Edge states and supersymmetric sigma models

Roberto Bondesan

UNIVERSITÉ PARIS 6 - PIERRE ET MARIE CURIE

et

INSTITUT DE PHYSIQUE THÉORIQUE - CEA/SACLAY

Thèse de doctorat

Spécialité

Physique Théorique

Sujet de la thèse:

Edge states and supersymmetric sigma models

---

présentée par

Roberto BONDESAN

pour obtenir le grade de

Docteur de l'Université Paris 6

Soutenue le 14 Septembre 2012 devant le jury composé de:

M.	Michel Bauer	Membre invité
M.	Sergio Caracciolo	Rapporteur
M.	Ilya Gruzberg	Examinateur
M.	Jesper Jacobsen	Membre invité (co-directeur de thèse)
M.	Hubert Saleur	Directeur de thèse
M.	Kareljan Schoutens	Rapporteur
M.	Jean-Bernard Zuber	Président du jury

Abstract

A fundamental property of the quantum Hall effect is the presence of edge states at the boundary of the sample, robust against localization and responsible for the perfect quantization of the Hall conductance. The transition between integer quantum Hall plateaus is a delocalization transition, which can be identified as a strong-coupling fixed point of a $1+1$-dimensional supersymmetric sigma model with topological θ-term. The conformal field theory describing this transition displays unusual features such as non-unitarity, and resisted any attempt of solution so far.

In this thesis we investigate the role of edge states at quantum Hall transitions using lattice discretizations of super sigma models. Edge states correspond to twisted boundary conditions for the fields, which can be discretized as quantum spin chains or geometrical (loop) models. For the spin quantum Hall effect, a counterpart of the integer quantum Hall effect for spin transport (class C), our techniques allow the exact computation of critical exponents of the boundary conformal field theories describing higher plateaus transitions. Our predictions for the mean spin conductance are validated by extensive numerical simulations of the related localization problems.

Envisaging applications to transport in network models of $2+1$-dimensional disordered electrons, and to quenches in one-dimensional gapless quantum systems, in this thesis we have also developed a new formalism for dealing with partition functions of critical systems in rectangular geometries. As an application, we derive formulas for probabilities of self-avoiding walks.

Key words: Loop models, quantum spin chains, boundary conformal field theory, edge states, supersymmetry, quantum Hall effect

Résumé

Une propriété fondamentale de l'effet Hall quantique est la présence des états de bord. Ils résistent à la localisation et sont responsables de la quantification parfaite de la conductance de Hall. La transition entre les plateaux d'effet Hall quantique entier est une transition de délocalisation, qui peut être identifiée comme un point fixe de couplage fort d'un modèle sigma supersymétrique en $1+1$-dimensions avec terme topologique θ. La théorie conforme décrivant cette transition présente des caractéristiques inhabituelles telles que la non-unitarité, et a résisté à toute tentative de résolution jusqu'à présent.

Dans cette thèse, nous étudions le rôle des états de bord dans les transitions d'effet Hall, en utilisant des discrétisations sur réseau de modèles sigma. Les états de bord correspondent aux conditions aux bord pour les champs des modèles sigma, et peuvent être discrétisés en terme de chaînes de spins quantiques ou de modèles géométriques (de boucles). Pour l'effet Hall de spin, un équivalent de l'effet Hall entier pour le transport de spin (classe C), nos techniques permettent le calcul exact des exposants critiques des théories conformes avec bord décrivant les transitions entre plateaux élevés. Nos prédictions pour la moyenne de la conductance de spin sont validées par des simulations numériques des problèmes de localisation correspondant.

Dans cette thèse, envisageant des applications au transport dans les modèles sur réseau des électrons désordonnés en $2+1$-dimensions, et aux trempes dans des systèmes quantiques à une dimension, nous avons également développé un nouveau formalisme pour calculer des fonctions de partition de systèmes critiques sur un rectangle. Comme application, nous dérivons des formules de probabilités pour les marches auto-évitantes.

Mots clés: Modèles de boucles, chaînes de spins quantiques, théories conformes avec bord, états de bord, supersymétrie, effet Hall quantique

Acknowledgments

I would like to express my gratitude to my supervisors Hubert and Jesper, for their constant support, teaching, encouragement and guidance during these three years of PhD. I have learned a lot from them.

I am also very grateful to the institutes where I have been equally shared during my graduate studies, the IPhT Saclay and the LPTENS, for the warm and scientifically rich atmosphere.

I thank Prof. Caracciolo and Prof. Schoutens for having accepted promptly to be referees on my manuscript and for their comments, and the other members of the committee, Prof. M. Bauer, Prof. I. Gruzberg, and Prof. J.-B. Zuber for their interest in my work. I am also particularly thankful to Prof. Caracciolo for his guidance and encouragement prior to the start of the PhD, to Prof. Gruzberg for his kind teaching and his support during the search of a postdoc, and to Dr. H. Obuse for our collaboration.

Many thanks to the students and postdocs in Saclay and at the LPTENS, among whom I found very good friends. I benefit from discussions (not necessarily about physics) with Alexandre, Axel, Azat, Bruno, Clément, Emanuele, Enrico, Eric, Francesco, Guillaume, Jean-Marie, Jérôme, Hirohiko, Piotr, Romain, Tristan and Vittore. Special thanks to Clément and Jean-Marie, and in particular to Jérôme for our collaboration and extremely useful discussions.

I am grateful to many people outside the scientific community for their support. First of all my family, and in particular my parents, who gave me the all the means to pursue my interests in life. Then, my tenderest thought goes to Laura, whose love completed my life and helped me to surmount the difficulties that doing a PhD abroad implies. I thank Axel, Adrien, Béa and Charles for all the good time we had playing together, and Alessandro, Daniele and Luca for our everlasting friendship.

Contents

Introduction

Conformal field theory (CFT) is an extremely powerful tool to study and classify possible critical behaviors in two dimensions. Starting with the seminal paper [19], many exact solutions of critical system have been obtained. Despite this success, there remain lattice systems and conformal field theories which have not been understood, demanding the development of new tools. Among those there are theories of Anderson transitions, between localized and delocalized phases in $2+1$-dimensional disordered non-interacting electrons.

The study of Anderson transitions is one of the most active research area in the context of disordered systems. In the last fifteen years, this field has witnessed a huge progress [78], in particular thanks to the completion of the the symmetry classification of disordered electrons [11, 204]. Field theoretical approaches to the localization transitions were developed during the eighties. The field theories associated to a $d+1$-dimensional disordered quantum system are d-dimensional quantum field theories (sigma models) describing disorder averaged products of (advanced and retarded) Green's functions. Although historically the first technique used to average over disorder was the replica trick [194], the single particle character of the systems under consideration, makes the supersymmetry method [75], leading to the study of rigorously defined super sigma models, a well suited way to formulate the problem.

Anderson transitions in $2+1$-dimensions exhibit a rich variety of critical behaviors [78]. On top of standard transitions separating insulating (localized) from metallic (extended) phases, the integer quantum Hall (IQH) effect provides an example of localization transition between two insulating phases, corresponding to different plateaus of the Hall conductance. In field theoretic terms this possibility is given by the presence of an additional topological θ-term in the action [163].

The perfect quantization of the Hall conductance has topological origin [188], and the presence of non-trivial topological insulating phases in several symmetry classes, has been by now fully understood in non-interacting systems in any dimension [128, 136, 179]. The research in this direction has been boosted by the recent theoretical [21, 123] and experimental [133] discovery of the quantum spin Hall effect, a counterpart of the IQH effect in time-reversal invariant systems. Other important cousins of the IQH effect are the so-called spin quantum Hall effect [183] and thermal quantum Hall effect [56], which may occur in disordered superconductors.

However, a good understanding of the field theories needed to describe the transitions

between these phases is still lacking. An important role in this direction has been played by network models discretizing the quantum dynamics, introduced by Chalker and Coddington [55] for the IQH transition. Network models allow for efficient numerical determination of the critical exponents, and from a theoretical perspective, they provide lattice regularizations of sigma models. These lattice regularizations can be formulated as non Hermitian spin chains, or as statistical mechanics models with non local degrees of freedom (loops), representing Feynman paths contributing to the disorder averaged Green's functions [18, 50, 101, 103, 132, 168, 170, 203]. Loop models are familiar from polymer physics [64], and, in their several variants (dense, dilute, colored, etc.), provide an intuitive and unifying geometrical language to approach critical phenomena, and a lot of exact results are available for them, using a variety of techniques [16, 17, 117, 153]. The lattice approach to the field theories has been very useful, and has allowed the exact solution of the spin quantum Hall transition [101].

From a technical point of view, difficulties in the study of the field theories describing the fixed points arise since one has to deal with so-called logarithmic conformal field theories, a family of CFTs exhibiting unusual properties such as non-unitarity, far less understood than ordinary unitary CFTs. In a more fundamental perspective, the lattice discretizations have proved to be very useful since common algebraic structures are shared between the lattice and the continuum [157], and this has allowed to improve our understanding of logarithmic CFTs [39, 92, 158, 170–172, 191].

The study of fixed points in supersymmetric sigma models benefits also from their relevance in high energy physics, in particular in the context of the AdS/CFT duality [161, 197], and progress in understanding these theories has picked up pace recently. Apart from the aforementioned lattice discretizations, other developments which made this possible are a better understanding of algebraic aspects of superalgebras [36, 98, 145, 166] and the use of the mini superspace technology [100, 181]. In spite of these results, finding the conformal field theory of the IQH transition remains an outstanding unsolved problem of theoretical physics.

Different quantum Hall phases can be distinguished by the presence of edge states at the boundary of the sample, which are robust against localization and responsible for a non-zero value of the Hall conductance [107]. Edge states are more generally an hallmark of topological character of phases of matter [108], and received a lot of attention recently. (However examples where strongly correlated topological phases do not support gapless boundary modes are known [31].) Among the several developments, the most exciting are related to applications to quantum computation [149], though systems like some fractional quantum Hall states, are usually proposed for that.

An interesting question of experimental relevance is then studying the boundary critical behavior at Anderson transitions. The role of edge states at the transitions manifests itself as conformal boundary conditions in the sigma models. Boundary properties for supersymmetric Wess Zumino Witten models are well understood [59, 60], and there has been recent progress for other models, such as the superprojective sigma models [38] of relevance for the spin quantum Hall effect [101, 170].

Boundary CFTs have also a broad range of applicability in several other areas of

condensed matter. For example they are central to our understanding of the Kondo effect [5], of the physics of quantum impurities or the Fermi edge singularity [7], and, more recently, of local and global quenches in one dimensional quantum systems [34, 72]. On the formal side boundary CFT plays also a fundamental role in the axiomatization of CFT [160], understanding of logarithmic conformal field theory [89, 171], or in the relationship between conformal field theory and the Schramm-Löwner Evolution formalism [16].

In this thesis we revisit the problem of edge states at quantum Hall transitions, by studying boundary sigma models through their lattice discretizations. Further, motivated by applications, we will present a new formalism of boundary states describing rectangular boundaries in CFT. We now outline the organization of the manuscript.

In chapter 1 we review loop models and boundary conformal field theory. Loop models are introduced from an algebraic perspective, as representations of the Temperley-Lieb algebra underlying the Potts model. We detail the relations between loops, the XXZ chain, and supersymmetric lattice models, the latter formulated in terms of both spin chains and coherent states path integrals. The Heisenberg chain is used as a useful guiding example for understanding the basic symmetry properties. We also discuss issues related to non-unitarity and indecomposable representations of the lattice algebras. We then move the focus to the continuum description, reviewing the mapping of the super spin chains introduced previously to sigma models on the complex projective superspace. In a second part of the chapter we give an introduction to boundary conformal field theory. After a brief general review of CFTs, and the definition of logarithmic CFTs, the emphasis is on the formalism of boundary states and boundary condition changing operators, and we present the construction of Cardy's states. Then we describe the boundary theory of critical loop models, and discuss recent extensions of it using blob algebras.

Chapter 2 develops the formalism of boundary states for fully open boundary conditions, introduced by the author in [26, 29]. There, we first discuss how conformal mappings can be implemented in terms of the Virasoro algebra, and how these ideas can be used to find the boundary states describing rectangular geometries for arbitrary CFTs. Then we construct rectangular amplitudes (partition functions), deriving some explicit results, and discussing their modular properties. Afterward, we turn to our main motivation, the calculation of partition functions for loop models. We introduce then lattice discretizations of the rectangle boundary states in loop models, and discuss a geometrical interpretation of conformal blocks. As an application of these ideas, we derive probability formulas for the logarithmic CFTs of self-avoiding walks.

In chapter 3, we introduce the network models for Anderson transitions and we make the link with the topics developed in the previous chapters. After a review of the phenomenology of the integer quantum Hall effect, and the formulation of quantum transport in the Chalker-Coddington model, we describe the supersymmetry method for computing disorder averaged Green's functions, and discuss the resulting spin chains and associated geometrical models. Then we provide the general framework of symmetry classification of disordered system, and focus on the spin quantum Hall effect. We will

discuss its phenomenology and how to employ network models to study the delocalization transition, adapting the previously defined supersymmetric theories to this case. We review how certain disorder averaged quantities can be mapped onto percolation, and use this mapping to derive explicit exact results, in particular for the conductance in the strip and cylinder geometries.

Finally, in chapter 4, we apply the tools developed previously to the study of edge states at quantum Hall transitions, following the articles [27, 28] by the author. We introduce new extensions of network models with extra edge channels, used to model edge states. For the spin quantum Hall case, we generalize the mapping to a geometrical model, this time being a model of loops intersecting at the boundary. The rest of the chapter is occupied by the solution of this new loop model. In particular we formulate the problem in terms of boundary conditions in super sigma models, discussing the relation between the topological θ-term and edge states. Then we launch into the technical problem of finding the critical exponents governing the decay of conductances at higher spin quantum Hall plateaus. The outcome of the analysis is that the exponents of percolation are modified to new irrational ones in the general case. These analytical predictions are finally compared to extensive numerical studies of the network model.

The material presented in this thesis in based on the following publications of the author:

- R. Bondesan, J. L. Jacobsen, and H. Saleur, *Edge states and conformal boundary conditions in super spin chains and super sigma models*, Nuclear Physics B **849** (2011), no. 2, 461–502.
- R. Bondesan, I. A. Gruzberg, J. L. Jacobsen, H. Obuse, and H. Saleur, *Exact exponents for the spin quantum Hall transition in the presence of multiple edge channels*, Phys. Rev. Lett. **108** (2012), 126801.
- R. Bondesan, J. Dubail, J. L. Jacobsen, and H. Saleur, *Conformal boundary state for the rectangular geometry*, Nuclear Physics B **862** (2012), no. 2, 553–575
- R. Bondesan, J. L. Jacobsen, and H. Saleur, *Rectangular amplitudes, conformal blocks, and applications to loop models*, Nuclear Physics B **867** (2013), no. 3, 913–949.

Further, sections 1.1.2 (subsection "Coherent states path integrals"), 3.1.5, and 3.2.3 (subsection "Conductance of a cylinder") contain material not published elsewhere.

Chapter 1

Boundary conformal field theory and loop models

The present chapter provides a review of some aspects of loop models and boundary conformal field theory serving as reference for the original research material presented in the next chapters. In section 1.1 we will introduce the algebraic approach to lattice models in the case of the Potts model, and discuss supersymmetric formulations. Section 1.2 contains an introduction to boundary conformal field theory, in particular to the formalism of boundary states, and discusses the continuum limit of (ordinary and blobbed) loop models.

1.1 The Potts model, loops and super sigma-models

The two dimensional Potts model provides an important laboratory to develop exact techniques in statistical mechanics [17]. It presents also many interesting mathematical aspects. Among those, the most fascinating are the relation to graph theory [185], and its algebraic formulation in terms of the Temperley-Lieb algebra [187]. Interestingly enough, Temperley-Lieb algebras appear also in the computation of the Jones polynomial of knot theory [125], placing the Potts model at the intersection among several branches of modern physics and mathematics.

We now define the Potts model. Consider a graph G with edge set E and vertex set V, and define a a spin configuration of the vertices by a map $s : V \to [Q]$, $[Q] := \{1, \dots, Q\}$. We assign an energy J if two adjacent vertices have the same spin, zero otherwise. The Potts model partition function is then

$$Z_G(J, Q) = \sum_{s:V\to[Q]} \exp\left(J \sum_{(ij)\in E} \delta(s_i, s_j) \right) ,$$

where the sum is over all spin configurations. It is illuminating to introduce $v = e^J - 1$,

so that we can rewrite it as (high temperature expansion)

$$Z_G(J,Q) = \sum_{s:V\to[Q]} \prod_{(ij)\in E} (1 + v\delta(s_i, s_j)) \ .$$

In this form, expanding out the product, we associate to each term an induced graph $H = (A, V)$ where the vertices i, j are connected if we take the term $\delta(s_i, s_j)$ in the expansion. Performing the sum over the possible spin values produces a factor of $Q^{k(H)}$, where $k(H)$ is the number of connected components (clusters[1]) of H, leaving us with Fortuin-Kasteleyn representation of the Potts model [82]:

$$Z_G(v,Q) = \sum_{A\subseteq E} v^{|A|} Q^{k(H)} \ . \tag{1.1}$$

The partition function is now a polynomial in Q, which is then promoted to a complex variable. The Potts model partition function encodes important properties of a graph since eq. (1.1) coincides with the Tutte polynomial of graph theory after a change of variables $(v, Q) \to (x, y)$. We refer the interested reader to [185] for more details on this connection. Varying the value of Q we cover a series of interesting models. For $Q = 2$ we get the Ising model, as evident from the initial spin formulation. The limit $Q \to 1$ corresponds to bond *percolation*, since if we set $v = p/(1-p)$ and look at the rescaled partition function

$$(1-p)^{|E|} Z = \sum_{A\subseteq E} p^{|A|}(1-p)^{|E|-|A|} Q^{k(H)} \ ,$$

edges in A are percolating with probability p. Another limit giving rise to an interesting geometrical model is $Q \to 0$. Let us first use the Euler relation $k(H) = |V| - |A| + c(H)$, where $c(H)$ is the cyclomatic number (i. e. , the number of linearly independent cycles) in eq. (1.1). Now sending $v, Q \to 0$ keeping $w = v/Q$ fixed, selects among the spanning subgraphs, the forests, having $c(H) = 0$. Further when $w \to 0$, one selects forests with a single component, called spanning trees or dense polymers. Percolation and dense polymers will play an important role in the coming developments.

We now restrict ourselves to planar graphs, for which there is a natural bijection between cluster configurations on G and on its dual G^*. We take an edge of G^* in A^* only if the associated edge of G is not taken in A and vice versa. Let us now draw the loops separating clusters from their duals. Such loops are non-intersecting and live on another graph (medial graph). When the graph is the square lattice—the case on which we focus below—the medial graph is the tilted square lattice, having vertices on links of the original square lattice, see figure 1.1. Using that the number of loops is given by $l(H) = k(H) + c(H)$, together with the Euler relation, yields the partition function in the loop representation:

$$Z_G(v,\beta) = \beta^{|V|} \sum_{A\subseteq E} \left(\frac{v}{\beta}\right)^{|A|} \beta^{l(H)} \ , \tag{1.2}$$

[1]Note that for a given spin configuration, adjacent vertices with the same value of the spin can be in different clusters.

where we defined $\beta := \sqrt{Q}$.

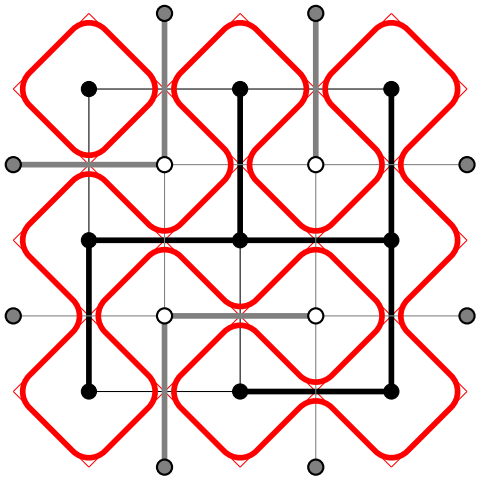

Figure 1.1: A cluster configuration on a 3×3 square lattice (thick black) and its dual (thick gray). Gray vertices are identified. In red the medial lattice where the loops (thick red) live.

The Potts model is called ferromagnetic if $v \geq 0$, as it is then favored for adjacent spins to take the same value; antiferromagnetic if $-1 \leq v \leq 0$, as it is then favored for adjacent spins to take different values; and unphysical otherwise ($v < -1$), as the weights are then no longer non-negative. We will mostly consider the ferromagnetic regime here. For v large spins are aligned, while if it is positive but small, spins are almost independent and one expects a phase transition at v_c. This value can be obtained by Kramers-Wannier duality [147] when $G = G^*$, like for the square lattice. A simple argument goes as follows. Note that sending G to G^* inverses v/β, since $|A^*| = |E| - |A|$. If the graph is self-dual v_c should be the same for G and G^*, implying $v_c = \beta$. At the critical point, the partition function counts the number of loops with a fugacity β:

$$Z_G(\beta) = \beta^{|V|} \sum_{\mathcal{L}} \beta^{\#(\text{loops})} ,$$

$\mathcal{L}$ being the set of loop configurations on the medial lattice of G.

1.1.1 Transfer matrices and the Temperley-Lieb algebra

A powerful approach to the computation of partition functions is the use of the transfer matrix, obtained by switching from a 2D to a 1+1D point of view. The partition function will then be represented as a suitable trace or matrix element, depending on boundary conditions, of a power of the transfer matrix. Let us focus now on the loop model on the tilted square lattice of figure 1.2(a), where we have open reflecting boundary conditions at the left and right boundaries of the strip. We use coordinates (i, j), $i = 0, \ldots, 2L-1$,

$j = 0, \ldots, 2L' - 1$ on the links of this lattice and introduce the set of even and odd column indices

$$I_A = \{0, 2, \ldots, 2L - 2\}\,, \quad I_B = \{1, 3, \ldots, 2L - 1\}\,. \tag{1.3}$$

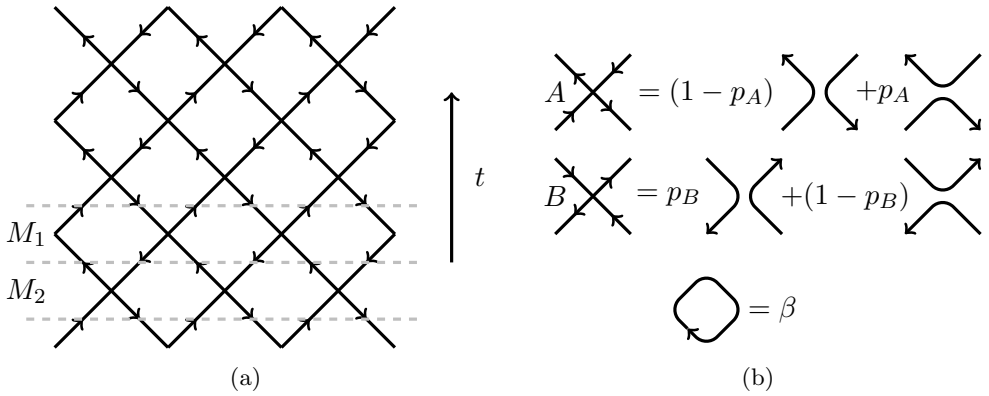

(a) (b)

Figure 1.2: (a) The two-dimensional lattice on which we define the loop model. Chiralities are associated to even and odd columns of links. The transfer matrix is a product of two transfer matrices acting on two consecutive layers $T = M_1 M_2$, imaginary time flows from bottom to top. The number of sites is $2L = 6$. (b) Vertices of the loop model. Loops formed weight β.

Referring to figure 1.2(a), we have associated a chirality to links (i, j), up-going if $i \in I_A$, and a down-going if $i \in I_B$ [2]. The transfer matrix T is diagonal-to-diagonal, evolving quantum states on a row by two layers of the lattice in the vertical (imaginary, discrete) time direction:

$$T = M_1 \times M_2\,; \quad M_1 = \prod_{i \in I_B^-} T_i^B\,, \quad M_2 = \prod_{i \in I_A} T_i^A\,. \tag{1.4}$$

$I_B^- = \{1, 3, \ldots, 2L - 3\}$ is the appropriate set of sites for open (reflecting) boundary conditions. T_i acts on two adjacent links and is given by the two possible events onto which a vertex can be decomposed: either the bits of loops on sites i and $i+1$ go through without interacting or they are contracted, see figure 1.2(b). Calling the operator implementing this contraction E_i we have:

$$\begin{aligned} T_i^A &= (1 - p_A) + p_A E_i \\ T_i^B &= p_B + (1 - p_B) E_i\,. \end{aligned}$$

[2] We stress that this orientation is a property of the underlying lattice, not of the loop itself. In particular, for a loop of a given position and shape, no sum over orientations is implied, and the states entering the loop representation do not contain any orientational information. This choice of a directed lattice is allowed since the interactions respect this chiralities, and thinking about a directed lattice is useful to make contact with the topic of chapter 3, quantum network models.

The sum over loop configurations in the partition function (1.2) is reproduced by the vertex decompositions in $T^{L'}$. See figure 1.3 for a typical loop configuration. When periodic boundary conditions in the horizontal direction are imposed one replaces I_B^- by I_B adding an additional operator E_{2L-1} acting onto the last and first strand.

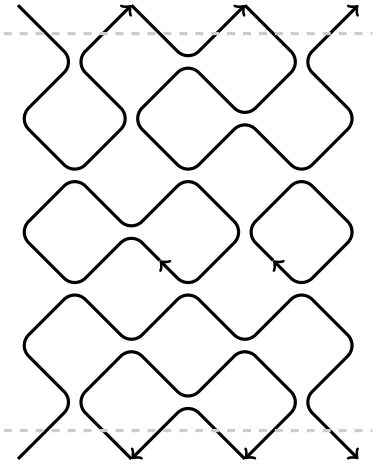

Figure 1.3: A typical loop configuration.

Above we allowed couplings with different strength in the vertical and horizontal direction, respectively v_A and v_B in the previous notation, which are related to p_s, $s = A, B$ by $(1-p_s)/p_s = \beta/v_s$. When $\beta = 1$, p_A and p_B are the probabilities of vertical and horizontal percolation bonds. The self-dual point at which the system is critical is $p_A = 1 - p_B$, which in the isotropic case $p_A = p_B$ gives $v = \beta$. It is useful to consider the very anisotropic continuous-time limit $p_A \to 0$ with $\epsilon = \sqrt{p_A/(1-p_B)}$ fixed, when $T \simeq \exp(-\sqrt{p_A(1-p_B)}H)$, where the quantum Hamiltonian H [3] is

$$H = -\epsilon \sum_{i \in I_A} (E_i - 1) - \epsilon^{-1} \sum_{i \in I_B^-} (E_i - 1)\,. \tag{1.5}$$

This is the Hamiltonian of a quantum mechanical system in one-dimension, a quantum spin chain. When $\epsilon \neq 1$ the chain is said to be staggered, and it is gapped, describing a massive integrable quantum field theory [81]. We anticipate here one of the key concepts which we will develop in several places below: the two extreme limits $\epsilon = 0$ and $\epsilon = \infty$ of dimerized spin chains, correspond in an open system to two different situations distinguished by the presence or not of a dangling edge state at the boundaries. See figure 1.4.

At the critical coupling $\epsilon = 1$ the gap between the ground state energy and the first excited state closes in the continuum limit (the chain is said to be gapless). In particular the dispersion relation of this chain is linear, characteristic of a conformal field theory, as we will see below.

[3] Note this is not the conserved Hamiltonian associated to an integrable system [200], but we expect the transfer matrix and the Hamiltonian to conceal the same physics.

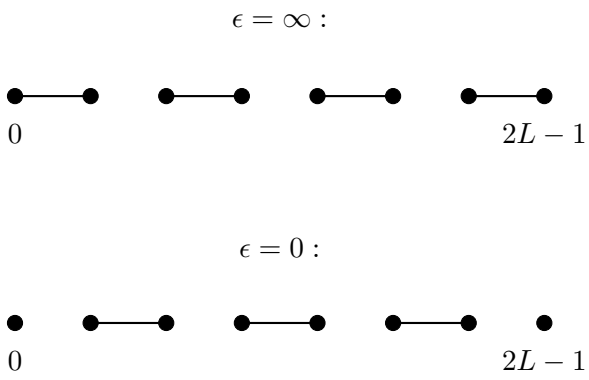

Figure 1.4: Schematic representation of the Hamiltonians in the extreme limits $\epsilon = 0$ and $\epsilon = \infty$. Dots denote sites and links are the couplings in the Hamiltonian.

We comment now on the algebraic properties of the transfer matrix (or Hamiltonian) for open boundary conditions. The operators used to construct the transfer matrix satisfy the Temperley-Lieb (TL) algebra TL_{2L}^{β} [187], which due to the graphical representation is in fact a diagram algebra. The TL algebra is generated by the identity I and the operators E_i, $i = 0, 1, \ldots, 2L-2$, subject to the relations:

$$\begin{aligned} (E_i)^2 &= \beta E_i \\ E_i E_{i\pm1} E_i &= E_i \\ [E_i, E_j] &= 0, \qquad \text{for } |i-j| \geq 2\,. \end{aligned} \tag{1.6}$$

In the loop representation of the Potts model, these relations are faithfully represented, meaning that the important information is the topology of connectivities of configurations. These connectivities are encoded in non crossing pairings on a rectangle with $2L$ points on opposite sides. The composition operation of the algebra $w \circ w' = ww'$, $w, w' \in TL_{2L}^{\beta}$, is obtained by stacking the diagram w on top of w'. See figure 1.5 for an illustration. With this point of view each configuration contributing to the partition function is a word in TL.

Supposing periodic boundary conditions in the vertical direction, the partition function will be given by

$$Z = \mathrm{Tr}_M\, T^{L'}\,, \tag{1.7}$$

where the symbol Tr_M is the so-called Markov trace (for a related discussion see [70]), standing for the operation of gluing the strands on the bottom and the top of the strip, to obtain the geometry of the annulus, and weighting each configuration according to the number of loops.

XXZ representation

In the algebraic framework introduced above, the spin and the cluster formulations of the Potts model correspond simply to different representations of the Temperley-Lieb

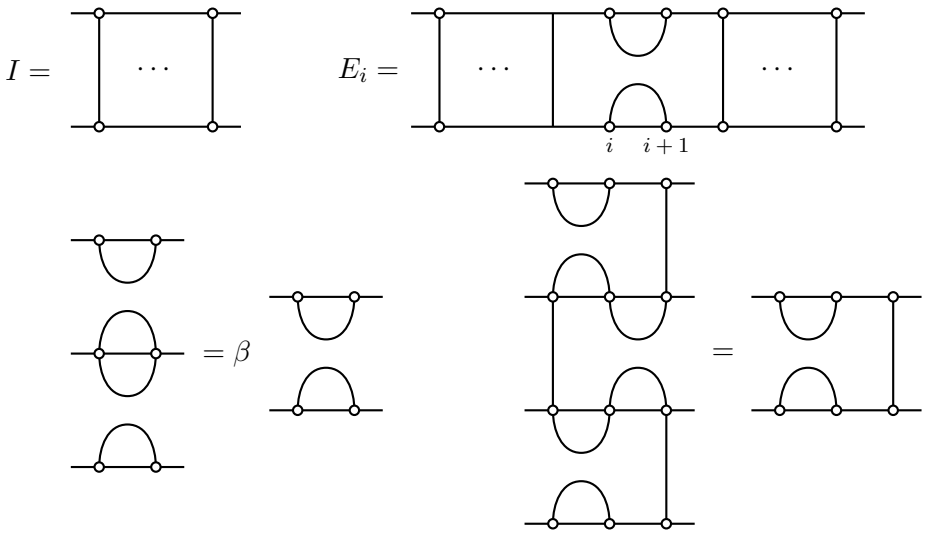

Figure 1.5: On top, the identity and the Temperley-Lieb generators in the diagrammatic (loop) representation. Below, the diagrammatic equations $(E_i)^2 = \beta E_i$ and $E_i E_{i+1} E_i = E_i$.

algebra. We refer to [142] for details. Another important representation we would like to discuss is the six-vertex/XXZ model.

It is possible to trade the Q-dimensional space of the spin representation for a 2-dimensional one, associated to dynamical orientations of loops, to obtain the six-vertex model [17]. This model is defined for arbitrary Q and has local, albeit complex, Boltzmann weights. The Hilbert space onto which the transfer matrix acts is $(\mathbb{C}^2)^{\otimes 2L}$, and the action of TL generators E_i can be written as:

$$E_i = -\frac{1}{2}\left(\sigma_i^x \sigma_{i+1}^x + \sigma_i^y \sigma_{i+1}^y\right) - \frac{q+q^{-1}}{4}\sigma_i^z \sigma_{i+1}^z - \frac{q-q^{-1}}{4}\left(\sigma_i^z - \sigma_{i+1}^z\right) + \frac{q+q^{-1}}{4}\,, \quad (1.8)$$

where

$$\sigma_i^a = \mathbf{1}_2 \otimes \cdots \otimes \mathbf{1}_2 \otimes \underbrace{\sigma^a}_{i} \otimes \mathbf{1}_2 \otimes \cdots \otimes \mathbf{1}_2\,,$$

σ^a, $a = x, y, z$, being Pauli matrices. Then the non trivial part of E_i in the basis $\{\uparrow,\downarrow\} \otimes \{\uparrow,\downarrow\}$ of sites $i, i+1$ is

$$E_i = \begin{pmatrix} 0 & 0 & 0 & 0 \\ 0 & q^{-1} & -1 & 0 \\ 0 & -1 & q & 0 \\ 0 & 0 & 0 & 0 \end{pmatrix}. \quad (1.9)$$

This operator satisfies relations (1.6) if q is related to β by $\beta = q + q^{-1}$. We will discuss later the representation theory of TL, but let us anticipate that the structure of modules (representation spaces) will change drastically if q is a root of unity. The six-vertex

model is then defined by using the above expression of E_i in the transfer matrix of eq. (1.4). The associated Hamiltonian is the XXZ Hamiltonian with boundary fields (up to an irrelevant constant):

$$H = \frac{1}{2}\sum_{i=0}^{2L-2}\left(\sigma_i^x\sigma_{i+1}^x + \sigma_i^y\sigma_{i+1}^y + \frac{q+q^{-1}}{2}\sigma_i^z\sigma_{i+1}^z\right) + \frac{q-q^{-1}}{2}\left(\sigma_0^z - \sigma_{2L-1}^z\right) . \tag{1.10}$$

We remark that for $q = 1$ ($\beta = 2$) this reduces to the celebrated XXX antiferromagnetic Heisenberg chain:

$$H = \frac{1}{2}\sum_{i=0}^{2L-2}\left(\sigma_i^x\sigma_{i+1}^x + \sigma_i^y\sigma_{i+1}^y + \sigma_i^z\sigma_{i+1}^z\right) . \tag{1.11}$$

Further we mention that another particularly important representation of the TL algebra is the RSOS one [12], on which there has been recently a renewal of interest for applications to anyonic chains [79, 112].

1.1.2 Replicas and supersymmetry

In the previous section we have seen the XXZ representation of TL, deforming the Heisenberg chain and keeping a two-dimensional space on every site. In this section we will describe other generalizations of the Heisenberg chain, where the $\mathfrak{sl}(2)$ symmetry becomes $\mathfrak{sl}(M)$ and $\mathfrak{sl}(N+M|N)$. These models will furnish new representations of TL, and will correspond to a replica and a supersymmetric version of the loop model introduced above.

$\mathfrak{gl}(M)$ vertex models

We begin by recalling the definition of $\mathfrak{gl}(M)$. Introduce the matrices E_{ab}, $a, b = 1, \dots, M$ having 1 in row a and column b and zero otherwise. The Lie algebra $\mathfrak{gl}(M)$ is then the span of the E_{ab}, and is defined by the commutation relations

$$[E_{ab}, E_{cd}] = \delta_{bc}E_{ad} - \delta_{da}E_{cb} .$$

We follow [4, 172] and associate to every up-going link of the tilted lattice of figure 1.2(a), the fundamental representation V of $\mathfrak{gl}(M)$, and to every down-going one the dual fundamental $V^\star$. The transfer matrix of this vertex model will act on the space of states:

$$\mathcal{H} = (V \otimes V^\star)^L . \tag{1.12}$$

We introduce bosons b_i^a, $i \in I_A$ and $\bar{b}_i^a$, $i \in I_B$, (recall def. (1.3)), $a = 1, \dots, M \geq 2$, satisfying canonical commutation relations, the non-trivial ones being $[b_i^a, b_j^{\dagger b}] = [\bar{b}_i^a, \bar{b}_j^{\dagger b}] = \delta_{ij}\delta^{ab}$. V and $V^\star$ are defined by the constraint that there is a single particle on a site (sum over repeated indices a will always be understood):

$$b_i^{\dagger a}b_i^a = 1 , \quad i \in I_A \tag{1.13}$$

$$\bar{b}_i^{\dagger a}\bar{b}_i^a = 1 , \quad i \in I_B , \tag{1.14}$$

on which the generators of $\mathfrak{gl}(M)$ are represented in terms of oscillators as $J_i^{ab} = b_i^{\dagger a} b_i^b$, $i \in I_A$, $J_i^{ab} = -\bar{b}_i^{\dagger b} \bar{b}_i^a$, $i \in I_B$. The tensor product $V \otimes V^\star$ (resp. $V^\star \otimes V$) decomposes as the adjoint plus the singlet. The most general (non-trivial) coupling can then be written as the projector onto the singlet, realized by pairwise contracting indices[4]. In terms of oscillators this projector can be written as the Hermitian operator:

$$E_i = \bar{b}_{i+1}^{\dagger a} b_i^{\dagger a} b_i^b \bar{b}_{i+1}^b \,, \quad i \in I_A$$
$$E_i = \bar{b}_i^{\dagger a} b_{i+1}^{\dagger a} b_{i+1}^b \bar{b}_i^b \,, \quad i \in I_B \,.$$

Thanks to the single particle constraint, one can verify that these furnish a faithful representation of TL, eq. (1.6) with $\beta = M$. Note that $\bar{b}_{i+1}^{\dagger a} b_i^{\dagger a} b_i^b \bar{b}_{i+1}^b = -J_{i+1}^{ab} J_i^{ba}$, and the bilinear $J^{ab} J^{ba}$ is the quadratic Casimir invariant of $\mathfrak{gl}(M)$. Moreover the vertex model defined by the transfer matrices (1.4) with E_i as above, enjoys a global $\mathfrak{sl}(M)$ or $\mathfrak{gl}(M)$ invariance, since the difference between the two algebras is the central element J^{aa}, and the global action is defined by $J^{ab} = \sum_i J_i^{ab}$.

The operator E_i acting on sites $i, i+1$ describes the annihilation of the particles on layer j, and the creation of new ones on layer $j+1$ with the same spin. Then the relation of this model with the loop model introduced above in section 1.1.1 should become apparent if we interpret the latter as a scattering process, and look at E_i as the contraction of wordlines of bosons. The partition function then is

$$Z = \mathrm{Tr}_{\mathcal{H}} \, T^{L'} \,,$$

where the trace is over the space of states of eq. (1.12). The fundamental representation flows on (contractible and not-contractible) loops, which thus get a weight $\mathrm{Tr}_V \, I = M$.

Supersymmetric formulation

The most interesting limits of loop fugacity equal to zero or one (dense polymers and percolation) are clearly ill-defined in the above formulation. This problem can be cured by introducing on top of bosons also fermions, an idea going back to Parisi and Sourlas [156]. We generalize then the above procedure and introduce oscillators b_i^a,f_i^α and $\bar{b}_i^a$,$\bar{f}_i^\alpha$ for $i \in I_A$ (even) and $i \in I_B$ (odd) respectively. We take the set of bosonic indices $a = 1, \ldots, N+M$ and fermionic ones as $\alpha = 1, \ldots, N$, where $N, M+N \geq 0$. Let us now consider the creation of two particles out of the vacuum and their annihilation on neighboring sites i (even) and $i+1$. This event produces a closed loop and will give a contribution

$$\langle 0 | \left(b_i^a \bar{b}_{i+1}^a + f_i^\alpha \bar{f}_{i+1}^\alpha \right) \left(\bar{b}_{i+1}^{\dagger b} b_i^{\dagger b} + \bar{f}_{i+1}^{\dagger \beta} f_i^{\dagger \beta} \right) |0\rangle = N + M - N = M \,, \tag{1.15}$$

[4]To relate the particle basis to the spin one, one has to define $|\mathrm{spin} = a\rangle = \epsilon_{ab} b^{\dagger b} |0\rangle$ on odd sites due to our choice of the dual representation. For the case of $\mathfrak{sl}(2)$ for example, one has $J^z b^{\dagger 1}|0\rangle = b^{\dagger 1}|0\rangle$ and $J^z b^{\dagger 2}|0\rangle = -b^{\dagger 2}|0\rangle$ for even sites but $J^z \bar{b}^{\dagger 2}|0\rangle = \bar{b}^{\dagger 2}|0\rangle$ and $J^z \bar{b}^{\dagger 1}|0\rangle = -\bar{b}^{\dagger 1}|0\rangle$ for odd ones. With this translation one finds $b_i^{\dagger 1} \bar{b}_{i+1}^{\dagger 1}|0\rangle + b_i^{\dagger 2} \bar{b}_{i+1}^{\dagger 2}|0\rangle = |\uparrow\downarrow\rangle - |\downarrow\uparrow\rangle$ as expected.

only if we choose the commutation relation of one species say $\bar{f}$ to be $[\bar{f}^\alpha, \bar{f}^{\dagger\beta}] = -\delta_{\alpha,\beta}$ and those of the other species as canonical ones (i. e. without minus signs). This extra minus sign will clearly produce some odd feature (e. g. the presence of negative norm states) but this is a necessary choice if we want to make sense for example of loops with fugacity zero, as demanded by physical applications. The presence of both bosons and fermions and interactions between the two, calls for a supersymmetric formulation of the problem which we will now review following [170,172], where now $M = 0$ or $M = 1$ are well defined.

We introduce oscillators a_i^p, $i \in I_A$, $\bar{a}_i^p$, $i \in I_B$ and define the $\mathbb{Z}_2$ grade of a^p and $\bar{a}^p$ as the grade $|\cdot|$ of the superindex: $|p| = 0$ if $p = 1, \dots, N + M$ and $p = 1$ if $p = N + M + 1, \dots, 2N + M$, that is

$$a^p = \begin{cases} b^p & \text{if } |p| = 0 \\ f^{p-(N+M)} & \text{if } |p| = 1 \end{cases} \quad ; \quad \bar{a}^p = \begin{cases} \bar{b}^p & \text{if } |p| = 0 \\ \bar{f}^{p-(N+M)} & \text{if } |p| = 1 \end{cases} .$$

Introduced the supercommutator $[a, b] = ab - (-1)^{|a||b|}ba$, a and $\bar{a}$ satisfy the following super-commutation relations (on top of trivial ones):

$$\begin{aligned} [a_i^p, a_j^{\dagger q}] &= \delta^{pq}\delta_{ij} \\ [\bar{a}_i^p, \bar{a}_j^{\dagger q}] &= (-1)^{|p||q|}\delta^{pq}\delta_{ij} . \end{aligned}$$

The minus sign if the two oscillators are fermionic is motivated by the cancellation of loops discussed above. Generalizing the bosonic construction of the previous section, we attach to every link (i, j) of the lattice the $\mathbb{Z}_2$-graded vector space $\mathbb{C}^{M+N|N}$, being the fundamental V of the Lie superalgebra $\mathfrak{gl}(M + N|N)$ for $i \in I_A$ and its dual $V^\star$ (which is different from the conjugate representation due to negative norm states) for $i \in I_B$. These spaces are constructed by imposing single particle constraints to the oscillators (repeated indices are summed over with Euclidean metric)

$$\begin{aligned} a_i^{\dagger p} a_i^p &= 1 , \quad i \in I_A \\ (-1)^{|p|}\bar{a}_i^{\dagger p}\bar{a}_i^p &= 1 , \quad i \in I_B . \end{aligned}$$

and defining the generators of $\mathfrak{gl}(M + N|N)$ as

$$\begin{aligned} J_i^{pq} &= a_i^{\dagger p} a_i^q , \quad i \in I_A \\ J_i^{pq} &= (-1)^{|p||q|+1}\bar{a}_i^{\dagger q}\bar{a}_i^p , \quad i \in I_B . \end{aligned}$$

They satisfy:

$$\begin{aligned} [J_{ab}, J_{cd}] &= J_{ab}J_{cd} - (-)^{(|a|+|b|)(|c|+|d|)}J_{cd}J_{ab} \\ &= \delta_{bc}J_{ad} - (-)^{(|a|+|b|)(|c|+|d|)}\delta_{da}J_{cb} . \end{aligned}$$

The transfer matrix eq. (1.4) acts on the space of states for a horizontal layer

$$\mathcal{H} = (V \otimes V^\star)^L , \tag{1.16}$$

where now the tensor product is of course the graded one, and

$$E_i = \bar{a}_{i+1}^{\dagger p} a_i^{\dagger p} a_i^q \bar{a}_{i+1}^q \,, \quad i \in I_A$$
$$E_i = \bar{a}_i^{\dagger p} a_{i+1}^{\dagger p} a_{i+1}^q \bar{a}_i^q \,, \quad i \in I_B \,.$$

Note that the TL generator is given by the quadratic Casimir $E_i = -\operatorname{Str} J_i J_{i+1}$. The partition function on an annulus is then given by:

$$Z = \operatorname{Str}_{\mathcal{H}} T^{L'} \,,$$

with the supertrace $\operatorname{Str}(\cdot) := \operatorname{Tr}((-1)^F \cdot)$, F the number of fermions. The fundamental representation V flows in closed loops, which then get a weight $\operatorname{Str}_V \mathbf{1} = M$ as desired.

Coherent states path integrals

We will now derive the coherent state path integral representation of transfer matrices of $\mathfrak{gl}(M)$ and $\mathfrak{gl}(N+M|N)$ vertex models. We will give more details in this section, since this approach has not been explicitly discussed in the literature.

We first deal with the $\mathfrak{gl}(M)$ case. Let us focus on two adjacent sites $V \otimes V^\star$. Since we are working in spaces fulfilling eq. (1.13)-(1.14), we introduce the projector onto the single particle subspace:

$$\mathcal{P} = b^{\dagger a} \bar{b}^{\dagger b} |0\rangle\langle 0| \bar{b}^b b^a \,,$$

where $b^a|0\rangle = \bar{b}^a|0\rangle = 0$. We project now the site transfer matrix onto this subspace

$$\begin{aligned} \tilde{T} &= \mathcal{P} \left((1-p) + p \bar{b}^{\dagger a} b^{\dagger a} b^b \bar{b}^b \right) \mathcal{P} \\ &= b^{\dagger a} \bar{b}^{\dagger b} |0\rangle \left((1-p)\delta_{ac}\delta_{bd} + p\delta_{ab}\delta_{cd} \right) \langle 0| \bar{b}^d b^c \,. \end{aligned}$$

$\tilde{T}$ is the operator we want to express in the coherent state basis.

Coherent state quantization is a standard method for deriving path integrals for quantum problems, we refer to [83] for reference. Given the bosonic Fock space associated to the harmonic oscillators b^a, we introduce complex variables x^a and define the coherent states

$$|x\rangle = \exp\left(x^a b^{\dagger a} \right) |0\rangle \,, \tag{1.17}$$

such that

$$b^a|x\rangle = x^a|x\rangle \,, \quad b^{\dagger a}|x\rangle = \partial_{x^a}|x\rangle \,.$$

The important point is that coherent states are (over-)complete and the resolution of the identity can be written as

$$\mathbf{1} = \int \mathrm{d}\mu(x) |x\rangle\langle x| \,,$$

where we introduced the Gaussian measure:

$$\mathrm{d}\mu(x) = \prod_a \frac{\mathrm{d}\Re(x^a)\mathrm{d}\Im(x^a)}{\pi} e^{-x^a x^{*a}} \,. \tag{1.18}$$

We express now $\tilde{T}$ in coherent state basis. We introduce variables $x_{0,0}, \bar{x}_{0,0}$ and $x_{0,1}, \bar{x}_{0,1}$ attached to the links meeting at the vertex under consideration, as in figure 1.6.

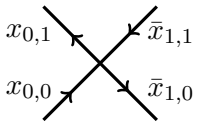

Figure 1.6: Labeling of bosonic variables at a vertex. The first index refers to columns, the second to rows. Overbars in $\bar{x}_{i,j}$ are used to stress the relation with dual representations $V^\star$ in the transfer matrix formulation.

We have:

$$\langle x_{0,1}, \bar{x}_{1,1}|\tilde{T}|x_{0,0}, \bar{x}_{1,0}\rangle = x^{*a}_{0,1}\bar{x}^{*b}_{1,1}\left((1-p)\delta_{ac}\delta_{bd} + p\delta_{ab}\delta_{cd}\right) x^c_{0,0}\bar{x}^d_{1,0} \,. \tag{1.19}$$

The deltas have a clear graphical interpretation, imposing the propagation of particles in the top direction, first term, or their contraction, second term.

We now consider the whole lattice and introduce on every link (ij) a complex variable x_{ij}, $i \in I_A$ and $\bar{x}_{ij}$, $i \in I_B$ (recall that I_A and I_B refer respectively to even and odd columns). Then we write the transfer matrix projected onto the single particle subspaces $\tilde{M}_1\tilde{M}_2$ acting say on horizontal layer j as

$$T = \int \mathrm{d}\mu(x,\bar{x})|(x,\bar{x})_{j+2}\rangle\langle(x,\bar{x})_{j+2}|\tilde{M}_1|(x,\bar{x})_{j+1}\rangle\langle(x,\bar{x})_{j+1}|\tilde{M}_2|(x,\bar{x})_j\rangle\langle(x,\bar{x})_j| \,, \tag{1.20}$$

where $\mathrm{d}\mu(x,\bar{x})$ denotes integration over all variables with coherent state measure (1.18) and

$$|(x,\bar{x})_j\rangle = \prod_{i\in I_A} |x_{i,j}, \bar{x}_{i+1,j}\rangle \,.$$

Since oscillators on different sites commute we have

$$\langle(x,\bar{x})_{j+1}|\tilde{M}_2|(x,\bar{x})_j\rangle = \prod_{i\in I_A}\langle x_{i,j+1}, \bar{x}_{i+1,j+1}|\tilde{T}_i|x_{i,j}, \bar{x}_{i+1,j}\rangle \,,$$

and analogously for $\tilde{M}_1$. For the L'-th power of the transfer matrix we just have to insert resolutions of the identity for each layer, and we then find ($J = \{0, 2, \ldots, 2L'-2\}$)

$$T^{L'} = \int \mathrm{d}\mu(x,\bar{x}) \prod_{j\in J}\prod_{i\in I'} \mathcal{T}^A_{i,j}(x,\bar{x}) \prod_{i\in I} \mathcal{T}^B_{i,j}(x,\bar{x})|(x,\bar{x})_{2L'}\rangle\langle(x,\bar{x})_0| \,,$$

where we defined

$$\mathcal{T}^A_{i,j}(x,\bar{x}) := (1-p_A)x^{*a}_{i,j+1}x^a_{i,j}\bar{x}^b_{i+1,j}\bar{x}^{*b}_{i+1,j+1} + p_A x^{*a}_{i,j+1}\bar{x}^{*a}_{i+1,j+1}\bar{x}^b_{i+1,j}x^b_{i,j}$$
$$\mathcal{T}^B_{i,j}(x,\bar{x}) := p_B x^{*a}_{i+1,j+1}x^a_{i+1,j}\bar{x}^b_{i,j}\bar{x}^{*b}_{i,j+1} + (1-p_B)x^{*a}_{i+1,j+1}\bar{x}^{*a}_{i,j+1}\bar{x}^b_{i,j}x^b_{i+1,j}\,.$$

Note now that the single particle constraint (1.13) when applied on coherent states imposes the variables to live on the real sphere S^{2N-1}, $x^a x^{*a} = 1$, since:

$$\langle x|x\rangle = \langle x|b^{\dagger c}b^c|x\rangle = x^{*c}x^c\langle x|x\rangle\,. \tag{1.21}$$

The partition function on an annulus $Z = \operatorname{Tr} T^{L'}$ is then obtained by tracing onto the single particle states on a layer giving

$$\langle 0|\prod_{i\in I_A} b_i^{a_i}\bar{b}_{i+1}^{a_{i+1}}|(x,\bar{x})_{2L'}\rangle\langle(x,\bar{x})_0|\prod_{i\in I_A} b_i^{\dagger a_i}\bar{b}_{i+1}^{\dagger a_{i+1}}|0\rangle = \prod_{i=0}^{2L-1} x^a_{i,2L'}x^{*a}_{i,0} = 1\,,$$

where we used the periodic boundary conditions $x^a_{i,0} = x^a_{i,2L'}$ and eq. (1.21). In the end the partition function of the Potts model in the coherent state representation is the following Gaussian integral:

$$Z = \operatorname{Tr} T^{L'} = \int \mathrm{d}\mu(x,\bar{x}) \prod_{j\in J}\prod_{i\in I'} \mathcal{T}^A_{i,j}(x,\bar{x}) \prod_{i\in I} \mathcal{T}^B_{i,j}(x,\bar{x})\,,$$

where $x^a_{i,0} = x^a_{i,2L'}$ is understood. We should also constrain the particles to live on a sphere, but since in this path integral we have only terms xx^* whose Gaussian integral is one, the result is the same also without imposing this. The index $a = 1,\dots,M$ is conserved along the wordlines of particles, and those wordlines close into loops. Each loop thus formed can be colored in M ways, so that it will get a weight M, and then we end up with the partition function of the loop model.

Further, note that alternatively we could have imposed the single particle constraint only at the end to find a less explicit formula:

$$\begin{aligned} Z = \operatorname{Tr} T^{L'} = \int \mathrm{d}\mu_S(x,\bar{x}) \prod_{j\in J}\prod_{i\in I_A} (1-p_A+p_A\bar{x}^{*p}_{i+1,j+1}x^{*p}_{i,j+1}x^q_{i,j}\bar{x}^q_{i+1,j}) e^{x^{*p}_{i,j+1}x^p_{i,j}} e^{\bar{x}^q_{i,j}\bar{x}^{*q}_{i,j+1}} \\ \times \prod_{i\in I_B} (p_B+(1-p_B)\bar{x}^{*p}_{i,j+2}x^{*p}_{i+1,j+2}x^q_{i+1,j+1}\bar{x}^q_{i,j+1}) e^{x^{*p}_{i+1,j+2}x^p_{i+1,j+1}} e^{\bar{x}^q_{i,j+1}\bar{x}^{*q}_{i,j+2}}\,, \end{aligned}$$

where

$$\mathrm{d}\mu_S(x,\bar{x}) = \mathrm{d}\mu(x,\bar{x}) \prod_j \prod_{i\in I_A} \delta(x^{*a}_{ij}x^a_{ij}-1) \prod_{i\in I_B} \delta(\bar{x}^{*a}_{ij}\bar{x}^a_{ij}-1)\,.$$

This formula is more standard since in general one has $\langle x|F(b,b^\dagger)|x'\rangle = F(x',x^*)e^{x^*x'}$. In our formula (1.19) the exponential is killed by the single particle requirement.

We would like now to derive a supersymmetric path integral representing the partition function. The generalization is straightforward. This time the projector onto single particle subspaces for adjacent sites $V\otimes V^\star$ is

$$\mathcal{P} = (-1)^{|p|}a^{\dagger q}\bar{a}^{\dagger p}|0\rangle\langle 0|\bar{a}^p a^q\,,$$

due to the extra minus-sign in the commutation relations of the fermions $\bar{f}$. We then project as before the transfer matrix

$$\begin{aligned}\tilde{T} &= \mathcal{P}\left((1-p) + p\bar{a}^{\dagger p}a^{\dagger p}a^q\bar{a}^q\right)\mathcal{P} \\ &= a^{\dagger q}\bar{a}^{\dagger p}|0\rangle\left((1-p)\delta_{pr}\delta_{ql}(-1)^{|p|} + p\delta_{pq}\delta_{lr}(-1)^{|p|+|r|}\right)\langle 0|\bar{a}^r a^l\,.\end{aligned}$$

Recall now that fermionic coherent states $|\eta\rangle$ for a fermion f, $\{f, f^\dagger\} = 1$, are defined by demanding $f|\eta\rangle = \eta|\eta\rangle$:

$$|\eta\rangle = e^{-\eta f^\dagger}|0\rangle = (1-\eta f^\dagger)|0\rangle\,; \quad \langle\eta| = \langle 0|e^{\eta^* f} = \langle 0|(1+\eta^* f)\,. \tag{1.22}$$

η and η^* are Grassmann variables anticommuting with $f, f^\dagger$. The resolution of the identity reads

$$\mathbf{1} = \int \mathrm{d}\eta^*\mathrm{d}\eta e^{-\eta^*\eta}|\eta\rangle\langle\eta|\,.$$

Introduce now the ordinary Grassmann variables $\bar{\eta}, \bar{\eta}^*$. Since $\{\bar{f}, \bar{f}^\dagger\} = -1$, we choose to define coherent states $|\bar{\eta}\rangle$ with an extra minus sign, $|\bar{\eta}\rangle = e^{\bar{\eta}\bar{f}^\dagger}|0\rangle$, so that we still have $\bar{f}|\bar{\eta}\rangle = \bar{\eta}|\bar{\eta}\rangle$. However, the identity in the Fock space of $\bar{f}$ is $\mathbf{1} = |0\rangle\langle 0| - \bar{f}^\dagger|0\rangle\langle 0|\bar{f}$ (one can verify that the minus sign is needed to be idempotent), so that the relation

$$\mathbf{1} = \int \mathrm{d}\eta^*\mathrm{d}\eta e^{-\bar{\eta}^*\bar{\eta}}|\bar{\eta}\rangle\langle\bar{\eta}|\,,$$

can only holds if $\langle\bar{\eta}| = \langle 0|e^{\bar{\eta}^*\bar{f}}$. In particular this implies that $\langle\bar{\eta}|\bar{f}^\dagger = -\langle\bar{\eta}|\bar{\eta}^*$.

Putting together bosonic and fermionic coherent states we define the super coherent states as

$$\begin{aligned}|\phi\rangle &= \exp(a^{\dagger p}\phi^p)|0\rangle\,; \quad \langle\phi| = \langle 0|\exp(\phi^{*p}a^p)\,, \\ |\bar{\phi}\rangle &= \exp((-1)^{|p|}\bar{a}^{\dagger p}\bar{\phi}^p)|0\rangle\,; \quad \langle\bar{\phi}| = \langle 0|\exp(\bar{\phi}^{*p}\bar{a}^p)\,.\end{aligned}$$

$\phi, \bar{\phi} \in \mathbb{C}^{N+M|N}$ are supervectors (similarly for $\bar{\phi}$)

$$\phi^p = \begin{cases} x^p & \text{if } |p| = 0 \\ \eta^{p-(N+M)} & \text{if } |p| = 1 \end{cases},$$

and we have the completeness relation

$$\mathbf{1} = \int \mathrm{d}\mu(\phi)\mathrm{d}\mu(\bar{\phi})|\phi, \bar{\phi}\rangle\langle\bar{\phi}, \phi|\,,$$

with

$$\mathrm{d}\mu(\phi) = \prod_{a=1}^{M+N}\frac{\mathrm{d}\Re(x^a)\mathrm{d}\Im(x^a)}{\pi}e^{-x^{*a}x^a}\prod_{b=M+N+1}^{M+2N}\mathrm{d}\eta^{*b}\mathrm{d}\eta^b e^{-\eta^{*b}\eta^b}\,, \tag{1.23}$$

and analogously for $\bar{\phi}$. We express now the operator $\tilde{T}$ in the coherent state basis:

$$\begin{aligned}\langle\phi_{0,1},\bar{\phi}_{1,1}|a^{\dagger q}\bar{a}^{\dagger p}|0\rangle\langle 0|\bar{a}^r a^l|\phi_{0,0},\bar{\phi}_{1,0}\rangle\left((1-p)\delta_{pr}\delta_{ql}(-1)^{|p|}+p\delta_{pq}\delta_{lr}(-1)^{|p|+|r|}\right)\\ =\phi^{*q}_{0,1}\bar{\phi}^{*p}_{1,1}\left((1-p)\delta_{pr}\delta_{ql}+p\delta_{pq}\delta_{lr}(-1)^{|r|}\right)\bar{\phi}^r_{1,0}\phi^l_{0,0}\\ =(1-p)\phi^{*q}_{0,1}\phi^q_{0,0}\bar{\phi}^{*p}_{1,1}\bar{\phi}^p_{1,0}+p\phi^{*q}_{0,1}\bar{\phi}^{*q}_{1,1}\phi^p_{0,0}\bar{\phi}^p_{1,0}\end{aligned} \quad (1.24)$$

We have the same graphical interpretation as in the bosonic case, and loops formed from inserting this decomposition at every vertex will weight M as wanted, thanks to correct ordering of fermions. Indeed let use compute for example the weight of the smallest loop one can have for the case of $M=0, N=1$. With the labeling of figure 1.7 one has to integrate over Gaussian measures (1.23) the following polynomial:

$$\begin{aligned}\phi^{*p}_{0,1}\bar{\phi}^{*p}_{1,1}\phi^{*q}_{0,2}\phi^q_{0,1}\bar{\phi}^{*r}_{1,2}\bar{\phi}^r_{1,1}\phi^s_{0,2}\bar{\phi}^s_{1,2}=\left(x^*_{0,1}\bar{x}^*_{1,1}+\eta^*_{0,1}\bar{\eta}^*_{1,1}\right)\left(x^*_{0,2}x_{0,1}+\eta^*_{0,2}\eta_{0,1}\right)\\ \times\left(\bar{x}^*_{1,2}\bar{x}_{1,1}+\bar{\eta}^*_{1,2}\bar{\eta}_{1,1}\right)\left(x_{0,2}\bar{x}_{1,2}+\eta_{0,2}\bar{\eta}_{1,2}\right),\end{aligned}$$

producing 0 as a result.

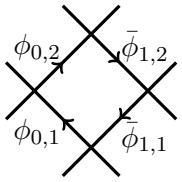

Figure 1.7: Labeling of edge variables.

Finally as in eq. (1.20) we insert coherent states on different links to have ($J\equiv\{0,2,\ldots,2L'-2\}$):

$$T^{L'}=\int \mathrm{d}\mu(\phi,\bar{\phi})\prod_{j\in J}\prod_{i\in I_A}\mathcal{T}^A_{i,j}(\phi,\bar{\phi})\prod_{i\in I_B}\mathcal{T}^B_{i,j}(\phi,\bar{\phi})|(\phi,\bar{\phi})_{2L'}\rangle\langle(\phi,\bar{\phi})_0|\,,$$

where we defined

$$\begin{aligned}\mathcal{T}^A_{i,j}(\phi,\bar{\phi})&:=(1-p_A)\phi^{*q}_{i,j+1}\phi^q_{i,j}\bar{\phi}^{*p}_{i+1,j+1}\bar{\phi}^p_{i+1,j}+p_A\phi^{*q}_{i,j+1}\bar{\phi}^{*q}_{i+1,j+1}\phi^p_{i,j}\bar{\phi}^p_{i+1,j}\\ \mathcal{T}^B_{i,j}(\phi,\bar{\phi})&:=p_B\phi^{*q}_{i+1,j+1}\phi^q_{i+1,j}\bar{\phi}^{*p}_{i,j+1}\bar{\phi}^p_{i,j}+(1-p_B)\phi^{*q}_{i+1,j+1}\bar{\phi}^{*q}_{i,j+1}\phi^p_{i+1,j}\bar{\phi}^p_{i,j}\,,\end{aligned}$$

and

$$\mathrm{d}\mu(\phi,\bar{\phi})=\prod_{j=0}^{2L'}\prod_{i\in I_A}\mathrm{d}\mu(\phi_{i,j})\prod_{i\in I_B}\mathrm{d}\mu(\bar{\phi}_{i,j})\,.$$

Taking the supertrace in eq. (1.16), amounts to evaluate the following expression

$$\begin{aligned}\prod_{i\in I_A}\langle 0|a_i^{p_i}\bar{a}_{i+1}^{p_{i+1}}|\phi_{i,2L'},\bar{\phi}_{i+1,2L'}\rangle\langle\phi_{i,0},\bar{\phi}_{i+1,0}|\bar{a}_{i+1}^{\dagger p_{i+1}}a_i^{\dagger p_i}|0\rangle(-1)^{p_i}\\ =\prod_{i\in I_A}\phi^{p_i}_{i,2L'}\bar{\phi}^{p_{i+1}}_{i+1,2L'}\bar{\phi}^{*p_{i+1}}_{i+1,0}\phi^{*p_i}_{i,0}(-1)^{p_i}=1\,.\end{aligned}$$

We do not have $(-1)^{p_{i+1}}$ in the product because the factor $(-1)^{p_{i+1}}$ from the supertrace is killed by the identical one coming from conjugation of $\bar{a}^\dagger|0\rangle$. Further in the last equality we used periodic boundary conditions in vertical direction together with the single particle constraint. This last indeed gives the real supersphere $S^{2N+2M-1|2N}$

$$\phi^{*p}\phi^p = x^{*a}x^a + \eta^{*\alpha}\eta^\alpha = 1$$
$$\bar{\phi}^{*p}\bar{\phi}^p = \bar{x}^{*a}\bar{x}^a + \bar{\eta}^{*\alpha}\bar{\eta}^\alpha = 1\,.$$

The expression of the partition function of the supersymmetric vertex model will then be

$$Z = \mathrm{Str}\, T^{L'} = \int \mathrm{d}\mu(\phi,\bar{\phi}) \prod_{j\in J}\prod_{i\in I_B} \mathcal{T}^B_{i,j}(\phi,\bar{\phi}) \prod_{i\in I_A} \mathcal{T}^A_{i,j}(\phi,\bar{\phi})\,,$$

with periodic boundary conditions of the fields in the vertical direction. As in the bosonic case, one should implement the supersphere constraint but since only factors of $\phi^*\phi$ appear, this will not change the result of the integral. If we started from the transfer matrix not projected onto single particle subspace and imposed the supersphere constraint only in the end, we would have obtained:

$$\begin{aligned} Z = \mathrm{Str}\, T^{L'} = \int \mathrm{d}\mu_S(\phi,\bar{\phi}) \prod_{j\in J}\prod_{i\in I_A} (1-p_A + p_A \phi^{*p}_{i,j+1}\bar{\phi}^{*p}_{i+1,j+1}\phi^q_{i,j}\bar{\phi}^q_{i+1,j}) e^{\phi^{*p}_{i,j+1}\phi^p_{i,j}} e^{\bar{\phi}^{*q}_{i,j+1}\bar{\phi}^q_{i,j}} \\ \times \prod_{i\in I_B} (p_B + (1-p_B)\phi^{*p}_{i+1,j+2}\bar{\phi}^{*p}_{i,j+2}\phi^q_{i+1,j+1}\bar{\phi}^q_{i,j+1}) e^{\phi^{*p}_{i+1,j+2}\phi^p_{i+1,j+1}} e^{\bar{\phi}^{*q}_{i,j+2}\bar{\phi}^q_{i,j+1}}\,, \end{aligned}$$

where

$$\mathrm{d}\mu_S(\phi,\bar{\phi}) = \mathrm{d}\mu(\phi,\bar{\phi}) \prod_j \prod_{i\in I_A} \delta(\phi^{*p}_{ij}\phi^p_{ij} - 1) \prod_{i\in I_B} \delta(\bar{\phi}^{*q}_{ij}\bar{\phi}^q_{ij} - 1)\,.$$

1.1.3 Algebraic analysis of the spectrum

The diagonalization of Hamiltonians (or transfer matrices) of a model is in general a problem demanding high computational resources since the dimension of the space of states grows exponentially with the system size. This very concrete problem motivates then an algebraic understanding which allows to diagonalize much smaller matrices by restricting to symmetry sectors. In this section we will discuss the algebraic aspects of the Heisenberg spin chain, and how to decompose more generally the spectrum of the loop model introduced above.

Heisenberg chain

At $\beta = 2$ ($q = 1$) the TL generators of eq. (1.9) are simply related to the permutation operator $P_{i,i+1}$, generating the symmetric group $\mathfrak{S}_N$, by

$$P_{i,i+1} = \begin{pmatrix} 1 & 0 & 0 & 0 \\ 0 & 0 & 1 & 0 \\ 0 & 1 & 0 & 0 \\ 0 & 0 & 0 & 1 \end{pmatrix} = \mathbf{1}_4 - E_i\,.$$

$TL_N^{\beta=2}$ is isomorphic to the projection of the group algebra of $\mathfrak{S}_N$ onto representations occurring in $\mathcal{H} = (\mathbb{C}^2)^N$. Recall that irreducible representations of $\mathfrak{S}_N$ (so-called Specht modules) are indexed by Young diagrams with N boxes [175]. Those occurring in the Heisenberg spin chain have at most two rows[5]. We label these Specht modules by the difference in length between the two rows $2j = 0, 2, \ldots, N$ (recall $N = 2L$), and call them S_j. S_j has basis given by standard tableaux (Young diagrams whose boxes are labeled with numbers $1, \ldots, N$ increasing to the right and to the bottom) and its dimension is readily computed using the hook-length formula [175]:

$$d_j = \binom{N}{N/2+j} - \binom{N}{N/2+j+1}. \tag{1.25}$$

Then we have the following decomposition of $\mathcal{H}$ onto irreducibles of TL_N^2:

$$\mathcal{H}|_{TL_N^2} = \bigoplus_{j=0}^{N/2} D_j S^j .$$

The multiplicities D_j's correspond to the number of states in the spin chain for each given standard tableau in S_j, $D_j = 2j+1$. Let us now look at the action of $\mathfrak{sl}(2)$ on the chain. This action commutes with permutation of sites, and irreducible representations ρ_j of dimension D_j are labeled by the same Young diagrams as before, where now j has the interpretation of spin sector. Then we have the decomposition onto irreducibles of $\mathfrak{sl}(2)$:

$$\mathcal{H}|_{\mathfrak{sl}(2)} = \bigoplus_{j=0}^{N/2} d_j \rho_j .$$

The multiplicity of spin j in the chain is known from standard Clebsh-Gordan formula and equals eq. (1.25). We have finally that the Hilbert space has a multiplicity-free decomposition as a $(TL_N^2, \mathfrak{sl}(2))$-bimodule:

$$\mathcal{H}|_{TL_N^2 \otimes \mathfrak{sl}(2)} = \bigoplus_{j=0}^{N/2} S_j \otimes \rho_j . \tag{1.26}$$

The Hamiltonian algebra, the TL algebra, acts on the first factor, while symmetries, $\mathfrak{sl}(2)$, act on the second one. This decomposition is well-known and is implied by the Schur-Weyl duality for $\mathfrak{sl}(2)$. This is a manifestation of the *double-commutant theorem* which we now state.

Consider the semisimple (or fully reducible as direct sum of irreducibles) action of the algebra A on V, with $\dim(V)$ finite. Let $B = Z(A)$ be the commutant algebra (centralizer) of A in V (the algebra of linear transformations of V commuting with A). The theorem states that

[5]For example, when $N = 3$ one cannot have the fully antisymmetric representation (associated to a Young diagram with a single column and three rows) using $e_a \otimes e_b \otimes e_c$, with e_a, e_b, e_c being basis of $\mathbb{C}^2$, so that $a, b, c = 1, 2$.

i. B acts also semisimply on V

ii. $Z(B) = A$ (double commutant property)

iii. V has the multiplicity-free decomposition

$$V = \bigoplus_j R_j^A \otimes R_j^B \,,$$

where j indices the (isomorphism classes of) irreducible representations R_j^A, R_j^B of A and B, which are in one-to-one correspondence.

If the dimension of R_j^A, R_j^B are respectively N_j, M_j, then clearly $\dim(V) = \sum_j N_j M_j$, and $\dim(A) = \sum_j N_j^2$, $\dim(B) = \sum_j M_j^2$, since A and B act on V as matrix algebras with blocks of dimension N_j and M_j. In a typical example of physical application of this theorem, A is the algebra of symmetries and B is that of Hamiltonians, as seen above and as will be discussed in section 3.1.6. This result can be expressed pictorially as in figure 1.8. The power of the theorem is that knowing the representations of an algebra, automatically determines representations of the dual one.

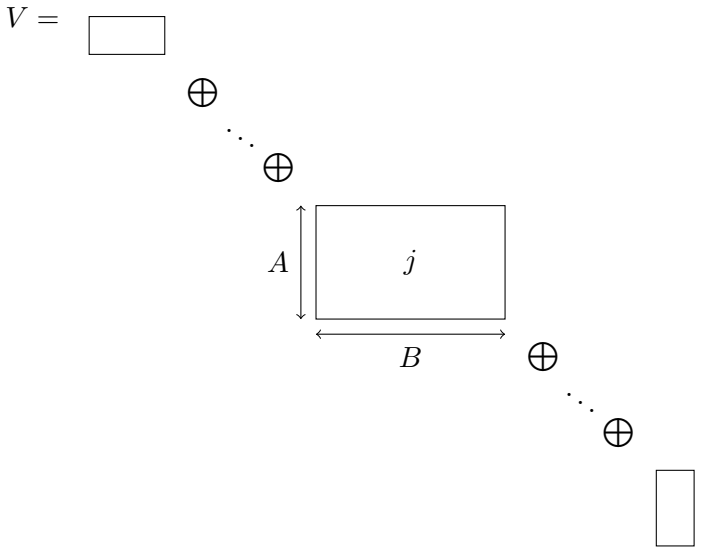

Figure 1.8: Decomposition of the space V under the semisimple action of the doubly commuting algebras A (symmetries) and B (Hamiltonians), acting on irreducible rectangular blocks j, vertically and horizontally respectively. To have commutativity, the action of A has to be the same on each column of the block, while that of B on each row.

We remark that for the Heisenberg chain we have

$$\dim(\mathcal{H}) = \sum_{j=0}^{N/2} d_j D_j = 2^N$$

$$\dim\left(TL_N^2\right) = \sum_{j=0}^{N/2} d_j^2 = \frac{1}{N+1}\binom{2N}{N}$$

$$\dim\left(\mathrm{U}(\mathfrak{sl}(2))^{(N)}\right) = \sum_{j=0}^{N/2} D_j^2 = \frac{(N+1)(N+2)(N+3)}{6}\ ,$$

which are respectively the (expected) dimension of the Hilbert space, the dimension of the TL algebra, the N-th Catalan Number, and the dimension of the commutant algebra $\mathrm{U}(\mathfrak{sl}(2))^{(N)}$, which is the image of the representation of $\mathfrak{sl}(2)$, or better, of its universal enveloping algebra $\mathrm{U}(\mathfrak{sl}(2))$, in $\mathcal{H}$ (usually called Schur algebra).

In the next section we will see how these ideas apply to the other models of interest.

Representations of TL at generic q

The considerations above apply directly to the TL model with $\beta = q + q^{-1}$ for $q = e^{i\pi/(p+1)}, p \notin \mathbb{Z}_{\geq 1}$ (generic case). This condition rules out the cases which are most interesting physically, but however conclusions about these cases can be still drawn by taking limits of generic formulas, as we will discuss later. Further, what happens at roots of unity will be discussed briefly in the next section.

The XXZ Hamiltonian (1.10) commutes with the generators of a quantum deformation of $\mathfrak{sl}(2)$, the quantum group $\mathrm{U}_q(\mathfrak{sl}(2))$ [6] [157], and this symmetry reduces to $\mathfrak{sl}(2)$ when $q = 1$ (Heisenberg chain). $\mathrm{U}_q(\mathfrak{sl}(2))$ (or more precisely the image of its representation on the chain) is the commutant of TL in $\mathcal{H}$. The problem of studying the representations of TL is equivalent to study those of the quantum group. The important point is that as long as q is not a root of unity its irreducible representations are one to one with those of ordinary $\mathfrak{sl}(2)$, and labeled by the spin j. For example $\mathbb{C}^4$ is decomposed onto ρ_0 the singlet $q^{-1/2}|\uparrow\downarrow\rangle - q^{1/2}|\downarrow\uparrow\rangle$ and the triplet ρ_1, spanned by $|\uparrow\uparrow\rangle$, $q^{1/2}|\uparrow\downarrow\rangle + q^{-1/2}|\downarrow\uparrow\rangle$, $|\downarrow\downarrow\rangle$. TL generators (1.8) are projectors onto the singlet as can be readily verified. Let us now describe the corresponding irreducible TL representations S_j. We use a "valence bond" basis where each basis state of the module indexed by j corresponds to a link state, with $(N-2j)/2$ arcs and $2j$ non-contractible lines, like the one in figure 1.9(a).

[6] The algebra $\mathrm{U}_q(\mathfrak{sl}(2))$ is generated by $q^{2S^Z}, q^{-2S^Z}, S^+, S^-$ subject to the relations [124]:

$$q^{2S^3} S^+ q^{-2S^3} = q^2 S^+\ , \quad q^{2S^3} S^- q^{-2S^3} = q^{-2} S^-$$

$$[S^+, S^-] = \frac{q^{2S^3} - q^{-2S^3}}{q - q^{-1}}\ .$$

In the classical limit $q \to 1$ we get the commutation relations of $\mathfrak{sl}(2)$ $[S^3, S^\pm] = \pm S^\pm, [S^+, S^-] = 2S^3$.

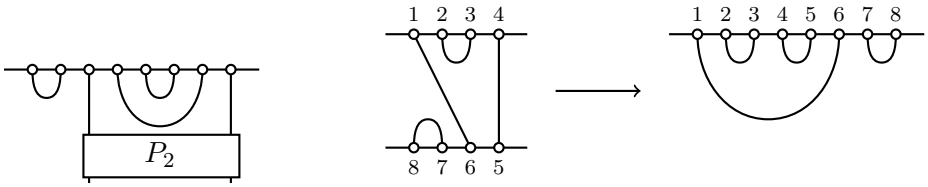

(a) (b)

Figure 1.9: (a) A link state with $2j = 2$ non-contractible lines for a chain of length $N = 8$. The through lines are projected by the operator P_2 to be non-contractible. (b) Unfolding a diagram to a link pattern.

The states in the chain corresponding to such diagrams are given by contracting the sites associated to arcs to form a singlet. Two states associated to two non-contractible lines are chosen such that application of the projector onto the singlet E_i gives zero. This is enforced by the projector P_2 in figure 1.9(a), as explained below. At $q = 1$ basis states with $2j$ non-contractible lines map to the Specht modules of the symmetric group introduced above. Then a decomposition like eq. (1.26) holds also in the generic case replacing $\mathfrak{sl}(2)$ by $\mathrm{U}_q(\mathfrak{sl}(2))$. In particular the dimensions d_j and D_j of the algebras are the same as in the $q = 1$ case. That the dimension of TL is the Catalan number for every value of q is actually obvious if one thinks about the diagram representation of the algebra and unfold each diagram to produce a link pattern[7], as in figure 1.9(b)

The operators projecting onto a sector with a given number of non-contractible lines (sites) are called Jones-Wenzl projectors P_k. P_{2j} is an element of the TL algebra projecting onto the j-th sector with spin j ($2j$ non-contractible lines), satisfying $P_k^2 = P_k$ and $E_i P_k = P_k E_i = 0$ for every $i < k$. The solution for such a P_k can be easily found recursively[142]:

$$P_{k+1} = P_k - \frac{[k]_q}{[k+1]_q} P_k E_k P_k \,,$$

[7]Counting link patterns is a well known combinatorial problem. Denote C_n the number of link patterns with n arcs ($C_0 = 1$). Given a configuration with $n > 0$, remove the rightmost arc. Then we are left with two smaller link patterns, leading to the following convolutional formula for C_n:

$$C_n = \sum_{n_1=0}^{n-1} C_{n_1} C_{n-1-n_1} \,.$$

Introducing the generating function $C(z) = \sum_{n\geq 0} C_n z^n$, the above relation implies $C(z) = 1 + zC(z)^2$, whose solution is

$$C(z) = \frac{1 - \sqrt{1-4z}}{2z} \,.$$

The coefficient C_n are thus:

$$C_n = \oint \frac{\mathrm{d}z}{2\pi i} z^{-n-1} C(z) = \frac{1}{n+1}\binom{2n}{n} \,.$$

with $P_1 = 1$ and where the quantum integers $[n]_q$ are $[n]_q = q^{n-1} + q^{n-3} + \cdots + q^{-(n-1)} = (q^n - q^{-n})/(q - q^{-1})$. For example one finds for the projector onto spin 1:

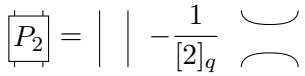

Note $[2]_q = q + q^{-1} = \beta$. Clearly the results above apply also to the $\mathfrak{gl}(M)$ and $\mathfrak{gl}(N + M|N)$ spin chains of section 1.1.2 when $M = q + q^{-1} \geq 2$, so that q is real. What changes however is the commutant of TL for these chains, so the multiplicities D_j in the decomposition of the spectrum. This commutant has been constructed in details in [172]. The value of D_j can be understood by a simple argument. Clearly $D_0 = 1$ and also $D_1 = M^2 - 1$, the dimension of the adjoint. Then we have the recursion relation

$$D_1 D_j = D_{j+1} + D_j + D_{j-1}\,,$$

which can be interpreted graphically as the fusion of 2 plus $2j$ non contractible lines on the left hand side to give either $2(j+1)$ non contracted lines, or $2j$ non contracted and 1 contracted, or $2(j-1)$ non contracted and 2 contracted. The solution of this recurrence relation with initial conditions D_0 and D_1 is

$$D_j = [2j+1]_q\,. \tag{1.27}$$

The results obtained so far allow to write down the decomposition of the $2L \times 2L'$ annulus partition function of the Potts model with $\beta = q + q^{-1}$ generic for the six-vertex/XXZ representation:

$$Z = \mathrm{Tr}_{\mathcal{H}}\, T^{L'} = \sum_{j=0}^{L} D_j\, \mathrm{Tr}_{S_j}\, T^{L'}\,. \tag{1.28}$$

For the XXZ chain $D_j = 2j + 1$ corresponds to weight non-contractible loops as $\delta = 2$. Indeed, to give a different weight $\delta = t + t^{-1} = [2]_t$ to non-contractible loops winding around the annulus, one introduces t^{2S^Z} into the trace, resulting in a different multiplicity $D_j = [2j+1]_t$ [170], consistent with the expression given for the $\mathfrak{gl}(N + M|N)$ spin chains. We have then expressed the Markov trace of the TL algebra introduced in eq. (1.7) for computing the partition function in the loop representation as a sum over the various sectors with fixed number of non-contractible lines. By continuity of the partition function of loop models with respect to the loop weight, this formula should be valid also at roots of unity. In this case, when both contractible and not-contractible loops are weighted the same, Z is trivial for dense polymers ($Z = 0$) and percolation ($Z = 1$), in the latter case after trivial rescaling of Z.

Scalar products and unitarity

We now introduce natural scalar products in the space of states of the TL models, and comment about unitarity. Consider first the XXZ chain. It is natural to define

a scalar product as in the $\mathfrak{sl}(2)$ case, treating the variable q as a formal parameter (i. e. no complex conjugation). For example, the norm associated to the $\mathrm{U}_q(\mathfrak{sl}(2))$ singlet $q^{-1/2}|\uparrow\downarrow\rangle - q^{1/2}|\downarrow\uparrow\rangle$, is $q+q^{-1}$. More generally, for some values of q, there are states in the representation spaces which have negative or zero norm (e. g. $q=i$ in the formula above). One can show that this does not happen for q real ($\beta \geq 2$), so that the irreducible modules introduced before are unitary in the case of $\mathfrak{gl}(M)$ spin chains. Otherwise, for $\beta < 2$, the scalar product is not positive-definite, spoiling unitarity of the representations [157]. Further, when q is a complex number of modulus one, the Hamiltonian of the XXZ chain eq. (1.10), is not Hermitian (however its eigenvalues are real).

The diagrammatic representations of TL can be also endowed with a scalar product. If $|s\rangle$ is a link state, we define its dual $\langle s|$ by turning it upside down and the bilinear form $\langle s_1|s_2\rangle$, which we call loop scalar product, by associating to the link states the diagram obtained by gluing $|s_2\rangle$ with $\langle s_1|$. The result is given by β^n, with n the number of loops thus formed, and we get zero if we contract two strings, as natural for our choice of basis. For instance we have

(1.29)

One comes to the same conclusion as for the XXZ chain, that the loop scalar product is not positive-definite, so that representations are not unitary.

We recall also that negative norm states appear in the super spin chains to ensure cancellations of closed loops, see eq. (1.15). The final moral is that non-unitarity of the theory is deeply related to the geometrical nature of problems (like polymers, percolation) we want to describe.

We will see below how these remarks are directly translated to the conformal field theories describing the continuum limit of these lattice models.

A look at indecomposability

To understand what happens in the more complicated case when q is a root of unity, it is instructive to proceed by examples, and here we will discuss the case of dense polymers $\beta = 0$. Specifically we consider the simplest case of the $\mathfrak{gl}(1|1)$ spin chain following [176].

We use the following convenient basis of $\mathfrak{gl}(1|1)$ w.r.t our notation of section 1.1.2: $E = 1/2(J^{11} + J^{22})$, $N = 1/2(J^{11} - J^{22})$, $F^+ = J^{12}$, $F^- = J^{21}$. E is central, and the other defining relations are

$$[N, F^{\pm}] = \pm F^{\pm}, \quad \{F^-, F^+\} = E\,.$$

In particular N counts the number of fermions. The choice of the Lie superalgebra $\mathfrak{gl}(1|1)$ is motivated by the fact that its representation theory is rather simple [99]. When dealing with the irreducible representations of superalgebras, we have to distinguish between typical or atypical representations. For $\mathfrak{gl}(1|1)$ typical representations are the

two-dimensional representations $\langle e, n\rangle$, $e \neq 0$, $n \in \mathbb{R}$, which read in matrix notation:

$$N = \begin{pmatrix} n-1 & 0 \\ 0 & n \end{pmatrix} \quad F^- = \begin{pmatrix} 0 & 1 \\ 0 & 0 \end{pmatrix} \quad F^+ = \begin{pmatrix} 0 & 0 \\ e & 0 \end{pmatrix} \quad E = \begin{pmatrix} e & 0 \\ 0 & e \end{pmatrix}.$$

The state annihilated by F^- is a boson. Atypical representations are the one-dimensional irreducible representations $\langle n\rangle$, which have $F^+ = F^- = E = 0, N = n$. This exhausts all irreducibles (up to isomorphism).

We are in a position to introduce the most important concept distinguishing the cases of roots of unity: *indecomposability*. Consider what happens for $\langle 0, n\rangle$: the vector $|0\rangle = (1,0)^T$ generates a one-dimensional invariant subspace, but there is not an invariant complement of the representation. Indeed $|1\rangle = (0,1)^T$ cannot be decoupled from the representation since $F^-|1\rangle = |0\rangle$. $\langle n, 0\rangle$ is indecomposable but not irreducible. To visualize this structure we write it in terms of the linking of its atypical constituents: $\langle n\rangle \to \langle n-1\rangle$, where the arrow represents the action of the algebra. Note that the largest proper submodule (radical) $\langle n-1\rangle$ is irreducible, and the quotient by this submodule, $\langle n\rangle$, is irreducible too.

Let us now look at the $\mathfrak{gl}(1|1)$ spin chain. It is built by alternating the fundamental $V = \langle 1, 1/2\rangle$ and the dual $V^\star = \langle -1, -1/2\rangle$. The TL generators can be written as quadratic in the fermions[8]:

$$E_i = (F_i^- + F_{i+1}^-)(F_i^+ + F_{1+1}^+)\,. \tag{1.30}$$

If we try to define a scalar product where F^+ is the conjugate of F^- we see that the scalar product is not positive-definite, since in $V^\star$, $\{F^+, F^-\} = -1$. Further, if we take the natural basis $|0,0\rangle, |1,0\rangle, |0,1\rangle, |1,1\rangle$ in $V \otimes V^\star$, then

$$\begin{aligned} E_0(|0,1\rangle - |1,0\rangle) &= 0 \\ E_0(|0,1\rangle + |1,0\rangle) &= 2(|0,1\rangle - |1,0\rangle)\,, \end{aligned}$$

so that E_0 (the Hamiltonian) is not diagonalizable in the tensor product, it can only be brought to a Jordan form in this two-dimensional subspace:

$$\begin{pmatrix} 0 & 1 \\ 0 & 0 \end{pmatrix}.$$

Note that $\mathcal{P}_1 := V \otimes V^\star$ is an indecomposable corresponding to the adjoint of $\mathfrak{gl}(1|1)$ [9]. Indeed using the usual coproduct formula (with graded tensor product) $J^{ab} = J_0^{ab} \otimes \mathbf{1} \oplus$

[8] The free fermionic character of the theory of dense polymers, or spanning trees, can be understood more directly from the matrix-tree theorem. See [116] for a discussion of that in the context of CFT, and [40] for the generalization to an interacting fermionic theory describing spanning forests.

[9] More generally the spin chain decomposes as [99]

$$(V \otimes V^\star)^{\otimes l} \simeq \bigoplus_{i=1-l}^{l-1} \binom{2l-2}{l-1+i} \mathcal{P}_i\,.$$

where $\mathcal{P}_n$ is an indecomposable four-dimensional representation playing the role of the projective cover of $\langle n\rangle$, that is it can never appear as a subrepresentation of a larger indecomposable and contains $\langle n\rangle$.

$\mathbf{1} \otimes J_1^{ab}$, the action of the generators in $\mathcal{P}_1$ is:

$$E = 0\,, \quad N = \begin{pmatrix} -1 & 0 & 0 & 0 \\ 0 & 0 & 0 & 0 \\ 0 & 0 & 0 & 0 \\ 0 & 0 & 0 & 1 \end{pmatrix}\,, \quad F^+ = \begin{pmatrix} 0 & 0 & 0 & 0 \\ -1 & 0 & 0 & 0 \\ 1 & 0 & 0 & 0 \\ 0 & 1 & 1 & 0 \end{pmatrix}\,, \quad F^- = \begin{pmatrix} 0 & 1 & 1 & 0 \\ 0 & 0 & 0 & 1 \\ 0 & 0 & 0 & -1 \\ 0 & 0 & 0 & 0 \end{pmatrix}$$

From the expression of N, we read that $\mathcal{P}_1$ is made up of atypical irreducibles $\langle 1\rangle$,$2\langle 0\rangle$,$\langle -1\rangle$, corresponding to the subspaces $|1,1\rangle$, $|0,1\rangle \pm |1,0\rangle$, $|0,0\rangle$, and has the following diamond structure:

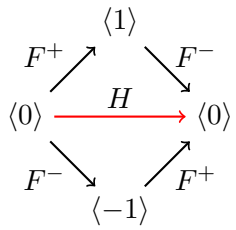

The arrows stand for the action of the elements of the algebra, and the red one corresponds to the action of the Hamiltonian $H = -E_0$, which can be also written as $H = -2C$, where C is the quadratic Casimir[10] of $\mathfrak{gl}(1|1)$ $C = (2N-1)E + 2F^-F^+$, as can be readily verified using the expression of generators above.

Note that we could have discussed the case of the XX chain ($q = i$) instead of the $\mathfrak{gl}(1|1)$ one, which after a Jordan-Wigner transformation is equivalent to (1.30). More generally, at roots of unity semisimplicity is lost and the TL algebra exhibits features similar to those discussed above. For example (for sufficiently large sizes) the tensor product of 1/2 representations does not decompose into irreducibles of TL and $\mathrm{U}_q(\mathfrak{sl}(2))$ no more, although it can still be written as a direct sum (of so-called tilting modules). The general theory is quite intricate and we refer to [171] for a discussion of these features.

There are however interesting quantities which do not need a detailed study of the algebraic structure to be computed. For example, as we have already remarked the annulus partition function of (1.28) being a trace of the transfer matrix does not see the Jordan cell structure at roots of unity. We will discuss this point further when studying rectangular amplitudes in chapter 2.

1.1.4 From spin chains to non linear sigma models

In this section we will derive the low energy effective field theories describing the vertex models introduced above. We will first illustrate the general procedure in the familiar case of the Heisenberg spin chain leading to the O(3) non-linear sigma model, and then generalize to the $\mathfrak{gl}(N+M|N)$ spin chains of interest for the Potts model.

[10] The quadratic Casimir is obviously defined up to any function of the central element E.

Spin coherent states

We have discussed in section 1.1.2 the path integral formulation of $\mathfrak{gl}(N+M|N)$ vertex models in terms of oscillator coherent states. It is useful to introduce a different basis of coherent states, which we will call spin coherent states. Our exposition follows [83], for the general theory of coherent states see [159].

Consider a single quantum mechanical spin and denote the highest weight of the $(2s+1)$-dimensional spin s representation $|0\rangle$: $S^+|0\rangle = 0, S^3|0\rangle = s|0\rangle$. The coherent state basis is defined by rotating $|0\rangle$ with the SU(2) matrix:

$$|\vec{n}\rangle = e^{i\theta(\vec{n}_0\times\vec{n})\cdot\vec{S}}|0\rangle\,.$$

Here $\vec{n}$ is a three-dimensional vector of unit length and $\vec{n}_0\cdot\vec{n} = \cos(\theta)$. If we choose $\vec{n}_0 = \hat{z} = (0,0,1)$ only S^1 and S^2 act on $|0\rangle$, so that coherent states are in one-to-one correspondence not with the whole group SU(2), but with its right coset SU(2)/U(1), where U(1) is the phase generated by the diagonal generator S^3. More generally coherent states differing by multiplications by rotations around the z-axis will differ by a phase, which in quantum mechanics is not observable, and are identified. Coherent states are (over-)complete:

$$\mathbf{1} = \int \mathrm{d}\mu_S(\vec{n})|\vec{n}\rangle\langle\vec{n}|\,,$$

where $\mathrm{d}\mu_S(\vec{n}) = (2s+1)/(4\pi)\mathrm{d}^3\vec{n}\delta(\vec{n}^2-1)$. We use now the Trotter formula to represent the partition function of the spin as:

$$Z = \mathrm{Tr}\, e^{-\beta H} = \lim_{N\to\infty}\lim_{\delta t\to 0}(e^{-\delta t H})^N\,,$$

and introduce resolutions of identity at every intermediate time step. From the definition of coherent states we have [83]:

$$\begin{aligned}\langle\vec{n}(t_j)|\vec{n}(t_{j+1})\rangle &= e^{is\Omega(\vec{n}(t_j),\vec{n}(t_{j+1}),\vec{n}_0)}\left(\frac{1+\vec{n}(t_j)\cdot\vec{n}(t_{j+1})}{2}\right)^s\\ \langle\vec{n}(t)|\vec{S}|\vec{n}(t)\rangle &= s\vec{n}(t)\,.\end{aligned}$$

$\Omega(\vec{n}(t_j),\vec{n}(t_{j+1}),\vec{n}_0)$ is the area associated to a spherical triangle with vertices in the three points. The term $e^{is\Omega}$ is usually referred to as Berry phase (see e. g. [10]). Then the resulting Euclidean path integral has action:

$$\mathcal{S} = -is\sum_j \Omega(\vec{n}(t_j),\vec{n}(t_{j+1}),\vec{n}_0) - s\log\left(\frac{1+\vec{n}(t_j)\cdot\vec{n}(t_{j+1})}{2}\right) + sH(\vec{n}(t_j))\,,$$

where $H(\vec{n})$ is obtained by replacing every occurrence of $\vec{S}$ with $\vec{n}$ in the Hamiltonian H. Note that the first term is complex (even thought we work in imaginary time), and in the limit of continuous time gives $\Omega(\vec{n})$, the total area of the cap on the sphere S^2 whose boundary is the trajectory $\vec{n}(t)$, see figure 1.10. Note that the ambiguity of

taking the upper or lower cap does not manifest itself since the difference of the two is the solid angle 4π, weighting $e^{4\pi i s} = 1$ in the partition function, thanks to quantization of the spin. The second term in the action becomes : $\sim m/2 \int_0^\beta \mathrm{d}t (\partial_t \vec{n})^2$, with the mass $m = s\delta t/2$ tending to zero.

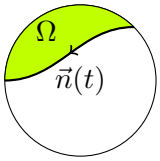

Figure 1.10: The area Ω enclosed by the trajectory $\vec{n}(t)$ on the sphere.

Consider now a spin chain of length L, $(\mathbb{C}^2)^{\otimes L}$, with antiferromagnetic Heisenberg coupling $J > 0$, see eq. (1.11):

$$H = J \sum_i \vec{S}_i \cdot \vec{S}_{i+1} \,,$$

and assume periodic boundary conditions. Introducing spin coherent states for each site, we find the action of the associated path integral to be:

$$\mathcal{S} = -is \sum_i \Omega(\vec{n}_i) + \frac{m}{2} \int_0^\beta \mathrm{d}t \sum_i (\partial_t \vec{n}_i)^2 + s^2 J \int_0^\beta \mathrm{d}t \sum_i \vec{n}_i(t) \cdot \vec{n}_{i+1}(t) \,. \tag{1.31}$$

Semiclassical approximation

The action (1.31) is dominated by the stationary points as $s \to \infty$ [11]. In this section we will derive the effective field theory in that limit, which was originally derived by Haldane [106]. Our arguments will be mostly heuristic, while one can obtain the same final result in a more controlled way by decomposing the field $\vec{n}$ into a soft mode becoming the sigma model field, and a hard mode which is integrated out [3, 83].

We first note that the large spin expansion is a perturbation around the classical solution [3, 106]. Indeed the commutator of quantum spins $[S^a, S^b] = i\epsilon^{abc} S^c$ is of order s, much smaller than the square of spin variables, of order s^2, so the commutator vanishes as $s \to \infty$ and the spins behave classically. This is an intuitive argument which can be made rigorous by expressing spins in terms of bosons and performing a $1/s$ expansion [3]. The ground state of the classical antiferromagnet is the Néel state with alternating up and down classical spins on neighboring sites, $S_i = (-1)^i \hat{z}$. Then, since we expect antiferromagnetic order in the large-s limit, we redefine the fields as:

$$\vec{n}_i \to (-1)^i \vec{n}_i \,,$$

[11] The method is applicable since Js stays finite as $s \to \infty$.

producing a staggering in the Berry phase term[12]:

$$\mathcal{S} = -is\sum_i (-1)^i \Omega(\vec{n}_i) + \frac{m}{2}\int_0^\beta \mathrm{d}t \sum_i (\partial_t \vec{n}_i)^2 + \frac{s^2 J}{2}\int_0^\beta \mathrm{d}t \sum_i (\vec{n}_i(t) - \vec{n}_{i+1}(t))^2 \,.$$

We want now to write an effective theory in the long wavelength, low energy limit. The second and third terms of the action give after appropriate rescaling of spacetime coordinates, the O(3) (or rather the O(3)/O(2)) non-linear sigma model action:

$$\mathcal{S}_0 = \frac{1}{2g_\sigma^2}\int \mathrm{d}^2x (\partial_\mu \vec{n})^2 \,,$$

with sigma model coupling

$$g_\sigma^2 = \frac{2}{s} \,.$$

Further, note that in the limit of large number of spins, the area difference can be approximated as:

$$\Omega(\vec{n}_{i+1}) - \Omega(\vec{n}_i) \simeq \int_0^\beta \mathrm{d}t \vec{n}_i \cdot ((\vec{n}_{i+1} - \vec{n}_i) \times \partial_t \vec{n}_i) \,,$$

since the width of the ribbon $|\vec{n}_{i+1} - \vec{n}_i|$ is supposed to be small (here is where we use the antiferromagnetic character of the large-s expansion), and recall that $|\vec{n}| = 1$. Performing the sum over sites yields the topological θ-term:

$$S_{\mathrm{top}} = \frac{i\theta}{8\pi}\int \mathrm{d}^2x \epsilon_{\mu\nu} \vec{n} \cdot (\partial_\mu \vec{n} \times \partial_\nu \vec{n}) \,,$$

where $\epsilon_{\mu\nu}$ is the Levi-Civita symbol, μ, ν are indices of worldsheet coordinates, and the θ angle is

$$\theta = 2\pi s \,. \tag{1.32}$$

Requiring finiteness of the action is equivalent to demand that at infinity $\vec{n}$ takes constant values in all directions in the plane:

$$\lim_{|\vec{x}|\to\infty} \vec{n}(\vec{x}) = \vec{n}_0 \,.$$

Thus topologically the worldsheet is compactified to a sphere and field configurations are maps from S^2 to S^2, thus falling into homotopy classes, indexed by integer values since $\pi_2(S^2) = \mathbb{Z}$. The topological character of S_{top} comes from the fact that

$$\mathcal{Q} = \frac{1}{8\pi}\int \mathrm{d}^2x \epsilon_{\mu\nu} \vec{n} \cdot (\partial_\mu \vec{n} \times \partial_\nu \vec{n}) \,,$$

[12]The transformation $\vec{n}_i \to (-1)^i \vec{n}_i$ changes the sign of the exchange term to a ferromagnetic one, and it is the Berry phase term which distinguishes ferromagnets from antiferromagnets. In the ferromagnetic case, the low energy field theory is not a sigma model, having quadratic dispersion relation [3].

counts the number of times $\vec{n}(t)$ wraps around the target space S^2 (it is called winding number or Pontryagin index of the field configuration $\vec{n}(\vec{x})$). Configurations with a given topological charge $\mathcal{Q}$ are called instantons. Clearly the physics will depend on θ (mod 2π) [13], thus the name of θ-angle. The topological action $S_{\rm top}$ has zero variation (it can be written as a total derivative, see below), so it does not enter the equations of motion. It does have however an important non-perturbative effect.

Recall first that if $\theta = 0$, the O(3) sigma model is massive and exhibits asymptotic freedom in g. In particular, since we are in 1+1D, massless particles cannot be produced from spontaneous breaking of the continuous O(3) symmetry (Mermin-Wagner theorem), and the particles acquire a mass under renormalization, due to infrared fluctuations. Instead masslessness emerges at $\theta = \pi$, as proved in [184]. The $\theta = \pi$ sigma model corresponds to the RG flow between the unstable fixed point at $g_\sigma = 0$, described by two free bosons[14] with central charge $c = 2$, and the non-trivial fixed point at strong coupling (g_c of order unity) with enhanced symmetry and described by the $SU(2)_1$ WZW model with $c = 1$. The proposed phase diagram is represented in figure 1.11. For further details see the discussion in [3].

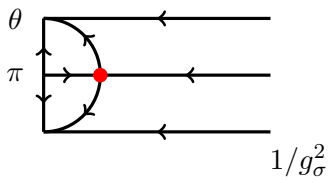

Figure 1.11: Phase diagram of the O(3) sigma model. The fixed point is governed by the $SU(2)_1$ WZW model. The diagram repeats itself in the θ-direction.

Masslessness of the $\theta = \pi$ sigma model was first proposed by Haldane [106], by assuming validity of the large-s mapping of the spin chain to the sigma model also for $s = 1/2$, in which case the microscopic theory can be solved exactly by Bethe Ansatz, and is massless. An important outcome of the analysis in [106] was the conjecture from the identification (1.32) that spin chains with s integer are gapped, while those with s half integer, are gapless. We note also that introducing a staggering in the spin chain, $\epsilon \neq 1$ in (1.5), is a relevant perturbation, changing the value as $\theta = 2\pi s + O(\epsilon - 1)$ [1].

It is finally useful to represent the O(3) sigma model using the spinor representation $\vec{n} = z^\dagger \vec{\sigma} z$, where $\vec{\sigma}$ are Pauli matrices and $z \in \mathbb{CP}^1$, that is, z_a is two-component complex vector satisfying $z^\dagger z = 1$ modulo U(1) phase transformations. Introducing also the non-dynamical Abelian gauge field

$$a_\mu = \frac{i}{2}\left(z_a^\dagger \partial_\mu z_a - (\partial_\mu z_a^\dagger) z_a\right) ,$$

allows to write explicitly the topological term as a total derivative. Then the Lagrangian

[13] Things change for a worldsheet with boundary, see chapter 4.

[14] Note that by rescaling the fields we can set $g_\sigma^2 = 1$ and working with non-trivial radius of the sphere $\vec{n}^2 = \rho^2$, $\rho = 1/g_\sigma$.

of the $\mathbb{CP}^1$ sigma model with topological θ-term is:

$$\mathcal{L} = \frac{1}{2g_\sigma^2}\Big((\partial_\mu - ia_\mu)z_a^\dagger(\partial_\mu + ia_\mu)z_a\Big) + \frac{i\theta}{2\pi}\epsilon_{\mu\nu}\partial_\mu a_\nu \,.$$

$\mathbb{CP}^{N+M-1|N}$ sigma models

The above mapping of the Heisenberg chain to the O(3) sigma model can be generalized [1] to other antiferromagnetic spin chains, that is, spin chains built by alternating an highest weight representation and its dual representation, with coupling favoring the singlet states. Spin coherent states associated to a given highest weight state can be constructed [169], and the associated field of the path integral, being the expectation value of the "spins" (generators of the group) in the coherent state basis, will now be an element of the manifold swept out by acting with all group elements on the highest weight. The resulting target space where the sigma models field Q lives, is then the symmetry group of the spin chain modulo the isotropy subgroup fixing the highest weight state $|\mathrm{hw}\rangle$, $Q = g|\mathrm{hw}\rangle\langle\mathrm{hw}|g^{-1}$. We have seen that for a representation of SU(2) of arbitrary spin this was $\mathrm{SU}(2)/\mathrm{U}(1) \simeq \mathbb{CP}^1$. In the case of U($N$), the elements fixing the highest weight state are products of factors U(m_i) for each m_i rows of the Young tableau with the same (possibly zero) length [1,169]. Considering a representation whose Young tableau is made of a single row of length n_c, the target space will be $\mathrm{U}(N)/\mathrm{U}(1)\times\mathrm{U}(N-1) \simeq \mathbb{CP}^{N-1}$. This consideration directly applies to the $\mathfrak{gl}(M)$ spin chains of section 1.1.2, and the mapping to the sigma model can be rederived [1,169], this time the semi-classical limit being associated to large representation n_c. Analogous discussions can be done for the supersymmetric case [170,203]. The target space of the sigma model for the $\mathfrak{gl}(N+M|N)$ spin chains is then found to be the complex projective superspace $\mathbb{CP}^{N+M-1|N}$.

We now define the sigma model on $\mathbb{CP}^{N+M-1|N}$, which is a direct generalization of that on $\mathbb{CP}^1$ discussed above. We first begin with superspace $\mathbb{C}^{N+M|N}$; the $N+M$ complex bosonic coordinates are denoted by z_a and we use ξ_a for the N fermionic directions. Within this complex superspace, consider the odd (real) dimensional supersphere defined by the equation

$$\sum_{a=1}^{N+M} z_a z_a^* + \sum_{a=1}^{N} \xi_a \xi_a^* = 1 \quad .$$

The supersphere $S^{2N+2M-1|2N}$ carries an action of U(1) by simultaneous phase rotations of all bosonic and fermionic coordinates,

$$z_a \longrightarrow e^{i\varpi} z_a \qquad , \qquad \xi_a \longrightarrow e^{i\varpi}\xi_a \quad . \tag{1.33}$$

Note that this transformation indeed leaves the constraint invariant. The complex projective superspace $\mathbb{CP}^{N+M-1|N}$ is the quotient space $S^{2N+2M-1|2N}/\mathrm{U}(1)$.

Functions on the supersphere $S^{2N+2M-1|2N}$ carry an action of the Lie supergroup $\mathrm{U}(N+M|N)$. These transformations include the phase rotations (1.33) which act trivially on $\mathbb{CP}^{N+M-1|N}$. The stabilizer subalgebra of a point on the projective superspace

is given by $\mathfrak{u}(1)\times\mathfrak{u}(N+M-1|N)$ where the first factor corresponds to the action (1.33). We conclude that $\mathbb{CP}^{N+M-1|N}$ is the following symmetric superspace:

$$\mathbb{CP}^{N+M-1|N} = \frac{\mathrm{U}(N+M|N)}{\mathrm{U}(1)\times\mathrm{U}(N+M-1|N)}\,.$$

Their simplest representative of interest to us is $\mathbb{CP}^{0|1}$, i.e. the space with just two real fermionic coordinates. The sigma model with this target space is equivalent to the theory of two symplectic fermions [126, 127].

The construction of the sigma model on $\mathbb{CP}^{N+M-1|N}$ closely parallels this geometric construction. The model involves a field multiplet $Z_\alpha = Z_\alpha(z,\bar z)$ with $N+M$ bosonic components $Z_\alpha = z_\alpha, \alpha = 1,\dots,N+M$ and N fermionic fields $Z_\alpha = \xi_{\alpha-N-M}, \alpha = N+M+1,\dots,2N+M+1$. To distinguish between bosons and fermions we use a grading function as before, $|\cdot|$, which is 0 when evaluated on the labels of bosonic and 1 on the labels of fermionic quantities. In addition we also need a non-dynamical U(1) gauge field a. With this field content, the action takes the form (with a summation convention on the index α)

$$S \;=\; \frac{1}{2g_\sigma^2}\int \mathrm{d}^2z\,(\partial_\mu - ia_\mu)Z_\alpha^\dagger(\partial_\mu + ia_\mu)Z_\alpha - \frac{i\theta}{2\pi}\int \mathrm{d}^2z\,\epsilon^{\mu\nu}\partial_\mu a_\nu \tag{1.34}$$

and the fields Z_α are subject to the constraint $Z_\alpha^\dagger Z_\alpha = 1$. This model is a direct generalization of that for $M=2, N=0$ discussed above. The integration over the Abelian gauge field can be performed explicitly and it leads to the replacement

$$a_\mu \;=\; \frac{i}{2}\left[Z_\alpha^\dagger\partial_\mu Z_\alpha - (\partial_\mu Z_\alpha^\dagger)Z_\alpha\right] \quad .$$

We recall also that the topological term multiplied by θ does not contribute to the equations of motion for a_μ. The manifold $\mathbb{CP}^{N+M-1|N}$ is homotopically equivalent to its bosonic base manifold $\mathbb{CP}^{N+M-1}$, whose second homotopy group is $\mathbb{Z}$, then the θ-term is not trivial. Note however that for symplectic fermions, the base manifold reduces to a point, and no theta term is present. As its bosonic counterpart, the $\mathbb{CP}^{N+M-1|N}$ sigma model on a closed surface possesses instanton solutions, whose corresponding instanton number is computed by the topological term $\mathcal{Q}$ that multiplies the parameter θ and is integer-valued. Then the parameter $\theta = \theta + 2\pi$ can be considered periodic as already noted before.

The target supermanifold being a symmetric superspace, the metric on the target space is unique up to a constant factor, so g_σ^2 and θ are the only coupling constants. The perturbative beta function is the same as the one for $\mathbb{CP}^{M-1}$ [195]

$$\frac{\mathrm{d}g_\sigma^2}{\mathrm{d}l} = \beta(g_\sigma^2) = Mg_\sigma^4 + O(g_\sigma^6)\,. \tag{1.35}$$

The beta function for θ is zero in perturbation theory, and that for g_σ^2 is independent of θ.

For $M > 0$, the coupling is weak at short length scales, but flows to strong values at large length scales. For $\theta \neq \pi \pmod{2\pi}$ the U$(N+M|N)$ symmetry is eventually restored, and the theory is massive. When $\theta = \pi \pmod{2\pi}$ and $M \leq 2$, the model flows to a non-trivial fixed point, whose bulk conformal field theory has been studied in [170, 171]. For $M > 2$ there are arguments supporting that the transition is first order using an $1/M$ expansion [62], and this fact can be also understood from the mapping of the Q-states Potts model to the sigma model with $M = Q^2$. For $M = 2$ and $N = 0$ we recover the flow in the O(3) sigma model. For $M = 0$, the beta function is in fact exactly zero, and the sigma model exhibits a line of fixed points [22, 37, 38, 170, 207] parametrized by g_σ^2 [15]. The case $M = 1$ is particularly interesting, because it is related with percolation as we have already discussed, and with the spin quantum Hall effect [101] (see section 3.2 below).

So far we have discussed the field theory for periodic boundary conditions. When open boundary conditions are imposed, the worldsheet of the sigma models is replaced with the strip (or the upper half plane). In this case the role of the θ-angle is affected by boundaries, but we postpone this discussion to section 4.1.3.

1.2 Boundary conformal field theory

The aim of this section is to give an introduction to the formal aspects of boundary conformal field theory (BCFT) and its applications to loop models.

1.2.1 The stress tensor and conformal data

When the continuum limit of a statistical system at the critical point is taken, the correlation length diverges and the critical fluctuations are described by a massless quantum field theory. The scale invariance gets generally promoted to invariance under conformal transformations, which preserve angles but not necessarily lengths [84] (see figure 1.12 for an example of conformal map).

In two dimensions, local conformal transformations coincide with holomorphic functions, so that conformal symmetry implies invariance under an infinite dimensional algebra, and it has proven to be extremely powerful.

[15] The critical theory of dense polymers, describing the continuum limit of the $\mathfrak{gl}(N|N)$ spin chains defined in section 1.1.2, corresponds to a particular value of g_σ^2 $(= 1)$. Other values can be obtained [37] by adding an exactly marginal interaction corresponding to the exchange of next nearest neighbors degrees of freedom V or V^* (since the products $V \otimes V$ or $V^* \otimes V^*$ decompose generically on two representations, this is the most generic next nearest neighbor coupling). In the Hamiltonian language, this means

$$H = -\sum_{i=0}^{2L-2} E_i + w \sum_{i=0}^{2L-3} P_{i,i+2}\,,$$

where $P_{i,i+2}$ is the operator permuting states in sites i and $i+2$. Note that the $P_{i,i+2}$ terms do not break the $\mathfrak{gl}(N+M|N)$ symmetry [37], i.e., it does not mix up the V and V^* spaces.

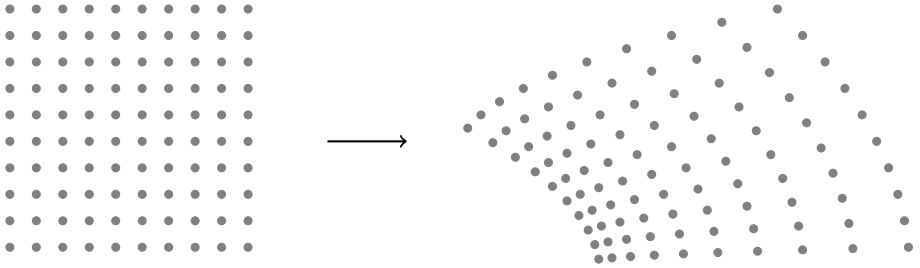

Figure 1.12: Example of a conformal transformation.

CFT in the complex plane

A prominent role in conformal field theory (CFT) is played by the stress tensor $T_{\mu\nu}$, a local field defined classically as the response of the action S under the infinitesimal transformation $x^\nu \to x^\nu + \epsilon^\nu$:

$$\delta S = -\frac{1}{2\pi}\int \mathrm{d}^2 x T_{\mu\nu}(x)\partial^\mu \epsilon^\nu(x)\,.$$

We consider first a CFT in the whole complex plane, and as customary we use complex coordinates $z, \bar{z}$. Then the only non-zero components of the stress tensor are a holomorphic one $T(z)$ and an antiholomorphic one $\bar{T}(\bar{z})$. We define the modes of T by

$$T(z) = \sum_{n\in\mathbb{Z}} L_n z^{-n-2}\,,$$

and analogously for $\bar{T}$. L_n's are the generators of conformal transformations of fields at the quantum level and satisfy the the celebrated Virasoro algebra (Vir):

$$[L_n, L_m] = (n-m)L_{m+n} + \frac{c}{12}n(n^2-1)\delta_{m+n,0}\,,$$

where c is the central charge of the CFT, and analogously for $\bar{L}_n$, generators of another copy of Vir. The subalgebra $L_0, L_{\pm 1}$ generates the global conformal transformations $\mathrm{SL}(2,\mathbb{C})$. The conformal transformations acting on functions rather than fields, are represented by $\ell_n = z^{n+1}\partial$, which satisfy the Witt algebra:

$$[\ell_n, \ell_m] = (m-n)\ell_{m+n}\,.$$

As every quantum field theory, a CFT is defined in terms of correlation functions $\langle\prod_i \phi_i(z_i,\bar{z}_i)\rangle_{\mathbb{C}}$ of fields $\phi(z,\bar{z})$. The fields are elements of a vector space F, which can be written as a direct sum of subspaces with given scaling dimension Δ. Generically F admits a decomposition into irreducible representations of Vir$\otimes$Vir:

$$F = \bigoplus_{i,j} N_{ij} V_i \otimes \bar{V}_j\,, \tag{1.36}$$

with multiplicities N_{ij}. However there are important exceptions to that in the case of logarithmic CFTs, when indecomposable but not irreducible Vir modules appear

(see discussion in section 1.2.2). If the sum above is finite, the theory is said to be rational[16]. The correlation functions are completely fixed once we know the operator product expansion (OPE) of the fields:

$$\phi_1(z_1,\bar{z}_1)\phi_2(z_2,\bar{z}_2) = \sum_\alpha f^\alpha_{\phi_1,\phi_2}(z_{12},\bar{z}_{12})\phi_\alpha(z_2,\bar{z}_2)\,, \tag{1.37}$$

where $z_{12} = z_1 - z_2$. The OPE allows us to reduce the computation of a correlation function of N fields to the that of a single one, and since we have translational invariance of correlators, one has $\langle\phi\rangle = 0$ unless ϕ has $\Delta = 0$. One demands also that the OPE is associative, and that correlators are invariant under permutations of fields.

We distinguish primary fields, whose correlators, as a consequence of conformal invariance, satisfy the conformal Ward identities (see e. g. [52])

$$\langle T(z)\prod_j \phi_j(z_j,\bar{z}_j)\rangle = \sum_j \left(\frac{h_j}{(z-z_j)^2} + \frac{1}{z-z_j}\partial_{z_j}\right)\langle\prod_j \phi_j(z_j,\bar{z}_j)\rangle\,,$$

and a similar one for $\bar{T}$, implying in particular that fields are factorized into a holomorphic $\phi(z)$ and an antiholomorphic $\bar{\phi}(\bar{z})$ component.

From an operator point of view, the space of states of the theory coincides with F, thanks to the state-fields correspondence $|\phi\rangle := \phi(0)|0\rangle$, where $|0\rangle$ is the $\mathrm{SL}(2,\mathbb{C})$-invariant vacuum of the theory. In the scheme of radial quantization [147] concentric circles in the plane correspond to surfaces of equal-time, and the Hamiltonian for this evolution is the dilatation operator $L_0 + \bar{L}_0$, whose (generalized) eigenvalues Δ organize the space of states. The primary fields can then be characterized as being highest weight vectors of (not necessarily irreducible) representations of the Virasoro algebra, such that $L_0\phi = h\phi$, $\bar{L}_0\bar{\phi} = \bar{h}\bar{\phi}$, and $L_m\phi = \bar{L}_m\bar{\phi} = 0$ if $m \geq 1$. Other states (descendant states) are then organized in conformal towers generated by acting with negative modes of Vir onto primary states.

In case eq. (1.36) holds, the OPE of primaries $\phi_1(z_1,\bar{z}_1), \phi_2(z_2,\bar{z}_2)$ with dimensions $(h_1,\bar{h}_1),(h_2,\bar{h}_2)$ takes the familiar form

$$\phi_1(z_1,\bar{z}_1)\phi_2(z_2,\bar{z}_2) = \sum_k C^{\phi_k}_{\phi_1,\phi_2} z_{12}^{h_k-h_1-h_2}\bar{z}_{12}^{\bar{h}_k-\bar{h}_1-\bar{h}_2}\phi_k(z_2,\bar{z}_2) + \dots\,,$$

where ϕ_k is a primary of dimension $(h_k,\bar{h}_k)$ and $C^{\phi_k}_{\phi_1,\phi_2}$ are bulk OPE structure constants. Since subleading terms (descendants) are determined only by conformal invariance, this can be stated also in terms of fusion product as:

$$\phi_1 \otimes_f \phi_2 = \sum_k \phi_k\,.$$

Primaries transform under the conformal map $(z,\bar{z}) \to (w,\bar{w})$ as tensors of conformal weight $h,\bar{h}$:

$$\phi(z,\bar{z})\mathrm{d}z^h\mathrm{d}\bar{z}^{\bar{h}} = \phi(w,\bar{w})\mathrm{d}w^h\mathrm{d}\bar{w}^{\bar{h}}\,. \tag{1.38}$$

[16]Sometimes an irrational theory can be organized into a finite number of representations of another chiral algebra, e. g. Kac Moody algebras or W-algebras. In this case the theory is still called rational.

The stress tensor is a field of conformal dimension $h = \bar{h} = 2$, and is not a primary (except for $c = 0$). Under a conformal mapping $z \to w$, T transforms as

$$T(z) = T(w)\left(\frac{\mathrm{d}w}{\mathrm{d}z}\right)^2 + \frac{c}{12}\{w; z\}\,, \tag{1.39}$$

where $\{w; z\}$ is the Schwarzian derivative

$$\{w; z\} \equiv \frac{\mathrm{d}^3 w/\mathrm{d}z^3}{\mathrm{d}w/\mathrm{d}z} - \frac{3}{2}\left(\frac{\mathrm{d}^2 w/\mathrm{d}z^2}{\mathrm{d}w/\mathrm{d}z}\right)^2 .$$

From an axiomatic point of view, CFTs on $\mathbb{C}$ are then fully determined by a small amount of data, a space of fields F, and their OPE. A CFT has thus the structure of an associative algebra with a product depending on a complex number, called a vertex operator algebra [121].

CFT on $\mathbb{H}$

Given a CFT in the complex plane $\mathbb{C}$, one can implement a boundary with the requirement that there is no energy flow across it, that is $T_{\parallel\perp} = 0$ along the boundary. If we choose as domain the upper half plane $\mathbb{H} = \{z \in \mathbb{C} | \Im(z) > 0\}$, then this implies the constraint

$$T(z) = \bar{T}(\bar{z})\,, \quad \text{for } z \in \mathbb{R}\,. \tag{1.40}$$

This is the condition which every CFT on $\mathbb{H}$ should respect, being equivalent to demand that a conformal transformation is constrained to respect the boundary. The consequence of eq. (1.40) is that chiral and antichiral sectors of the theory are no longer independent: $\bar{T}(\bar{z})$ on $\mathbb{H}$ can be regarded as the analytic continuation of $T(z)$ on the lower half plane, and only a single Vir algebra organizes the theory.

The dependence on anti-holomorphic coordinates $\bar{z}$'s in the correlator $\langle \prod_i \phi_i(z_i, \bar{z}_i)\rangle$ of N fields on $\mathbb{H}$, are regarded as holomorphic dependence on $z^* = \bar{z}$ on the lower half plane (method of images [41]). Then this correlator coincides with the *chiral* correlator of $2N$ fields $\langle \prod_i \phi_i(z_i) \prod_i \phi_i(z_i^*)\rangle_{\mathbb{C}}$ in the whole plane. Correlators of primaries are constrained by the conformal Ward identity in $\mathbb{H}$

$$\langle T(z) \prod_j \phi_j(z_j, \bar{z}_j)\rangle = \sum_j \left(\frac{h_j}{(z - z_j)^2} + \frac{1}{z - z_j}\partial_{z_j} + \frac{\bar{h}_j}{(\bar{z} - \bar{z}_j)^2} + \frac{1}{\bar{z} - \bar{z}_j}\partial_{\bar{z}_j}\right) \times \langle \prod_j \phi_j(z_j, \bar{z}_j)\rangle\,.$$

In a BCFT on $\mathbb{H}$ one distinguishes bulk fields which live inside $\mathbb{H}$ and which we have already encountered, from boundary fields, living on the boundary $\mathbb{R}$, see figure 1.13, where we can put several different conformal boundary conditions.

We introduce then a vector space of boundary fields B, which is a direct sum of subspaces distinguished by (generalized) eigenvalues h of L_0. Clearly B depends on the

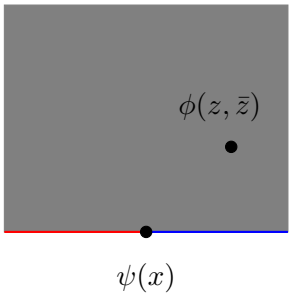

Figure 1.13: Bulk $\phi(z,\bar{z})$ and boundary $\psi(x)$ fields in a BCFT on $\mathbb{H}$. The boundary support two different boundary conditions, red and blue.

boundary conditions chosen, and there are in general many boundary spaces for a given bulk theory. If we consider for instance a conformal boundary condition labeled a on $\mathbb{R}^{<0}$ and b on $\mathbb{R}^{>0}$, we denote the associated primary boundary fields as $\psi_i^{a,b}$. If the bulk theory contains only irreducible representations i of Vir, B_{ab} decomposes as

$$B_{ab} = \bigoplus_i n_{ab}^i V_i \,,$$

We have also a boundary OPE associating to two boundary fields their short distance expansion, in a similar way to the bulk case (1.37). Suppose that a, b, c are labels associated to conformal boundary conditions, and call the primary boundary fields living at the interface between a, b and b, c, $\psi_i^{a,b}(x), \psi_j^{b,c}(y)$. If we assume that the labels i, j correspond to Vir irreducibles (of conformal dimensions h_i and h_j), then the boundary OPE takes the form of a sum of irreducibles $\psi_k^{a,c}$ $(x > y)$:

$$\psi_i^{a,b}(x)\psi_j^{b,c}(y) = \sum_s (x-y)^{h_s-h_i-h_j} C_{ijs}^{abc} \psi_s^{a,c}(y) + \dots \,, \tag{1.41}$$

where C_{ijs}^{abc} are called boundary OPE coefficients.

In a BCFT one considers in general correlators of mixed boundary and bulk fields $\langle \phi_1(z_1,\bar{z}_1)\cdots\psi_1(x_1)\cdots\rangle$. The interaction between boundary and bulk fields is given by the bulk-boundary OPE, associating to a bulk field its short distance expansion near the boundary in terms of boundary operators [53]. For $\phi_i(z)$ a primary transforming as the Vir irreducible i, and a uniform boundary condition a on the boundary, it is:

$$\phi_i(z) = \sum_k {}^a C_i^k (2\Im(z))^{h_k-2h_i} \psi_k^{aa}(\Re(z)) + \dots$$

where ${}^a C_i^k$ are the bulk-boundary OPE structure constants. We summarize in figure 1.14 the possible OPEs in a BCFT. Note that the one-point functions of bulk fields are not trivial like in the case of a CFT on $\mathbb{C}$ (the boundary breaks translational invariance) and depend on boundary conditions imposed, see discussion in section 1.2.3.

To summarize, a CFT on $\mathbb{H}$ is specified by the following data: a bulk CFT, a space of boundary fields B, the boundary OPE, and the bulk-boundary OPE. For a more precise

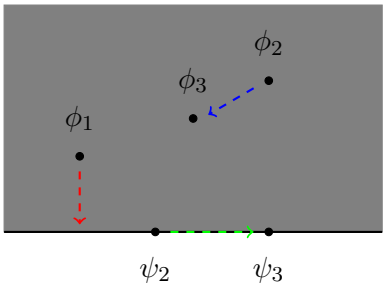

Figure 1.14: Different types of OPE in a boundary conformal field theory: bulk (blue), bulk-boundary (red), boundary (green).

discussion of the role between boundary and bulk CFTs, in particular in the case of logarithmic CFTs, we refer to [174].

We find notationally convenient to introduce here a parametrization of the central charge for CFTs which we will often consider in the following:

$$c = 1 - \frac{6}{p(p+1)}\,, \tag{1.42}$$

with p arbitrary and we will use standard Kac table notation to denote the conformal weights:

$$h_{r,s} = \frac{((p+1)r - ps)^2 - 1}{4p(p+1)}\,. \tag{1.43}$$

A canonical example of CFTs is that of unitary minimal models, the only unitary CFTs with $c < 1$. They have central charge (1.42) with $p \in \mathbb{Z}^{\geq 2}$. The field content is given by Vir irreducibles whose highest weights are in Kac notation $\phi_{r,s}$, $1 \leq r < p$, $1 \leq s < r$ [85].

1.2.2 Logarithmic conformal field theories

In this section we discuss some aspects of logarithmic CFTs. This subject is quite technical and here we limit ourselves to the main concepts and examples. We refer the reader to the review [87] for more details.

General aspects

In a unitary CFT, the generator of dilatations is Hermitian $L_0^\dagger = L_0$, hence can be diagonalized, leading to usual power law behavior of correlation functions. For unitary CFTs the space of states is a direct sum of irreducible representations of Vir. In non-unitary theories instead non irreducible (indecomposable) representations for which diagonalizability of L_0 is lost, may appear, resulting in logarithmic singularities of correlators.

Consider the two-point function $\langle \phi_1(w)\phi_2(0)\rangle$ of two fields which do not need to be primary. Invariance of the out vacuum under $\mathrm{SL}(2,\mathbb{C})$, $\langle 0|L_{\pm 1,0} = 0$, implies in particular

[174]

$$\begin{aligned}0 &= \oint_{C_\infty} \mathrm{d}zz\langle T(z)\phi_1(w)\phi_2(0)\rangle \\ &= \oint_{C_w} \mathrm{d}zz\langle T(z)\phi_1(w)\phi_2(0)\rangle + \oint_{C_0} \mathrm{d}zz\langle T(z)\phi_1(w)\phi_2(0)\rangle \\ &= \langle((L_0 + wL_{-1})\phi_1)(w)\phi_2(0)\rangle + \langle\phi_1(w)(L_0\phi_2)(0)\rangle\,,\end{aligned}$$

where we expanded T around w and 0 in the two pieces. In turn this gives the differential equation:

$$-w\frac{\mathrm{d}}{\mathrm{d}w}\langle\phi_1(w)\phi_2(0)\rangle = \langle(L_0\phi_1)(w)\phi_2(0)\rangle + \langle\phi_1(w)(L_0\phi_2)(0)\rangle\,. \tag{1.44}$$

If ϕ_1 and ϕ_2 are ordinary primary fields, $L_0\phi_i = h\phi_i, i = 1, 2$, then the solution to this equation is the familiar one: const $\times\, w^{-2h}$. Instead a nilpotent part in L_0 produces logarithmic singularities. Indeed suppose now that L_0 has the following Jordan form in the subspace with basis the two states ϕ, ψ:

$$L_0 = \begin{pmatrix} h & 1 \\ 0 & h \end{pmatrix}.$$

Solving eq. (1.44) gives:

$$\begin{aligned}\langle\phi(w)\phi(0)\rangle &= 0 \\ \langle\phi(w)\psi(0)\rangle &= \frac{b}{w^{2h}} \\ \langle\psi(w)\psi(0)\rangle &= \frac{\theta - 2b\log(w)}{w^{2h}}\,.\end{aligned}$$

ϕ must be a null field, and ψ is called its logarithmic partner. The parameter θ is not fundamental and can be reabsorbed in a redefinition of the fields, while b is called the indecomposability parameter [105] characterizing the the Jordan cell of L_0 [17].

Examples

We discuss now how logarithms appear in correlation functions using as an example the chiral four point function of primary fields degenerate at level two. Consider

$$C(z_1, z_2, z_3, z_4) = \langle\phi(z_1)\phi(z_2)\phi(z_3)\phi(z_4)\rangle\,,$$

with ϕ being $\phi_{1,2}$ or $\phi_{2,1}$ in Kac notation (1.43). The computation of this correlator is a standard exercise [84]. First invariance under global conformal transformations fixes it up to a function of a single parameter, the anharmonic ratio

$$\zeta = \frac{z_{12}z_{34}}{z_{13}z_{24}}\,.$$

[17] See [71, 190, 191] for recent developments regarding the measure of b on a lattice for the logarithmic CFTs describing loop models.

Called h the conformal weight of ϕ, one has

$$C(z_1,z_2,z_3,z_4)=\left(\frac{z_{13}z_{24}}{z_{12}z_{23}z_{14}z_{34}}\right)^{2h}\mathcal{G}(\zeta)\,.$$

Further ϕ has a null state at level two, $(2(2h+1)L_{-2}-3L_{-1}^2)\phi=0$. Its decoupling in correlation functions gives a differential equation after rewriting the action of Vir modes as differential operators. In this case one finds the hypergeometric equation:

$$\zeta(1-\zeta)\mathcal{G}''+\{\gamma-(1+\alpha+\beta)\zeta\}\,\mathcal{G}'-\alpha\beta\mathcal{G}=0\,.$$

with parameters

$$\alpha=-4h,\beta=\frac{1}{3}-\frac{4}{3}h,\gamma=\frac{2}{3}-\frac{8}{3}h\,.$$

Looking for solutions in the form of power series (say around ~ 0) produces the two solutions:

$$\mathcal{G}^0(\zeta)=\,{}_2F_1\left(\frac{1}{3}-\frac{4h}{3},-4h;\frac{2}{3}-\frac{8h}{3};\zeta\right) \tag{1.45}$$

$$\mathcal{G}^1(\zeta)=\zeta^{\frac{8h}{3}+\frac{1}{3}}\,{}_2F_1\left(\frac{1}{3}-\frac{4h}{3},\frac{4h}{3}+\frac{2}{3};\frac{8h}{3}+\frac{4}{3};\zeta\right)\,. \tag{1.46}$$

The OPE of ϕ fields is (for simplicity we have absorbed the OPE coefficients in the definitions of fields):

$$\phi(z)\phi(0)=z^{-2h}\left(\phi_0(0)+z^{h_1}\phi_1(0)\right)+\dots\,,$$

where ϕ_0 is the identity and ϕ_1 is degenerate at level three and has weight $h_1=8h/3+1/3$. Substituting in the correlation function, we see from the behavior as $z_{12},z_{34}\to 0$ ($\zeta\to 0$), that $\mathcal{G}^0(\zeta)$ and $\mathcal{G}^1(\zeta)$ correspond respectively to the fusion channels of the identity and of ϕ_1. We call these functions conformal blocks.

The important remark now is that the validity of these solutions is for $\gamma=1-h_1\notin\mathbb{Z}$. If γ is integer either the solutions coincide or one is ill defined. We want to discuss two cases of interest for applications, $c=-2$ and $\phi=\phi_{1,2}$, $h=-1/8$ (dense polymers), and $c=0$ and $\phi=\phi_{2,1}$, $h=5/8$ (dilute polymers). The reason for these names will become clear when we will discuss the continuum limit of loop models in section 1.2.4. In these cases, we have the following behavior of conformal blocks (parametrize $c=1-6/(p(p+1))$, $\epsilon=p-1$ in (1.47), $\epsilon=p-2$ in (1.48)):

$$\lim_{\epsilon\to 0}\mathcal{G}^0(\zeta)=\frac{2}{\pi}K(\zeta)\,;\qquad \lim_{\epsilon\to 0}\mathcal{G}^1(\zeta)=\frac{2}{\pi}K(\zeta)\,; \tag{1.47}$$

$$\mathcal{G}^0(\zeta)=\frac{15}{16\epsilon}S_2(\zeta)+O(\epsilon)\,;\qquad \lim_{\epsilon\to 0}\mathcal{G}^1(\zeta)=S_2(\zeta)\,. \tag{1.48}$$

K is the complete elliptic integral of the first kind of parameter ζ and

$$S_2(\zeta):=\zeta^2\,{}_2F_1\left(-\frac{1}{2},\frac{3}{2};3;\zeta\right)\,. \tag{1.49}$$

For dense polymers, due to the degeneracy $\mathcal{G}^0 \to \mathcal{G}^1$, one has to replace one conformal block with the missing solution of the differential equation which generally is given by a derivation procedure, and here can be written as ($\epsilon = p - 1$)

$$\lim_{\epsilon \to 0} \frac{\mathcal{G}^1(\zeta) - \mathcal{G}^0(\zeta)}{\epsilon} \propto K(1-\zeta) - \frac{\log(16)}{\pi} K(\zeta)\,.$$

Now standard identities give

$$K(1-\zeta) = \log(\zeta) K(\zeta) + H(\zeta)$$

with $H(\zeta)$ regular at $\zeta = 0$, so that the solution contains a logarithm. In terms of fusion rules this behavior is stated as the degeneracy of the two fields ϕ_0 and ϕ_1, which are replaced by the identity Ω and its logarithmic partner ω under the Virasoro algebra [104]:

$$\phi_{1,2}(z)\phi_{1,2}(0) = z^{1/4}\left(\omega(0) + \Omega(0)\log(z)\right) + \dots\,.$$

From the discussion above Ω has vanishing two-point function and that of ω contains logarithms. The description of this indecomposable module can be found in [87].

For dilute polymers, $\mathcal{G}^0$ here has to be replaced by the logarithmic conformal block, which can be written as ($\epsilon = p - 2$)

$$\lim_{\epsilon \to 0} \frac{1}{F_{02}} \left(\mathcal{G}^0(\zeta) - F_{00}\mathcal{G}^0(1-\zeta)\right) = (1-\zeta)^2\, {}_2F_1\left(-\frac{1}{2}, \frac{3}{2}; 3; 1-\zeta\right) = S_2(1-\zeta)\,.$$

F_{ij} are the fusing matrices of four ϕ fields at generic central charge which relates conformal blocks in different basis $\mathcal{G}_i(\zeta) = \sum_j F_{ij}\mathcal{G}_j(1-\zeta)$. These fusing matrices can be derived from standard hypergeometric identities, and read as:

$$\begin{pmatrix} F_{00} & F_{02} \\ F_{20} & F_{22} \end{pmatrix} = \begin{pmatrix} \frac{1}{\beta} & \frac{\Gamma\left(-\frac{8h}{3}-\frac{1}{3}\right)\Gamma\left(\frac{2}{3}-\frac{8h}{3}\right)}{\Gamma\left(\frac{1}{3}-\frac{4h}{3}\right)\Gamma(-4h)} \\ \frac{\Gamma\left(\frac{8h}{3}+\frac{1}{3}\right)\Gamma\left(\frac{8h}{3}+\frac{4}{3}\right)}{\Gamma\left(\frac{4h}{3}+\frac{2}{3}\right)\Gamma(4h+1)} & -\frac{1}{\beta} \end{pmatrix}, \tag{1.50}$$

where we defined $\beta = 2\sin\left(\pi(8h+1)/6\right) = 2\cos(\pi/(p+1))$, if we parametrize as usual $c = 1 - 6/(p(p+1))$. β plays the role of the weight of loops in the study of loop models.

Also in this case the $z \sim 0$ expansion of $S_2(1-\zeta)$ contains logarithmic singularities. From the point of view of OPE this is stated as the degeneracy of the stress tensor $T(z)$ and the field $\phi_{3,1}$. Indeed the $c \to 0$ limit in the OPE is ill-defined (this is general for a field with $h \neq 0$ fusing in the identity)

$$\phi_{2,1}(z)\phi_{2,1}(0) = z^{-2h}\left(\phi_{1,1}(0) + \frac{2h}{c} z^2 T(0) + z^{h_{3,1}}\phi_{3,1}(0)\right) + \dots$$

The way out to this "catastrophe" proposed in [105] was to suppose that $\phi_{3,1}$ diverges in a way to make the limit meaningful. The result of the limit procedure is

$$\phi_{2,1}(z)\phi_{2,1}(0) = z^{-2h}\left(\phi_{1,1}(0) + \frac{h}{b} z^2 \left(T(0)\log(z) + t(0)\right)\right) + \dots$$

t is the logarithmic partner of T and the indecomposability parameter $b = 5/6$ shows up in the expansion of the logarithmic conformal blocks.

1.2.3 The annulus partition function

So far the discussion has been rather abstract. It will be the purpose of this section to make it more concrete by computing the partition function of a CFT on an annulus. The results presented are standard, and mostly derived by J. Cardy in [41] in the context of rational unitary conformal field theory. Very good reviews on this subject and classification of boundary conditions exist, see e. g. [86, 160, 180].

Boundary states

The first object we want to introduce are boundary states. States in a bulk CFT are defined in radial quantization on concentric circles in the plane. Calling z the coordinate on $\mathbb{H}$, we map then $\mathbb{H}$ to the complement of the unit disk $\{\zeta \in \mathbb{C}, |\zeta| > 1\}$ by $\zeta = (z+i)/(z-i), \bar{\zeta} = (\bar{z}-i)/(\bar{z}+i)$. Using the transformation law of the stress tensor eq. (1.39), the conformal boundary condition (1.40) becomes

$$\zeta^2 T(\zeta) = \bar{\zeta}^2 \bar{T}(\zeta)\,, \quad \text{for } |\zeta| = 1$$

Going to a mode expansion, it implies that a boundary state $|B\rangle$ lies in the subspace satisfying the following gluing condition

$$\left(L_n - \bar{L}_{-n}\right)|B\rangle = 0\,. \tag{1.51}$$

We now look for a basis of states, solutions of these conditions. We assume the decomposition (1.36) of the space of bulk fields F, then we can solve the condition (1.51) in each direct summand separately. Taking $n = 0$ gives $i = j$, and the unique solution in $V_i \otimes \bar{V}_i$ is given by so-called Ishibashi states [115]. Each term V_i corresponds to a highest state (primary) $|i\rangle$, and other states in V_i are given by an orthonormal basis $|i; N\rangle$ of descendants, and similarly for $\bar{V}_i$. The Ishibashi states $|i\rangle\rangle$ are associated to each diagonal bulk field:

$$|i\rangle\rangle = \sum_{N=0}^{\infty} |i; N\rangle \otimes \overline{|i; N\rangle}\,, \tag{1.52}$$

A generic boundary state $|a\rangle$ corresponding to a boundary condition a, can then be decomposed onto Ishibashi states:

$$|a\rangle = \sum_i c_a^i |i\rangle\rangle\,, \tag{1.53}$$

with some constants c_a^i. The formalism of boundary states is used in the computation of correlators and partition functions in BCFT. For example the one-point function of the bulk field $\phi_1(\zeta, \bar{\zeta})$ in $\{\zeta \in \mathbb{C}, |\zeta| > 1\}$ can be computed using invariance of $|a\rangle$ and $\langle 0|$ under conformal transformations generated by $L_n - \bar{L}_{-n}$ (explicitly using the commutator of Vir generators with primary fields, see eq. (2.5) below):

$$\langle \phi(\zeta, \bar{\zeta})\rangle_a = \langle 0|\phi(\zeta, \bar{\zeta})|a\rangle = \frac{c_a^i}{(\bar{\zeta}\zeta - 1)^{2h}}$$

where ϕ has dimension $h, \bar{h} = h$. This result can be transformed to the geometries of interest, for example to $\mathbb{H}$ to yield

$$\begin{aligned}\langle \phi(z,\bar{z})\rangle_a &= \left(\frac{\mathrm{d}\zeta}{\mathrm{d}z}\right)^h \left(\frac{\mathrm{d}\bar{\zeta}}{\mathrm{d}\bar{z}}\right)^{\bar{h}} \langle \phi(\zeta,\bar{\zeta})\rangle_a \\ &= \frac{c_a^i}{|z-\bar{z}|^{2h}}\,.\end{aligned}$$

The c_a^i are thus related to bulk-boundary OPEs [53].

To determine the c_a^i's, below we will rederive Cardy conditions [44] and draw their consequence on the spectrum of the boundary theory.

Boundaries in free theories

We turn now to the concrete example of free bosons and free fermions theories, for which a Lagrangian description is possible and boundary conditions can be obtained by varying the action.

We start from the CFT of a (not-compactified) free boson ϕ. This theory has chiral $i\partial\phi$ and anti-chiral $i\bar{\partial}\phi(\bar{z})$ fields of dimension one, having the mode expansions

$$\begin{aligned} i\partial\phi &= \sum_{n\in\mathbb{Z}} a_n z^{-n-1} \\ i\bar{\partial}\phi &= \sum_{n\in\mathbb{Z}} \bar{a}_n \bar{z}^{-n-1}\,, \end{aligned}$$

where a_n, $\bar{a}_n$, are harmonic oscillators generating a U(1) current algebra (Heisenberg algebra):

$$\begin{aligned} [a_n, a_{-m}] &= m\delta_{m+n,0} \\ [\bar{a}_n, \bar{a}_{-m}] &= m\delta_{m+n,0} \\ [a_n, \bar{a}_{-m}] &= 0\,. \end{aligned}$$

The space of states of the theory is the Fock space generated by acting with negative modes of $J, \bar{J}$ on the vacuum $|0\rangle$, annihilated by non-negative modes. The Virasoro generators admit the representation

$$\begin{aligned} L_n &= \frac{1}{2}\sum_{m\in\mathbb{Z}} a_{n-m}a_m\,, \quad \text{if } n \neq 0\,, \\ L_0 &= \frac{1}{2}a_0^2 + \sum_{m\geq 1} a_{-m}a_m\,. \end{aligned} \tag{1.54}$$

From variation of the U(1)-invariant action

$$S = \frac{1}{4\pi}\int \mathrm{d}^2 z \partial\phi\bar{\partial}\phi\,,$$

with $z = x + iy$, coordinates on say a semi-infinite cylinder with boundary at $y = 0$, one finds two types of boundary conditions, Neumann (N) and Dirichlet (D):

$$N : \partial_x \phi|_{y=0} = 0 \quad ; \quad D : \partial_y \phi|_{y=0} = 0 \, .$$

The map $w = e^{-iz}$ sends the cylinder to $\mathbb{H}$, allowing to rewrite the above conditions in terms of the modes of the U(1) currents and as conditions for the boundary states:

$$(a_n + \Omega \bar{a}_{-n})|B_\Omega\rangle = 0 \, , n \in \mathbb{Z}$$

N corresponds to $\Omega = 1$ and D to $\Omega = -1$. Note that both imply the conformal boundary condition for the stress tensor since Vir generators are bilinears in a_n, eq. (1.54). Taking $n \geq 1$ above we see that the solution is an eigenvector of the annihilation operator a_n, which has the form of a bosonic coherent state, eq. (1.17). Then the solution to this constraint is[18]

$$|B_\Omega\rangle \propto \exp\left(-\Omega \sum_{k=1}^{\infty} \frac{1}{n} a_{-n} \bar{a}_{-n} \right) |0\rangle \, .$$

Further, after some algebraic manipulations [25] the states can be cast in the form of an Ishibashi state, not for the Virasoro algebra but for the extended chiral U(1) algebra[19]. More general conformal boundary conditions breaking this symmetry are also understood [86].

We consider next the case of a Majorana fermion described by the action

$$S = \frac{1}{4\pi} \int \mathrm{d}^2 z \left(\psi \partial \psi + \bar{\psi} \partial \bar{\phi} \right) \, ,$$

with ψ and $\bar{\psi}$ analytic and anti-analytic components. The fermionic modes are defined via the expansion of the bulk fermionic fields

$$\psi(z) = \sum_{r \in I} \frac{\psi_r}{z^{r+1/2}} \, , \quad \bar{\psi}(\bar{z}) = \sum_{r \in I} \frac{\bar{\psi}_r}{\bar{z}^{r+1/2}} \, ,$$

[18] More generally the quantization of free bosons leads to Fock spaces labeled by the momentum π_0, such that $a_0|\pi_0\rangle = \bar{a}_0|\pi_0\rangle = \pi_0|\pi_0\rangle$. In this case one has a D boundary state for every real value of π_0, while $\pi_0 = 0$ for N.

[19] More generally, in a theory with an extended symmetry generated by currents $J, \bar{J}$ with dimension h_J one can look for a subset of the conformal boundary conditions which preserve the extended chiral algebra. In this case the left- and right-moving fields corresponding to unbroken symmetries are related on the real axis by

$$J(z) = \Omega \left(\bar{J}(\bar{z}) \right) \, ,$$

where J and $\bar{J}$ are generators of the symmetry that is preserved by the boundary, and Ω denotes an automorphism of the algebra of fields that leaves the stress tensor invariant[180]. The gluing relation is then

$$\left(J_n - (-1)^{h_J} \Omega \bar{J}_{-n} \right) |B\rangle_\Omega = 0 \, .$$

Considering extended symmetry is important since often a theory is rational with respect to the extended symmetry and not with respect to Vir, for which the only rational theories are the minimal models $c < 1$.

where we consider for simplicity only the Neveu-Schwartz sector $I = \mathbb{Z} + 1/2$, where fermions are periodic in the plane, and antiperiodic on the cylinder. The Hilbert space of the theory is the fermionic Fock space generated by $\psi_{-r}, \bar{\psi}_{-s}$, $r, s \geq 1/2$ acting on $|O\rangle$, where $\psi_{p+1/2}|O\rangle = \bar{\psi}_{p+1/2}|O\rangle = 0, p \in \mathbb{Z}_{\geq 0}$. The OPEs

$$\psi(z)\psi(w) = \frac{1}{z-w}\,, \quad \bar{\psi}(\bar{z})\bar{\psi}(\bar{w}) = \frac{1}{\bar{z}-\bar{w}}$$

lead to

$$\{\psi_r, \psi_s\} = \left\{\bar{\psi}_r, \bar{\psi}_s\right\} = \delta_{r+s,0}\,.$$

Considering the cylinder geometry, variation of the action leads as in the free boson case to two types of boundary conditions, Dirichlet (D) and Neumann (N) [35]. We set coordinates $w = x + iy$ on the cylinder, and using the mapping to the plane as above, the mode expansion now reads

$$\psi(x,y) = (-i)^{1/2} \sum_r \psi_r e^{irx-ry}\,,$$
$$\bar{\psi}(x,y) = i^{1/2} \sum_r \bar{\psi}_r e^{-irx-ry}\,.$$

The boundary conditions are then

$$\bar{\psi}(x, y=0) = \epsilon\psi(x, y=0)\,, \tag{1.55}$$

where $\epsilon = 1$ for N and -1 for D. The boundary state associated to these equations has now the form of (fermionic) coherent states, see eq. (1.22),

$$|B^p_\psi\rangle \propto \exp\left(\epsilon i \sum_{p=0}^{\infty} \psi_{-p-1/2}\bar{\psi}_{-p-1/2}\right)|O\rangle\,.$$

Now imagine doing the same problem in a geometry rotated by $\pm\pi/2$, obtained by the mapping $w' = \pm iw$. Majorana fermions are objects of dimension $1/2$, and thus under a conformal mapping transform as $\psi(w')(dw')^{1/2} = \psi(w)(dw)^{1/2}$, and similarly for $\bar{\psi}$. Hence the equations characterizing the boundary state now would read $\bar{\psi} = \pm\epsilon i\psi$ instead of (1.55): when dealing with fermions, the D or N boundary condition is not represented by a unique equation, but depends on the orientation of the boundary[35].

We remark that this fermionic theory describes the Ising CFT $c = 1/2$, and D and N boundary conditions correspond to fixed and free conditions of Ising spins.

After these examples, we will discuss in the next sections how the computation of the annulus partition function allows to compute boundary states and classify boundary conditions in more complicated CFTs.

Boundary condition changing operators

Consider now the case of an infinitely long strip with boundary conditions a, b at the left and right boundary. The upper half plane can be mapped conformally onto this geometry by $z \to iL/\pi \log(z)$, and if $a \neq b$, the change of boundary condition may be though of as produced by the insertion of a *boundary condition changing* (BCC) field at the origin and at infinity [44]. BCC operators are defined by demanding that their correlation function be equal to the ratio of partition functions for a given domain, with and without change of boundary condition. For example, consider the case of figure 1.15, where one has three boundary conditions a, b, c on the boundary of the domain, and BCC operators are inserted where they change. Calling $Z(a, b, c)$ and Z the partition functions when there are three different boundary conditions and when there is a uniform boundary condition, one has

$$\langle \psi_i^{a,b}(x_1)\psi_j^{b,c}(x_2)\psi_k^{c,a}(x_3)\rangle := \frac{Z(a,b,c)}{Z} .$$

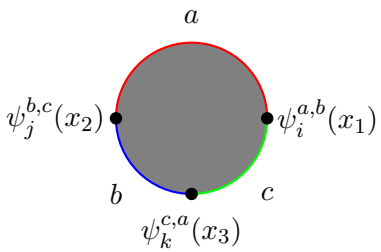

Figure 1.15: Boundary condition changing operators.

This remark is a powerful one since the BCC operators $\psi^{a,b}$ are primaries corresponding to the fields of lowest dimension in the boundary spectrum of a strip with boundary conditions a, b.

Cardy states and bulk-boundary correspondence of BCFT

We will see now how to relate the two concepts of BCC operators and boundary states. Consider a strip of length L' and width L, supporting boundary conditions a and b on left and right boundaries. We assume periodic boundary conditions in the other direction to form an annulus. We will show following [44] how equating the description of the partition function in the open and closed channel, see figure 1.16, will constrain the possible boundary conditions.

Call H_{ab} the Hamiltonian on the strip

$$H_{ab} = \frac{\pi}{L}\left(L_0 - \frac{c}{24}\right) .$$

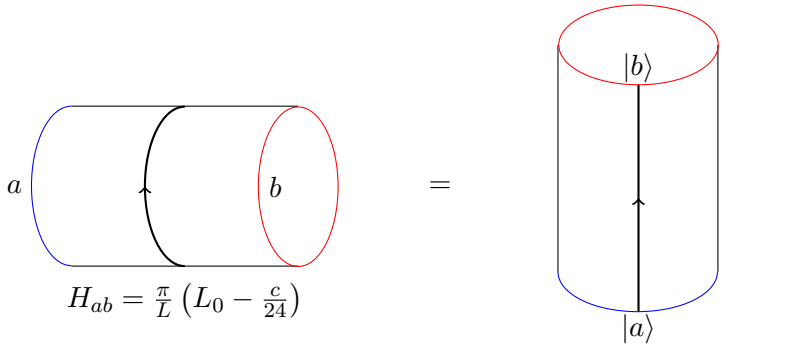

Figure 1.16: Open (left) and closed (right) channels. Arrows indicate the direction of imaginary time.

The partition function for the annulus is then

$$Z_{ab}(\tau) = \mathrm{Tr}_{B_{ab}}\, \hat{q}^{L_0 - c/24}\,,$$

where we recall that B_{ab} is the space of states of the boundary theory under consideration and we introduced the following notation for the modular parameter:

$$\hat{q} := \sqrt{q}\,; \quad q = e^{2\pi i \tau}\,; \quad \tau = iL'/L\,.$$

We assume now that B_{ab} has the form of eq. (1.36), a direct sum of Vir irreducibles V_i with positive or zero integer multiplicities n_{ab}^i, and we introduce the Vir character of the representation i:

$$\chi_i(\tau) = q^{-c/24}\,\mathrm{Tr}_{V_i}\, q^{L_0}\,.$$

Further we assume that there is a modular S matrix (which is the case for at least rational CFTs [84]), allowing to transform characters under modular inversion $\tau \to -1/\tau$:

$$\chi_i(\tau) = \sum_j S_{ij}\chi_j\left(-\tfrac{1}{\tau}\right)\,.$$

Then the partition function on the annulus can be written as

$$Z_{ab}(\tau) = \sum_{ij} n_{ab}^i S_{ij}\chi_j\left(-\tfrac{2}{\tau}\right)\,.$$

When we switch the role of L and L' by a modular inversion, it is more natural to describe the partition function as a matrix element of the evolution operator of the periodic system

$$H_P = \frac{2\pi}{L'}\left(L_0 + \bar{L}_0 - \frac{c}{12}\right)\,,$$

between boundary states. That is, defining the inverse modular parameter

$$\tilde{q} := e^{-2\pi i/\tau} ,$$

we can write the partition function as

$$\begin{aligned} Z_{ab}(\tau) &= \langle b|\tilde{q}^{L_0+\bar{L}_0-\frac{c}{12}}|a\rangle \\ &= \sum_{ij}(c_b^j)^*\langle\langle i|\tilde{q}^{L_0+\bar{L}_0-\frac{c}{12}}|j\rangle\rangle c_a^i \\ &= \sum_j c_a^j(c_b^j)^*\chi_j\left(-\tfrac{2}{\tau}\right) . \end{aligned}$$

Here we used the decomposition of boundary states (1.53), and that from the explicit form of Ishibashi states eq. (1.52) one has that their overlap gives the chiral character

$$\langle\langle i|\tilde{q}^{L_0+\bar{L}_0-\frac{c}{12}}|j\rangle\rangle = \delta_{ij}\sum_N\sum_{p=1}^{d_i(N)}\tilde{q}^{2(h_i+N-(c/24))} = \delta_{ij}\chi_i\left(-\tfrac{2}{\tau}\right) .$$

Now consistency of the two expressions we have derived implies (assuming that characters are linearly independent):

$$n_{ab}^i = \sum_j S_{ij}c_a^j(c_b^j)^* . \tag{1.56}$$

This is a very restrictive constraint for determining the allowed boundary conditions. The states satisfying it are called Cardy states[20]. Note that (1.56) contains information about the bulk theory since the index j runs over bulk Ishibashi states onto which the boundary states are decomposed.

In some cases one can also go further and solve completely the boundary theory [44], as we now explain. One set of solutions to Cardy constraint can be found by associating a boundary state to each irreducible representation V_i as

$$|\tilde{i}\rangle = \sum_l \frac{S_{il}}{\sqrt{S_{0l}}}|l\rangle\rangle .$$

From eq. (1.56), we see that the associated multiplicities n_{ij}^k are exactly the fusion multiplicities of the Verlinde formula for for a bulk rational CFT[21]:

$$N_{ij}^k = \sum_l \frac{S_{il}S_{jl}^*S_{kl}}{S_{0l}} .$$

[20] We remark however that Cardy states are not automatically guaranteed to be the right physical ones satisfying other sewing constraints from the associativity of OPE, whose validity should in principle be verified [86].

[21] Note that N_{ij}^k are not positive for some non-unitary CFTs and we exclude them from the present discussion.

N_{ij}^k are the fusion multiplicities defined by $\phi_i \otimes_f \phi_j = \sum_k N_{ij}^k \phi_k$, with $\otimes_f$ the fusion product of two bulk chiral primary fields ϕ_i, ϕ_j. Then in this case the fusion of boundary conditions gives precisely which representations occur in the strip with boundary conditions i, j, see figure 1.17. In particular we can construct a state (called Cardy brane) $|\tilde{0}\rangle = \sum_l \sqrt{S_{0l}} |l\rangle\rangle$ for which only the identity (vacuum) representation occurs and this provides the simplest example of a boundary conformal field theory: $B = V_0$. More generally if we put 0 on one side and i on the other side of the strip, then the spectrum consists of only the irreducible i, $B = V_i$.

The above solutions are exhaustive if one assumes that the set of boundary conditions $|a\rangle$ is complete [160]:

$$\sum_a c_a^i (c_a^j)^* = \delta^{ij} \,,$$

because then one can interpret eq. (1.56) as the eigenvalue equation $\sum_b (n_i)_{ab} c_b^j = S_{ij} c_a^j$, implying in particular that the number of boundary states equals that of Ishibashi's ones, so that of bulk primaries via the correspondence exhibited above. We remark further that the classification of boundary conditions above applies only to the "fundamental" boundary conditions, which are orthogonal, while in general one has to deal with linear combinations of those [86].

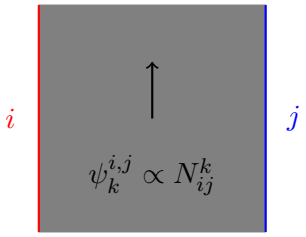

Figure 1.17: The Cardy case: the boundary fields $\psi_k^{i,j}$ which can propagate in the strip with boundary conditions corresponding to representations i, j are given by the fusion multiplicities N_{ij}^k.

The above procedure applies directly to the case of the unitary rational conformal field theories, like the minimal models $\mathcal{M}(p, p+1)$, giving the full answer for the classification of conformal boundary conditions. The prototype of this is the Ising CFT, the minimal model with $p = 3$, $c = 1/2$. In the bulk one has

$$F = \left(V_I \otimes \bar{V}_I\right) \oplus \left(V_\epsilon \otimes \bar{V}_\epsilon\right) \oplus \left(V_\sigma \otimes \bar{V}_\sigma\right) \,,$$

where the L_0 eigenvalues of I, ϵ, σ are $0, 1/2, 1/16$. Using the S-matrix [84], one finds

three possible boundary states:

$$
\begin{aligned}
|\tilde{0}\rangle &= \frac{1}{\sqrt{2}}|0\rangle\rangle + \frac{1}{\sqrt{2}}|\frac{1}{2}\rangle\rangle + \frac{1}{2^{1/4}}|\frac{1}{16}\rangle\rangle \\
|\frac{\tilde{1}}{2}\rangle &= \frac{1}{\sqrt{2}}|0\rangle\rangle + \frac{1}{\sqrt{2}}|\frac{1}{2}\rangle\rangle - \frac{1}{2^{1/4}}|\frac{1}{16}\rangle\rangle \\
|\frac{\tilde{1}}{16}\rangle &= |0\rangle\rangle - |\frac{1}{2}\rangle\rangle\,,
\end{aligned}
$$

corresponding respectively to fixed ± 1 and free boundary conditions of Ising spins.

Beyond the Cardy case

We question now the applicability to more general CFTs. In particular the assumption that the space of states is given by irreducible representations i with positive coefficients (multiplicities) is violated in logarithmic CFTs, see section 1.2.2. Some work has been done in the past to understand what happens in these cases, for both rational [88,89,174] and irrational [60,158,171] logarithmic CFTs. Recall that in the logarithmic case, fusion of two irreducible representations can produce an indecomposable but irreducible one. It has been found in the above examples that again the spectrum of the boundary theory agrees with the fusion rules, where now indecomposable representation are allowed to be generated by the fusion process.

Further the bulk-boundary correspondence valid for unitary rational CFTs, does not need to hold for more complicated theories. A striking example of the richness of non-unitary irrational cases is given by the conformal boundary loop models of section 1.2.5 for which boundary labels are arbitrary real numbers. In the approach to boundary loop models we will discuss below, we focus only on the boundary theory. Reconstructing the bulk theory from the boundary data in the non-unitary (logarithmic) case remains in general an interesting open question [174].

1.2.4 Continuum limit of loop models

In this section we will first recall how conformal invariance constrains the eigenvalues of the transfer matrix of a critical lattice model, and then discuss in particular the BCFT describing the continuum limit of the loop models introduced in section 1.1.1.

Finite size scaling of transfer matrices

Conformal invariance fixes the scaling of eigenvalues of transfer matrices of a two-dimensional critical lattice model [42]. Consider now a lattice system with boundary, say an infinite vertical strip of width L with boundary conditions labeled a and b. A correlation function of local lattice observables $\phi^{\rm lat}(x,y)$ (e. g. magnetization in the Ising model) can be expressed in a transfer matrix T_{ab} formalism as

$$
\langle \phi^{\rm lat}(x_1,y_1)\phi^{\rm lat}(x_2,y_2)\rangle = \langle 0|\hat{\phi}^{\rm lat}(x_1)(T_{ab}/\Lambda_0)^{y_2-y_1}\hat{\phi}^{\rm lat}(x_2)|0\rangle\,. \tag{1.57}
$$

Here $|0\rangle$ is the ground state with eigenvalue Λ_0 and on the right hand side $\hat{\phi}^{\rm lat}$ denotes a local operator acting onto the Hilbert space of the transfer matrix. If we insert now a complete basis $\{|n\rangle\}$ of eigenstates of T the correlation function decays as $(\Lambda_n/\Lambda_0)^{y_2-y_1}$, for $\langle 0|\hat{\phi}^{\rm lat}|n\rangle \neq 0$. In the continuum limit $L \to \infty$, the lattice observables become scaling fields $\phi = L^h \phi^{\rm lat}$, with h dictating the change under a dilatation, coinciding thus with the conformal dimensions of fields introduced above. In the continuum only states with $\log(\Lambda_n/\Lambda_0)$ scaling like $1/L$ are kept (low-energy states). The proportionality constant in the scaling formula can be obtained from conformal invariance. Indeed consider now a two-point function of boundary fields on the upper half plane $\mathbb{H}$:

$$\langle \psi(u_1)\psi(u_2)\rangle \propto |u_1 - u_2|^{-2h} .$$

Mapping it to the infinite strip via $z = u + iv \to w = x + iy = iL/\pi \log(z)$, it transforms as

$$\langle \psi(y_1)\psi(y_2)\rangle \propto \left(\frac{\pi}{2L} \frac{1}{\sinh\left(\frac{\pi}{2L}|y_1 - y_2|\right)} \right)^{2h} .$$

In the limit $|y_1 - y_2| \ll L$ one recovers the upper half plane result, while for $|y_1 - y_2| \gg L$ one finds $\exp(-\frac{\pi h}{L}|y_1 - y_2|)$. Comparing with the previous discussion, we get to first order

$$\log\left(\frac{\Lambda_n}{\Lambda_0}\right) \simeq \frac{\pi h}{L} . \tag{1.58}$$

By taking the limit $y_1 \to -\infty$ in (1.57), the only state $|n\rangle$ which survives is the one associated to the boundary operator ψ (lowest eigenvalue such that $\langle 0|\hat{\phi}^{\rm lat}|n\rangle \neq 0$). One can also associate to each eigenvector $|n\rangle$ an operator by computing the correlation function in this excited state so that upon transforming back to $\mathbb{H}$ an operator with dimension $L/\pi \log(\Lambda_n/\Lambda_0)$ is inserted at the origin. We come to the important conclusion that, as far as low-lying states are concerned, there is a one-to-one correspondence between eigenvectors of the transfer matrix in the strip and boundary operators. In particular the lowest eigenvector is associated to the BCC operator.

The ground state energy itself contains important information [2, 24]

$$\log(\Lambda_0) = L f_b + 2 f_s - \frac{c\pi}{24L} + \mathcal{O}\left(\frac{1}{L^2}\right) ,$$

where f_b, f_s are bulk and surface free energies, and c the central charge of the CFT. The above reasoning can be generalized to anisotropic lattices and in particular to quantum spin chains. In this case one has the following scaling for the energy of the n-th excited state:

$$\mathcal{E}_n = L f_b + 2 f_s - \frac{v c_{\rm eff} \pi}{24L} + \mathcal{O}\left(\frac{1}{L^2}\right) . \tag{1.59}$$

$c_{\rm eff} = c - 24 h_n$ and v is the so-called Fermi velocity, appearing in the linear dispersion relation of the quantum chain[22]. Note that bulk and surface energies do not depend on n, so they cancel in (1.58).

[22] For the Potts model $v = (p+1)\sin\left(\frac{\pi}{p+1}\right)$ if $\beta = 2\cos\left(\frac{\pi}{p+1}\right)$.

The above results provide a way to extract universal quantities of the CFT from finite size scaling of eigenvalues of the transfer matrix or Hamiltonian.

BCFT of loop models

The Potts model has a second order phase transition for $Q \leq 4$ and a first order one for $Q > 4$. The conformal field theory description of the critical region, parametrizing $\beta = \sqrt{Q} = q + q^{-1} = 2\cos(\pi/(p+1))$ can be obtained by studying finite size scaling of eigenvalues as discussed above. Indeed the XXZ model is amenable to exact solution by Bethe Ansatz [8], and finite size scaling of eigenvalues gives the dimension of fields present in the CFT. Further the six-vertex model can be mapped to a height model and then to a free boson theory with background charge (Coulomb gas method) allowing to deduce the exponents of the CFT [51, 177]. We will not reproduce here the calculations, but rather directly give the results and comment about the algebraic features. It is important to distinguish the cases q root of unity or not, as we have discussed for the lattice model in section 1.1.3. Here we take q generic. Using the parametrization above, the central charge of the CFT is (1.42). For $p \in \mathbb{Z}^{\geq 3}$ this coincides with that of the minimal models $\mathcal{M}(p, p+1)$, unitary and rational conformal field theories. However in our setting p is arbitrary and we expect in general non-unitary non-rational CFTs. When p is integer, the continuum limit of loop models is described by so-called logarithmic minimal models [158, 172]. The case of minimal models $\mathcal{M}(p, p+1)$ is recovered by restricting to the RSOS representation of TL [12].

The boundary spectrum of the continuum loop model is given by boundary primary operators ψ_j, $j \in \mathbb{Z}^{\geq 0}$, with j standing for the representation of Vir with weight $h_j = h_{1,1+2j}$, using Kac label notation (1.43). ψ_j are highest weight states and the general theory [84] associates a Verma module to them, obtained by acting freely with negative modes of the algebra $L_{-\gamma_1} \cdots L_{-\gamma_L} \psi_j$, γ a partition of n, $n \in \mathbb{Z}^{\geq 1}$. However this construction gives for the values h_j we are considering null states, that is, states which have zero norm and thus have to be removed to obtain an irreducible representation. The null vector for generic q occurs at conformal weight $h_{1,-1-2j}$. In particular this implies the following fusion rules [84]:

$$j_1 \otimes_f j_2 = \bigoplus_{j=|j_1-j_2|}^{j_1+j_2} j \,. \tag{1.60}$$

Despite the theory is irrational, fusion produces only a finite number of terms (quasirationality). The Vir character of this representation is computed by subtracting the null vector and its descendants:

$$\chi_j(\hat{q}) = \mathrm{Tr}_{V_j}\, \hat{q}^{L_0} = \frac{\hat{q}^{h_{1,1+2j}} - \hat{q}^{h_{1,-1-2j}}}{P(\hat{q})}$$

with $P(q)$ the generating function of partitions

$$P(\hat{q}) = \prod_{n=1}^{\infty} (1 - \hat{q}^n) \,.$$

We have then the space of boundary states

$$B = \bigoplus_{j=0}^{\infty} V_j$$

associated to the homogeneous reflecting R boundary condition in the lattice model[23]. The set of boundary labels one can use as boundary conditions is $\{j\}_{j\in\mathbb{Z}_{\geq 0}\cup R}$. Specifying at the boundaries of the strip two representations j_1, j_2 of Vir as boundary conditions, the resulting boundary fields $\psi_j^{j_1,j_2}$ can be obtained by the fusion of j_1, j_2, eq. (1.60), as in the Cardy case.

These results can also be understood by taking the continuum limit of the XXZ spin chain algebraically. Indeed the fusion rules can be implemented on a finite system by joining two chains, say in sector j_1 and j_2 to form a unique representation j [172]. This geometry, see figure 1.18, is quite natural also from the BCFT point of view, where this corresponds to inserting the fields ψ_{j_1}, ψ_{j_2} at bottom in the two half-strips. If we interpret those fields as changing boundary conditions from j_1 to 0 and 0 to j_2, respectively, we know that at the tip of the slit these have fused to $\psi_j^{j_1,j_2}$.

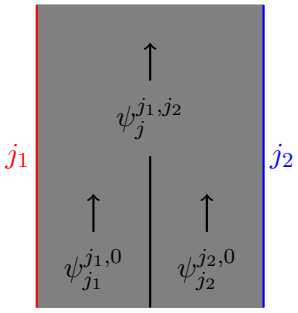

Figure 1.18: Fusion of boundary operators in the strip-slit geometry.

Going back to the lattice model and called two irreducible representations of $\mathrm{U}_q(\mathfrak{sl}(2))$ ρ_{j_1}, ρ_{j_2} their tensor product at generic q is the same as the usual one for $\mathfrak{sl}(2)$:

$$\rho_{j_1} \otimes \rho_{j_2} = \bigoplus_{j=|j_1-j_2|}^{j_1+j_2} \rho_j \,,$$

reproducing exactly the fusion rules of ψ_j's. Further, thanks to the centralizing property of $\mathrm{U}_q(\mathfrak{sl}(2))$ and TL, the same formula must apply also for tensoring TL representations. As the system size is increased TL irreducibles S_j grow and in the continuum limit they

[23] We refrain from adding pedantically the boundary labels $\psi_j^{R,R}$.

(more precisely, their low-lying parts) become exactly the Vir modules V_j. Further, on top of the identification of L_0 with the lattice Hamiltonian, also appropriate combinations of TL become the Vir generators [134]. In the same spirit one expects that the lattice scalar product converges to the bilinear form of the CFT, as we will discuss in more details in section 2.3.

The continuum limit of the annulus partition function of eq. (1.28) can now be taken. Note that the multiplicities D_j given by eq. (1.27) do not depend on the system size, and that according to the previous discussion

$$\mathrm{Tr}_{S_j} T^{L'} \to \chi_j(\hat{q}) \,,$$

where $\hat{q} = e^{-\pi L'/L}$ and the arrows indicates the universal part of the quantity on the left when the limit $L, L' \to \infty$, L/L' fixed is taken. Then the CFT annulus partition function is

$$Z = \sum_{j=0}^{\infty} D_j \chi_j(\hat{q}) \,. \tag{1.61}$$

Parametrized $q = e^{i\gamma}$, $D_j = [2j+1]_q$ can also be written as $D_j = \frac{\sin((2j+1)\gamma)}{\sin(\gamma)} = U_{2j}(\beta)$, $\beta = q + q^{-1}$ and $U_i(x)$ is the Chebyshev polynomial of the second kind. Although we derived the CFT annulus partition function assuming that q was generic, we remark that the result applies also when q is a root of unity by continuity.

The algebraic way of taking the continuum limit of a lattice model [172] is a general and powerful one, and has been applied to other models based on diagram algebras similar to TL, like the blob algebra [118], and the Brauer algebra [39], and it will be the guiding principle for the analysis of the models of edge states in section 4.2.1. The major point is that there are symmetry considerations which do not depend actually on the system size and carry on to the CFT. In particular these considerations are useful for the study of logarithmic CFTs [158, 172]. We stress that the above results for the continuum limit of critical loop models, can be used to study the conformal field theories governing non-trivial fixed points of $\mathbb{CP}^{N+M-1|N}$ sigma models introduced in section 1.1.4.

1.2.5 Boundary loop models

According to the discussion of the Cardy case of section 1.2.3, one would expect that irreducible summands of the space of states of the bulk CFT will correspond to admissible boundary conditions. The torus partition function of loop models, from which the operator content of the bulk fields can be read [43], has been constructed in [65, 170], and the representations j's (first column of the Kac table) obtained in the BCFT above are only a subset. We will see now how to construct from the lattice an infinity of conformal boundary conditions using the blob algebra.

The blob algebra

Consider a loop model on a strip of size $2L$, and choose to mark the loops touching say the left boundary, with a blob, see figure 1.19. Fugacities of unblobbed and blobbed

loops are denoted by β and β_1.

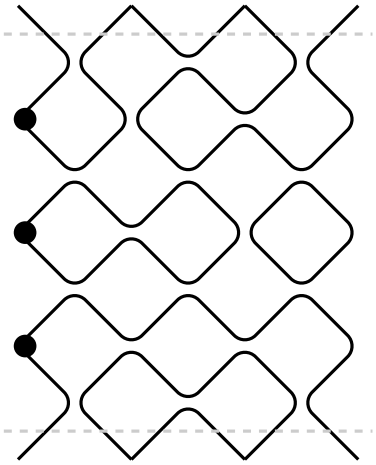

Figure 1.19: A configuration of the loop model based on the blob algebra.

This lattice model is based on a boundary extension of the TL algebra, called the blob algebra [141], or one-boundary TL algebra (1BTL). It is defined by adding to the TL algebra an extra generator b_1, marking the leftmost strand with a filled circle as depicted in figure 1.20. The relations satisfied in addition to the TL relations (1.6) are

$$\begin{aligned} b_1^2 &= b_1 \\ E_0 b_1 E_0 &= \beta_1 b_1 \\ [E_i, b_1] &= 0\,, \text{ for } i > 0\,, \end{aligned}$$

where E_0 is the TL generator acting on strands $0, 1$ of the lattice. Analogously, we introduce a blob operator b_2 marking the rightmost strand of the lattice with a filled gray circle, see figure 1.20, and we choose to weight loops touching only the right boundary as β_2. When b_1 and b_2 are both present we call the algebra the two boundary TL algebra (2BTL). In this case we have to choose how to weight loops touching both boundaries, allowing to reduce words of the algebra containing both b_1 and b_2. We impose the following additional relation, which gives a fugacity β_{12} to loops touching both boundaries:

$$\left(\prod_{i\,\text{even}} E_i\right) b_1 b_2 \left(\prod_{i\,\text{odd}} E_i\right) \prod_{i\,\text{even}} E_i = \beta_{12} \prod_{i\,\text{even}} E_i\,.$$

The transfer matrix of the model is defined by

$$T = b_1 b_2 T_0\,,$$

where T_0 is the transfer matrix of the Potts model, eq. (1.4). A more general case would be to consider $T = (1 + \lambda_1 b_1)(1 + \lambda_2 b_2) T_0$, but we anticipate that as long as $\lambda_{1,2} > 0$

Figure 1.20: The two additional generators b_1, b_2 of the two boundary TL algebra.

the values of the critical exponents do not depend on this parameter[24] and we make the choice $\lambda_{1,2} = \infty$ [118]. The associated Hamiltonian reads

$$H = -b_1 - b_2 + H_0 \,,$$

H_0 being the TL Hamiltonian (1.5). Again we could have considered a general boundary coupling, but we set it to one thanks to the universality of the result.

The TL algebra is recovered by setting $\beta_1 = \beta_2 = \beta_{12} = \beta$. Also in 2BTL there are exceptional values of the parameters at which the algebra is not semisimple and indecomposable modules appear, but the structure is clearly richer. For example in the one boundary case, given the usual parametrization $\beta = 2\cos(\pi/(p+1)$, they occur at $\beta_1 = \frac{\sin((r_1+1)\pi/(p+1))}{\sin(r_1\pi/(p+1))}$, when r_1 is integer [118,141]. We will discuss the generic case only here.

Irreducible representations will still be indexed by the number of through lines $2j$ as in the case of TL. The leftmost (rightmost) through line of a link state can carry black (resp. gray) blobs, being an eigenstate of the projector b_1 (resp. b_2). But it can also be unblobbed, that is eigenstate of the projector $1-b_1$ $(1-b_2)$. When $j > 0$, we distinguish then four subsectors, according to the fact that the leftmost and rightmost lines are blobbed or unblobbed. Another way to state this is that since the blob operators are projectors, once a through line is blobbed, it cannot be unblobbed, so that the transfer matrix has a tridiagonal block structure indexed by the number of through lines and the blobbed/unblobbed characters of leftmost and rightmost through lines.

Boundary TL algebras admit a representation as XXZ chains with boundary terms, we refer to [151] for that and for a discussion of the symmetry properties.

Operator content

For any values of $\beta_1, \beta_2, \beta_{12}$ the loop model based on 2BTL flows in the continuum limit to a boundary CFT whose central charge is given by β in the same way as for the usual loop model. The boundary spectrum present very interesting features and it was fully conjectured for the one boundary case in [118] and the two boundary case was solved in [70]. More than that, the authors of [70,118] were able to conjecture the full annulus partition function, which is given similarly to that of the Potts model (1.61), by the

[24] This arbitrariness's on the boundary coupling can also be understood from the Yang-Baxter equations of the model. Indeed writing the boundary matrix as $B(u) = 1 + g(u)b$, u the spectral parameter and b the blob operator, the Sklyanin equation gives rise to a solution for $g(u)$ that depends on an arbitrary parameter ζ, see eq. (40) of [67], analogously to the arbitrariness of the boundary coupling.

sum of characters of each sector weighted by non-trivial "multiplicities" depending on the weight of loops winding around the annulus. Here we limit ourselves to report the spectrum of primary operators.

Using the parametrization

$$\begin{aligned} \beta_1 &= \frac{\sin\left((r_1+1)\frac{\pi}{p+1}\right)}{\sin\left(r_1\frac{\pi}{p+1}\right)}\,, \qquad \beta_2 = \frac{\sin\left((r_2+1)\frac{\pi}{p+1}\right)}{\sin\left(r_2\frac{\pi}{p+1}\right)} \\ \beta_{12} &= \frac{\sin\left((r_1+r_2+1-r_{12})\frac{\pi}{2(p+1)}\right)\sin\left((r_1+r_2+1+r_{12})\frac{\pi}{2(p+1)}\right)}{\sin\left(r_1\frac{\pi}{p+1}\right)\sin\left(r_2\frac{\pi}{p+1}\right)}\,, \end{aligned} \tag{1.62}$$

it was found that in the sector with no non-contractible lines, the conformal weights appearing are [70]

$$h_{r_{12}-2n,r_{12}}\,, \tag{1.63}$$

with $n \in \mathbb{Z}$, while with $2j > 0$ non-contractible lines they are

$$h_{\epsilon_1 r_1+\epsilon_2 r_2-1-2n,\epsilon_1 r_1+\epsilon_2 r_2-1+2j}\,. \tag{1.64}$$

The sign $\epsilon_1 = \pm 1$ indicate whether the leftmost non-contractible line is required to touch the left boundary (for $\epsilon_1 = +1$, referred to as the blobbed sector), or forbidden from doing so (for $\epsilon_1 = -1$, referred to as the unblobbed sector). The sign ϵ_2 similarly describe the choice of blobbed/unblobbed sectors at the right boundary, and $n \in \mathbb{N}$. The parameters r_1, r_2 and r_{12} are related to the weight of marked loops through the formulas (1.62). The case $\beta_2 = \beta$ and $\beta_{12} = \beta_1$ corresponds to the one-boundary loop model (1BLM), where the exponents reduce to [118]

$$h_{r_1,r_1+2j\epsilon_1}\,. \tag{1.65}$$

We stress that the findings above are valid for arbitrary real values of r_1, r_2, r_{12}. They are mostly the result of an educated guess based on numerical diagonalizations of transfer matrices and algebraic considerations. When r_1 is integer, the 1BTL model can be realized in terms of the TL algebra [118], and the spectrum can be computed [177].

The spectrum of the boundary theory is very complicated, and clearly encodes a lot of possible boundary critical phenomena in 2D statistical mechanics models. In particular the arbitrariness of choosing β_{12} and the presence of an infinite number of primaries in the sector $j = 0$ reveals the difficulty in understanding the fusion in this irrational theory.

Chapter 2

Fully open boundaries in conformal field theory

In this chapter we will discuss the computation of CFT partition functions on a rectangle, using a new formalism of "fully open" boundary states. In section 2.1 we outline the formalism, discussing the differences with respect to the usual concept of cylinder boundary states and giving explicit results for the case of free theories. In section 2.2 we study amplitudes (partition functions), and compare the approaches using the open boundary states with the approach using conformal mappings and conformal blocks. In section 2.3 we address the discretization of boundary states introduced previously in terms of lattice boundary states in loop models. Correspondingly, the amplitudes are related to partition functions of loop models with lines inserted at the corners, and we use this geometrical interpretation to derive probability formulas for self-avoiding walks. This chapter contains material published by the author in [26, 29].

2.1 Conformal boundary state for the rectangular geometry

2.1.1 Gluing condition

A boundary condition in conformal field theory has to preserve conformal symmetry. We have seen in section 1.2.1 the conformal boundary condition gluing left- and right-moving modes of the stress tensor (1.40). This allowed to define boundary states $|B^p\rangle$ describing in radial quantization, a circular boundary at radius $|z| = 1$. Here the subscript p stands for periodic since the boundary is defined on a circle, in contrast to the "fully open" boundary states to be defined below. Recall that the constraint for the disk was

$$\left(L_n - \bar{L}_{-n}\right)|B^p\rangle = 0\,,$$

and that a basis of solutions was given by the so-called Ishibashi states (1.52).

Using the transformation law of the stress tensor, also more complicated boundaries can be described by gluing conditions. In this section we will discuss the geometry of

the bottom of the rectangle, see figure 2.1. In the $1+1$D Hamiltonian description of the CFT, the boundary state now lives in the Hilbert space of the 1D theory defined on a segment instead of a circle. To proceed, we choose coordinates $z = x + iy$ in the plane and consider the semi-rectangular region $0 \leq x \leq L, y \geq 0$ of Fig. 2.1, where we allow different boundary conditions on the sides, and derive the gluing condition for the stress-energy tensor in this geometry (for analogous discussions see [113, 114, 199]).

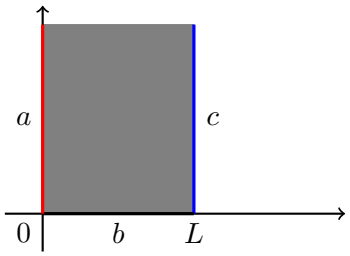

Figure 2.1: The semi-rectangular geometry defining the boundary state.

Conformal invariance of the boundary on the bottom side is $T_{xy} = 0$, and at the boundaries $z = iy$ and $z = L + iy$, $y > 0$ is realized by setting

$$\bar{T}(\bar{z}) = T(2L - \bar{z})\,,$$

and imposing periodic boundary conditions in the x direction of period $2L$: $T(z+2L) = T(z)$ (same for $\bar{T}$).

Care is needed to treat properly the effect of corners. The stress tensor T has a singularity as its argument approaches the corners. To see this we start more generally by the singularity in the upper half plane when an operator of weight h is inserted at the origin. In this case the most singular term is

$$T(w) \approx \frac{h}{w^2}\,.$$

We then fold the upper half plane by the mapping $z = w^{1/2}$ to have a corner in $z = 0$. After using the transformation law of the stress tensor (1.39), we get

$$T(z) \approx \left(4h - \frac{c}{8}\right)\frac{1}{z^2}\,. \tag{2.1}$$

Also if $h = 0$, at a corner there is an anomaly, which reflects itself in a non-trivial scaling dependence of physical quantities [54], as will be discussed in section 2.2.1 in more details.

As a consequence the condition on T defining the boundary state $|B^o\rangle$ at $y = 0$ is

$$\Big(T(x) - T(-x) + 4\pi i\left(\tilde{h}_l\delta'(x) + \tilde{h}_r\delta'(x-L)\right)\Big)\,|B^o\rangle = 0\,,$$

where we have used

$$\frac{1}{(x-i\epsilon)^2}-\frac{1}{(x+i\epsilon)^2}\approx\frac{4i\epsilon x}{(x^2+\epsilon^2)^2}\to-2\pi i\delta'(x)\,,$$

and defined the "effective conformal weight" at the corners

$$\tilde{h}:=2h-\frac{c}{16}\,,$$

h_l (h_r) being the weight of the operator inserted at the left (right) corner. Since the system is periodic with period $2L$, we can go to a mode expansion

$$T(x)=-\frac{\pi^2}{L^2}\left(\sum_n L_n e^{-i\pi nx/L}-\frac{c}{24}\right)\,,$$

to get the gluing condition (for $n\in\mathbb{Z}^{>0}$)

$$\left(L_n-L_{-n}-2n\left(\tilde{h}_l+(-)^n\tilde{h}_r\right)\right)|B^o\rangle=0\,. \tag{2.2}$$

Note in particular that in this case one not only identifies L_n and $\bar{L}_{-n}$, but also relates L_n to L_{-n}, since the semi-rectangular geometry is obtained by two consecutive folding of the plane.

2.1.2 Computation of the boundary states

Let us consider the rectangle bottom of figure 2.1 and call the condition on the left side a, that on the bottom b and that on the right c. Boundary condition changing (BCC) operators $\phi_i^{a|b}$, $\phi_j^{b|c}$, will then sit at the left and right corners. We choose for convenience the corners to be in $\zeta=-1,0$ in the ζ-plane. To discuss boundary states in radial quantization it is more appropriate to map the rectangle bottom to the region $\mathcal{D}=\{z\in\mathbb{C}:\Im(z)>0,|z|>1\}$, left of figure 2.2, by $z=e^{-i\pi\zeta}$. The gluing condition (so the boundary state) is not changed. We denote the boundary state we want to determine $|B^b_{ac}\rangle$, which is thus associated graphically to:

$|B^b_{ac}\rangle =$ 

If $X=\Phi(z_1,\bar{z}_1)\cdots\phi(x)\cdots$ is a chain of arbitrary bulk and boundary operators, the boundary state $\left|B^b_{ac}\right\rangle$ is defined by

$$\langle X\rangle_{\mathcal{D}}=\langle 0|X|B^b_{ac}\rangle\,,$$

where $\langle X\rangle_{\mathcal{D}}$ is the correlator in the geometry $\mathcal{D}$. On the other hand, we can map $\mathcal{D}$ to $\mathbb{H}$ using the Joukowsky map $f(z)=z+z^{-1}$, see figure 2.2. Suppose now that at the operator level, this conformal map can be implemented by conjugation by an operator $\hat{G}_f$, then

$$\langle X\rangle_{\mathcal{D}}=\langle 0|\hat{G}_f^{-1}X\hat{G}_f\phi_i^{a|b}(-2)\phi_j^{b|c}(2)|0\rangle\,,$$

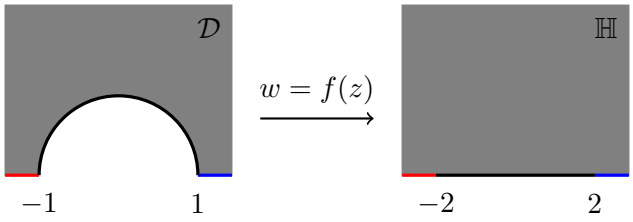

Figure 2.2: Mapping of semicircular region $\mathcal{D}$ to the upper half plane $\mathbb{H}$ $f(z) = z + z^{-1}$ (Joukowsky map).

(if $\hat{G}_f = e^{\sum_n \epsilon_n L_n}$, then $\hat{G}_f^{-1} = e^{-\sum_n \epsilon_n L_n}$), and the right term is a correlation function on the upper half plane. Since the out-vacuum $\langle 0|$ is invariant under the mapping f, one has

$$|B^b_{ac}\rangle = \hat{G}_f \phi_i^{a|b}(-2)\phi_j^{b|c}(2)|0\rangle\,. \tag{2.3}$$

The problem of finding the boundary state is then reduced to that of constructing the operator $\hat{G}_f$. This can be done using standard methods of CFT [15, 137, 182] which we discuss in the next section.

Conformal maps

A primary $\phi(z)$ of dimension h transforms under the conformal map $z \to f(z)$ as

$$\phi(z) = \big(f'(z)\big)^h\, \phi(f(z))\,. \tag{2.4}$$

In radial quantization, the equal-time commutator of L_n with the primary $\phi(z)$ is [147]

$$[L_n, \phi(z)] = \big(h(n+1)z^n + z^{n+1}\partial\big)\,\phi(z)\,. \tag{2.5}$$

From (2.4) we interpret this action of L_n as the infinitesimal variation

$$L_n \leftrightarrow z \to f(z) = z + \epsilon z^{n+1}\,.$$

Then under an infinitesimal transformation $z \to z+\epsilon(z)$, $\epsilon(z) = \sum_n \epsilon_n z^{n+1}$, $\phi(z)$ changes as $[\sum \epsilon_n L_n, \phi] = h\epsilon'\phi + \epsilon\partial\phi$.

We now exponentiate the infinitesimal action of eq. (2.5) and construct the operator $\hat{G}_f$ implementing the finite transformation (2.4) by conjugation demanding

$$\big(f'(z)\big)^h\, \phi(f(z)) = \hat{G}_f^{-1}\phi(z)\hat{G}_f\,.$$

Such operators have been discussed in the context of open string field theory [137, 182] and SLE [15]. Since this is not a very standard result, we give some details. We first

ask what is the conformal map associated to $\hat{G}_f = \exp(-\epsilon L_n)$ (n positive or negative), which acts as:

$$\begin{aligned}\hat{G}_f^{-1}\phi(z)\hat{G}_f &= \exp\left(\mathrm{ad}\left(\epsilon L_n\right)\right)\phi(z) \\ &= \sum_{k\geq 0}\frac{\epsilon^k}{k!}\left(h(n+1)z^n + z^{n+1}\partial\right)^k\phi(z) \end{aligned} \tag{2.6}$$

with the adjoint action $\mathrm{ad}(L_n)\phi = [L_n, \phi]$ of eq. (2.5). The map f is [137] ($\hat{G}_f$ is called U_f^{-1} there)

$$f(z) = \exp\left(\epsilon z^{n+1}\partial\right) z = \frac{z}{(1-\epsilon n z^n)^{1/n}}\,, \tag{2.7}$$

as can be readily verified by comparing the ϵ expansions of $\left(f'(z)\right)^h \phi(f(z))$ with eq. (2.6).

More generally the operator

$$\hat{G}_f = \exp\left(-\sum_{n\geq 1}\epsilon_n L_n\right)\,, \tag{2.8}$$

will then implement the map

$$\begin{aligned} f(z) &= \exp\left(\sum_{n\geq 1}\epsilon_n z^{n+1}\partial\right) z \\ &= z + \epsilon_1 z^2 + \left(\epsilon_1^2 + \epsilon_2\right) z^3 + \left(\epsilon_1^3 + \tfrac{5}{2}\epsilon_1\epsilon_2 + \epsilon_3\right) z^4 + \ldots \end{aligned}$$

Given a map $f(z)$ analytic inside a disk around the origin, the above result allows to associate by determining the ϵ's, the corresponding Hilbert space operator to insert in correlation functions. Instead considering the operator

$$\hat{G}_f = \exp\left(-\sum_{n\leq -1}\epsilon_n L_n\right)\,, \tag{2.9}$$

will implement the map

$$\begin{aligned} f(z) &= \exp\left(\sum_{n\leq -1}\epsilon_n z^{n+1}\partial\right) z \\ &= z + \epsilon_{-1} + \epsilon_{-2}\frac{1}{z} + \left(\epsilon_{-3} - \tfrac{1}{2}\epsilon_{-2}\epsilon_{-1}\right)\frac{1}{z^2} + \ldots \end{aligned}$$

which allow to associate Hilbert space operators to conformal maps analytic inside a disk containing $z = \infty$. If a map f is well defined in a region containing both 0 and ∞ and $f(0) = 0$ and $f(\infty) = \infty$, then eq. (2.8) and (2.9) associate to the same map two different operators in the Hilbert space. This is because in the two regions of convergence of the

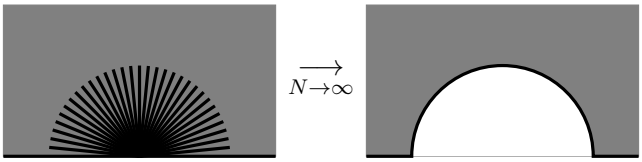

Figure 2.3: The geometry $\mathcal{D}$ emerging as the $N \to \infty$ limit of the multi-slit geometries.

formulas for $\hat{G}_f$, f has different power series expansions, respectively $f(z) = \sum_{n\geq 1} a_n z^n$ and $f(z) = \sum_{n\leq 1} b_n z^n$.

We now come back to the problem of finding $\hat{G}_f$, where $f(z) = z + z^{-1}$. Let us first remark that from eq. (2.7) we have

$$\hat{G}_{g_k} = e^{-\frac{2}{k}L_{-k}}\,, \quad g_k(z) = \left(z^k + 2\right)^{1/k}\,.$$

which for $k > 0$ has the correct asymptotic behavior as $z \to \infty$. Then note that composing g_{2^N} yields the map $f(z)$ in the limit $N \to \infty$ (and $|z| > 1$) :

$$\begin{aligned} g_2 \circ g_4 \circ \cdots \circ g_{2^N}(z) &= \sqrt{\sqrt{\ldots\sqrt{\sqrt{z^{2^N}+2}+2}\cdots+2}+2} \\ &= z + \frac{1}{z} + O(z^{1-2^{N+1}})\,. \end{aligned}$$

Since $\hat{G}_f\hat{G}_g = \hat{G}_{f\circ g}$ by definition, the operator $\hat{G}_f$ will be then given by the following product formula:

$$\hat{G}_f = \lim_{N\to\infty} e^{-\frac{1}{2^{N-1}}L_{-2^N}} \ldots e^{-\frac{1}{2}L_{-4}} e^{-L_{-2}}\,.$$

This formula has an appealing geometrical interpretation [26, 69]. Let us define the half-plane minus $k-1$ slits of size $2^{1/k}$

$$\mathbb{H}_k = \mathbb{H} \setminus \left\{ z | z^k \in [-2, 2] \right\}\,.$$

We now note that g_{2^N} is a conformal mapping from $\mathbb{H}_{2^N}$ onto $\mathbb{H}_{2^{N-1}}$, so that $g_2 \circ g_4 \circ \cdots \circ g_{2^N}$ is a mapping from $\mathbb{H}_{2^N}$ onto the half-plane $\mathbb{H}$. Then the geometry $\mathcal{D}$ can intuitively be though as the limit of infinite slits, as in figure 2.3.

Solution for homogeneous boundaries

After the above preparations, we can give the general formula for the boundary state solving the rectangular gluing condition, eq. (2.2). Let us discuss first the case of homogeneous boundary conditions $h_l = h_r = 0$, no BCC in (2.3). We have

$$\begin{aligned} |B^o\rangle &= \hat{G}_f\,|0\rangle \\ &= |0\rangle - L_{-2}|0\rangle - \frac{1}{2}L_{-4}|0\rangle + \frac{1}{2}L_{-2}^2|0\rangle + \ldots\,. \end{aligned} \tag{2.10}$$

One can actually show explicitly that this state solves the gluing constraint, see [26]. We will comment below in section 2.2.1 about the normalization of the state $|B^o\rangle$. In the following we will continue to use the normalization fixed in equation (2.10). The conjugate state $\langle B^o|$ is defined as (recall that if $|\Phi\rangle = \Phi(0)|0\rangle$, $\langle\Phi| = \langle 0|I\circ\Phi(0)$, with $I(z) = -1/z$):

$$\langle B^o| = \langle 0|\hat{G}_f^\dagger = \langle 0|\hat{G}_{I\circ f}\,,$$

where $I\circ f = -\frac{z}{1+z^2}$.

We note now that a very similar expression appeared in the open string field theory literature to describe the so-called identity string field [76]. That object is a boundary state defined as [167]:

$$\langle\mathcal{I}| := \langle 0|\hat{G}_{f_\mathcal{I}}\,,$$

where $f_\mathcal{I}$ is the conformal map sending the upper half disk $\{|z|\leq 1, \Im z\geq 0\}$ to the upper half plane $\mathbb{H}$:

$$f_\mathcal{I}(z) = \frac{z}{1-z^2} = I\circ\left(z-\tfrac{1}{z}\right)\,.$$

In [76] it was found

$$\langle\mathcal{I}| = \langle 0|\hat{G}_h\hat{G}_{f_2}\hat{G}_{f_3}\hat{G}_{f_4}\cdots$$

with

$$h(z) = \frac{z}{(1-2z^2)^{1/2}}\,;\quad f_n(z) = \frac{z}{(1+2z^{2^n})^{1/2^n}}\,,$$

and

$$\hat{G}_h = e^{L_2}\,;\quad \hat{G}_{f_n} = \exp\left(-\tfrac{1}{2^{n-1}}L_{2^n}\right)\,.$$

The expression of $\langle B^o|$ can be obtained from that of $\langle\mathcal{I}|$ by noting that

$$h^{-1}\circ h^{-1}\circ f_\mathcal{I} = I\circ f_f\,,$$

with $h^{-1}(z) = z/\sqrt{1+2z^2} = f_1(z)$, which implies

$$\hat{G}_{I\circ f} = \left(\hat{G}_h^{-1}\right)^2\hat{G}_{f_\mathcal{I}}\,.$$

This gives a consistency check of our result for the rectangular boundary state with that of [76] for the identity string field.

General solution and basis states

From eq. (2.3) we now have the solution for the more general case of BCC insertions in the corners. Using boundary OPE (1.41) it can written

$$|B^b_{ac}\rangle = \sum_s C^{abc}_{ijs}\sqrt{C^{aca}_{ss0}}|_i{}^s{}_j\rangle\,, \tag{2.11}$$

where we defined the *basis states* $|_i{}^s{}_j\rangle$ by

$$|_i{}^s{}_j\rangle := \hat{G}_f\, 4^{h_s-h_i-h_j} \sum_{n\geq 0}\sum_{\gamma\vdash n} 4^n \beta^{s,\gamma}_{i,j} L_{-\gamma}|\phi_s\rangle \tag{2.12}$$

$$= 4^{h_s-h_i-h_j}\left[|\phi_s\rangle + \sum_{n\geq 1}\sum_{\gamma\vdash n} \alpha^{s,\gamma}_{i,j} L_{-\gamma}|\phi_s\rangle\right], \tag{2.13}$$

where $\gamma \vdash n$ is a partition $(\gamma_1,\dots,\gamma_L)$ of n, and we used the shorthand $L_{-\gamma} := L_{-\gamma_1}\cdots L_{-\gamma_L}$. The coefficients $\beta^{s,\gamma}_{i,j}$, appear in the OPE of chiral fields ϕ_i,ϕ_j in the term corresponding to the descendant of ϕ_s, $L_{-\gamma}\phi_s$. Recursion relations for these coefficients can be obtained [84]. The term $\sqrt{C^{aca}_{ss0}}$ in the eq. (2.11) is needed in order to define the basis state as an element of the Verma module of the primary ϕ_s without any information about the boundary conditions. The knowledge of boundary OPE coefficients C^{abc}_{ijs} is equivalent to that of the F-matrices of the theory since [80, 173]:

$$C^{abc}_{ijs} = F_{bs}\left[\begin{array}{cc} a & c \\ i & j \end{array}\right]. \tag{2.14}$$

The F-matrices relate conformal blocks $\mathcal{F}$ building correlation functions in the following way [146]:

$$\mathcal{F}^s_{ij;kl}(\zeta) = \sum_r F_{sr}\left[\begin{array}{cc} i & l \\ j & k \end{array}\right]\mathcal{F}^r_{il;jk}(1-\zeta)\,. \tag{2.15}$$

We will see below several examples of this relation. Here we would like just to point out that they are a priori known data.

The basis states $|_i{}^s{}_j\rangle$ span the space of boundary states solving eq. (2.2) and are the analogues for the rectangular geometry of Ishibashi states (1.52). For determining the coefficients α's in eq. (2.13) one could work out the algebra in (2.12) or directly solve the constraint (2.2) for different values of n. It is well known however that the combinatorics of the Virasoro algebra is complicated and does not allow to get a closed formula for the coefficients in the above expansions, be it $\beta^{s,\gamma}_{i,j}$ or $\alpha^{s,\gamma}_{i,j}$. An exception is the case of free theories, when the Virasoro generators admit an expression in terms of bosonic or fermionic oscillators, see the discussion in section 2.1.3. We note then the following difference between Ishibashi states for the cylinder geometry and the basis states for the rectangle: rectangle basis states depend on the boundary operators inserted at the corners, so on their fusion, which does not give access to an explicit expression. Instead Ishibashi states are known explicitly from eq. (1.52).

Note that the normalization of the identity ϕ_0 (0 is the label for the identity) is fixed by demanding $\phi_0^{aa}\phi_i^{ab} = \phi_i^{ab}$, which implies

$$C^{aab}_{0ij} = \delta_{ij} \tag{2.16}$$

for every a, i. Note also that taking different OPEs of the three point function $\langle\phi_i^{ab}\phi_j^{bc}\phi_k^{ca}\rangle$ one has the cyclic relation

$$C^{abc}_{ijk}C^{aca}_{kk0} = C^{bca}_{jki}C^{aba}_{ii0}\,.$$

The state $|B^b_{ac}\rangle$ is directly given by a basis state if the fusion $\phi_i^{a,b} \otimes_f \phi_j^{b,c}$ produces only one channel. This is of course the case for homogeneous boundary conditions, when no BCC operators are present:

$$|B^a_{aa}\rangle = (C^{aaa}_{000})^{3/2}|_0{}^0{}_0\rangle = \hat{G}_f|0\rangle\,,$$

where $|\phi_0\rangle \equiv |0\rangle$, and we used (2.16). This is also the case when there is only a single BCC operator. Indeed, if $a = b$, calling the BCC operator $\phi_s^{a,c}$, one has

$$\begin{aligned}|B^a_{ac}\rangle &= C^{aac}_{0ss}\sqrt{C^{aca}_{ss0}}|_0{}^s{}_s\rangle \\ &= \sqrt{C^{aca}_{ss0}}\hat{G}_f\phi_s(2)|0\rangle = \sqrt{C^{aca}_{ss0}}\hat{G}_f\exp(2L_{-1})|\phi_s\rangle\,,\end{aligned}$$

since L_{-1} generates translations and $|\phi_s\rangle$ inserts the operator at the origin. C^{aca}_{ss0} is not fixed by (2.16) and could be set to one, see [173].

The discussion presented so far solves implicitly the problem of finding the boundary states for the rectangular geometry. Before moving on, let us define the conjugate states of eq. (2.11)

$$\langle B^b_{ac}| = \sum_s C^{abc}_{ijs}\sqrt{C^{aca}_{ss0}}\langle{}^i{}_s{}^j|\,,$$

which is associated graphically to

$$\langle B^b_{ac}| = \quad a \;\; b \;\; c$$

$\langle{}^i{}_s{}^j|$ is the adjoint of $|_i{}^s{}_j\rangle$, and we introduce also the following graphical notation for the basis states:

$$|_i{}^s{}_j\rangle = \quad \phi_i \;\; s \;\; \phi_j$$

2.1.3 Free theories

While the expression (2.10) is general, there are more natural ways to think of the boundary state in the case of free theories. There, like when the boundary is a circle instead of a segment, expressions as coherent states over the bosonic/fermionic modes are possible, this time however involving only the chiral half of oscillators.

Free boson

The simplest case is the free boson. The BCFT and the boundary states for the disk geometry have been discussed in 1.2.3. In the case of homogeneous boundary conditions, the gluing equation (2.2) takes the following simple form expressing Virasoro modes in terms of bosonic oscillators (see (1.54)):

$$\left(\sum_{m\in\mathbb{Z}} a_{n-m}a_m - \sum_{m\in\mathbb{Z}} a_{-n+m}a_{-m} + \frac{n}{4}\left[1+(-1)^n\right]\right)|B^o_\phi\rangle = 0\,.$$

The solution is of the form:

$$|B^o_\phi\rangle = \exp\left(-\sum_{n>0}\frac{1}{2n}a^2_{-n}\right)|0\rangle\,,$$

as can be verified using twice

$$(a_m + a_{-m})\,|B^o_\phi\rangle = 0\,, \quad m>0\,.$$

Alternatively one could also express L_n in (2.10) using (1.54) and check that the two expressions agrees for $c=1$.

Open boundary states for the free boson have been discussed in more generality in [26, 113, 199].

Ising model

The case of the Majorana fermion describing the Ising model is less straightforward. Going through the derivation of the gluing conditions for fermions using the doubling trick of section 2.1.1, produces a step function (say for D boundary conditions along the rectangle)[26]:

$$[\psi(x,y=0) + \mathrm{sign}(x) i\psi(-x,y=0)]\,|B^o_\psi\rangle = 0\,.$$

The sign function can be traced back to the transformation properties of fermions involving a purely imaginary factor, see the discussion of free theories of section 1.2.3. The solution to this can again be written as the coherent state

$$|B^o_\psi\rangle = \exp\left(\sum_{0\le m<n}^{\infty} G_{m,n}\psi_{-m-1/2}\psi_{-n-1/2}\right)|O\rangle\,. \tag{2.17}$$

The matrix $G_{m,n}$ can be easily computed using a different strategy involving correlation functions. As done in section 2.1.2 we define the boundary state in the geometry denoted by $\mathcal{D}$ (fig. 2.2 (left)), and consider the mapping to the upper half plane $\mathbb{H}$ (fig. 2.2 (right)), viz. $w = z + z^{-1}$. We thus consider D boundary conditions on all sides of the boundary of $\mathcal{D}$, so that $|B^o_\psi\rangle$ should be the state representing this boundary. Calling $|O\rangle$ the ground state of the model at infinity in $\mathbb{H}$ we have

$$\begin{aligned}\langle\psi(z_1)\psi(z_2)\rangle_{\mathcal{D}} &= \langle O|\psi(z_1)\psi(z_2)|B^o_\psi\rangle \\ &= \left(\frac{\partial w_1}{\partial z_1}\frac{\partial w_2}{\partial z_2}\right)^{1/2}\langle\psi(w_1)\psi(w_2)\rangle_{\mathbb{H}}\,,\end{aligned} \tag{2.18}$$

where on the rhs the correlator is evaluated in $\mathbb{H}$ with the usual D boundary conditions. Using that this correlator must simply be $1/(w_1-w_2)$ (since it involves only right movers, which are not affected by the boundary), and evaluating derivatives, gives straightforwardly that

$$\langle O|\psi(z_1)\psi(z_2)|B^o_\psi\rangle = \frac{1}{z_1-z_2}\frac{\sqrt{1-\frac{1}{z_1^2}}\sqrt{1-\frac{1}{z_2^2}}}{1-\frac{1}{z_1 z_2}}\,.$$

From the result (2.17) we can write the boundary state as

$$|B^o_\psi\rangle = :\exp\left(\oint \frac{dz}{2i\pi}\oint \frac{dz'}{2i\pi}\psi(z)G(z,z')\psi(z')\right):|O\rangle\,,$$

where $G(z,z')$ corresponds to the generating function of the numbers $G_{m,n}$ introduced above. Evaluating eq. (2.18) using Wick's theorem, we find in the end that

$$G(z_1,z_2) = \frac{1}{2(z_2-z_1)}\left(\frac{\sqrt{1-\frac{1}{z_1^2}}\sqrt{1-\frac{1}{z_2^2}}}{1-\frac{1}{z_1 z_2}} - 1\right).$$

We consider this expression in the domain $|z_1|, |z_2| > 1$ (because of the geometry of our problem), and expand it as

$$G(z_1,z_2) = \frac{1}{2z_1 z_2}\sum_{m,n=0}^{\infty}\frac{G_{mn}}{z_1^m z_2^n}\,.$$

(Observe that on top of $G_{mn} = -G_{nm}$, we have $G_{mn} = 0$ if $m+n$ is even.) As a result, we now have the generating function for the the quadratic form appearing in (2.17). The first few values of $G_{m,n}$ read:

$$\begin{aligned} G_{01} &= \frac{1}{2} \\ G_{03} = \frac{1}{8}, G_{12} &= \frac{5}{8} \\ G_{05} = \frac{1}{16}, G_{14} = \frac{3}{16}, G_{23} &= \frac{5}{8} \\ G_{07} = \frac{5}{128}, G_{16} = \frac{13}{128}, G_{25} = \frac{25}{128}, G_{34} &= \frac{81}{128}\,. \end{aligned}$$

We can then compare the result for the boundary state found in this section with the specialization at $c = 1/2$ of formula (2.10) by expressing the Virasoro modes in a standard way in terms of fermionic ones:

$$L_n = \frac{1}{2}\sum_{k\,\in\,\mathbb{Z}+\frac{1}{2}} k :\psi_{-k+n}\psi_k:\,, \quad n\in\mathbb{Z}\,.$$

We have verified the agreement for the first few descendants up to level 8 in the Virasoro modes.

The computation of the boundary state can be generalized to the case of different boundary conditions on the sides of the rectangle by considering correlators involving BCC operators and the spectator fermions used above. This can be done since for the Ising model higher point correlation functions are known explicitly [13]. Without entering details of the derivation, we present here the solution for the boundary state describing free Ising spins on the left and right sides and fixed say + in between, $|B^+_{ff}\rangle$.

This change of boundary conditions is mediated by $\sigma^{f,+}$. From the fusion rules of these BCC operators

$$\sigma^{f,+} \otimes_f \sigma^{+,f} = I^{f,f} + \psi^{f,f} ,$$

we know that this state is composed of two basis states, one in the sector of the identity $|{}^{I}_{\sigma}{}_{\sigma}\rangle$ and one in that of the energy $|{}^{\psi}_{\sigma}{}_{\sigma}\rangle$:

$$|B^{+}_{ff}\rangle \propto |{}^{I}_{\sigma}{}_{\sigma}\rangle + C|{}^{\psi}_{\sigma}{}_{\sigma}\rangle .$$

The numerical value of C is

$$C = 4^{h_\psi} \frac{C^{f,+,f}_{\sigma,\sigma,\psi}}{C^{f,+,f}_{\sigma,\sigma,I}} = 4^{-h_\psi}\sqrt{2} , \tag{2.19}$$

following using F-matrices for the Ising model (see e. g. [138]) after identification of boundary conditions with Virasoro representations $f \equiv \sigma$, $+ \equiv I$ and normalizing two point functions to one.

For the basis state one has a coherent state form (2.17), where in $|{}^{\psi}_{\sigma}{}_{\sigma}\rangle$ the vacuum must be replaced by the energy $\psi_{-1/2}|O\rangle$. The first few terms read:

$$\begin{aligned}
|{}^{I}_{\sigma}{}_{\sigma}\rangle &= 4^{-2h_\sigma}\left[1 + \frac{3}{2}\psi_{-1/2}\psi_{-3/2} + \frac{7}{8}\psi_{-1/2}\psi_{-7/2} + \frac{3}{8}\psi_{-3/2}\psi_{-5/2} + \dots\right]|O\rangle \\
|{}^{\psi}_{\sigma}{}_{\sigma}\rangle &= 4^{h_\psi-2h_\sigma}\left[1 - \frac{1}{2}\psi_{1/2}\psi_{-5/2} - \frac{3}{8}\psi_{1/2}\psi_{-9/2} - \frac{5}{16}\psi_{1/2}\psi_{-13/2} - \right. \\
&\qquad \left. \frac{9}{8}\psi_{-3/2}\psi_{-5/2} - \frac{5}{8}\psi_{-3/2}\psi_{-9/2} + \dots\right]\psi_{-1/2}|O\rangle .
\end{aligned}$$

The full expression for the generating functions $G(z_1, z_2)$ for these two basis states is quite lengthy and we refer the interested reader to [29] for that.

We have also verified the expressions for the above boundary states and the coefficients (2.19) from the solution of the Ising spin chain, as reported in [26, 29].

2.2 Rectangular amplitudes

Having discussed in details the construction of boundary states for the bottom of the rectangle, we study now the partition functions resulting from the overlap of such boundary states. Recall that generically we expect the partition function of a critical system to behave as

$$Z = e^{f_{\rm b} LL'} e^{f_{\rm s}(L+L')} Z_{\mathcal{R}}(L, L') ,$$

where $f_{\rm b}$ and $f_{\rm s}$ are bulk and surface energies, and $Z_{\mathcal{R}}(L, L')$ should be described by the CFT. We stress that this formula holds in the continuum limit of lattice models $L, L' \to \infty$, L'/L fixed.

2.2.1 Homogeneous boundary conditions

We first consider the amplitude associated to the boundary state with no BCC field insertions, eq. (2.10), for a generic CFT. Since we have the same boundary condition on each side, we note that the partition function for a rectangle of length L and width L' will have to be a modular form

$$Z_{\mathcal{R}}(L, L') = Z_{\mathcal{R}}(L', L)\,. \tag{2.20}$$

Define as usual $\tau := iL'/L$, $q := e^{2\pi i\tau}$ and the Dedekind eta function as

$$\eta(\tau) = q^{1/24}\prod_{n=1}^{\infty}(1-q^n)\,.$$

The partition function $Z_{\mathcal{R}}(L, L')$ was computed in [129]:

$$Z_{\mathcal{R}}(L, L') = L^{c/4}\eta(\tau)^{-c/2} \tag{2.21}$$

$$= L^{c/4}q^{-c/48}\left(1 + \frac{c}{2}q + \frac{c(c+6)}{8}q^2 + \dots\right)\,. \tag{2.22}$$

Each corner contributes $c/16\log(L)$ to the free energy (corner free energy) [54] due to the anomalies of the stress tensor, and the non-trivial scaling $L^{c/4}$ is the sum of these contributions[1].

Equation (2.20) then follows from the transformation properties of the η function:

$$\eta(-1/\tau) = \sqrt{-i\tau}\eta(\tau) \tag{2.23}$$

$$\eta(\tau+1) = e^{i\pi/12}\eta(\tau)\,. \tag{2.24}$$

[1] As an illustrative example of this fact we consider a semi-infinite rectangular geometry of width L in the y-direction and uniform boundary conditions. If we perform the transformation $x \to x, y \to y + \delta L\Theta(y - y_0)$, $0 < y_0 < L$, the response of the system is given by the change in free energy F as [65]:

$$\delta F = \frac{1}{2\pi}\int \mathrm{d}^2 r\langle T_{\mu\nu}\rangle\partial^\mu\alpha^\nu = -\frac{\delta L}{\pi}\int_0^\Lambda \mathrm{d}x\,\langle T(y_0)\rangle\,,$$

with Λ a cutoff, set to ∞ at the end, α the coordinate transformation, and we used $T_{22} = -T_{11} = -(T + \bar{T})$. The mapping to $\mathbb{H}$ (where $\langle T(z)\rangle = 0$) is $z = \cosh(w\pi/L)$, so using (1.39):

$$\frac{\delta F}{\delta L} = \frac{c\pi}{24L^2}\int_{iy_0}^{\Lambda+iy_0}\mathrm{d}w\left(1 + \frac{3}{\sinh(w\pi/L)^2}\right) = \frac{c\pi}{24L^2}\left(\Lambda - \frac{3iL}{\pi}\cot\left(\frac{\pi y_0}{L}\right) - \frac{3L}{\pi}\coth\left(\frac{\pi(\Lambda + iy0)}{L}\right)\right)\,.$$

When $\Lambda \to \infty$, $y_0 \to 0$ the corner free energy predicted by CFT is:

$$\Delta F = -\frac{c}{8}\log(L)\,.$$

As expected, we have a logarithmic dependence on L and the result is in agreement with the presence of an exponent $-c/16$ associated to the corner. A similar computation gives the partition function for a rectangle (2.21), and note that when BCC operators $\phi_1\cdots\phi_n$ are present, the variation of the free energy is given by replacing $\langle T_{\mu\nu}\rangle$ with $\frac{\langle T_{\mu\nu}\phi_1\cdots\phi_n\rangle}{\langle\phi_1\cdots\phi_n\rangle}$.

As it was observed in [130], this partition function can actually be derived only from modularity arguments.

In the limit of very tall rectangle $L' \gg L$ ($q \to 0$) we note from the expansion (2.22) that the free energy per unit length has the correct behavior [84] of that for the infinite strip:

$$-\frac{\log(Z_{\mathcal{R}}(L,L'))}{L'} \sim -\frac{c\pi}{24L}\,.$$

Further, we remark that for the $c = 1$ and $c = -2$ CFTs of free bosons and symplectic fermions (related to spanning trees via matrix-tree theorem [185]), the partition function is simply given by the Laplacian of the rectangle, whose expression [73] agrees with that given above.

Now we can take the scalar product of the boundary state with itself to form the amplitude

$$A_{\mathcal{R}}(\tau) := \langle B^o|\hat{q}^{L_0-c/24}|B^o\rangle = \hat{q}^{-c/24}\sum_{n\geq 0} c_n \hat{q}^n\,, \tag{2.25}$$

where $\hat{q} := \sqrt{q}$ is the relevant combination of L'/L appearing in the transfer matrix on a strip, and the arrow is the direction of imaginary time. The following relation between this amplitude and the partition function $Z_{\mathcal{R}}(L,L')$ should hold

$$A_{\mathcal{R}}(\tau) = L^{-c/4} Z_{\mathcal{R}}(L,L') = \eta(\tau)^{-c/2}\,. \tag{2.26}$$

We have verified this relation by computing the first coefficients c_n in (2.25) using the commutation relations of the Virasoro algebra and comparing them with the power series of $\eta^{-c/2}$, confirming the validity of our derivation up to a very high order ($n = 52$) in $\hat{q}$. We note that as expected from the left-right symmetry of the boundary conditions of the problem, the boundary states couple only to descendants of the identity of even level (so that $c_{2n+1} = 0$ in eq. (2.25)).

We comment now on the normalization of the boundary state $|B^o\rangle$ and of rectangle partition functions. First we note that the state $|B^o\rangle$ is not normalizable. Indeed from (2.26), we have that

$$\langle B^o|B^o\rangle = \lim_{q\to 1}\eta(\tau)^{-c/2} = \begin{cases}\infty & \text{if } c>0,\\ 0 & \text{if } c<0,\\ 1 & \text{if } c=0.\end{cases}$$

A similar situation happens for the Ishibashi states in the cylinder geometry. However in the case of cylinder states, one can fix a possible multiplicative constant in the definition, which is not fixed by the gluing condition on the disk (1.51), by requiring the equality of the cylinder amplitude to the annulus partition function, as discussed in section 1.2.3. We do not know how to fix a possible multiplicative constant α in the definition $|B^o\rangle = \alpha \hat{G}_f\,|0\rangle$. This issue is related to the very definition of a partition function on a rectangle, containing the factor $L^{c/4}$ in (2.21), which depends on the unit of measure of length we adopt.

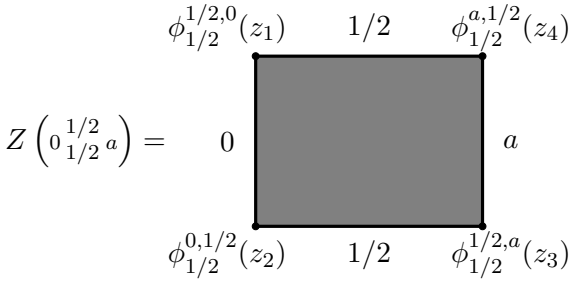

Figure 2.4: The partition functions for one-leg insertion at the corners z_i.

2.2.2 Conformal blocks and modular properties

Example: one-leg insertions

We discuss the general properties of rectangular amplitudes starting with an example, that of the partition function of a loop model with one-leg operators inserted at the corners. Using the labels $i \equiv (1, 1+2i)$ where $(1, 1+2i)$ is Kac notation (1.43), we would like to compute the partition functions $Z\left(0\,{}^{1/2}_{1/2}\,a\right)$, see figure 2.4, where $a = 0, 2$, so that the BCC operators in the corners are $\phi_{1/2}^{0,1}$ or $\phi_{1/2}^{2,1}$.

We note that this partition function is the same as that of the Q-states Potts model with fixed boundary conditions on left and right boundaries and free on the top and bottom sides. In this language the two values $a = 0, 2$ correspond to the two situations of fixed spins in an equal state ($a = 0$) or fixed spins in different states ($a = 2$). This is consistent with the known fusion rules [48] since $1/2 \otimes_f 1/2 = 0 \oplus 1$. The partition functions $Z\left(0\,{}^{1/2}_{1/2}\,a\right)$ have been already computed in [48] and here we reproduce the results and comment about boundary states and modular properties.

If $a = 0$, at the corners on the bottom sit BCC operators $\phi_{1/2}^{0,1/2}$ and $\phi_{1/2}^{1/2,0}$, whose OPE coefficients are clearly $C_{1/2,1/2,s}^{0,1/2,0} \propto \delta_{s,0}$ so that only the identity channel propagates. For $a = 1$ we insert instead $\phi_{1/2}^{0,1/2}$ and $\phi_{1/2}^{1/2,1}$ whose OPE coefficients are $C_{1/2,1/2,s}^{0,1/2,1} \propto \delta_{s,1}$ so that only the ϕ_1-channel is left. Called z_i the position of the corners, by definition of BCC operators, the partition functions will be

$$Z\left(0\,{}^{1/2}_{1/2}\,a\right) = Z_{\mathcal{R}}(L, L')\langle \phi_{1/2}^{1/2,0}(z_1)\phi_{1/2}^{0,1/2}(z_2)\phi_{1/2}^{1/2,a}(z_3)\phi_{1/2}^{a,1/2}(z_4)\rangle\,,$$

where $Z_{\mathcal{R}}(L, L')(\tau)$ is the partition function for no field insertion (2.21), and the correlator is in the rectangle geometry. For computing a correlator of the fields on the rectangle, we map it to the upper half plane w using a Schwarz-Cristoffel transformation:

$$z = \int_0^w \mathrm{d}t \frac{1}{\sqrt{(1-t^2)(1-k^2t^2)}}\,.$$

It maps the points on the real line $(-1/k, -1, 1, 1/k)$ to the corners of a rectangle with $L = 2K$ and $L' = K'$, $(-K + iK', -K, K, K + iK')$, where K is the complete elliptic integral of the first kind of modulus k and K' the complementary one, see figure 2.5.

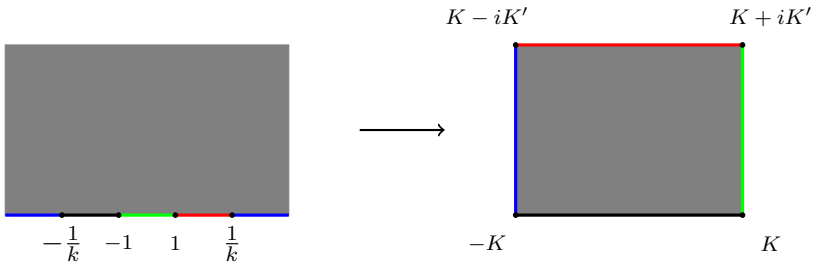

Figure 2.5: The Schwarz-Cristoffel transformation sending the upper half plane to the rectangle.

The Jacobian J of this transformation is singular at the corners, but when the boundary operators sit at the corners, the transformation law of primary fields, eq. (1.38), continues to hold since as the argument of the field approaches the corner in z_c, the field itself goes to zero as $(z - z_c)^h \phi(z_c)$, where h is the dimension of the field. Then we look at the Jacobian as the coefficient of the first term in the expansion around the position of the corners. The result for general field insertion is

$$J = k^{-h_i - h_l}(1 - k^2)^{h_i + h_j + h_k + h_l}\,, \tag{2.27}$$

so that in the case we are after:

$$J = k^{-2h}(1 - k^2)^{4h}\,.$$

The correlator on the upper half plane can be written using the fusion procedure depicted as:

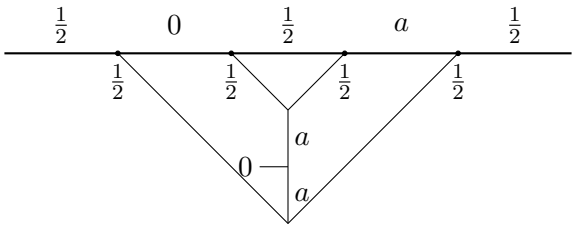

giving:

$$\langle \phi_{1/2}^{1/2,0}(w_1)\phi_{1/2}^{0,1/2}(w_2)\phi_{1/2}^{1/2,a}(w_3)\phi_{1/2}^{a,1/2}(w_4)\rangle = \left(\frac{w_{13}w_{24}}{w_{12}w_{23}w_{14}w_{34}}\right)^{2h} \times C_{1/2,1/2,a}^{0,1/2,a} C_{1/2,1/2,a}^{0,1/2,a} C_{aa0}^{0a0} \mathcal{G}^a(1-\zeta)\,.$$

The explicit expressions for the blocks $\mathcal{G}^a$ were given in eq. (1.45), (1.46), and recall that the anharmonic ratio ζ is defined as

$$\zeta = \frac{w_{12}w_{34}}{w_{13}w_{24}}\,,$$

with $w_{ij} = w_i - w_j$. We now let $(w_1, w_2, w_3, w_4) = (-1/k, -1, 1, 1/k)$ and express everything in terms of τ,

$$\begin{aligned} k &= \left(\frac{\theta_2(2\tau)}{\theta_3(2\tau)}\right)^2 \\ \zeta &= \left(\frac{\theta_4(\tau)}{\theta_3(\tau)}\right)^4 . \end{aligned} \tag{2.28}$$

After a little algebra we finally get (recall $L = 2K$):

$$Z\left(\begin{smallmatrix} 0 & 1/2 \\ 1/2 & a \end{smallmatrix}\right) = \mathcal{N}^a L^{c/4-8h}\eta^{-c/2}\theta_3^{16h}\mathcal{G}^a(1-\zeta)\,. \tag{2.29}$$

An important feature is the presence of $c/4 - 8h$, the modular weight of the rectangular partition functions [54] already discussed in section 2.1.1. In the above formula we wrote a normalization factor $\mathcal{N}^a$, which will be fixed by a physical requirement below.

Before doing that, we express this partition function using the formalism of boundary states introduced above. The relevant boundary states are (omitting the OPE coefficients appearing in the general formulas (2.11))

$$|B^{1/2}_{0a}\rangle \propto |{}^{a}_{1/2\ 1/2}\rangle$$

Parametrizing c as in (1.42) the first few terms of these basis states have the complicated explicit form

$$\begin{aligned} 4^{2h_{1/2}}|{}^{0}_{1/2\ 1/2}\rangle = |0\rangle &+ \left(7 - \frac{24}{p+3}\right) L_{-2}|0\rangle \\ &+ \left(-\frac{40}{3p+5} + \frac{24}{p+3} - \frac{1}{2}\right) L_{-4}|0\rangle + \left(\frac{200}{9p+15} - \frac{48}{p+3} + \frac{19}{6}\right) L_{-2}^2|0\rangle + \dots \end{aligned}$$

and

$$\begin{aligned} 4^{2h_{1/2}-h_1}|{}^{1}_{1/2\ 1/2}\rangle = |\phi_1\rangle &+ \frac{5p-1}{3p+1}L_{-2}|\phi_1\rangle - \frac{2(p+1)}{3p+1}L_{-1}^2|\phi_1\rangle \\ &+ \frac{34p^3+21p^2+44p-3}{60p^3+86p^2+40p+6}L_{-4}|\phi_1\rangle - \frac{16(p-2)p(p+1)}{(2p+1)(3p+1)(5p+3)}L_{-3}L_{-1}|\phi_1\rangle \\ &- \frac{p^2+34p-3}{30p^2+28p+6}L_{-2}^2|\phi_1\rangle + \frac{20p^3+58p^2+44p+6}{30p^3+43p^2+20p+3}L_{-2}L_{-1}^2|\phi_1\rangle \\ &- \frac{2(p+1)^2(2p+3)}{30p^3+43p^2+20p+3}L_{-1}^4|\phi_1\rangle + \dots \end{aligned}$$

One can now take the overlap of the basis states to compute the rectangular amplitudes:

$$\langle {}^{1/2\ \ 1/2}_{0}|\hat{q}^{L_0-c/24}|{}^{0}_{1/2\ \ 1/2}\rangle = 4^{-4h_{1/2}} q^{-c/48}\left(1+\frac{(3-7p)^2(-2+p)}{2p(1+p)(3+p)}q+\dots\right)$$
$$\langle {}^{1/2\ \ 1/2}_{1}|\hat{q}^{L_0-c/24}|{}^{1}_{1/2\ \ 1/2}\rangle = 4^{2h_1-4h_{1/2}} q^{-c/48+h_1/2} \times\left(1+\left(\frac{9}{2}-\frac{3}{p}-\frac{45}{1+p}+\frac{80}{1+3p}\right)q+\dots\right).$$

We have verified that this small-q expansion matches the exact expression (2.29) up to order $\hat{q}^{10}$. Note that only even powers of $\hat{q}$ (even and odd of q, recall $\hat{q}=\sqrt{q}$) appear, since only even level descendants are present in the boundary states due to the left-right symmetry of the problem (odd level descendants are odd under left-right reversal, so do not appear).

Finally, we fix the normalization $\mathcal{N}^a$ following Cardy [48]. We demand that in the limit $\zeta \to 0$ of an infinitely long rectangle, the normalized conformal blocks[2] behave as

$$\mathcal{N}^a \mathcal{G}^a(1-\zeta) = 1 + O(\zeta)\,. \tag{2.30}$$

This because for a very long rectangle, one has in both cases $a=0$, $a=1$, the partition function of a horizontal strip with free boundary conditions on the sides. Both conformal blocks should give one in that limit. We have:

$$\mathcal{N}^0 = \frac{1}{F_{00}} = 2\sin\left(\frac{\pi}{6}(8h+1)\right) = \beta \tag{2.31}$$
$$\mathcal{N}^1 = \frac{1}{F_{20}} = \frac{\Gamma\left(\frac{4h}{3}+\frac{2}{3}\right)\Gamma(4h+1)}{\Gamma\left(\frac{8h}{3}+\frac{1}{3}\right)\Gamma\left(\frac{8h}{3}+\frac{4}{3}\right)}\,.$$

Here β is the fugacity of loops and F_{ij} are the F-matrices, eq. (1.50).

The results derived so far are valid for both dense and dilute loops, where in the first case the relation between the BCFT labels i and the Vir representations in Kac notation is $i \equiv (1, 1+2i)$, while in the second is $i \equiv (1+2i, 1)$.

We have seen in section 1.2.2 that at logarithmic points describing polymers (dense polymers $h=-1/8, c=-2$ and dilute polymers $h=5/8, c=0$) some conformal blocks are ill defined. The presence of a divergence is clearly a difficulty for the interpretation of the partition function as that of a statistical model. We will see in section 2.3.2 what is the precise geometrical interpretation of the partition functions $Z\left(0\,{}^{1/2}_{1/2}\,a\right)$. One expects physically that these partition functions should be well defined for every value of loop fugacity β, also at $\beta=0$, which is the case we are after for polymers. The solution to this is simply hidden in the normalization of the partition function, eq. (2.29). In the case of dense polymers $\mathcal{N}^0 = \mathcal{N}^1 = 0$. This does not come as a surprise, and should

[2]The relation between OPE coefficients and F-matrices (2.14) holds for a certain choice of normalization of fields [173]. Redefining $\phi_i^{ab} \to \lambda_i^{ab}\phi_i^{ab}$ and $|0\rangle \to \alpha|0\rangle$ we can eventually fix $\lambda_{1/2}^{0,1/2}$ and $\lambda_{1/2}^{1,1/2}$ so that the OPE structure constants satisfy the behavior of eq. (2.30)

be traced back to the presence of a single loop on the rectangle. Factorizing this trivial zero, one then gets for dense polymers the result:

$$Z\left(\begin{smallmatrix}0 & 1/2\\ 1/2 & 1\end{smallmatrix}\right)(h=-1/8) = Z\left(\begin{smallmatrix}0 & 1/2\\ 1/2 & 0\end{smallmatrix}\right)(h=-1/8) = \sqrt{L}\eta\theta_3^{-2}\frac{2}{\pi}K(1-\zeta)$$
$$= \sqrt{L}\eta\,,$$

K is the complete elliptic integral of the first kind of parameter ζ and we used the identity $2K(1-\zeta(\tau)) = \pi\theta(\tau)^3$. This result agrees with the Laplacian of the rectangle with D,N,D,N boundary conditions [29]. For dilute polymers one has

$$\mathcal{N}^0 \to \frac{\pi}{2}\epsilon + O(\epsilon^2)$$
$$\mathcal{N}^1 \to \frac{15}{32}\pi + O(\epsilon)\,.$$

Note that the indecomposability parameter $b = 5/6$ [105] is present explicitly in the coefficient, $h^2/b = 15/32$. The zero of $\mathcal{N}^0$ kills the divergence of $\mathcal{G}^0$, and finally we predict again degeneracy of both partition functions

$$Z\left(\begin{smallmatrix}0 & 1/2\\ 1/2 & 1\end{smallmatrix}\right)(h=5/8) = Z\left(\begin{smallmatrix}0 & 1/2\\ 1/2 & 1\end{smallmatrix}\right)(h=5/8) = L^{-5}\theta_3^{-10}S_2(1-\zeta)\,,$$

with S_2 defined in (1.49). The degeneracy we have observed could be understood more fundamentally as the gluing of the two sectors ϕ_0 and ϕ_1 in an indecomposable module corresponding to a single boundary condition.

We now discuss transformation properties of the partition function

$$Z\left(\begin{smallmatrix}0 & 1/2\\ 1/2 & a\end{smallmatrix}\right)(\tau) =$$

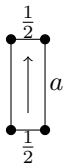

under modular inversion, $S : \tau \to -1/\tau$. Modular inversion interchanges length and width. At the same time a partition function can obviously be described either using time flowing say up or right, without changing the result. Then we expect that under S we have:

$$Z\left(\begin{smallmatrix}0 & 1/2\\ 1/2 & a\end{smallmatrix}\right)(-1/\tau) =$$

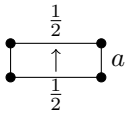

$$=$$

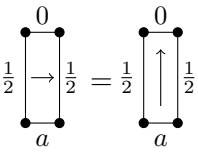

$$=$$

$$= Z\left(\begin{smallmatrix}1/2 & 0\\ a & 1/2\end{smallmatrix}\right)(\tau)\,.$$

One can then check that our result (2.29) satisfy this relation using standard transformation properties of theta functions under modular inversion (see e. g. [84]). In particular one uses that under S:

$$\mathcal{G}^a(1-\zeta) \to \mathcal{G}^a(\zeta)\,,$$

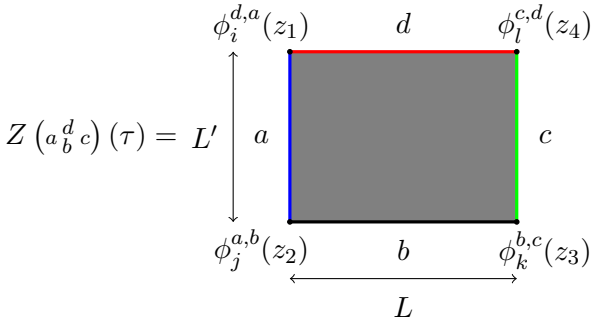

Figure 2.6: The partition function with different boundary conditions and operator insertion at the corners z_i.

and standard hypergeometric identities to write:

$$\mathcal{G}^a(\zeta) = \sum_{b=0,1} F_{ab}\mathcal{G}^b(1-\zeta)\,.$$

For explicit expressions of the the matrices $F_{ab} = F_{ab}\left[\begin{smallmatrix} 1/2 & 1/2 \\ 1/2 & 1/2 \end{smallmatrix}\right]$, see eq. (1.50).

General result

We now generalize the discussion presented above to the case of arbitrary boundary conditions a, b, c, d around the rectangle, see figure 2.6. We present here the results and refer for details to [29].

A partition function with generic boundary conditions can be written as:

$$Z\left(\begin{smallmatrix} & d & \\ a & & c \\ & b & \end{smallmatrix}\right) = \mathrm{a}\boxed{\begin{smallmatrix} \mathrm{d} \\ \uparrow \\ \mathrm{b} \end{smallmatrix}}\mathrm{c} = L^{w(i,j,k,l)}\langle B^d_{ac}|\hat{q}^{L_0-c/24}|B^b_{ac}\rangle \tag{2.32}$$

$$= L^{w(i,j,k,l)}\sum_s C^{adc}_{ils}C^{abc}_{jks}C^{aca}_{ss0}\mathcal{A}^{i,j,k,l}_s(\tau)\,. \tag{2.33}$$

The modular weight $w(i,j,k,l)$ is determined by general arguments [54] and is given by the anomaly at the corners (2.1):

$$w(i,j,k,l) = \frac{c}{4} - 2(h_i + h_j + h_l + h_k)\,. \tag{2.34}$$

We defined the amplitudes involving basis states as:

$$\mathcal{A}^{i,j,k,l}_s(\tau) = \begin{array}{ccc} \phi_i & & \phi_l \\ & \boxed{s}\uparrow & \\ \phi_j & & \phi_k \end{array} := \langle \begin{smallmatrix} i & l \\ & s \end{smallmatrix}|\hat{q}^{L_0-c/24}|\begin{smallmatrix} s \\ j & k \end{smallmatrix}\rangle$$
$$= \hat{q}^{h_s-c/24}\sum_{n\geq 0} c_n\hat{q}^n\,.$$

Inserting expressions of boundary states (2.12) in practice allows to obtain only the first few coefficients c_n of the power series. As shown in the example above, closed formulas can be obtained using CFT correlators. Now the amplitude contains only the channel s of the correlator of BCC fields at the corners, and has the following expression [29]:

$$\mathcal{A}_s^{i,j,k,l}(\tau) = 4^{-\frac{1}{3}(h_i+h_j+h_k+h_l)}\eta(\tau)^{-2w(i,j,k,l)}\mathcal{F}^s_{il;jk}(1-\zeta(\tau))\,, \tag{2.35}$$

where $\zeta(\tau)$ is given in eq. (2.28), and the conformal block[3] $\mathcal{F}^s_{il;jk}$ behaves for small argument as

$$\mathcal{F}^s_{il;jk}(z) \sim z^{h_s-\frac{1}{3}(h_i+h_j+h_k+h_l)}\,,$$

so that the normalization is consistent with that of our boundary states (2.13). We note that in the case of four $\phi_{1/2}$ fields discussed above, we found it convenient to introduce the functions $\mathcal{G}^a$, which are related to the functions $\mathcal{F}^a$ by:

$$\mathcal{G}^a(\zeta) = (\zeta(1-\zeta))^{4h/3}\mathcal{F}^a_{1/2,1/2;1/2,1/2}(\zeta)\,.$$

We now discuss the modular properties of rectangular amplitudes in the general case. We have already encountered the F-duality stating the associativity of the fusion product, relating conformal blocks singular near $\zeta = 0$ to those singular near $\zeta = 1$, eq. (2.15), which we recall:

$$\mathcal{F}^s_{ij;kl}(\zeta) = \sum_r F_{sr}\left[\begin{array}{cc} i & l \\ j & k \end{array}\right]\mathcal{F}^r_{il;jk}(1-\zeta)\,.$$

Another transformation acting in the space of conformal blocks is braiding, exchanging the position of ϕ_j and ϕ_k:

$$\mathcal{F}^s_{ij;kl}(\zeta) = \sum_r B_{sr}\left[\begin{array}{cc} i & l \\ j & k \end{array}\right]\mathcal{F}^r_{ik;jl}\left(\frac{1}{\zeta}\right)\,.$$

Let us remark now that the space of conformal blocks furnishes a representation of the modular group $\Gamma = \mathrm{PSL}(2,\mathbb{Z})$ with the following natural action:

$$M \circ \mathcal{F}(\zeta(\tau)) = \mathcal{F}(\zeta(M\tau))\,, \quad M \in \Gamma\,.$$

[3] A four point function can always be written as

$$\langle\phi_1(w_1)\phi_2(w_2)\phi_3(w_3)\phi_4(w_4)\rangle = \prod_{i<j} w_{ij}^{\mu_{ij}} G(\zeta)\,, \quad \mu_{ij} = \frac{1}{3}\left(\sum_{k=1}^4 h_k\right) - h_i - h_j\,,$$

where the function $G(\zeta)$ is a linear combination of conformal blocks. There several well-known ways for representing conformal blocks. There is a representation in terms of power series determined only by Virasoro algebra [84], and there is an integral representation in terms of Dotsenko-Fateev integrals [68]. Further, conformal blocks form a basis of solutions to null-vector differential equations associated to degenerate fields in the correlator as exploited above in the case of fields degenerate at level two.

Indeed one can relate $\zeta(M\tau)$ to $\zeta(\tau)$ using the explicit expression of the anharmonic ratio in terms of the modular parameter, eq. (2.28). For the generators $S:\tau\to-1/\tau$ and $T:\tau\to\tau+1$, one has

$$\zeta(S\tau)=1-\zeta(\tau)\,;\quad \zeta(T\tau)=\frac{1}{\zeta(\tau)}\,,$$

so that the action of T and S on conformal blocks is

$$\begin{aligned}S\circ\mathcal{F}^{s}_{ij;kl}(\zeta)&=\sum_r F_{sr}\left[\begin{smallmatrix} i & l\\ j & k\end{smallmatrix}\right]\mathcal{F}^{r}_{il;jk}(\zeta)\\ T\circ\mathcal{F}^{s}_{ij;kl}(\zeta)&=\sum_r B_{sr}\left[\begin{smallmatrix} i & l\\ j & k\end{smallmatrix}\right]\mathcal{F}^{r}_{ik;jl}(\zeta)\,.\end{aligned}$$

This action transfers immediately into modular covariance of rectangular amplitudes using eq. (2.35). Modular inversion S acts in an obvious way on the rectangle by interchanging its length and width:

$$\begin{aligned}S\circ\mathcal{A}^{i,j,k,l}_{s}(\tau)&=\mathcal{A}^{l,i,j,k}_{s}(-1/\tau)\\ &=\tau^{-w(i,j,k,l)}\sum_r F_{sr}\left[\begin{smallmatrix} i & l\\ j & k\end{smallmatrix}\right]\mathcal{A}^{i,j,k,l}_{r}(\tau)\,,\end{aligned}$$

where $\mathcal{A}^{l,i,j,k}_{s}(-1/\tau)=\langle {}^{l}_{s}\,{}^{k}|\hat{\tilde{q}}^{L_0-c/24}|{}_{i}^{\,s}\,{}_{j}\rangle$, $\hat{\tilde{q}}=e^{-i\pi/\tau}$. Note the appearance of the modular weight $w(i,j,k,l)$ from the transformation of η (2.23) (not present if considering the modular inversion of the full CFT partition function). Modular translation T instead deforms a rectangle to a rhombus, and its meaning could be understood from:

$$\begin{aligned}T\circ\mathcal{A}^{i,j,k,l}_{s}(-1/\tau)&=\mathcal{A}^{i,j,k,l}_{s}(-1/(\tau+1))\\ &=e^{i\pi w(i,j,k,l)/3}(\tau+1)^{-w(i,j,k,l)}\eta(\tau)^{-2w(i,j,k,l)}\mathcal{F}^{s}_{ij;kl}\left(\frac{1}{\zeta(\tau)}\right)\\ &=e^{i\pi w(i,j,k,l)/3}\left(\frac{\tau+1}{\tau}\right)^{-w(i,j,k,l)}\\ &\qquad\times\sum_r B_{sr}\left[\begin{smallmatrix} i & l\\ j & k\end{smallmatrix}\right]\mathcal{A}^{i,k,j,l}_{r}(-1/\tau)\,,\end{aligned}\tag{2.36}$$

where we used the transformation of η (2.24). Note that the amplitude $\mathcal{A}^{i,k,j,l}_{r}(-1/\tau)$ can be thought as the r-channel amplitude of a rectangle whose bottom, where operators $\phi^{a,b}_{j}$ and $\phi^{b,c}_{k}$ sit, has been twisted by π:

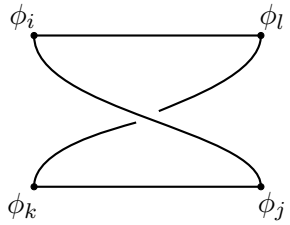

Recall that for the torus a Dehn twist by 2π at fixed time is exactly T; here we have $\hat{q}$ so the twist is the half. This should be the way to understand modular translation of rectangular amplitudes. In particular if the twisted amplitude is equal to the original one, as happens when $k = j$, we expect to have invariance (in the sense of equation (2.36)) under modular translations.

More generally modular transformations are powerful tools for constraining the objects we want to compute, and their usefulness are well appreciated for CFTs on cylinders and tori [43, 44]. For example we have seen in section 1.2.3 that for the cylinder geometry it gives the so-called Cardy states. The natural constraint for the rectangle[4] comes from imposing the consistency of the partition function upon switching the direction of imaginary time from vertical to horizontal:

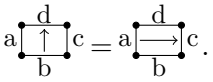

The resulting consistency equation

$$\sum_s C_{ijs}^{dab} C_{kls}^{bcd} C_{ss0}^{dbd} F_{sr}\left[\begin{array}{cc} i & l \\ j & k \end{array}\right] = C_{ilr}^{adc} C_{jkr}^{abc} C_{rr0}^{aca}$$

is simply stating the associativity of the fusion product of boundary fields, the so-called sewing constraint coming from crossing symmetry of correlators[138]. It has been shown in [173] that its solution is given by (2.14). Then, since we defined directly our boundary states in terms of physical boundary OPEs, consistency under modular inversion does not give any additional constraint.

2.3 Geometrical description of conformal blocks

2.3.1 Lattice boundary states

We now use the loop models to discretize the rectangular boundary states. The BCFT of loop models was discussed in section 1.2.4, and we recall that the primary fields are given by $\{\phi_j\}$, $j \in \frac{1}{2}\mathbb{Z}^{\geq 0}$, where the boundary labels are related to the Kac labels (1.43) by $j \equiv (1, 1+2j)$.

Define the normalized link state $|_i{}^s_j\rangle_L$ as:

$$|_i{}^s_j\rangle_L := \frac{1}{\sqrt{{}_L\langle {}^i_s |_i{}^s_j\rangle_L}}$$

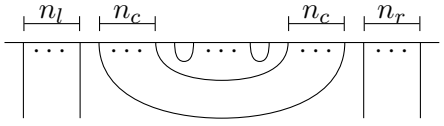

(2.37)

with

$$n_l + n_c = i\,; \quad n_r + n_c = j\,; \quad n_l + n_r = s\,.$$

[4] The action of the modular group on a rectangle has been discussed in [66, 130] in the case of percolation.

The norm of the state $\sqrt{{}_L\langle {}^{i}_{s}{}^{j}|{}_{i}{}^{s}_{j}\rangle_L}$ is computed using the loop scalar product, see the discussion around eq. (1.29). The link state has $s = n_l + n_r$ through lines, which as before, are supposed to be non-contractible, that is, the state is projected to the sector with exactly s non-contractible lines. The n_c lines inserted at the left corner are paired with the n_c ones inserted at the right corner, and during the time evolution of the state, these lines can propagate through the system or being contracted. Then we claim that $|{}_{i}{}^{s}_{j}\rangle_L$ flows in the continuum limit to the following basis state:

$$|{}_{i}{}^{s}_{j}\rangle_L \xrightarrow{\text{(FP)}} \alpha^{s}_{ij}|{}_{i}{}^{s}_{j}\rangle\,.$$

The limit to be taken is $L \to \infty$ with i, j, s fixed, and we keep only the finite part (noted as (FP)) which is supposed to be described by the CFT, as will be discussed more precisely below. This identification corroborates the interpretation of the boundary operators ϕ_j and ϕ_i as inserting respectively $j = n_r + n_c$ lines at the right corner and $i = n_l + n_c$ lines at the left corner. In the simplest case of no line insertion the boundary state is simply

$$|{}_{0}{}^{0}_{0}\rangle_L := \tfrac{1}{\sqrt{\beta^L}}|\cup\cdots\cup\rangle \xrightarrow{\text{(FP)}} \alpha^{0}_{00}|{}_{0}{}^{0}_{0}\rangle\,.$$

The precise sense in which these lattice boundary states are discretization of the CFT ones is the following. Denote by $|k\rangle_L$ the k-th eigenvector (normalized according to the loop scalar product) of the Hamiltonian of the loop model restricted to the sector with s through lines. Due to the anomaly at the corners (see eq. (2.34)), scalar products between a lattice rectangular boundary state $|B\rangle_L$ and $|k\rangle_L$, are expected to scale as:

$$-\log({}_L\langle B|k\rangle_L) = a_0 L + a_1 \log L + a_2 + \frac{a_3}{L} + \frac{a_4}{L^2} + O\left(\frac{1}{L^3}\right)\,,$$

with

$$a_1 = 2(h_l + h_r) - \frac{c}{8}\,,$$

h_l, h_r being the weights of BCC operators in the corners. The value of the CFT scalar product $\langle B|k\rangle$ is then extracted from

$$a_2 = \gamma - \log(\langle B|k\rangle)\,,$$

γ determined normalizing $\langle B|0\rangle = 4^{h_s - h_i - h_j}$, see eq. (2.13). In [26, 29] we reported the details of the numerical computations for first few excited states $|k\rangle$, supporting the above identification of lattice boundary states. Finally, we note that the state defined in (2.37) is of course not the only microscopic state giving rise to $|{}_{i}{}^{s}_{j}\rangle$ in the continuum limit. Any similar state obtained via local modifications (e. g. by allowing a finite number of arches between the through lines etc.) would obey the same property, albeit with a different value of the coefficient α^{s}_{ij}. Then these coefficients are then expected to be non-universal and cannot be predicted by the CFT.

Given a CFT rectangle boundary state $|B^b_{ac}\rangle = \sum_s C^{abc}_{ijs}\sqrt{C^{aca}_{ss0}}|_i{}^s_j\rangle$, and the discretization of basis states introduced above in eq. (2.37), we can define the more general lattice boundary state as combination of lattice basis states

$$|B^b_{ac}\rangle_L = \sum_s D^{abc}_{ijs}|_i{}^s_j\rangle_L \,.$$

We expect then that $|B^b_{ac}\rangle_L \xrightarrow{\text{(FP)}} |B^b_{ac}\rangle$ if

$$D^{abc}_{ijs} := C^{abc}_{ijs}\sqrt{C^{aca}_{ss0}}\frac{1}{\alpha^s_{ij}} \,. \tag{2.38}$$

With these objects by construction one discretizes CFT rectangle partition functions. Note indeed that $|B^b_{ac}\rangle_L$ are normalized in order to obtain in the continuum the CFT states $|B^b_{ac}\rangle$, and the CFT partition functions (2.32), when taking overlaps. In particular they provide a way to impose conformal boundary conditions on the lattice, so to discretize in generality correlators of BCC operators. Conformal boundary conditions from loop models were discussed in particular in [158].

Using the lattice boundary state one can obtain more explicit results. We just mention that as the crossing symmetry of correlation functions (or rectangular amplitudes) is a powerful tool for constraining OPE structure constants in the continuum theory, also lattice crossing symmetry allows to derive constraints for the coefficients D's appearing in eq. (2.38) and to compute ratios of the coefficients α's from a lattice computation. See figure 2.7 for an illustration of lattice crossing symmetry. The details can be found in [29].

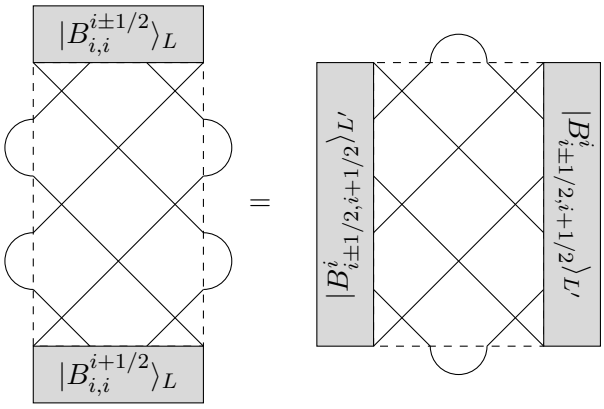

Figure 2.7: Example of lattice crossing symmetry for the case of one-leg insertions at the corners (boundary labels change by $\pm 1/2$) for a lattice of size $L \times L'$.

Always referring to the CFT of loop models, we note that the BCC operator between two boundary conditions labeled by j, j' is $\phi^{j,j'}_{|j-j'|}$ (lowest eigenstates of the strip Hamiltonian), and the fusion rules of these operators are:

$$\phi^{i,j}_{|i-j|} \otimes_f \phi^{j,k}_{|j-k|} = \sum_{s\in\mathcal{I}'} \phi^{i,k}_s \,.$$

The allowed fusion channels, those for which the OPE coefficients are not zero, are $\mathcal{I}' = (\{|i-k|, |i-k|+2, \ldots, i+k\} \cap \{||i-j|-|j-k||, ||i-j|-|j-k||+2, \ldots, |i-j|+|j-k|\})$. This restriction comes from the compatibility of the number of lines inserted by the fields in the corners and that which is allowed by the boundary conditions. We depict in figure 2.8 the geometric interpretation of the two-point function of BCC operators as the contraction of $|i-j|$ lines originating from the point in which the boundary condition is changed from i to j and terminating at the point in which we change from j to i.

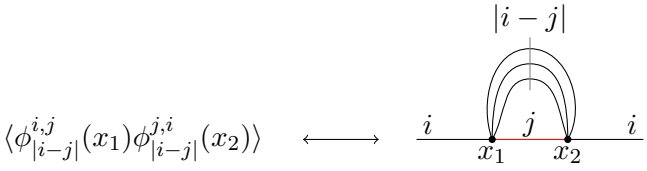

Figure 2.8: Geometric interpretation of the two-point function of BCC operators.

2.3.2 Probabilistic interpretation

Given the geometrical interpretation of boundary states in terms of lines insertions in the loop model, we can now push the discussion further and associate a geometric picture in terms of loop configurations to conformal blocks building the correlator of BCC operators. The amplitude $\mathcal{A}_s^{i,j,k,l}(\tau) = \langle {}^{i\ \ l}_{\ s} | \hat{q}^{L_0 - c/24} | {}_{j}^{\ s}{}_{k} \rangle$ is associated to

$$ {}_L\langle {}^{i\ \ l}_{\ s} | T^{L'} | {}_{j}^{\ s}{}_{k} \rangle_L \xrightarrow{\text{(FP)}} \alpha^s_{jk}\alpha^s_{il}\mathcal{A}_s^{i,j,k,l}(\tau)\,. $$

T is the transfer matrix of the loop model and $|{}_{j}^{\ s}{}_{k}\rangle_L$ are the discretizations of the basis states $|{}_{j}^{\ s}{}_{k}\rangle$ discussed above. We depict in figure 2.9 two configurations contributing to the lattice amplitude ${}_L\langle {}^{1\ \ 1}_{\ 1} | T^{L'} | {}_{1}^{\ 1}{}_{1} \rangle_L$, and one to the amplitude ${}_L\langle {}^{1\ \ 1}_{\ 2} | T^{L'} | {}_{1}^{\ 2}{}_{1} \rangle_L$, drawing only lines inserted at the corners.

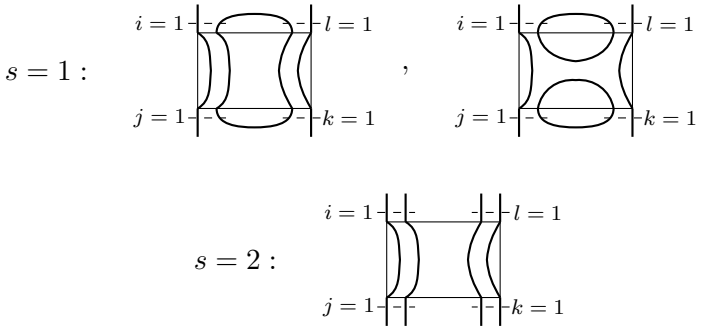

Figure 2.9: Configurations contributing to the lattice amplitudes ${}_L\langle {}^{1\ \ 1}_{\ s} | T^{L'} | {}_{1}^{\ s}{}_{1} \rangle_L$ for $s = 1, 2$.

We see that $\mathcal{A}_s^{i,j,k,l}(\tau)$ is then associated to the continuum limit of lattice amplitudes where we insert $2i$ lines in the top left corner, $2l$ in the top right, $2j$ in the bottom left and $2k$ in the bottom right. $2s$ of the lines at the bottom and at the top (the most exterior ones) are forced to propagate. The other lines instead can or not be contracted. Only if $s = i+l = j+k$ ($s = 2$ in the example of figure 2.9), the amplitude is associated to configurations where all lines inserted at the corners are forced to propagate. For example, the CFT partition function of figure 2.10 will be $Z\left(\begin{smallmatrix} 0 & i \\ i & i+j \end{smallmatrix}\right) \propto L^w \mathcal{A}_{i+j}^{i,i,j,j}$.

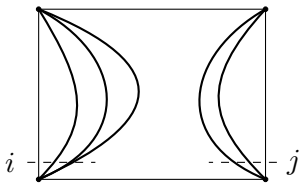

Figure 2.10: A schematic illustration of the partition function for a loop model where we insert i lines in the bottom left corner and j in the bottom right one, and we impose that $s = i + j$ lines propagate vertically.

The only term in the amplitude sensible to the changing of the number of through lines (associated to different fusion sectors) is the conformal block. Then we are led to the geometrical identification of conformal blocks which we schematically represent as

$\mathcal{F}_{il;jk}^s(1-\zeta) \longleftrightarrow$ 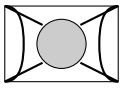

where the diagram on the right has a fixed number s of through lines and the bubble stays for the possibility of contracting or not the other lines inserted at the corner.

We recall that a partition function Z is given in general by a sum of amplitudes from the relation (2.33), and its geometric interpretation follows from that of the amplitude.

We can easily obtain interesting results from the discussion above as follows. Let us now specify to the case of one line insertion at every corner, $i = j = k = l = 1/2$, for which explicit expressions of the amplitude has been given in section 2.2.2. The partition function

$$Z\left(\begin{smallmatrix} 0 & 1/2 \\ 1/2 & 1 \end{smallmatrix}\right)(\tau) = \mathcal{N}^1 \eta^{-c/2}(\tau)\theta_3^{16h}(\tau)\mathcal{G}^1(1-\zeta) \propto L^w \mathcal{A}_1(\tau)$$

is unambiguously the (universal part of the) continuum limit of a loop model where the two lines inserted at left and right bottom corners are constrained to propagate in the vertical direction. Consequently

$$Z\left(\begin{smallmatrix} 1/2 & 0 \\ 1 & 1/2 \end{smallmatrix}\right)(\tau) = \mathcal{N}^1 L^w \eta^{-c/2}(\tau)\theta_3^{16h}(\tau)\mathcal{G}^1(\zeta(\tau)) \propto (L')^w \mathcal{A}_1(-1/\tau)\,,$$

is then the partition function of a loop model with the two lines inserted at left bottom and left top corners constrained to propagate in the horizontal direction. Then one can interpret the conformal blocks $\mathcal{G}^a$ as in the top of figure 2.11. The geometric interpretation of every other amplitude involving boundary states with $\phi_{1/2}$

insertions at the corners will follow from the decomposition in terms of $\mathcal{A}_1(\tau)$ and $\mathcal{A}_1(-1/\tau)$. For example for $\mathcal{A}_0(\tau)$, we can use the hypergeometric identity $\mathcal{G}^0(1-\zeta) = 1/F_{10}\mathcal{G}^1(\zeta) - F_{11}/F_{10}\mathcal{G}^1(1-\zeta) \propto \mathcal{G}^1(\zeta) + 1/\beta\mathcal{G}^1(1-\zeta)$, F_{ij} F-matrices (1.50), see the bottom of figure 2.11.

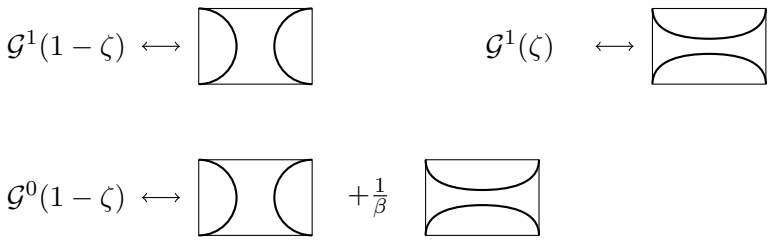

Figure 2.11: Geometric interpretation of the conformal blocks $\mathcal{G}^1$ and $\mathcal{G}^0$. Thick lines represent the non-contractible lines created by the one-leg operators in the corners propagating or not through the system (time is flowing upwards).

We have seen that the two elementary events which can happen when inserting a line in each corner are described by $\mathcal{G}^1(1-\zeta)$ and $\mathcal{G}^1(\zeta)$. Then, the probability of having these two lines flowing vertically is:

$$P(\tau) = \frac{\square\!\square}{\square\!\square + \square\!\square} = \frac{Z\left(\begin{smallmatrix}0 & 1/2\\ 1/2 & 1\end{smallmatrix}\right)(\tau)}{Z\left(\begin{smallmatrix}0 & 1/2\\ 1/2 & 1\end{smallmatrix}\right)(\tau) + Z\left(\begin{smallmatrix}1/2 & 0\\ 1 & 1/2\end{smallmatrix}\right)(\tau)} = \frac{\mathcal{G}^1(1-\zeta)}{\mathcal{G}^1(1-\zeta)+\mathcal{G}^1(\zeta)} \tag{2.39}$$

and horizontally it is $1 - P(\tau)$. Note that whatever normalization drops out since it is common to both partition functions.

We first consider the case of percolation, for which $\beta = 1$, corresponding to $c = h = 0$. We have:

$$\begin{aligned} P_{c=0,\text{dense}}(\zeta) &= \frac{(1-\zeta)^{\frac{1}{3}}{}_2F_1\left(\frac{1}{3},\frac{2}{3};\frac{4}{3};1-\zeta\right)}{(1-\zeta)^{\frac{1}{3}}{}_2F_1\left(\frac{1}{3},\frac{2}{3};\frac{4}{3};1-\zeta\right) + \zeta^{\frac{1}{3}}{}_2F_1\left(\frac{1}{3},\frac{2}{3};\frac{4}{3};\zeta\right)} \\ &= \frac{\Gamma(\frac{2}{3})}{\Gamma(\frac{4}{3})\Gamma(\frac{1}{3})}(1-\zeta)^{\frac{1}{3}}{}_2F_1\left(\frac{1}{3},\frac{2}{3};\frac{4}{3};1-\zeta\right) \\ &= \frac{\Gamma\left(\frac{2}{3}\right)}{\Gamma\left(\frac{1}{3}\right)\Gamma\left(\frac{4}{3}\right)}(1-\zeta)^{\frac{1}{3}}\left(1-\frac{1}{6}(1-\zeta)+\frac{5}{63}(1-\zeta)^2+O\left((1-\zeta)^3\right)\right). \end{aligned}$$

This quantity is precisely the crossing probability computed by Cardy [45, 48], that is, the probability that there is at least one Fortuin-Kasteleyn (FK) crossing cluster spanning the rectangle in the vertical direction. We now comment on this relation. Microscopically, the configurations of loops contributing to the numerator of our formula are those where the two lines inserted at the corners propagate from bottom to top. In terms of FK clusters (for the relation between loops and clusters see figure 1.1), this corresponds to count cluster configurations with "wired" boundary conditions on top

and bottom rows, and to the constraint that there is at least one spanning cluster crossing the rectangle, see figure 2.12. Call such ensemble of cluster configurations $\mathcal{S}_w$.

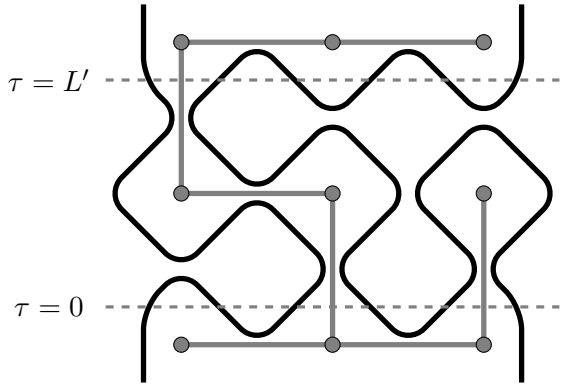

Figure 2.12: A configuration of loops (black) and the corresponding configuration of Fortuin-Kasteleyn clusters (gray). The through lines inserted at the bottom corners are forced to propagate to the top, and wired boundary conditions (all bonds open) are imposed on the links of the bottom and top rows of the lattice where the Fortuin-Kasteleyn clusters live. $\tau = 0$ and $\tau = L'$ are initial and final discrete imaginary times of the transfer matrix evolution in the vertical direction.

Instead the configurations counted by Cardy's formula, which we denote by $\mathcal{S}$, are simply those with at least one spanning cluster, without imposing wired boundary conditions. We now show that

$$\#(\mathcal{S}) = 2^L \times 2^L \times \#(\mathcal{S}_w)\,, \tag{2.40}$$

where $\#(E)$ is the number of elements of the set E. First note that changing the status (open or closed) of links in the bottom and top rows of the lattice where FK clusters live, transforms a configuration $s \in \mathcal{S}$ into another $s' \in \mathcal{S}$. Then we can group the spanning configurations $\mathcal{S}$ in classes whose elements differ only by the status of bottom and top links, and for each class we choose the representative with all the bottom and top links open. Since there are $2^L \times 2^L$ (first factor for the possible status of top links and second for those of bottom links) elements in each class, eq. (2.40) follows. Now note that also the set of all possible (not only spanning) cluster configurations can be divided in classes with elements differing by the status of top and bottom links as before. Then, if we compute the crossing probability by dividing the number of spanning configurations $\#(\mathcal{S})$ by the number of all possible configurations, the multiplicative factor $2^L \times 2^L$ drops out, and the equality of our formula with Cardy's one is established. The above argument does not work anymore when we have generic weight of clusters β, since spanning configurations cannot be regrouped then due to the different powers of β weighting each configuration. Crossing probabilities for generic fugacity β have been computed using SLE methods, see [16].

We assume now that the geometric interpretation of boundary states goes through also in the dilute case, then in particular (2.39) should also be valid, where now the value

of h in (1.46) is $h_{2,1}$. It is of interest to see then what is the behavior of probabilities (2.39) at the logarithmic points discussed above, $c = -2$ dense and $c = 0$ dilute. The outcome is that probabilities are well defined but their expansion shows logarithmic terms. For a tall rectangle $1 - \zeta \to 0$ we have (K is the complete elliptic integral of the first kind)

$$\begin{aligned} P_{c=-2,\text{dense}}(\zeta) &= \frac{K(1-\zeta)}{K(1-\zeta)+K(\zeta)} \\ &= \frac{\pi}{\pi - \log\left(\frac{1-\zeta}{16}\right)} + \frac{\pi(1-\zeta)}{2\left(\pi - \log\left(\frac{1-\zeta}{16}\right)\right)^2} + O\left((1-\zeta)^2\right) . \end{aligned}$$

and (S_2 is the hypergeometric function defined in (1.49))

$$\begin{aligned} P_{c=0,\text{dilute}}(\zeta) &= \frac{S_2(1-\zeta)}{S_2(1-\zeta)+S_2(\zeta)} \\ &= \frac{15\pi}{32}(1-\zeta)^2 + \frac{15\pi}{32}(1-\zeta)^3 \\ &\quad + \frac{75\pi\left(12\log\left(\frac{1-\zeta}{16}\right) + 12\pi - 1\right)}{4096}(1-\zeta)^4 + O\left((1-\zeta)^5\right) . \end{aligned}$$

We are not aware of a previous derivations of these probability formulas for for self avoiding walks.

Note that since $P(1-\zeta) = 1 - P(\zeta)$, the same series plus the constant term holds for a very long rectangle ($\zeta \to 0$) replacing $1 - \zeta$ by ζ. We have already seen how rectangular amplitudes contain the OPE structure constants, and now we see that for logarithmic CFTs the indecomposability parameters [105] (contained in the F-matrices), here $b = 5/6$ for dilute polymers, show up in geometric observables.

Note also that expressing the anharmonic ratio in terms of the modular parameter q through eq. (2.28)

$$\log(1-\zeta) = \log(16) + \log(\sqrt{q}) - 8\sqrt{q} + \dots$$

integer powers of τ enter explicitly the expression of the probability. This feature is a consequence of the Jordan form of the transfer matrix in these cases.

More generally one could replace the ill-behaved conformal blocks in the logarithmic cases by a combination of them which has probabilistic interpretation and which is expected to be well defined even if the conformal blocks themselves are singular or degenerate. Unfortunately writing down explicitly such a probabilistic basis in the space of conformal blocks does not seem to be simple for higher number of line insertions. Indeed we do not know how to associate precisely a conformal block to a given propagation of lines (as discussed at the beginning of section 2.3.2), but more importantly, we do not know how to fix the normalization.

Chapter 3

Quantum network models and classical geometrical models

This chapter is a review chapter where we relate the geometrical models and the conformal field theories introduced previously to the network models describing quantum Hall transitions. Section 3.1 contains a description of the integer quantum Hall effect and of the Chalker-Coddington model. After a pedagogical discussion of the bosonic representation of quantum transport observables in the network model, we develop the supersymmetry method for performing disorder average, and we establish the relations to geometrical models of 2D statistical mechanics. The emphasis is put on symmetry aspects of the various theories. Then we describe the general framework of symmetry classes of disordered fermions, and introduce the spin quantum Hall effect, studied in section 3.2. There we adapt the tools developed before to the spin quantum Hall network model and derive the mapping of certain disorder averaged quantities to percolation. This mapping is used to infer several exact properties for the spin quantum Hall transition, in particular we derive the exact conductance for the strip and cylinder geometry using conformal field theory.

3.1 The Chalker-Coddington model

3.1.1 Integer quantum Hall effect

The experimental discovery

The classical Hall effect predicts that in the presence of a magnetic field, the passage of a current induces a voltage perpendicular to the direction of the current flow (or alternatively that current flows in a direction perpendicular to an applied electric field). The experimental setup is as in figure 3.1. The Hall resistivity is then predicted to be proportional to the intensity of the magnetic field.

Von Klitzing discovered in 1980 that at low temperature and high magnetic field, the Hall resistance (equal in 2D to the resistivity) of a two-dimensional electron gas shows

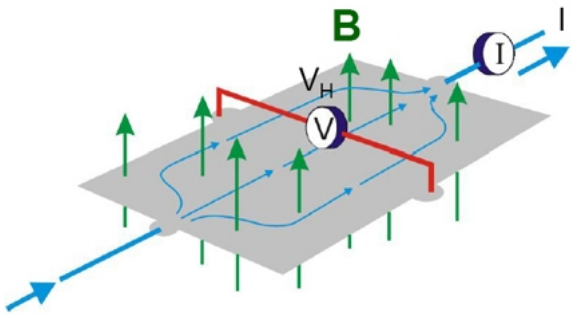

Figure 3.1: Setup for measurement of the Hall resistance. B is the magnetic field perpendicular to the two-dimensional sample, I is the current and V_H is the measured Hall voltage. The Hall resistance is $R_H = V_H/I$.

very well defined plateaus at integer fractions ν of h/e^2 [193], see figure 3.2:

$$R_H = \frac{1}{\nu}\frac{h}{e^2}\,. \tag{3.1}$$

Equivalently, the Hall conductance $\sigma_H = 1/R_H$ is quantized. In the plateau region the longitudinal conductance $\sigma_{xx} = R_{xx}$ vanishes. This phenomenon is called the integer quantum Hall effect (IQHE), and its discovery had such an impact that Von Klitzing was awarded the Nobel prize in 1985. The quantization of the Hall conductance does not depend much on the microscopic details of the sample and its accuracy is so high that it is used as a standard method in metrology.

Phenomenological theory of the IQHE

From a theoretical perspective the IQHE is a very interesting problem. Here we will discuss the basic explanation of the effect, on which several good reviews exist, such as [63, 96, 119, 162].

The starting point for a theoretical approach is the quantum mechanical Hamiltonian for a single spinless electron in two dimensions in a perpendicular magnetic field

$$H_0 = \frac{1}{2m}\left(\vec{p} + e\vec{A}\right)^2\,.$$

$\vec{A}$ is the vector potential (chosen in the gauge $A = B(0, x, 0)$), m is the effective mass containing the effect of lattice atoms and interactions, $-e$ is electron charge. The system is translational invariant along y, and the problem takes the form of a harmonic oscillator (along x) whose solution is well known. The energy levels (Landau levels) are quantized

$$E_n = \left(n + \frac{1}{2}\right)\hbar\omega_c\,, \quad n = 0, 1, \ldots$$

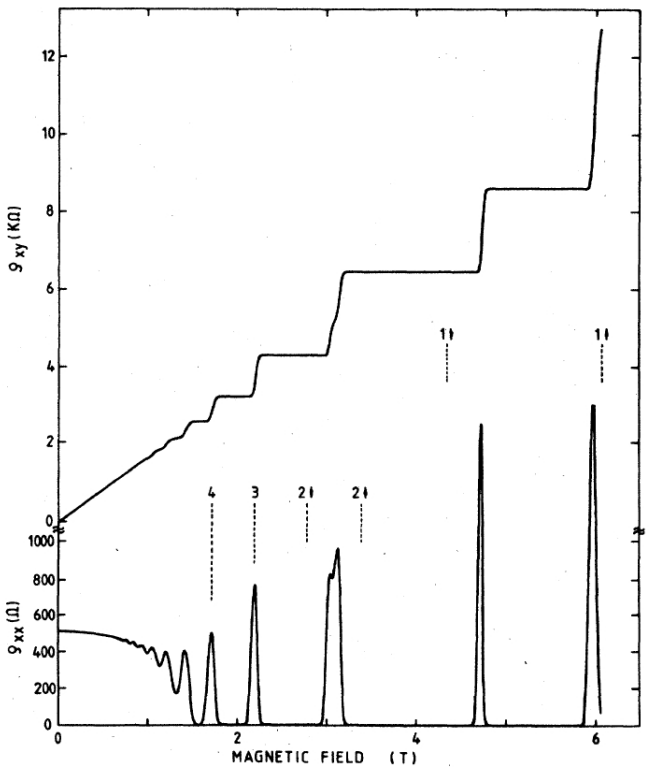

Figure 3.2: Experimental curves of Hall resistance $R_H = \rho_{xy}$ and longitudinal resistivity ρ_{xx} as a function of the magnetic field at fixed carrier density. Increasing the magnetic field the resistance departs from the classical linear behavior. Picture taken from [193].

with $\omega_c = eB/m$ called the cyclotron frequency. The spatial extension of Landau states is governed by the magnetic length $\ell = \sqrt{\hbar/eB}$, and since E_n does not depend on k, the momentum along y, they have huge degeneracy. The number of occupied Landau levels is given by the filling fraction ν:

$$\nu = 2\pi\ell^2\rho = \frac{\rho}{B/\phi_0}\,,$$

with ρ the density of states, and ϕ_0 the flux quantum. Integer values of ν correspond to the Hall resistance of (3.1). However this does not explain the plateau, since changing ρ we provide additional particles able to carry current continuously. The explanation of the IQHE requires two more ingredients, *disorder* and *edge states*. Disorder is induced by impurities in the sample and is modeled as a random potential $V(\vec{r})$ in the Hamiltonian:

$$H = H_0 + V(\vec{r})\,.$$

Its qualitative effect on the energy spectrum is to broaden Landau levels into bands as in figure 3.3.

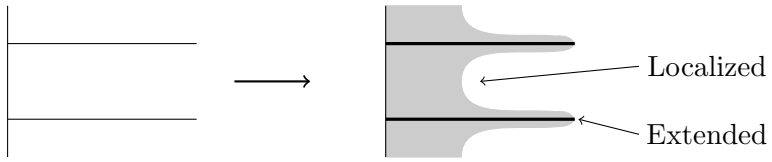

Figure 3.3: Broadening of Landau levels into bands (here plotted energy versus density of states) as disorder is switched on. At the band center extended states exist, while in the tails states are localized.

The band tails correspond to states whose wavefunctions are exponentially localized to the extent of the localization length ξ:

$$|\psi^2(\vec{r})| \sim \exp\left(-|\vec{r}|/\xi\right)\,.$$

This is the phenomenon of Anderson localization. Exponentially decaying functions cannot contribute to electrical transport, meaning that in particular for filling fractions corresponding to the energy regions of localized states, the longitudinal conductance vanishes. Near the band center however extended states appear, which spread across the entire system and contribute to transport. At this point the localization length ξ diverges and the system undergoes the plateau transition.

Clearly this picture still does not explain what are the states responsible of carrying current contributing to the Hall conductance. The answer is given by the presence of a boundary in the real sample, where there are edge states escaping Anderson localization. In a clean system, the presence of a confining potential at a boundary modifies the Landau levels [107] as in figure 3.4.

The Fermi energy intersects a given number of edge states N corresponding to the bulk Landau level N. Edge states acquire longitudinal velocity [33]:

$$v_{nk} = \frac{1}{\hbar}\frac{\mathrm{d}E_{nk}}{\mathrm{d}k} = \frac{1}{\hbar}\frac{\mathrm{d}E_{nk}}{\mathrm{d}x_0}\frac{\mathrm{d}x_0}{\mathrm{d}k}\,,$$

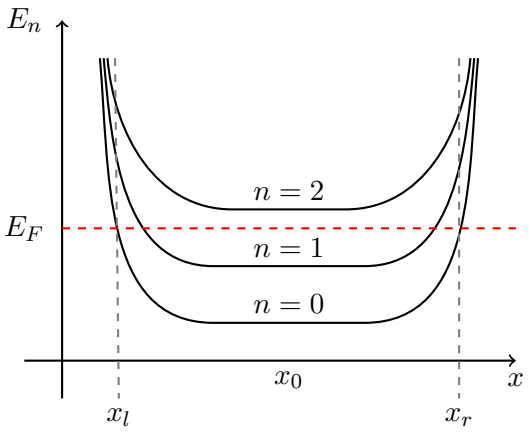

Figure 3.4: Energy levels E_n in a system with confining potential (walls at x_l and x_r). x_0 is the center of cyclotron motion. E_F is the Fermi energy intersecting the number of edge states contributing to transport.

whose sign depends on the slope of the energy as a function of the position x. We have then chiral counter propagating edge states at the two boundaries which are responsible of carrying the current. Note that at the band center x_0 ($x_0 = -k\ell^2$ from the wave functions of the harmonic oscillator) the electrons do not carry any current. When disorder is considered, the final picture we have is that electrons in the bulk do not contribute to transport (are localized), while at the boundaries chiral edge states occur, see figure 3.5.

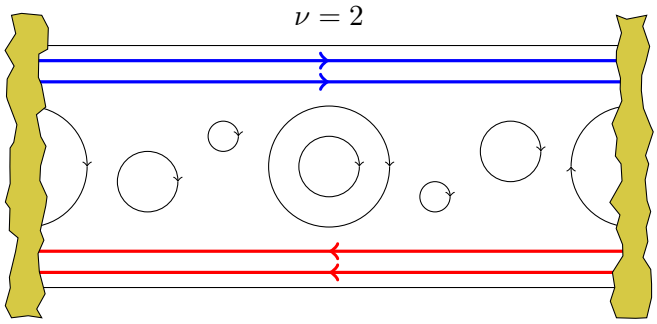

Figure 3.5: In an integer quantum Hall sample bulk states are localized due to disorder (loops), while there are extended chiral edge states at the boundary contributing to transport. The conductor is connected to reservoirs at the extremities.

Assuming that the width of the sample is big enough to have suppression of backscattering (destructive interaction between the edge states at the two boundaries), one can show [33] using the Landauer-Büttiker formalism for quantum transport, that the presence of ν edge states in a disordered conductor gives in the experimental setup (four-

terminal measurement) the observed Hall resistance (3.1).

We concentrate now on the physics of the plateau transition and discuss first an appealing semiclassical description of the quantum Hall effect based on a percolation model.

The percolation model

We consider now the motion of an electron in a smooth random potential. We assume that the magnetic field is very large so that the magnetic length is very small compared to the scale over which the potential varies. This assumption corresponds to a semiclassical limit where the wave functions live on contour lines of constant energy in the landscape of the random potential, thick lines in figure 3.6. The motion is directed due to the presence of the magnetic field. Low lying states will be along contours in "deep valleys" (minus signs in figure 3.6), while high energy levels will encircle high "mountains top" (plus signs in figure 3.6). At an intermediate energy, isopotential lines percolate, and there will be extended states, corresponding to the plateau transition. It is useful to think about the Fermi energy as the level of water poured in the random landscape [96]. If the system has boundaries, the confining potential will allow trajectories (edge states) for electrons which connect the contacts.

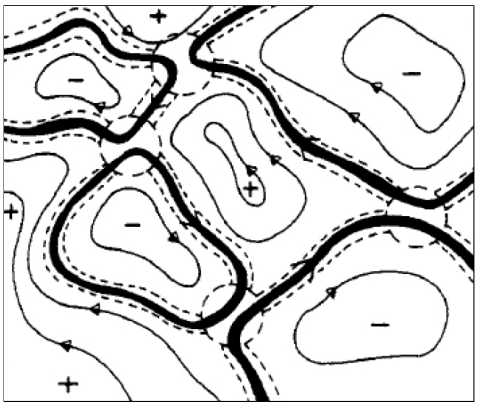

Figure 3.6: Landscape of a disordered potential whose minima and maxima are denoted by $+$ and $-$. Thick lines are contour levels at given potential V_0 and arrows stand for the directed motion of electrons. Figure taken from [55].

Then we may argue that the plateau transition occurs at a critical energy E_c corresponding to the classical percolation threshold. The localization length would coincide with the correlation length in percolation, which implies [189]

$$\xi \sim |E - E_c|^{-\nu} ,$$

with $\nu = 4/3$. This picture although being useful as intuition, is wrong, since the critical behavior observed by direct study of disordered Schrödinger equations has an exponent ν

larger, of the order of ~ 2.3, which agrees with the value determined experimentally (see references in [63] for example). The above picture neglects quantum tunneling between different isopotentials, occurring at circular regions in figure 3.6, corresponding to the saddle points of the potential. Chalker and Coddington in [55] have shown that one can obtain a larger exponent, of the order of the expected one, if one includes in the percolation picture quantum tunneling[1]. This model is an example of network model whose properties will be discussed in details in the next sections.

3.1.2 Quantum transport in the network model

The Chalker-Coddington (CC) model [55] is a lattice model proposed to describe the universality class of the IQH transition. As discussed above, under the assumptions of slowly varying potential on the scale of the magnetic length, the motion of guiding centers of electrons is confined to isopotential lines. This motion is unidirectional due to the presence of a magnetic field, breaking time reversal invariance. At a saddle point of the disordered potential, wave functions can tunnel. This quantum dynamics is encoded in a scattering matrix S, relating incoming waves to outgoing ones. There are two possibilities according to the chiralities of links, that we label as vertices of type A or B, see figure 3.7. Call $\psi(e)$ the wavefunction amplitude on link e of the lattice, so that S_s, $s = A, B$, is defined by:

$$\begin{pmatrix} \psi(e_1') \\ \psi(e_2') \end{pmatrix} = S_s \begin{pmatrix} \psi(e_1) \\ \psi(e_2) \end{pmatrix} = \begin{pmatrix} \alpha & \beta \\ \gamma & \delta \end{pmatrix} \begin{pmatrix} \psi(e_1) \\ \psi(e_2) \end{pmatrix} . \tag{3.2}$$

Figure 3.7: Vertices corresponding to saddle points. A and B are the two sublattices.

Since we want to model a disordered potential, we choose to take the scattering matrices as random U(2) matrices. $S_s \in \mathrm{U}(2)$ admits the polar decomposition:

$$S_s = \begin{pmatrix} e^{i\varphi_1} & 0 \\ 0 & e^{i\varphi_2} \end{pmatrix} \begin{pmatrix} \sqrt{1-t_s^2} & t_s \\ -t_s & \sqrt{1-t_s^2} \end{pmatrix} \begin{pmatrix} e^{i\varphi_3} & 0 \\ 0 & e^{i\varphi_4} . \end{pmatrix} \tag{3.3}$$

which we interpret as assigning random phases φ_i's to links rather than to nodes, while t parametrizes an orthogonal matrix, describing tunneling at the node. Note that taking all transitions amplitudes to be positive would violate unitarity.

[1]The value of ν determined numerically with the network model heavily suffers from finite size corrections. However the most recent estimate of this exponent at the moment of writing, is [155] $\nu = 2.62 \pm 0.06$. This value is actually larger than the one observed experimentally, questioning the validity of the Chalker and Coddington model (and more generally of a single particle model) as a theory for the IQH transition, but we will not discuss this issue here.

Describing the situation of figure 3.6 would require to study a topologically disordered network. Instead, following [55] we suppose that randomness in link phases alone is sufficient, and we study only a directed square network, like that of figure 3.8, where "+" and "−" correspond to valleys and hills of the disordered potential. We choose to

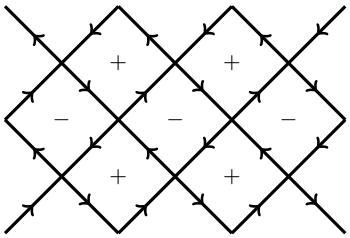

Figure 3.8: The square directed network of the Chalker-Coddington model. Vertices are the saddle points of the disordered potential, dividing maxima (+) and minima (−).

take the parameters t_s in (3.3) to depend only on the type of sublattice A, B, and not on the node under consideration. t_A^2 (t_B^2) is the probability for the scatterers to turn right (left) at node A (B). The isotropic point is $t_A^2 + t_B^2 = 1$. We remark that the lattice is the same as the medial lattice of the classical Potts model of section 1.1.

The wave function of the network at given time t is the collection of link wave functions $\psi_t(e)$, and we consider the discrete time evolution given by the scattering matrices S. Calling the unitary evolution operator $\mathcal{U}$, the dynamics is

$$\psi_{t+1}(e') = \mathcal{U}(e', e)\psi_t(e)\,.$$

$\mathcal{U}$ is an $|E| \times |E|$ sparse matrix ($|E|$ being the number of links in the lattice) whose building blocks are given by (3.3).

While the phases of (3.3) are taken to be random, the parameter t is not. To understand why, it is useful to consider the geometry of a strip, and take the two extreme limits $t_A = 1, t_B = 0$, or $t_A = 0, t_B = 1$, see figure 3.9. In the first case left turns are suppressed and only closed loops corresponding to localized states are present, and the system is in an insulating phase, with zero conductance. In the second case right turns are suppressed, and while in the bulk of the system there are closed loops corresponding to localized states, at the boundaries there are chiral edge states escaping localization, and the system is in the $\nu = 1$ quantum Hall state, with non-zero Hall conductance. We see that t plays the role of filling fraction ν in the IQHE, and we expect the plateau transition to occur at the symmetric value $t_A = t_B = 1/\sqrt{2}$ (at the isotropic point), where probabilities for turning left or right at a node are equal.

We define the Green function for propagation from link e to e' in the network as[2]:

$$G(e, e'; z) = \langle e | \left(1 - z\mathcal{U}\right)^{-1} | e' \rangle \tag{3.4}$$

[2]In the case of continuous time, one has the usual definition using the resolvent $(E \pm i0 - H)^{-1}$, $\pm$ corresponding to advanced and retarded Green functions.

Figure 3.9: Extreme limits of the Chalker-Coddington model. Left, $t_A = 1, t_B = 0$, the system is insulating phase, right $t_A = 0, t_B = 1$ the system is in a quantum Hall phase. The plateau transition occurs at $t_A = t_B = 1/\sqrt{2}$.

where $|e\rangle$ are states corresponding to the wavefunctions $\psi(e)$. $\epsilon = -i\log(z)$, $|z| < 1$, plays the role of quasi-energies (related to the eigenphases of the evolution operator). Retarded and advanced Green functions are defined by $G_{R,A}(e, e'; e^{i\epsilon}) = G(e, e'; e^{i\epsilon \pm i0})$. An important quantity for studying the transition is the diffusion propagator [78] $\Pi(e, e'; \omega) = \langle G_R(e, e'; e^{i(\epsilon+\omega/2)}) G_A(e, e'; e^{i(\epsilon-\omega/2)}) \rangle$, whose behavior is power law in the delocalized regime and exponentially decaying in the localized phase. We can define in a standard way the local density of states as the discontinuity of the Green function across $|z = e^{i\epsilon}| = 1$:

$$\rho(e, \epsilon) = \frac{1}{2\pi} \left(G_R(e, e; e^{i\epsilon}) - G_A(e, e; e^{i\epsilon}) \right) . \tag{3.5}$$

The evolution operator $\mathcal{U}$ is defined for a closed network where each link starts and ends at a node. We discuss now transport properties of the open system. Cutting an oriented link of the network produces two halves, one going into the network i and the other out o. Current can be injected in i and drained in o. We define now the point contact conductance (PCC) [120]. Cut two links of a closed network in disjoint parts i_1, o_1 and i_2, o_2, see figure 3.10.

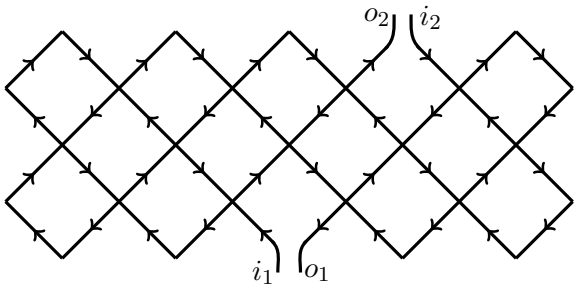

Figure 3.10: Open links where current can be injected (i_1, i_2) and drained (o_1, o_2).

The amplitudes at these links are related by a scattering matrix:

$$\begin{pmatrix} \psi(o_1) \\ \psi(o_2') \end{pmatrix} = \begin{pmatrix} r_{1,1} & t_{1,2} \\ t_{2,1} & r_{2,2} \end{pmatrix} \begin{pmatrix} \psi(i_1) \\ \psi(i_2) \end{pmatrix} ,$$

consisting of transmission t_{ab} and reflection coefficients r_{ab}. The Landauer formula states then that the dimensionless PCC from the in-link b to the out-link a, is given by the transmission probability

$$g = |t_{ab}|^2 . \tag{3.6}$$

The transmission amplitude can be written in terms of $\mathcal{U}$ if we impose boundary conditions on the evolution operator $\mathcal{U}|o_1\rangle = \mathcal{U}|o_2\rangle = \mathcal{U}^\dagger|i_1\rangle = \mathcal{U}^\dagger|i_2\rangle = 0$, as $t_{ab} = \langle o_a| (1-\mathcal{U})^{-1} \mathcal{U}|i_b\rangle$. Assuming that the two point contacts are separated by more than one lattice unit, $\langle o_a|\mathcal{U}|i_b\rangle = 0$, then

$$t_{ab} = \langle o_a| (1-\mathcal{U})^{-1} |i_b\rangle . \tag{3.7}$$

More generally we will be interested in considering a set of incoming edges $C_{\text{in}} = \{i_b\}$, to form one contact and another set of outgoing edges $C_{\text{out}} = \{o_a\}$ to form the other contact. The transmission matrix between these contacts is a rectangular matrix with entries t_{ab} of eq. (3.7). The conductance will be given by the multi-channel Landauer formula:

$$g = \sum_{a \in C_{\text{out}}} \sum_{b \in C_{\text{in}}} |t_{ab}|^2 = \operatorname{Tr} t t^\dagger . \tag{3.8}$$

Typically we will consider a two-terminal probe where contacts are put on the bottom and top of a strip (or cylinder).

3.1.3 Bosonic representation of observables

The Green function introduced in (3.4) has a natural Feynman expansion (for $|z| < 1$) in terms of directed paths $\gamma(e, e')$:

$$G(e, e', z) = \langle e| (1 - z\mathcal{U})^{-1} |e'\rangle = \sum_{\gamma(e,e')} \cdots z U_{e_j} s_j \cdots \tag{3.9}$$

$\gamma(e, e')$ is an ordered collection of neighboring links starting at e and ending at e'. A given link can be visited an arbitrary number of times, and can coincide with the starting or ending point. Each link e_j visited contributes to the weight of the path by the random phase $U_{e_j} = e^{i\varphi_{e_j}}$, the fugacity z, and the matrix element $s_j = \sqrt{1-t^2}$ or $s_j = \pm t$ according to the the right or left turn at next step.

This interpretation of quantum mechanical amplitudes as classical paths (albeit with in general complex Boltzmann weights), allows us to write the interesting observables in the network model, a quantum mechanical system in 2+1D, as a 2D statistical mechanics problem. In this way the solution of the network model can be investigated using tools of statistical mechanics like those developed in chapters 1 and 2. The discussion of the consequences of this remark will occupy the majority of the rest of the thesis.

Path integrals and transfer matrices

A path integral representation of the sum over Feynman paths contributing to the Green function is readily obtained using Gaussian integral representations of matrix elements of the resolvent $(1 - z\mathcal{U})^{-1}$. Introduce complex variables $x(e)$ for each link e of the lattice. Then

$$G(e_i, e_o, z) = \frac{1}{Z} \int \mathrm{d}\mu(x) x(e_i) x^*(e_o) \exp\left(z x^*(e')\mathcal{U}(e', e) x(e)\right) , \tag{3.10}$$

with the Gaussian measure

$$\mathrm{d}\mu(x) = \prod_{e \in E} \frac{\mathrm{d}\Re x(e) \mathrm{d}\Im x(e)}{\pi} e^{-x^*(e)x(e)} ,$$

and partition function:

$$Z = (\mathrm{Det}(1 - z\mathcal{U}))^{-1} = \int \mathrm{d}\mu(x) \exp\left(z x^*(e')\mathcal{U}(e', e) x(e)\right) .$$

This is the bosonic representation of G. Consider now the vertex of figure 3.11, where we spelled out the S-matrix elements of eq. (3.2).

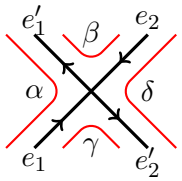

Figure 3.11: A vertex together with S-matrix elements $\alpha, \beta, \gamma, \delta$.

The corresponding evolution operator in the path integral formulation for this vertex is (we set $z = 1$ for convenience):

$$\exp\left(\beta x^*(e_1')x(e_2) + \alpha x^*(e_1')x(e_1) + \delta x^*(e_2')x(e_2) + \gamma x^*(e_2')x(e_1)\right) . \tag{3.11}$$

We want to derive the transfer matrix in terms of bosonic oscillators $b_i, b_i^\dagger, \bar{b}_j, \bar{b}_j^\dagger$ satisfying canonical commutation relations (b_i, $\bar{b}_j$ are associated to different sites, so commute), for which this is the expression in coherent state basis, see section 1.1.2. We then make the change of variables

$$x(e_2) \leftrightarrow x^*(e_2) , \quad x^*(e_2') \leftrightarrow x(e_2') ,$$

in the path integral, such that (3.11) becomes

$$\exp\left(\beta x^*(e_1')x^*(e_2) + \alpha x^*(e_1')x(e_1) + \delta x^*(e_2)x(e_2') + \gamma x(e_2')x(e_1)\right) .$$

Then the transfer matrix for this node is[3]:

$$T_{01} = e^{\beta b^\dagger \bar{b}^\dagger} \alpha^{b^\dagger b} \delta^{\bar{b}^\dagger \bar{b}} e^{\gamma b \bar{b}} ,$$

Expanding the exponential, this expression has a geometrical interpretation associating to occupation numbers of bosons, bits of Feynman paths [103]. 0 and 1 stand for labels of sites (adjacent links on the same row of the lattice). T_{01} acts on the tensor product of Fock spaces living at sites 0 and 1, spanned by $b^{\dagger m}\bar{b}^{\dagger n}|0\rangle$, $|0\rangle$ being the vacuum. In the coherent states picture the single Fock space corresponds to the polynomial algebra $\mathbb{C}[x]$, and the action of $b, b^\dagger$ is given by x, ∂.

The diagonal-to-diagonal transfer matrix T for the evolution in one step of time along the vertical direction of the lattice can be constructed analogously to that for the Potts model, described in section 1.1.1 by concatenating transfer matrices acting on adjacent links. This time however T acts on the product of Fock spaces for every site in a row. In the derivation of the path integral (3.10) we supposed a network with periodic boundary conditions in the vertical (discrete imaginary time) direction, of length say L'. That expression can be written using T as [103] :

$$G(e_i, e_o) = \frac{\mathrm{Tr}\, \mathrm{T}_\tau b_{r_i}(\tau_i) b^\dagger_{r_o}(\tau_o) T^{L'}}{\mathrm{Tr}\, T^{L'}} , \tag{3.12}$$

where the coordinates of the links are $e_i = (r_i, \tau_i)$, $e_o = (r_o, \tau_o)$, and T_τ ensures time ordering.

Observables more complicated than a single Green function require the introduction of more species of bosons (replicas). For example, for representing the PCC of eq. (3.6), we introduce two types of bosons, retarded b_+ and advanced b_-, so that

$$\begin{aligned} g &= \langle o| \left(1 - \mathcal{U}\right)^{-1} |i\rangle\langle i| \left(1 - \mathcal{U}^\dagger\right)^{-1} |o\rangle \\ &= \frac{1}{|Z|^2} \int \mathrm{d}\mu(x_+, x_-) x_+(e_o) x^*_+(e_i) x_-(e_i) x^*_-(e_o) \\ &\qquad \times \exp\left(x^*_+(e')\mathcal{U}(e', e) x_+(e) + x^*_-(e)\mathcal{U}^*(e', e) x_-(e')\right) . \end{aligned}$$

Correspondingly, we introduce bosons of opposite U(1) charges b_+, b_- and the two-sites transfer matrix associated to the computation of the conductance is

$$T_{01} = e^{\beta b^\dagger_+ \bar{b}^\dagger_+ + \beta^* b^\dagger_- \bar{b}^\dagger_-} \alpha^{b^\dagger_+ b_+} (\alpha^*)^{b^\dagger_- b_-} \delta^{\bar{b}^\dagger_+ \bar{b}_+} (\delta^*)^{\bar{b}^\dagger_- \bar{b}_-} e^{\gamma b_+ \bar{b}_+ + \gamma^* b_- \bar{b}_-} . \tag{3.13}$$

Note that the Fock space on site 0 is

$$\mathcal{F} = \mathrm{span}\{b^{\dagger n}_+ b^{\dagger m}_- |0\rangle, m, n \in \mathbb{Z}^{\geq 0}\} ,$$

and on site 1

$$\bar{\mathcal{F}} = \mathrm{span}\{\bar{b}^{\dagger n}_+ \bar{b}^{\dagger m}_- |0\rangle, m, n \in \mathbb{Z}^{\geq 0}\} .$$

[3]Note that evaluating $\alpha^{b^\dagger b}$ and $\delta^{\bar{b}^\dagger \bar{b}}$ in coherent states basis produces the terms $e^{\alpha x^*(e'_1) x(e_1)}$ and $e^{\delta x^*(e_2) x(e'_2)}$ coming from the norm of the coherent states.

They correspond in coherent state basis to the polynomial algebra $\mathbb{C}[x_+, x_-]$ and $\mathbb{C}[\bar{x}_+, \bar{x}_-]$.

We now discuss the symmetry of the transfer operator (3.13) following [102, 103]. Define the pseudounitary group $\mathrm{U}(1,1)$ as the group of matrices g satisfying

$$g^\dagger = \sigma_z g^{-1} \sigma_z \,, \tag{3.14}$$

with the metric $\sigma_z = \mathrm{diag}(1,-1)$ in advanced-retarded space. The Lie algebra $\mathfrak{u}(1,1)$ consists of matrices

$$Y = \begin{pmatrix} A & B \\ C & D \end{pmatrix} \tag{3.15}$$

satisfying (from the parametrization $g = e^{iY}$) $Y^\dagger = \sigma_z Y \sigma_z$, so that $A = A^*, D = D^*, C = -B^*$. The generators E^{ab} of $\mathrm{u}(1,1)$ satisfy the commutation relations

$$[E^{ab}, E^{cd}] = -\delta^{bc} E^{ad} + \delta^{ad} E^{bc} \,,$$

where the presence of the minus sign distinguishes these from those of $\mathfrak{u}(2)$. $\mathfrak{u}(1,1)$ is represented on Fock space $\mathcal{F}$ by $E_{ab} \mapsto J_{ab}$:

$$J = \begin{pmatrix} b_+ b_+^\dagger - \frac{1}{2} & b_+ b_- \\ -b_+^\dagger b_-^\dagger & -b_-^\dagger b_- - \frac{1}{2} \end{pmatrix} \,,$$

and on $\bar{\mathcal{F}}$ by

$$\bar{J} = \begin{pmatrix} -\bar{b}_+^\dagger \bar{b}_+ - \frac{1}{2} & -\bar{b}_+^\dagger \bar{b}_-^\dagger \\ \bar{b}_+ \bar{b}_- & \bar{b}_- \bar{b}_-^\dagger - \frac{1}{2} \end{pmatrix} \,.$$

It is a straightforward computation now to show that the transfer matrix T_{01} of eq. (3.13) has *global* $\mathfrak{u}(1,1)$ symmetry:

$$[J + \bar{J}, T_{01}] = 0 \,.$$

This result holds only if the parameters $\alpha, \beta, \gamma, \delta$ are the matrix elements of a *unitary* S-matrix [102, 103], and establishes the global $\mathfrak{u}(1,1)$ invariance of the diagonal-to-diagonal transfer matrix T.

Random matrix limit and Howe duality

We now give more symmetry considerations by focusing on the simplest case of a network consisting of a single node with a directed edge traversing it, closing to a loop. Some remarks presented in this section appeared in [32, 205]. Call the amplitude for propagation through this node α, which is constrained by unitarity to $|\alpha|^2 = 1$. First we note that in this setup the equivalence between path integral and transfer matrix formulation is transparent. For example, Z is

$$Z = \frac{1}{1-\alpha} = \int \mathrm{d}^2 x e^{-x^*(1-\alpha)x} = \mathrm{Tr}_{\mathcal{F}}\, \alpha^{b^\dagger b} = \sum_{n \geq 0} \alpha^n \,,$$

where $-\log(\alpha)$ plays the role of chemical potential. Now we consider a more general situation where we have n species of advanced and retarded bosons b_+^a, b_-^a, with the

(flavor) index $a = 1, \ldots, n$. We also allow to have N channels in the network, like in figure 3.12. The scattering amplitude at this node is given by $U \in \mathrm{U}(N)$. This is the random matrix limit since the whole amplitude is given by a single unitary random matrix, although for the moment no integration over the realization of U is implied. We write $U = \exp\left(\sum_{k,l=1}^{N} X^{kl} E^{kl}\right)$, where E^{kl} are the generators of the Lie algebra $\mathfrak{u}(N)$, and introduce another (color) index for bosons $b_+^{a,k}, b_-^{a,k}$, $k = 1, \ldots, N$.

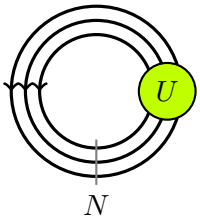

Figure 3.12: The single node network with N channels.

We consider the partition function given by:

$$|Z|^{2n} = |\det(1-U)|^{-2n} = \mathrm{Tr}_{\mathcal{F}} \exp\left(\sum_{a=1}^{n}\sum_{k,l=1}^{N} X^{kl}\left(b_+^{k,a\dagger} b_+^{l,a} - b_-^{l,a\dagger} b_-^{k,a}\right)\right) .$$

$\mathcal{F}$ is the Fock space spanned by monomials of the bosons, and corresponds to the symmetric algebra

$$\mathcal{F} = S\left(\mathbb{C}^N \otimes \mathbb{C}^{2n}\right) = \bigoplus_{d=0}^{\infty} S^d\left(\mathbb{C}^N \otimes \mathbb{C}^{2n}\right) ,$$

with $S^d(V)$ means the quotient of $V^{\otimes d}$ to the symmetric power. Now we note that there are two algebras (and corresponding Lie groups by exponentiation) acting on $\mathcal{F}$. The first is $\mathfrak{u}(N)$ whose action is given by

$$X \mapsto \sum_{a=1}^{n}\sum_{k,l=1}^{N} X^{kl}\left(b_+^{k,a\dagger} b_+^{l,a} - b_-^{l,a\dagger} b_-^{k,a}\right) .$$

The other action is that of $\mathfrak{u}(n,n)$, defined by replacing σ_z in the definitions of $\mathfrak{u}(1,1)$, eq. (3.14), with $\sigma_z \otimes \mathbf{1}_n$. Denoting $Y \in \mathfrak{u}(n,n)$ as in (3.15), with now A, B, C, D $n \times n$ blocks, the representation on Fock space is

$$Y \mapsto \sum_{k=1}^{N}\sum_{a,b=1}^{n}\left(A^{ab} b_+^{k,a} b_+^{k,b\dagger} + B^{ab} b_+^{k,a} b_-^{k,b} - C^{ab} b_+^{k,a\dagger} b_-^{k,b\dagger} - D^{ab} b_-^{k,a\dagger} b_-^{k,b}\right) .$$

Note that generators for one group are obtained by tracing the bosons on the degrees of freedom of the other group. The natural commuting action of $\mathfrak{u}(N)$ and $\mathfrak{u}(n,n)$ on $\mathbb{C}^N \otimes \mathbb{C}^{2n}$ (they act on different indices) induces a commuting action on Fock space. Further

this property is maximal, the algebra of $\mathfrak{u}(N)$-invariants in the space of transformations of the Fock space (the Weyl algebra) is generated by $\mathfrak{u}(n,n)$ and vice-versa. $(\mathfrak{u}(N),\mathfrak{u}(n,n))$ is a dual pair in the sense of R. Howe [110] (see also the review [57], in particular in the context of Lie superalgebras). As a consequence, one can use the general theory to study the algebraic aspects of the computation of partition functions we are after. The main consequence of the centralizing property is that the Fock space admits a multiplicity free decomposition into irreducible representations as a $(\mathfrak{u}(N),\mathfrak{u}(n,n))$-bimodule:

$$\mathcal{F} = \bigoplus_{\lambda} V_\lambda \otimes \tilde{V}_\lambda \,. \tag{3.16}$$

V_λ is an irreducible representation of $\mathfrak{u}(N)$ and $\tilde{V}_\lambda$ is the corresponding irreducible of $\mathfrak{u}(n,n)$. This result follows from Schur-Weyl duality on each summand S^d of $\mathcal{F}$ [57]:

$$S^d\left(\mathbb{C}^N \otimes \mathbb{C}^{2n}\right) = \bigoplus_{\substack{\lambda\vdash d \\ \ell(\lambda)\leq \min(N,2n)}} V_\lambda \otimes \tilde{V}_\lambda \,,$$

where $\lambda \vdash d$ means partition of d, and $\ell(\lambda)$ is the number of parts (rows of the associated Young diagram). The modules in (3.16) are infinite dimensional.

Let us now restrict to the case of interest for the CC model, $N=1$. Representations of U(1) are labeled by the value of the integer charge $\sum_{a=1}^n \left(b_+^{a\dagger}b_+^a - b_-^{a\dagger}b_-^a\right)$ (this is the generator of the algebra). In particular we will be interested below in U(1) singlets, representations where the charge vanishes. The Howe duality construction give access to the corresponding $\mathfrak{u}(n,n)$ representation (or its supersymmetric generalizations).

3.1.4 Supersymmetry method

The observables in the network models are random variables. To compare the theoretical predictions with experiments, one is interested not in the value of an observable for a given realization of disorder, but rather in its statistics, like its mean value and its moments. Denote the disorder average by overlines, which in the CC model amounts to integrating over the uniform measure of U(1) link phases, and let us consider first the mean value of a single Green function $\overline{G(e,e';z)}$. Clearly the problem is the presence of the denominator in our expression (3.10). To get rid of it two tricks are mainly used, replicas and supersymmetry. If we think about the graphical expansion of G in terms of Feynman paths, the role of the denominator is divide out loops which do not connect the points e, e'. Giving a weight zero to these loops is precisely what replicas (involving an a priori ill-defined zero limit of the number of replicas) and supersymmetry do. We will consider supersymmetry only here. The supersymmetry method for performing the disorder average was introduced and popularized by Efetov [75]. In the context of network models it was discussed among others in [103] and [50, 206].

Let us introduce Grassmann variables $\eta(e), \eta^*(e)$ for each link e of the network, so that the inverse of the partition function Z^{-1} appearing in (3.10) can be written as:

$$Z^{-1} = (\mathrm{Det}(1-z\mathcal{U})) = \int \mathrm{d}\mu(\eta)\exp\left(z\eta^*(e')\mathcal{U}(e',e)\eta(e)\right) \,,$$

where

$$\mathrm{d}\mu(\eta) = \prod_{e\in E} \mathrm{d}\eta^*(e)\mathrm{d}\eta(e)e^{-\eta^*(e)\eta(e)}\,.$$

If we define the supervector $\phi \in \mathbb{C}^{1|1}$

$$\phi = \begin{pmatrix} x \\ \eta \end{pmatrix},$$

then the supersymmetric representation of the Green function is:

$$G(e_i, e_o, z) = \int \mathrm{d}\mu(\phi)\phi^1(e_i)\phi^{*1}(e_o)\exp\left(z\phi^{*p}(e')\mathcal{U}_{e',e}\phi^p(e)\right)\,. \tag{3.17}$$

Recalling the form of the evolution operator for the CC model, we can define the non-random (real) evolution operator $\tilde{\mathcal{U}}$ by

$$\mathcal{U}(e', e) = \tilde{\mathcal{U}}_{e',e}e^{i\varphi(e)}\,.$$

Integrating over the phases $\varphi(e)$, one readily finds that:

$$\overline{G(e_i, e_o, z)} = \delta_{io}\,.$$

The local density of states eq. (3.5) is trivial for the CC model. Let us compute now the mean value of the conductance $\bar{g}$. Introducing retarded and advanced supervectors ϕ_+, ϕ_-, g can be written as:

$$\begin{aligned} g = \int \mathrm{d}\mu(\phi_+, \phi_-)&\phi_+^1(o)\phi_+^{*1}(i)\phi_-^1(i)\phi_-^{*1}(o) \\ &\times \exp\left(\tilde{\mathcal{U}}_{e',e}\left(e^{i\varphi(e)}\phi_+^{*p}(e')\phi_+^p(e) + e^{-i\varphi(e)}\phi_-^{*q}(e)\phi_-^q(e')\right)\right)\,. \end{aligned}$$

As in section 1.1.2, we define the grade of the superindex p by $|p| = 0$ if bosonic or $|p| = 1$ if fermionic. It is convenient to perform the change of variables $\phi_-^p \to (-1)^{|p|}\phi_-^{*p}$, $\phi_-^{*p} \to \phi_-^p$, so that:

$$\begin{aligned} g = \int \mathrm{d}\mu(\phi_+, \phi_-)&\phi_+^1(o)\phi_+^{*1}(i)\phi_-^{*1}(i)\phi_-^1(o) \\ &\times \exp\left(\tilde{\mathcal{U}}_{e',e}\left(e^{i\varphi(e)}\phi_+^{*p}(e')\phi_+^p(e) + e^{-i\varphi(e)}\phi_-^{*q}(e')\phi_-^q(e)\right)\right)\,. \end{aligned}$$

Let us now integrate over a single phase $\varphi(e)$. Define

$$\hat{\phi}_\sigma(e) := \tilde{\mathcal{U}}(e', e)\phi_\sigma^{*p}(e')\,,$$

then the result of integration can be written compactly as

$$\Omega = \int_0^{2\pi} \frac{\mathrm{d}\varphi}{2\pi}\exp\left(e^{i\varphi}\hat{\phi}_+^p\phi_+^p + e^{-i\varphi}\hat{\phi}_-^q\phi_-^q\right) = \sum_{m\geq 0}\frac{1}{(m!)^2}\left(\hat{\phi}_+^p\phi_+^p\hat{\phi}_-^q\phi_-^q\right)^m\,. \tag{3.18}$$

This imposes that the number of advanced and retarded particles on a given link must be equal, and is the interaction produced by disorder averaging.

Let us discuss how this result is expressed in terms of the transfer matrix associated to this coherent state path integral. We introduce fermions $f_\sigma, \bar{f}_\sigma$, $\sigma = \pm$. As already discussed for the Potts model if section 1.1.2 we choose that f satisfies canonical anticommutation relations, and $\bar{f}_\sigma$ the modified ones $\{\bar{f}, \bar{f}^\dagger\} = -1$. This is necessary to ensure cancellation of closed loops not contributing to the conductance. Recall also the compact notation for superoscillators

$$a^p_\sigma = \begin{cases} b^p_\sigma & \text{if } |p| = 0 \\ f^{p-2}_\sigma & \text{if } |p| = 1 \end{cases} \quad ; \quad \bar{a}^p_\sigma = \begin{cases} \bar{b}^p_\sigma & \text{if } |p| = 0 \\ \bar{f}^{p-2}_\sigma & \text{if } |p| = 1 \end{cases} .$$

The transfer matrix in the supersymmetric theory associated to the coherent state path integral representing conductances is (see eq. (3.13))

$$T_{01} = e^{\beta a^{p\dagger}_+ \bar{a}^{p\dagger}_+ + \beta^* a^{q\dagger}_- \bar{a}^{q\dagger}_-} \alpha^{a^{p\dagger}_+ a^p_+} (\alpha^*)^{a^{q\dagger}_- a^q_-} \delta^{(-)^{|p|} \bar{a}^{p\dagger}_+ \bar{a}^p_+} (\delta^*)^{(-)^{|q|} \bar{a}^{q\dagger}_- \bar{a}^q_-} e^{\gamma \bar{a}^p_+ a^p_+ + \gamma^* \bar{a}^q_- a^q_-} .$$

In the representation of observables using the supersymmetric transfer matrices, the trace of eq. (3.12) is replaced by the supertrace $\mathrm{Str}(\cdot) = \mathrm{Tr}((-1)^F \cdot)$, appropriate to weight zero spurious loops, as discussed in section 1.1.2. The extra minus for δ and δ^* is due to the fact that the number of $\bar{f}_\sigma$ fermions is $-\bar{f}_\sigma f_\sigma$. This transfer matrix acts in the tensor product of bosonic and fermionic Fock spaces. For example on site 0 the space of states is spanned by $(b^\dagger_+)^n (b^\dagger_-)^m (f^\dagger_+)^i (f^\dagger_-)^j |0\rangle$, $m, n \in \mathbb{Z}^{\geq 0}, i, j \in \{0, 1\}$, and corresponds to the supersymmetric algebra

$$\mathcal{F} = \mathcal{S}(\mathbb{C}^1 \otimes \mathbb{C}^{2|2}) = S(\mathbb{C}^2) \otimes \bigwedge(\mathbb{C}^2) ,$$

with $\bigwedge(\mathbb{C}^2)$ the antisymmetric algebra corresponding in coherent states picture to the Grassmann algebra of polynomials in η, η^*. All the statements done above in the bosonic case generalize quite easily to the supersymmetric setting. The transfer matrix T has global invariance under the Lie superalgebra $\mathfrak{u}(1, 1|2)$ for any realization of the disorder [4] [102, 103]. The disorder average projects the Fock space onto the subspace with equal

[4] The supergroup $\mathrm{U}(1, 1|2)$ is defined by replacing σ_z in eq. (3.14) by $\Lambda = \mathrm{diag}(1, 1, -1, 1)$ in advanced-retarded base. The algebra $\mathfrak{u}(1, 1|2)$ acts on Fock space by the following representation of generators in terms of oscillators:

$$J = \begin{pmatrix} b_+ b^\dagger_+ - \frac{1}{2} & b_+ f^\dagger_+ & b_+ b_- & b_+ f_- \\ f_+ b^\dagger_+ & f_+ f^\dagger_+ - \frac{1}{2} & f_+ b_- & f_+ f_- \\ -b^\dagger_- b^\dagger_+ & -b^\dagger_- f^\dagger_+ & -b^\dagger_- b_- - \frac{1}{2} & -b^\dagger_- f_- \\ f^\dagger_- b^\dagger_+ & f^\dagger_- f^\dagger_+ & f^\dagger_- b_- & f^\dagger_- f_- - \frac{1}{2} \end{pmatrix}$$

$$\bar{J} = \begin{pmatrix} -\bar{b}^\dagger_+ \bar{b}_+ - \frac{1}{2} & -\bar{b}^\dagger_+ \bar{f}_+ & -\bar{b}^\dagger_+ \bar{b}^\dagger_- & -\bar{b}^\dagger_+ \bar{f}^\dagger_- \\ -\bar{f}^\dagger_+ \bar{b}_+ & -\bar{f}^\dagger_+ \bar{f}_+ - \frac{1}{2} & -\bar{f}^\dagger_+ \bar{b}^\dagger_- & -\bar{f}^\dagger_+ \bar{f}^\dagger_- \\ \bar{b}_- \bar{b}_+ & \bar{b}_- \bar{f}_+ & \bar{b}_- \bar{b}^\dagger_- - \frac{1}{2} & \bar{b}_- \bar{f}^\dagger_- \\ -\bar{f}_- \bar{b}_+ & -\bar{f}_- \bar{f}_+ & -\bar{b}_- \bar{b}^\dagger_- & -\bar{f}_- \bar{f}^\dagger_- - \frac{1}{2} \end{pmatrix} .$$

$\mathfrak{u}(1, 1|2)$ is a non-compact real form of $\mathfrak{gl}(2|2)$, and representations of $\mathfrak{u}(1, 1|2)$ are also representations

number of advanced and retarded particles (recall that due to commutation relations, for $\bar{f}$ fermions, $-\bar{f}^\dagger \bar{f}$ is the number of particles):

$$b_+^\dagger b_+ + f_+^\dagger f_+ = b_-^\dagger b_- + f_-^\dagger f_-$$
$$\bar{b}_+^\dagger \bar{b}_+ - \bar{f}_+^\dagger \bar{f}_+ = \bar{b}_-^\dagger \bar{b}_- - \bar{f}_-^\dagger \bar{f}_- .$$

The representations left after disorder average have been discussed in few papers [102, 103, 203]. The space left on site 0 is the irreducible representation V given by the linear span of all the states satisfying the above constraint. The fact that the representation is irreducible is also guaranteed by the supersymmetric version of Howe duality [57]. Its highest weight λ is given by the eigenvalues of Cartan generators J^{aa}, $a = 1, \dots, 4$ on the vacuum, which is the highest weight vector. This yields $\lambda = \frac{1}{2}(1, 1, -1, -1)$. The space on on site 1 is the dual space V^* with highest weight $\bar{\lambda} = -\lambda$. The space of states of the transfer matrix for a system of width $2L$, will then be $(V \otimes V^*)^{\otimes L}$. Calling the projector onto this subspace $\mathcal{P}$, then the transfer matrix used to compute the disorder averaged conductance is

$$\overline{T} = \mathcal{P} T \mathcal{P} .$$

Expanding the transfer matrix $\overline{T}$ as $t_s \to 0$ (keeping $t_A/t_B = \epsilon$ fixed), allows to derive the quantum spin chain describing the anisotropic limit [102, 168, 203]:

$$H = -\epsilon \sum_{i \in I_A} \mathrm{Str}\, J_i \bar{J}_{i+1} - \epsilon^{-1} \sum_{i \in I_B^-} \mathrm{Str}\, \bar{J}_i J_{i+1} , \tag{3.19}$$

where J and $\bar{J}$ are the generators of $\mathfrak{u}(1,1|2)$ acting on V and $\bar{V}$ respectively, and I_A, I_B^- are defined as in section 1.1.1, $I_A = \{0, 2, \dots, 2L-2\}$, $I_B^- = \{1, 3, \dots, 2L-3\}$. Setting $\epsilon = 1$ we reach the critical point of the CC model. This chain has the form of the Heisenberg chain (1.11), given by the quadratic Casimir of the algebra and which we have already encountered in the study of the Potts model. However in that case the space of states was the alternation of the fundamental and dual representations. In the present case we are dealing with infinite dimensional irreducible representations, and this makes the study of the problem very difficult even to approach. In section 3.1.5 we will discuss a geometrical formulation of the problem and the idea of truncation of the space to a finite dimensional one, as possible strategies to attack the study of this spin chain. Before that we will discuss the field theory associated to the spin chain describing the conductance.

Sigma models

The relation between sigma models and antiferromagnetic spin chains was discussed in section 1.1.4. We apply now that procedure to derive the field theory describing the

of $\mathfrak{gl}(2|2)$. The generators of $\mathfrak{gl}(2|2)$ (see e. g. section 1.1.2) can be obtained from those of $\mathfrak{u}(1,1|2)$ by performing a canonical transformation to new bosons $c^* = -b_-, c = b_-^\dagger$, $\bar{c}^* = -b_+, \bar{c} = b_+^\dagger$, after which however c^* and $\bar{c}^*$ are no more the adjoint of c and $\bar{c}$. See also the discussion in [207].

conductance in the CC model starting from the the super-spin chain whose Hamiltonian is (3.19). In this case the sigma model field Q belongs to the symmetric superspace $\mathrm{U}(1,1|2)/\mathrm{U}(1|1)\times\mathrm{U}(1|1)$. Indeed $\mathrm{U}(1,1|2)$ is the symmetry group of that spin chain, and $\mathrm{U}(1|1)\times\mathrm{U}(1|1)$ is the isotropy group of the highest weight, the vacuum, since it corresponds to transforming the advanced and retarded sectors independently. The bosonic base of this target space is $H^2\times S_2$, where $H^2\simeq\mathrm{U}(1,1)/\mathrm{U}(1)\times\mathrm{U}(1)$ is the (non-compact) hyperboloid and $S_2\simeq\mathrm{U}(2)/\mathrm{U}(1)\times\mathrm{U}(1)$ is the (compact) sphere. The presence of a non-compact part is a new feature with respect to the case of $\mathbb{CP}^{M+N-1|N}$ models discussed in 1.1.4. Topological properties are determined by the compact sector only, and the field theory admits a θ-term. The Lagrangian of the sigma model (which can be derived in a semiclassical limit of large representation weight, as in 1.1.4) will then be of the same type of (1.34):

$$S \;=\; \frac{1}{16g_\sigma^2}\int \mathrm{d}^2z\ \mathrm{Str}\,\partial_\mu Q\partial_\mu Q - \frac{\theta}{16\pi}\int \mathrm{d}^2z\,\epsilon_{\mu\nu}\,\mathrm{Str}\,Q\partial_\mu Q\partial_\nu Q\,. \tag{3.20}$$

Here the field Q is a matrix parametrizing the coset $\mathrm{U}(1,1|2)/\mathrm{U}(1|1)\times\mathrm{U}(1|1)$:

$$Q = g\begin{pmatrix}\mathbf{1}_2 & 0\\ 0 & -\mathbf{1}_2\end{pmatrix}g^{-1}\,,$$

$g\in\mathrm{U}(1,1|2)$, on which $\mathrm{U}(1,1|2)$ acts globally by $Q\mapsto hQh^{-1}$. The variables Z_a (satisfying $Z^\dagger Z=1$) used in the definition of the action (1.34) of the $\mathbb{CP}^{M+N-1|N}$ models can be expressed in terms of a matrix field Q as

$$Q_{ab} = 2Z_a^*Z_b - \delta_{ab}\,,$$

to obtain an expression for (1.34) identical to (3.20)—though with different target spaces. Other formulations in terms of more natural coordinates on the target space, and many more insights can be found in [203].

The field theory (3.20), or rather its replica formulation where $Q\in\mathrm{U}(2n)/\mathrm{U}(n)\times\mathrm{U}(n)$ with $n=0$, was proposed by Pruisken [163] some years before the CC model was invented, and the supersymmetric version we have reproduced here appeared first in [196]. The idea of [163] was to identify the sigma model coupling with the bare longitudinal conductivity and the topological angle with the bare Hall conductivity:

$$g_\sigma^2 = \frac{1}{2\sigma_{xx}}\,,\quad \theta = 2\pi\sigma_{xy}\,. \tag{3.21}$$

Note that the θ-term breaks parity and is then consistent with the presence of a magnetic field in the microscopic theory. Then a renormalization group flow qualitatively similar to that of the O(3) sigma model of figure 1.11 was proposed [163], where non-trivial critical points at $\sigma_{xy}=\mathbb{Z}+\frac{1}{2}$ correspond to the plateau transitions. This picture is usually accepted to be the correct one.

3.1.5 Geometrical models

We have seen that for the study of spin chains related to to the Potts model, a good understanding of the geometrical formulation of these models in terms of loops was crucial. In this section we want to discuss more precisely what are the geometrical models associated to the the above supersymmetric formulation of conductance in the CC model.

We derive the graphical interpretation from the coherent state path integrals using the supersymmetric Wick's theorem, which is a direct generalization of its bosonic counterpart. Consider for example the simple integral

$$I_2 = \int \mathrm{d}\mu(\phi)(\phi^{*p}\phi^p)^2\,,$$

where we allow now $\phi \in \mathbb{C}^{N+M|N}$, and $\mathrm{d}\mu(\phi)$ is the notation for Gaussian measure. A direct computation gives $I_2 = M^2 + M$. Graphically this is obtained by considering two diagrams, one where the lines connect planarly to form two loops plus another where they are permuted, they cross and give only a single loop, see figure 3.13. Since loops weight M, then we get the expected result. Clearly it coincides with a M bosonic replica formulation where $\phi \in \mathbb{C}^M$, as one should have expected.

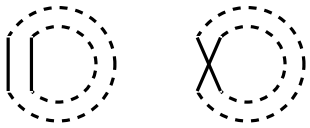

Figure 3.13: The two diagrams contributing to the integral I_2. The diagram on the left weights M^2, that on the right M.

As a starting point we describe the geometrical model for computing the Green function in a clean version of the CC model, where the random phases are set to zero[5] in (3.17). Consider a vertex in coherent state basis. Naming edges as in figure 3.11, and expanding the exponential it is:

$$\mathcal{T} = \sum_{m,n,k,l} z^{m+n} \frac{\left(\phi^{*p}(e_1')\phi^p(e_1)\sqrt{1-t^2}\right)^k}{k!} \frac{(\phi^{*p}(e_2')\phi^p(e_1)(-t))^{m-k}}{(m-k)!}$$
$$\times \frac{\left(\phi^{*p}(e_1')\phi^p(e_2)\sqrt{1-t^2}\right)^l}{l!} \frac{(\phi^{*p}(e_2')\phi^p(e_2)t)^{n-l}}{(n-l)!}\,.$$

The vertices of the associated loop model are clear. First, $\phi^p(e)\phi^q(e')\delta_{pq}$ corresponds to a path connecting e, e'. Second, integration over fields imposes the constraint that the

[5]Note that this restricts phases to be real, changing the symmetry class of the model (class D in notation of section 3.1.6). This problem is described in the continuum by a Dirac fermion (equivalent to two uncoupled Ising models) with central charge $c = 1$ plus a $\beta - \gamma$ ghost system ($c = -1$) for the bosonic part. See [139].

number of lines, say i, leaving the vertex on the edge $e = (v, v')$, should be the same as that of lines entering the vertex v' and further, these i lines are joined in $i!$ ways. For each choice of m, n, k, l we have $m! \times n!$ vertices with the same local weight, and all vertices of the model are obtained by varying m, n, k, l. The geometrical model is obtained by joining all these vertices in all possible ways. See figure 3.14 for an example of a vertex. The weights of vertices are not positive since they correspond to quantum mechanical amplitudes, and the resulting geometrical model is not unitary. The Green function $G(e, e; z)$ will then be given by all the closed loops passing through the edge e weighted by z^l, l being the number of monomers of the loop. Any other loop formed which does not contain e weights zero.

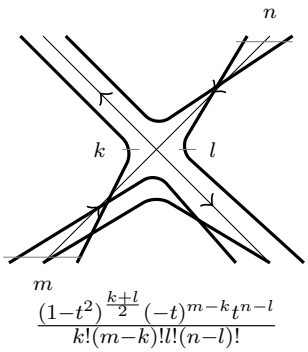

Figure 3.14: A vertex of the loop model associated to single Green function in the clean (no random phases) CC model. Here $m = 3, n = 2, k = 1, l = 1$.

We now move to the geometrical model associated to the mean conductance in the CC model. Before disorder averaging, the geometrical model is exactly two copies (corresponding to retarded and advanced paths) of that described above for a single Green function (though different boundary conditions are concerned). Let us now consider what we obtain after disorder averaging. We have seen in the previous section that averaging constrains the number of advanced particles (bosons plus fermions) to be equal to that of retarded particles. Explicitly, the vertex of the resulting model is:

$$\begin{aligned}\mathcal{T} = \sum_{m,n\geq 0} \sum_{i+k=j+l} & \frac{\left(\phi_+^{*p}(e_1')\phi_+^{p}(e_1)\sqrt{1-t^2}\right)^i}{i!} \frac{\left(\phi_+^{*p}(e_2')\phi_+^{p}(e_1)(-t)\right)^{m-i}}{(m-i)!} \\ & \times \frac{\left(\phi_-^{*q}(e_1')\phi_-^{q}(e_1)\sqrt{1-t^2}\right)^j}{j!} \frac{\left(\phi_-^{*q}(e_2')\phi_-^{q}(e_1)(-t)\right)^{m-j}}{(m-j)!} \\ & \times \frac{\left(\phi_+^{*r}(e_1')\phi_+^{r}(e_2)t\right)^k}{k!} \frac{\left(\phi_+^{*r}(e_2')\phi_+^{r}(e_2)\sqrt{1-t^2}\right)^{n-k}}{(n-k)!} \\ & \times \frac{\left(\phi_-^{*r}(e_1')\phi_-^{r}(e_2)t\right)^l}{l!} \frac{\left(\phi_-^{*r}(e_2')\phi_-^{r}(e_2)\sqrt{1-t^2}\right)^{n-l}}{(n-l)!}\end{aligned}$$

Clearly if $i + k \neq j + l$ the Gaussian integration gives zero, since on outgoing links the number of advanced paths is different from that of retarded ones, so we have restricted the sum above. On link e_1 and e_2 there are respectively m and n bits of advanced and retarded paths. A vertex of this geometrical model is illustrated in figure 3.15. As above every closed loop formed weights zero.

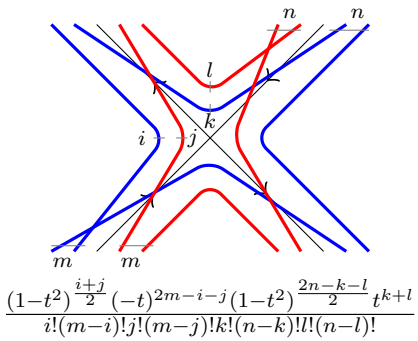

Figure 3.15: A vertex of the geometrical model for computing mean conductance in the CC model. Red and blue paths correspond to advanced and retarded ones.

Again the weight of a vertex can be negative and the model is not unitary. An interesting remark has been made recently in [23], where the authors are able to partly resum these paths and obtain a geometrical formulation in terms of "pictures" with positive definite Boltzmann weights.

Truncations

The main practical problem in studying the vertex models above is clearly the presence of an infinite number of possible interactions at the vertex. Indeed usual methods of statistical mechanics, like those discussed in chapter 1 for the Potts model, work for models with a finite number of degrees of freedom. Recently it was proposed then to truncate the space of states to obtain a finite (dilute, two-colors) loop model which can be solved [111]. This is reminiscent of what done for the O(n) spin model on the hexagonal lattice [152]: the spin model defined by the action $JS_i \cdot S_j$ with $S_i \in S^{n-1}$, the $(n-1)$-dimensional sphere, can be mapped to a geometrical model where edges can be visited an arbitrary number of times, but the substitution $JS_i \cdot S_j \to \log(JS_i \cdot S_j)$ lead to a finite loop model preserving the O(n) symmetry of the original spin model.

To illustrate the truncation for the CC model, we first introduce for each link e fugacities $z_n(e)$ for the presence of n monomers. The N-th truncation [111] is then defined by setting $z_n(e) = 0$ if $n > N$. The original model had $z_n(e) = 1$ for every n. This corresponds to restricting the sum over states in the path integral formulation,

eq. (3.18) to

$$\Omega_N = \sum_{m=0}^{N} \frac{z_m}{(m!)^2} \left(\hat{\phi}_+^p \phi_+^p \hat{\phi}_-^q \phi_-^q \right)^m .$$

The couplings $z_m(e)$ are now free parameters. This procedure has clearly an equivalent within the formulation in terms of transfer matrices. There it corresponds to quotient the space of states V, V^* by relations $(b^\dagger)^{N+1}|0\rangle = 0$. In this form, but considering a slightly different model than the CC one, the truncations were considered earlier in [132, 140].

In [111] the first truncation $N = 1$ was considered. The parameter $z = z_1(e)$ plays the same role as the monomer fugacity in the O(n) model and we expect that at a critical value the length of loops becomes infinite[111]. The first truncation however does not describe the physics of the original model. Indeed the divergence of the correlation length has been determined numerically to be governed by an exponent $\nu \simeq 1.1$, more than two times smaller than the one of the untruncated CC model.

The hope is that studying the truncations leads to understand the full untruncated theory. We note that studying numerically higher truncations than the first requires however big computational resources. Numerical studies of the geometrical model of pictures defined in [23] could be more efficient.

3.1.6 Symmetry classes

Disordered non-interacting electronic systems fit into a classification scheme referred to as the Altland-Zirnbauer classification [11, 204]. In this perspective the IQHE is a possible type of universal behavior in a particular symmetry class. The classification applies in any dimension, and is a classification of random matrices. It describes the space of possible Hamiltonians for a quantum mechanical system respecting a given symmetry. Very good reviews exist on this topic [78, 208, 209]. We mention also that this classification has recently found applications in the homotopy classification of topological insulators and superconductors [128, 179]. Here we will only state the results and the main ideas, which we use to put network models in this general scheme.

The outcome of the classification is that there exists (in the sense explained below) only ten classes[6], which are in correspondence with classical compact symmetric spaces. This statement has been proved rigorously in [109]. Before proceeding we recall that symmetric spaces of compact type are constructed in the following way. Let U be a connected compact Lie group ($U = \mathrm{SO}(N), \mathrm{Sp}(N), \mathrm{SU}(N)$) and τ an involutive ($\tau^2 = 1$) automorphism of U. Let $K \subset U$ be the subgroup of τ-fixed points $\tau(k) = k$. Then the coset space U/K is a compact symmetric space. Denoting $\mathfrak{u}$ and $\mathfrak{k}$ the Lie algebras of U and K, then $\mathfrak{u}$ decomposes into positive and negative eigenspaces of the linearized involution $\mathrm{d}\tau$: $\mathfrak{u} = \mathfrak{k} \oplus \mathfrak{p}$. $\mathfrak{p}$ is the tangent space to U/K which does not have a structure

[6] By considering the Dirac structure of the Hamiltonian a refinement can be done to obtain 13 classes [20].

of Lie algebra in general. Non compact symmetric spaces U^*/K are constructed from the Lie algebra $\mathfrak{u}^* = \mathfrak{k} \oplus i\mathfrak{p}$. Note also that compact Lie groups K themselves are symmetric spaces by choosing $U = K \times K$ and $\tau(k, k') = (k', k)$.

The first column in table 3.1 corresponds to the name given by Cartan to the symmetric space to which the evolution operator e^{itH} belongs. We distinguish three subclasses: Wigner-Dyson (WD), chiral and superconductor (BdG, Bogoliubov De Gennes) classes. The last column refers to the target space of the low energy effective supersymmetric field theory describing products of retarded and advanced Green functions. This space also depends only on symmetries and is fixed by the space to which the microscopic Hamiltonian belongs. The precise definition requires the notion of Riemannian symmetric superspaces developed by Zirnbauer in [204].

H-class	e^{itH}	NLσM
A	$\mathrm{U}(N)$	$\mathrm{GL}(n\|n)/\mathrm{GL}(n_-\|n_-)\times\mathrm{GL}(n_+\|n_+)$
AI	$\mathrm{U}(N)/\mathrm{O}(N)$	$\mathrm{Osp}(2n\|2n)/\mathrm{Osp}(2n_-\|2n_-)\times\mathrm{Osp}(2n_+\|2n_+)$
AII	$\mathrm{U}(2N)/\mathrm{Sp}(2N)$	$\mathrm{Osp}(2n\|2n)/\mathrm{Osp}(2n_-\|2n_-)\times\mathrm{Osp}(2n_+\|2n_+)$
AIII	$\mathrm{U}(p+q)/\mathrm{U}(p)\times\mathrm{U}(q)$	$\mathrm{GL}(n\|n)$
BDI	$\mathrm{O}(p+q)/\mathrm{O}(p)\times\mathrm{O}(q)$	$\mathrm{GL}(2n\|2n)/\mathrm{Osp}(2n\|2n)$
CII	$\mathrm{Sp}(p+q)/\mathrm{Sp}(p)\times\mathrm{Sp}(q)$	$\mathrm{GL}(2n\|2n)/\mathrm{Osp}(2n\|2n)$
C	$\mathrm{Sp}(2N)$	$\mathrm{Osp}(2n\|2n)/\mathrm{GL}(n\|n)$
CI	$\mathrm{Sp}(2N)/\mathrm{U}(N)$	$\mathrm{Osp}(2n\|2n)$
D	$\mathrm{SO}(2N)$	$\mathrm{Osp}(2n\|2n)/\mathrm{GL}(n\|n)$
DIII	$\mathrm{SO}(2N)/\mathrm{U}(N)$	$\mathrm{Osp}(2n\|2n)$

Table 3.1: The ten classes. First column H-class is the Cartan label corresponding to the compact symmetric space type to which the evolution operator $\exp(iH)$ belongs. N, p, q are related to size of the Hilbert space. The column NLσM contains the target space of the super sigma model description of corresponding localization problems. n_+, n_- and $n = n_+ + n_-$ are related to the number of retarded and advanced particles needed to represent products of Green functions. The first three are WD, next three chiral, last four BdG classes.

We discuss now WD classes with some details of the main ideas and then present only the results for the other classes. In his threefold way [74] Dyson reverses the usual reasoning in quantum mechanics of starting from a Hamiltonian and then discussing the symmetries, and instead assumes the knowledge of the (finite-dimensional) Hilbert space V of a quantum system and of the group G of symmetries. V will be reducible in general and the goal is to enumerate the possible Hamiltonians occurring in each irreducible block which commute with G. In general $G = G_0 \cup TG_0$, where G_0 is the group of unitary symmetries and T is antiunitary: $T(z\psi) = \bar{z}T\psi$ for $z \in \mathbb{C}, \psi \in V$, and $\langle T\psi_1, T\psi_2\rangle = \overline{\langle \psi_1, \psi_2\rangle}$. We choose the antiunitary symmetry to be time reversal, and in that case $T^2 = \pm 1$. Instead of Hamiltonians, one focuses for convenience on time

evolution operators U, such that

$$U = g_0 U g_0^{-1} = g_1 U^{-1} g_1^{-1} ,$$

for $g_0 \in G_0$ and $g_1 \in TG_0$. The idea behind Dyson's classification is a familiar tool when discussing symmetries, the Schur duality, used to transfer information from the symmetries to the Hamiltonians (see the discussion in section 1.1.3). The Hilbert space is supposed to have the following decomposition under the reductive action of the unitary symmetries G_0:

$$V = \bigoplus_\lambda V_\lambda = \bigoplus_\lambda \mathbb{C}^{m_\lambda} \otimes R_\lambda . \tag{3.22}$$

R_λ are irreducible representations of G_0 (e. g. spaces of given spin for SU(2) representations) and $\mathbb{C}^{m_\lambda}$ are multiplicity spaces. Note now that the space of evolution operators we are looking for is precisely defined as the centralizer Z of G_0 in $\mathrm{U}(V)$. The double commutant theorem discussed in section 1.1.3 then applies, and $\mathbb{C}^{m_\lambda}$ are recognized as representation spaces of evolution operators, so that Z is the direct product of unitary groups:

$$Z \simeq \prod_\lambda \mathrm{U}(m_\lambda) .$$

Focus sing on a single summand of the decomposition (3.22), we have found that the evolution operator of a system in presence of only unitary symmetries, are unitary matrices (and the corresponding Hamiltonians are Hermitian). This is class A. The IQHE provides a realization of this class, the breaking of time reversal symmetry being caused by the magnetic field.

Suppose now that time reversal symmetry is present. If T acting on a summand V_λ of (3.22) produces another $V_{\lambda'}$, $\lambda' \neq \lambda$, no further constraints arise and one is back to class A. Consider now $\lambda' = \lambda$ and focus on V_λ, and denote $\mathrm{U} = \mathrm{U}(m_\lambda)$. The set of evolutions we are looking for is

$$M = \{u \in \mathrm{U} | u = \tau(u)^{-1}\} ,$$

where τ is the involutive automorphism given by $\tau(u) = TuT^{-1}$. Call K the set of τ-fixed points $k = \tau(k)$. An element of M can be written as $u = k\tau(k)^{-1}$, and M is given by the symmetric space U/K. The precise reasoning for finding K is a bit intricate [208, 209]. The idea is that the condition $k = \tau(k)$ can be written as the invariance under K of a bilinear form associated to T. If $T^2 = 1$ the bilinear form is symmetric and $K = \mathrm{O}(N)$, if $T^2 = -1$ the form is skew symmetric and $K = \mathrm{Sp}(N)$ (N even). Then we get two more possibilities in the WD classification scheme, classes AI and AII of table 3.1. AI class arises typically in systems with time reversal and spin conservation, while AII is obtained by breaking spin symmetry, for example by strong spin orbit scatterers[7].

[7] From fundamental principles of quantum mechanics an electron has spin 1/2, so global time reversal (the product of time reversal acting on $\mathbb{C}^m$, denoted by T in the text, and that acting on R_λ), if present, squares to -1. The action of time reversal in the representation space R_λ of SU(2) also squares to -1 [209], and this implies that the sign of T^2, acting on $\mathbb{C}^m$, must be $+1$.

We now follow [11] and ask the classification question for superconducting systems described at mean field level by the Hamiltonian:

$$H = \sum_{\alpha,\beta=1}^{N} h_{\alpha,\beta} c_\alpha^\dagger c_\beta + \frac{1}{2} \sum_{\alpha,\beta=1}^{N} \left(\Delta_{\alpha,\beta} c_\alpha^\dagger c_\beta^\dagger - \Delta_{\alpha,\beta}^* c_\alpha c_\beta \right) .$$

$c^\dagger, c$ are fermionic creation and annihilation operators satisfying canonical anticommutation relations, and indices refer to position and spin degrees of freedom. New classes arise by asking the classification questions in this setting because of the extra structure given by the fermionic Fock space $\wedge(V)$ [209]. These new constraints are built in the particle-hole form of the Hamiltonian $H = (c^\dagger, c)\mathcal{H}(c, c^\dagger)^T$, with the BdG-Hamiltonian $\mathcal{H}$ given by:

$$\mathcal{H} = \begin{pmatrix} h & \Delta \\ -\Delta^* & -h^T \end{pmatrix} ,$$

where Hermiticity ($\mathcal{H}^\dagger = \mathcal{H}$) implies $h = h^\dagger, \Delta^T = -\Delta$. This structure corresponds to the relation

$$\mathcal{H} = -\tau_x \mathcal{H}^T \tau_x ,$$

with $\tau_x = \sigma_x \otimes \mathbf{1}_N$. This condition is defining (in an appropriate basis, that of Majorana fermions $c_\alpha + c_\alpha^\dagger$, $i(c_\alpha - c_\alpha^\dagger)$) the $\mathfrak{so}(2N)$ algebra (class D), which is the space of Hamiltonians of a superconductor without any symmetry, $G = \mathrm{Id}$.

Consider now a BdG Hamiltonian with spin rotation invariance $G = \mathrm{SU}(2)$. The Hamiltonian reads

$$H = \sum_{ij}^{N} \left(h_{ij} \sum_{a=\uparrow,\downarrow} c_{ia}^\dagger c_{ja} + \Delta_{ij} c_{i\uparrow}^\dagger c_{j\downarrow}^\dagger + \Delta_{ij}^* c_{j\downarrow} c_{i\uparrow} \right) . \tag{3.23}$$

Hermiticity requires $h = h^\dagger$ and spin rotation invariance $\Delta^T = \Delta$. These conditions give the symmetry property ($\tau_y = \sigma_y \otimes \mathbf{1}_N$):

$$\mathcal{H} = -\tau_y \mathcal{H}^T \tau_y , \tag{3.24}$$

which characterize the Lie algebra $\mathfrak{sp}(2N)$ (class C). We will discuss d-wave superconductors belonging to class C and exhibiting the spin quantum Hall effect in section 3.2. When time reversal is present two more classes corresponding to the following symmetric spaces are found: DIII: $\mathrm{SO}(2N)/\mathrm{U}(N)$ and CI: $\mathrm{Sp}(2N)/\mathrm{U}(N)$.

A last set of symmetry classes is given by Hamiltonians with a chiral form:

$$H = \begin{pmatrix} 0 & h \\ h^\dagger & 0 \end{pmatrix} .$$

These Hamiltonians satisfy $\tau_z H \tau_z = -H$, $\tau_z = \sigma_z \otimes \mathbf{1}_N$, a condition which singles out the symmetric space $\mathrm{U}(p+q)/\mathrm{U}(p) \times \mathrm{U}(q)$ (in the case of h being a $p \times q$ matrix) for the corresponding evolution operator. A typical realization of chiral symmetry in

mesoscopic physics is the block structure of random fermions hopping on a bipartite lattice [90, 91]. In analogy with WD classes, time reversal symmetry singles out an orthogonal $\mathrm{O}(p+q)/\mathrm{O}(p)\times\mathrm{O}(q)$ (class BDI) and symplectic $\mathrm{Sp}(p+q)/\mathrm{Sp}(p)\times\mathrm{Sp}(q)$ (class CII) structure.

Each of the ten classes can be realized by a network model by trading the U(1) phases of the CC model for matrices belonging to the appropriate symmetric space [135]. In the next section we will see a realization of class C.

3.2 The spin quantum Hall transition

3.2.1 Physics of the spin quantum Hall effect

The spin quantum Hall effect (SQHE) is the quantization of the spin Hall conductance, analogously to the charge conductance quantization in the IQHE. For spin transport, the role of the electric field is played by an external Zeeman magnetic field, and the spin Hall conductance σ^s_{xy} is defined as the response to the spatial variation of the field. Suppose the Zeeman field $B^z(y)$ to be directed along z and to depend only on the coordinate y. Denoting the z component of the spin current along the x direction j^z_x, σ^s_{xy} is defined by:

$$j^z_x = \sigma^s_{xy}\left(-\frac{\mathrm{d}B^z(y)}{\mathrm{d}y}\right).$$

The SQHE may occur in singlet superconductors described by the Hamiltonian H of eq. (3.23). For a superconductor particle number is not a conserved quantity and there is not transport of charge. However since the gap function Δ_{ij} is symmetric, H commutes with the generators of global spin rotations

$$\vec{S} = \frac{1}{2}\sum_i \sum_{a,b=\uparrow,\downarrow} c^\dagger_{ia}\vec{\sigma}_{ab}c_{ib}\,,$$

and spin is conserved. If Δ is complex, time reversal is broken[8] and σ^s_{xy} can have non-zero value. Recall from section 3.1.6 that SU(2) invariance and no time reversal symmetry, defines class C. Note that relation (3.24) implies that eigenvalues of $\mathcal{H}$ occurs in pairs $(\epsilon,-\epsilon)$.

Consider now a $d+id$ superconductor, for which the gap function Δ has Fourier transform

$$\Delta_k = \Delta_0\cos(2\theta_k) - i\Delta_{xy}\sin(2\theta_k)\,,$$

with $\tan(\theta_k) = k_y/k_x$. This form allows for the SQHE, and computing spin transport shows that [183]:

$$\sigma^s_{xy} = 2\,\mathrm{sgn}(\Delta_{xy})\,.$$

[8] Time reversal symmetry for spinful fermions is defined by

$$Tc_\uparrow T^{-1} = c_\downarrow\,,\quad Tc_\downarrow T^{-1} = -c_\uparrow$$
$$Tc^\dagger_\uparrow T^{-1} = c^\dagger_\downarrow\,,\quad Tc^\dagger_\downarrow T^{-1} = -c^\dagger_\uparrow\,.$$

We see that in the time reversal invariant case $\Delta_{xy} = 0$, the system is in a (spin) insulating phase. For $\Delta_{xy} \neq 0$, a value $\sigma^s_{xy} = \pm 2$ defines a spin quantum Hall phase, topologically distinct from the insulating phase [192]. Analogously to the IQH case, on a system with boundary, transport is carried by chiral edge states which come in couples (up and down spin). These edge states are robust to weak disorder (hence it is the quantization of spin Hall conductance), but for strong enough disorder the system undergoes an Anderson transition from localized to quantum Hall phase [183], see figure 3.16.

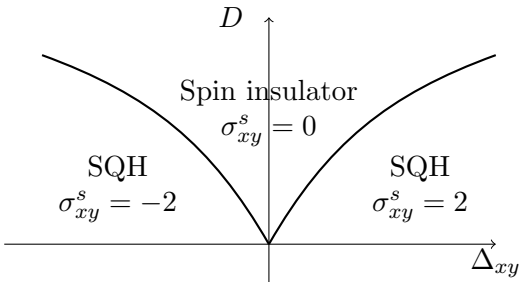

Figure 3.16: Schematic phase diagram as a function of Δ_{xy} and disorder D [183]. SQH refers to the spin quantum Hall phase.

The nature of this phase transition will be investigated in the rest of this chapter using the network model description, and in chapter 4 we will discuss boundary critical phenomena at the SQH transitions and their relation to topological properties and edge states.

Before presenting the network model, we point out that despite a great theoretical understanding of the SQH transition, no experimental realization exists up to date, though there are some proposals in the literature [183].

3.2.2 The network model

The network and symmetries

To study the plateau transition in the SQHE, we introduce a network model which generalizes the CC model for the IQHE [122]. We associate the links of the network to internal edge states separating puddles of spin quantum Hall fluid, so that each link will now carry a doublet of complex fluxes. Specifically we consider the same network as that of the CC model, figure 3.8, and the wavefunction now will be given by $\psi(e)_\sigma$, $\sigma = \uparrow, \downarrow$ corresponding to spin degrees of freedom.

Symmetry properties of class C (3.24) require the evolution operator $\mathcal{U} = e^{i\mathcal{H}}$ of the network to satisfy:

$$\mathcal{U} = \tau_y \mathcal{U}^* \tau_y \,, \tag{3.25}$$

so that $\mathcal{U} \in \mathrm{Sp}(2N)$, where N is the number of links. As in the CC case, $\mathcal{U}$ has a block structure connecting only wavefunctions on adjacent links and we denote again

the two types of vertices $s = A, B$. Random U(1) phases of the CC model are replaced by Sp(2) = SU(2) random matrices mixing up and down particles on links. The node scattering matrix $\tilde{S}_s$ is chosen diagonal in spin index $\tilde{S}_s = \tilde{S}_{s\uparrow} \oplus \tilde{S}_{s\downarrow}$, with

$$\tilde{S}_{s\sigma} = \begin{pmatrix} \sqrt{1-t_{s\sigma}^2} & t_{s\sigma} \\ -t_{s\sigma} & \sqrt{1-t_{s\sigma}^2} \end{pmatrix} .$$

The system is isotropic when $t_{A\sigma}^2 + t_{B\sigma}^2 = 1$, and $t_{A\sigma} = t_{B\sigma} = 1/\sqrt{2}$ is the critical point at which the SQH transition occurs. Repeating the argument of section 3.1.2 about the extreme limit values of $t_{s\sigma}$'s we see that on a strip the SQH phase is characterized correctly by two chiral counter-propagating edge states, responsible for a value of the spin Hall conductance $\sigma_{xy}^s = 2$. Note that taking $t_{s\uparrow} \neq t_{s\downarrow}$ breaks SU(2) symmetry and splits the transition into two IQH transitions.

An important difference between the SQH and the IQH transitions is given by the behavior of the density of states $\rho(\epsilon)$, eq. (3.5). As discussed above in class C it has the property $\rho(\epsilon) = \rho(-\epsilon)$, and as $\epsilon \sim 0$, the value at which the SQH occurs, it is critical:

$$\rho(\epsilon) \sim \epsilon^{\alpha} ,$$

as will be derived below.

The Green functions $G(e, e'; z) = \langle e|(1 - z\mathcal{U})^{-1}|e'\rangle$ are SU(2) matrices (we omit the spin index in the notation $|e\rangle$), which thanks to the symmetry (3.25) are related by

$$G^{\dagger}(e, e'; z) = \mathbf{1}_2 \delta_{ee'} - G(e', e; (z^*)^{-1}) .$$

At the transition $\epsilon = 0$ (corresponding to z real, recall $z = e^{i(\epsilon \pm i0)}$), the above relation is between retarded and advanced Green functions.

PCC of an open system will be given in terms of the transmission matrix t (3.7) by the multi-channel Landauer formula, $g = \mathrm{Tr}\, tt^{\dagger}$, where the trace is over spin degrees of freedom. We remark that t (or G) being a linear combination of products of SU(2) matrices can be written in the form $t = \lambda \tilde{t}$, with $\lambda \in \mathbb{R}$ and $\tilde{t} \in$ SU(2). This follows from the representation

$$U = \cos(\alpha) + i(\vec{\sigma} \cdot \vec{n}) \sin(\alpha) , \tag{3.26}$$

for any $U \in$ SU(2). Then $\mathrm{Det}(t) = \lambda^2$ and $tt^{\dagger} = \lambda^2 \mathbf{1}$, so the PCC is [18]

$$g = 2\,\mathrm{Det}(t) \tag{3.27}$$

This equation is another way of rephrasing the SU(2) symmetry relating advanced and retarded Green functions.

Supersymmetry method for the SQH network

The supersymmetry method discussed in section 3.1.4 for the CC model can be adapted straightforwardly to the case we are after in this section. The following discussion is

based on [50, 101]. We consider a single Green function first. For each lattice link e and $\sigma = \uparrow, \downarrow$ we introduce the supervectors $\phi_\sigma(e), \phi^*_\sigma(e) \in \mathbb{C}^{1|1}$:

$$\phi_\sigma(e) = \begin{pmatrix} x_\sigma \\ \eta_\sigma \end{pmatrix} ,$$

and ϕ^* is defined similarly by conjugating the complex variables x and introducing fermions η^*_σ. Denote the ensemble average in the supersymmetric lattice field theory as:

$$\langle \bullet \rangle = \int \mathrm{d}\mu(\phi) \bullet \exp\left(z \phi^{*p}_\gamma(e') \mathcal{U}_{\gamma\delta}(e', e) \phi^p_\delta(e) \right) ,$$

with $\mathrm{d}\mu(\phi)$ Gaussian measure over all bosons and fermions and as needed, $\langle 1 \rangle = 1$. The supersymmetric representation of the Green function then is:

$$G_{\alpha\beta}(e_i, e_o, z) = \langle x_\alpha(e_i) x^*_\beta(e_o) \rangle = \langle \eta_\alpha(e_i) \eta^*_\beta(e_o) \rangle .$$

Representing the PCC conductance does not need the introduction of replicas, thanks to eq. (3.27). Noting that $\langle x(o)x^*(i)\rangle\langle \eta(o)\eta^*(i)\rangle = \langle x(o)x^*(i)\eta(o)\eta^*(i)\rangle$, we have:

$$g = 2\,\mathrm{Det}(t) = 2\langle \tfrac{1}{\sqrt{2}} \left(x_\uparrow(o)\eta_\downarrow(o) - x_\downarrow(o)\eta_\uparrow(o) \right) \tfrac{1}{\sqrt{2}} \left(x^*_\uparrow(i)\eta^*_\downarrow(i) - x^*_\downarrow(i)\eta^*_\uparrow(i) \right) \rangle . \quad (3.28)$$

Clearly the ensemble average above is understood for an open system with appropriate boundary conditions for $\mathcal{U}$ and where we set $z = 1$.

This formalism can be rewritten in terms of transfer matrices acting on a Fock space spanned by bosonic and fermionic oscillators for up and down particles. The transfer matrix associated to the evolution operator is easy to guess having done the exercise for the CC model in section 3.1.4. Keeping notation of that section, the two sites transfer matrix acting at a vertex of type A (a act on site 0, $\bar{a}$ on site 1), is [101]:

$$T_{01} = \prod_{\sigma=\uparrow,\downarrow} e^{t_{A\sigma} a^{p\dagger}_\sigma \bar{a}^{p\dagger}_\sigma} \left(1 - t^2_{A\sigma}\right)^{\frac{1}{2}\left(a^{p\dagger}_\sigma a^p_\sigma + (-)^{|p|} \bar{a}^{p\dagger}_\sigma \bar{a}^p_\sigma \right)} e^{-t_{A\sigma} \bar{a}^p_\sigma a^p_\sigma} . \quad (3.29)$$

This transfer matrix commutes with combinations of bosonic and fermionic operators which are SU(2) singlets, in analogy with the case of the CC model, for which the (global) symmetry was given by U(1) singlets. These operators are the generators of an $\mathfrak{osp}(2|2) = \mathfrak{sl}(2|1)$ Lie superalgebra [101] (see appendix of [186] for details). We remark that $\mathfrak{sl}(2|1)$ and SU(2) (or rather $\mathfrak{osp}(2|2)$ and Sp(2)) form an Howe pair [57], but we will not discuss here more of these representation theoretic aspects.

3.2.3 Exact solutions

Disorder average

We now proceed to the computation of disorder averaged quantities. There are several articles discussing from different point of view this computation [18, 50, 101, 143]. Here we follow [50], but with some modifications (we use in particular half of the fields used

there). Disorder averaging (noted as overlines) is defined as the integration over the Haar measure of SU(2) on every link. Parametrizing $U \in \mathrm{SU}(2)$ as in (3.26), the integration is

$$\int_{\mathrm{SU}(2)} \mathrm{d}U = \frac{2}{\pi} \int_0^\pi \mathrm{d}\alpha \sin^2(\alpha) \int \mathrm{d}\vec{n}\,,$$

$\vec{n}$ being a unit vector, and the moments of U are very simple:

$$\overline{U^k} = c_k \mathbf{1}\,, \quad c_k = \begin{cases} 1 & \text{if } k = 0 \\ -\frac{1}{2} & \text{if } k = \pm 2 \\ 0 & \text{otherwise.} \end{cases}$$

This result has very remarkable consequences for the solution of the SQH network model. Indeed, considering the sum over Feynman paths associated to the Green function (3.9), we see that paths visiting a node a number of times different from 0 or 2 will not contribute. This has to be compared with the case of the IQH transition, where also after disorder average, an infinite number of paths contribute to the (products of two) Green functions.

We will now translate this remark in the supersymmetric formalism. Define the non-random (real) evolution operator $\tilde{\mathcal{U}}$ acting as identity in spin indices by factoring out the random SU(2) matrix on link e:

$$\mathcal{U}_{\alpha\beta}(e', e) = \tilde{\mathcal{U}}(e', e)(U_e)_{\alpha\beta}\,.$$

Then define

$$\hat{\phi}^p_\sigma(e) := z\phi^{*p}_\sigma(e')\tilde{\mathcal{U}}(e', e)\,.$$

For example, for a link e_1 entering a vertex of type A, with labeling of of figure 3.7, it would be $\hat{\phi}^p_\sigma(e_1) = -zt_A\phi^{*p}_\sigma(e'_1) + z\sqrt{1-t_A^2}\phi^{*p}_\sigma(e'_2)$, where we set $t_s = t_{s\uparrow} = t_{s\downarrow}$ as will be assumed from now on. Then the integration on a single link will be:

$$\Omega = \int_{\mathrm{SU}(2)} \mathrm{d}U \exp\left(\hat{\phi}^p_\alpha U_{\alpha\beta}\phi^p_\beta\right)\,.$$

A general integral of this type can be written as a modified Bessel function of the first kind $I_\nu(z)$:

$$\begin{aligned}
\Omega &= \frac{1}{2\pi^2} \int_0^\pi \mathrm{d}\alpha \sin^2\alpha \int_0^\pi \mathrm{d}\theta \sin\theta \int_0^{2\pi} \mathrm{d}\phi \\
&\quad \times \exp\left[B^0 \cos\alpha + i \sin\alpha \left(\sin\theta \sin\phi B^1 + \sin\theta\cos\phi B^2 + \cos\theta B^3\right)\right] \\
&= \frac{2}{\sqrt{B^\mu B^\nu \Lambda_{\mu,\nu}}} I_1\left(\sqrt{B^\mu B^\nu \Lambda_{\mu,\nu}}\right) \\
&= \sum_{k\geq 0} \left(\frac{B^\mu B^\nu \Lambda_{\mu,\nu}}{4}\right)^k \frac{1}{k!(k+1)!}\,,
\end{aligned}$$

where $\Lambda_{\mu,\nu}$ is the matrix $\mathrm{diag}(+,-,-,-)$. In our case ($\sigma^\mu = (\mathbf{1}, \vec{\sigma})$)

$$B^\mu = z\hat{\phi}^p_\alpha \sigma^\mu_{\alpha,\beta}\phi^p_\beta \,,$$

so that

$$B^\mu B^\nu \Lambda_{\mu\nu} = z^2 \hat{\phi}^p_\alpha \phi^p_\beta \hat{\phi}^q_\gamma \phi^q_\delta \left(\sigma^\mu_{\alpha\beta}\sigma^\nu_{\gamma\delta}\Lambda_{\mu\nu}\right) = 2z^2 \hat{\phi}^p_\alpha \phi^p_\beta \hat{\phi}^q_\gamma \phi^q_\delta (\delta_{\alpha\beta}\delta_{\gamma\delta} - \delta_{\alpha\delta}\delta_{\beta\gamma}) \,.$$

The terms with $\beta = \delta$ or $\alpha = \gamma$ gives zero, meaning that only SU(2) singlets contribute[9]. Since bosonic SU(2) singlets vanish, $x_\uparrow x_\downarrow - x_\downarrow x_\uparrow = 0$, disorder average gives only three terms:

$$\Omega = 1 + z^2 \left[\hat{\eta}_\downarrow \hat{\eta}_\uparrow\right] \left[\eta_\uparrow \eta_\downarrow\right] + z^2 \left[\tfrac{1}{\sqrt{2}} \left(\hat{x}_\uparrow \hat{\eta}_\downarrow - \hat{x}_\downarrow \hat{\eta}_\uparrow\right)\right] \left[\tfrac{1}{\sqrt{2}} (x_\uparrow \eta_\downarrow - x_\downarrow \eta_\uparrow)\right] . \tag{3.30}$$

Integration over the SU(2) invariant Haar measure projects the Fock space $\mathcal{F} = \mathcal{S}(\mathbb{C}^2 \otimes \mathbb{C}^{1|1})$ onto the irreducible three-dimensional singlet representation. Note that the supersymmetric structure is spoiled, and this suggests introducing new supervectors $\Psi, \Psi^* \in \mathbb{C}^{2|1}$ corresponding to the only particles which can propagate:

$$\Psi = \left(1, \eta_\uparrow \eta_\downarrow, \tfrac{1}{\sqrt{2}}(x_\uparrow \eta_\downarrow - x_\downarrow \eta_\uparrow)\right)$$
$$\Psi^* = \left(1, \eta^*_\downarrow \eta^*_\uparrow, \tfrac{1}{\sqrt{2}}(x^*_\uparrow \eta^*_\downarrow - x^*_\downarrow \eta^*_\uparrow)\right) .$$

We now consider the interaction vertex of type A in the notation of figure 3.7, which is given by $\Omega(e_1)\Omega(e_2)$, where $\Omega(e)$ is defined in (3.30). Expanding the product and expressing the result in terms of Ψ, Ψ^* (dropping terms which are not singlets and whose integral is zero), we get

$$\Omega(e_1)\Omega(e_2) = (1 - t_A^2)\Psi^{*p}(e'_1)\Psi^p(e_1)\Psi^q(e_2)\Psi^{*q}(e'_2) + t_A^2 \Psi^{*p}(e'_1)\Psi^p(e_2)\Psi^q(e_1)\Psi^{*q}(e'_2) \,.$$

After redefinition $\Psi^*(e'_2) \leftrightarrow \Psi(e'_2)$, $\Psi(e_2) \leftrightarrow \Psi^*(e_2)$, we find the interaction vertices (1.24) of the coherent state representation of the percolation model with identification:

$$p_A = t_A^2 \,, \quad p_B = 1 - t_B^2 \,.$$

This result can actually be understood more straightforwardly using the transfer matrix formulation, as done in the original paper [101]. Indeed, after disorder average, the SU(2) singlets on up links

$$|0\rangle \,, \quad \frac{1}{\sqrt{2}}(b^\dagger_\uparrow f^\dagger_\downarrow - b^\dagger_\downarrow f^\dagger_\uparrow)|0\rangle \,, \quad f^\dagger_\uparrow f^\dagger_\downarrow |0\rangle \,,$$

constitute the fundamental representation V of $\mathfrak{sl}(2|1)$. On down links,

$$|0\rangle \,, \quad \frac{1}{\sqrt{2}}(\bar{b}^\dagger_\uparrow \bar{f}^\dagger_\downarrow - \bar{b}^\dagger_\downarrow \bar{f}^\dagger_\uparrow)|0\rangle \,, \quad -\bar{f}^\dagger_\uparrow \bar{f}^\dagger_\downarrow |0\rangle \,,$$

[9] Note that more generally for a group G, integrating over the G-invariant Haar measure will project the integrand over G singlets.

constitute the dual fundamental $V^\star$. The transfer matrix on neighboring sites, eq.(3.29) will now act on the tensor product $V \otimes V^\star$, which decomposes as (one-dimensional) singlet plus (eight-dimensional) adjoint representation [99]. Then the most general coupling will be given by the projector onto the singlet (since projector onto singlet and adjoint sum to identity), and the correct weights are readily found, leaving us with the supersymmetric vertex model of percolation, which was discussed in section 1.1.2.

Mapping to percolation and results

We have seen in the previous section that the disorder averaged paths contributing to Green functions and conductance are percolation loops (also called hulls). This allows for the exact computation of several quantities at the SQH transition.

Loops of classical percolation correspond to localized states, and the length of these loops diverges at the critical point $p_c = 1/2$. The correlation length diverges as $\xi \sim |p - p_c|^{-4/3}$, and we find that the exponent of the quantum localization length is $\nu = 4/3$. While the percolation model for the IQHE discussed in 3.1.1 does not provide the right exponent, percolation turns out to exactly describe localized states in the SQHE.

In the following discussion we will focus on the computation of a single Green function and the conductance. We mention however that the mapping to percolation allows also to derive some multifractal exponents governing scaling of moments of wavefunctions at Anderson transitions [143, 186].

Let us consider first the single Green function. Since single bosons or fermions cannot propagate alone, $\overline{G(e_o, e_i; z)}$ will be zero unless $e_o = e_i$. In this case, one can insert at no cost a pair of fermionic fields $\eta_\downarrow(e)\eta^*_\downarrow(e)$ in the correlator $\langle \eta(e)_\uparrow \eta^*_\uparrow(e) \rangle$, where now $\langle \bullet \rangle$ denotes ensemble average in the disorder averaged model. Then $\overline{G(e, e; z)}$ is given by a correlation function of $(\eta\eta)$ fields running along a single loop, which is weighted as z^{2L}, L being the length of the loop. This shows that [18, 101]

$$\operatorname{Tr} \overline{G(e, e; z)} = \begin{cases} 2 - \sum_{L>0} P(L, e) z^{2L} & \text{if } |z| < 1 \\ \sum_{L>0} P(L, e) z^{-2L} & \text{if } |z| > 1 \end{cases} .$$

$P(L, e)$ is the probability that the edge e belongs to a loop of length L. Note that the energy is the conjugate variable to the length of loops. The local density of states defined as the discontinuity of the Green functions (3.5) (which now are traced over spin indices), can be written in terms of percolation probabilities as [18, 101]:

$$\overline{\rho(e, \epsilon)} = \frac{1}{2\pi} \left(1 - \sum_{L>0} P(L, e) \cos(2L\epsilon) \right) . \tag{3.31}$$

If we consider the point e in the bulk of the system, then the length of a loop is related to its size ξ by $L \sim \xi^{d_f}$, with d_f the fractal dimension, which for percolation is given by the dimension of the two-leg bulk operator $h_b = 1/4$ as $d_f = 2 - h_b = 7/4$ [178]. This implies using standard scaling arguments $P(e, L) \sim L^{h_b/(2-h_b)} = L^{-8/7}$, and the

following behavior of the bulk LDOS[10]:

$$\overline{\rho^b(e,\epsilon)} \sim |\epsilon|^{1/7} .$$

If the point e is located at the boundary, which is a natural case when the strip geometry is considered, then $P(e,L) \sim L^{-1-h_s/d_f}$ ($L \sim \xi^{d_f}$ holds also if loops touch the boundary since we consider an ordinary surface transition, driven by the divergence of bulk correlation length). Using the dimension of the boundary two-leg exponent $h_s = 1/3$, $P(e,L) = L^{-25/21}$, giving the boundary LDOS scaling [186]:

$$\overline{\rho^s(e,\epsilon)} \sim |\epsilon|^{4/21} .$$

We now consider the PCC conductance. From the mapping to percolation, we find that after disorder average (3.28) is given by twice the probability $P(i,o)$ that a percolation hull connects the incoming link i to the outgoing one, o:

$$\bar{g} = 2P(i,o) .$$

If more generally a set of incoming edges $C_{\rm in} = \{i_b\}$, and another $C_{\rm out} = \{o_a\}$ of outgoing ones, is considered, Landauer formula (3.8) gives

$$\bar{g} = 2 \sum_{a \in C_{\rm out}} \sum_{b \in C_{\rm in}} P(i_b, o_a) ,$$

which, after regrouping of configurations in the sum, is the mean number of lines connecting incoming to outgoing links. The probability $P(i,o)$ coincides with the probability that the two points lie on the same loop since the segment joining i to o comes always paired with another going back from o to i. Then $P(i,o)$ is given by the two point function of two-leg operators. If the two point are in the bulk at a distance r, $\bar{g} \sim r^{-1/2}$, while if the points are on the boundary (of the upper half plane) $\bar{g} \sim r^{-2/3}$.

We remark that not every observable in the SQHE can be computed using percolation. Indeed percolation describes the averaged paths contributing to the product of up to three Green functions only [143]. All higher powers of Green functions require to introduce bosonic and fermionic replicas, and to deal with a theory with an infinite number of degrees of freedom on each link, sharing similar difficulties with the model for the IQHE.

Conductance of a strip

Now we consider the more realistic case of a two terminal probe, when the SQH network has the geometry of a strip of width $2L$ and length $2L_T$, and contacts are connected to the bottom and the top of the strip. We recall that in this situation all configurations of the loop model fall into disjoint sectors labeled by the number of *through lines* $2k$.

[10] The absolute value comes from the fact that eigenenergies $(\epsilon, -\epsilon)$ occur in pairs in class C, as discussed above.

The lowest energy state in each sector corresponds in the CFT to the boundary $2k$-leg (primary) field of dimension $h_{1,1+2k}$, see section 1.2.4.

We put the source of current at the bottom and the drain at the top (an equal result would be obtained by switching drain and source) and consider the mean conductance given by the average number of through lines going from the source to the drain of the current, times 2 for spin:

$$\bar{g} = 2\sum_{k=1}^{\infty} kP(k, L_T/L, L_T/\xi)\,. \tag{3.32}$$

$P(k, L_T/L, L_T/\xi)$ is the probability that exactly $2k$ paired through lines (k connecting source to drain) run through the system, and ξ is the bulk correlation length. At the transition, $\xi = \infty$, and for large L_T/L we expect that $P(k, L_T/L, 0) \sim e^{-\pi h_{1,1+2k} L_T/L}$ from conformal invariance. For $L_T/L \gg 1$ the sum in eq. (3.32) for $\bar{g}$ is dominated by $k = 1$, and the first subleading correction is controlled by the two-leg exponent $h_{1,3} = 1/3$.

One can do more than that, and compute the exact conductance (3.32), as shown by Cardy in [47, 48]. The idea behind this computation is simple and thanks to our discussion of rectangular partition functions, the computation is immediate. Consider now the loop model with generic fugacity of loops β. Denote the ensemble averaging over loop configurations as $\langle\bullet\rangle$, and the number of loops touching the bottom boundary, the top, both or none as N_b, N_t, N_c, N_o respectively, see figure 3.17.

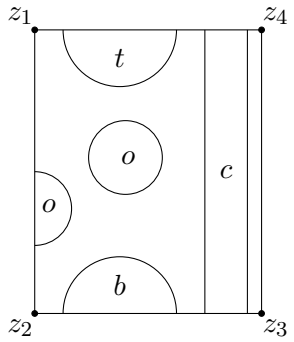

Figure 3.17: Loops touching the boundary on the bottom (b), top (t), both (c) and none of the two (o).

Then the conductance will be given by $2\langle N_c\rangle$, which can be written as:

$$\langle N_c\rangle = \lim_{\beta\to 1} \frac{\partial}{\partial\beta}\langle\beta^{N_c}\rangle$$

This would require the knowledge of the partition function for a rectangle where we count loops touching both boundaries β and all the other as 1. It should be possible to obtain this result using boundary loop models, but we do not have developed the formalism of rectangular amplitudes in this direction yet. Instead we use the following

trick [47]. If we call $Z(\beta_1, \beta_2)$ the partition function where loops touching the bottom are weighted β_1 and those touching the top β_2, then

$$Z(\beta,\beta) = \langle \beta^{N_b+N_t+N_c+N_o} \rangle \,, \quad Z(1,\beta) = \langle \beta^{N_t+N_o} \rangle$$
$$Z(\beta,1) = \langle \beta^{N_b+N_o} \rangle \,, \quad Z(1,1) = \langle \beta^{N_o} \rangle \,.$$

In terms of these partition functions the mean number will be:

$$\begin{aligned} \langle N_c \rangle &= \lim_{\beta\to 1} \frac{\partial}{\partial\beta} \left(Z(\beta,\beta) - Z(1,\beta) - Z(\beta,1) + Z(1,1) \right) \\ &= \lim_{\beta\to 1} \frac{\partial}{\partial\beta} \frac{Z(\beta,\beta)Z(1,1)}{Z(\beta,1)Z(1,\beta)} \,, \end{aligned} \tag{3.33}$$

where in the second line we used the fact that every partition function is one at the percolation point $\beta = 1$. Again the computation of these partition functions would require in principle the knowledge of rectangular amplitudes for boundary loop models. However their expression can be obtained easily by thinking in terms of Fortuin-Kasteleyn clusters. Indeed loops touching a boundary get a weight one if the cluster they encircle is weighted one. Then $Z(\beta,\beta)$ corresponds to the partition function of the Potts model in the FK representation with free boundary conditions on every side, $Z(1,\beta)$ and $Z(\beta,1)$ to that with fixed boundary conditions on top and bottom respectively, and $Z(1,1)$ to the case of fixed on both bottom and top boundaries. The boundary condition changing operator between fixed (F) and free (f) boundary conditions in the Potts model is $\phi_{1,2}^{F,f}$ as discussed in section 2.2.2, whose weight we will denoted here by h. According to the discussion of that section, these partition functions are given by

$$\begin{aligned} Z(\beta,\beta) &= Z_{\mathcal{R}}(L,L') \\ Z(1,\beta) &= Z_{\mathcal{R}}(L,L') \langle \phi_{1,2}^{f,F}(z_2) \phi_{1,2}^{F,f}(z_3) \rangle \\ Z(\beta,1) &= Z_{\mathcal{R}}(L,L') \langle \phi_{1,2}^{F,f}(z_1) \phi_{1,2}^{f,F}(z_4) \rangle \\ Z(1,1) &= Z_{\mathcal{R}}(L,L') \langle \phi_{1,2}^{F,f}(z_1) \phi_{1,2}^{f,F}(z_2) \phi_{1,2}^{F,f}(z_3) \phi_{1,2}^{f,F}(z_4) \rangle \,, \end{aligned}$$

where $Z_{\mathcal{R}}(L,L')$ is the partition function for homogeneous boundary conditions, eq. (2.21). We transform the correlators to the upper half plane w. The expression of the Jacobian was given in (2.27), and we have

$$\frac{Z(\beta,\beta)Z(1,1)}{Z(\beta,1)Z(1,\beta)} = \frac{\langle \phi_{1,2}^{F,f}(w_1) \phi_{1,2}^{f,F}(w_2) \phi_{1,2}^{F,f}(w_3) \phi_{1,2}^{f,F}(w_4) \rangle_{\mathbb{H}}}{\langle \phi_{1,2}^{f,F}(w_1) \phi_{1,2}^{F,f}(w_4) \rangle_{\mathbb{H}} \langle \phi_{1,2}^{f,F}(w_2) \phi_{1,2}^{F,f}(w_3) \rangle_{\mathbb{H}}} \,.$$

The four point function involved is precisely a correlator computed in section 2.2.2 (F and f correspond to boundary labels 0 and 1/2 in notation that section, $\zeta = w_{12}w_{34}/w_{13}w_{24}$):

$$\langle \phi_{1,2}^{F,f}(w_1) \phi_{1,2}^{f,F}(w_2) \phi_{1,2}^{F,f}(w_3) \phi_{1,2}^{f,F}(w_4) \rangle_{\mathbb{H}} = \mathcal{N}^0 \left(\frac{w_{13}w_{24}}{w_{12}w_{23}w_{14}w_{34}} \right)^{2h} \mathcal{G}^0(1-\zeta) \,.$$

with $\mathcal{G}^0$ given by (1.45) and $\mathcal{N}^0 = \beta$ (2.31). The two point functions are

$$\langle \phi_{1,2}^{f,F}(w_1)\phi_{1,2}^{F,f}(w_4)\rangle_{\mathbb{H}} \langle \phi_{1,2}^{f,F}(w_2)\phi_{1,2}^{F,f}(w_3)\rangle_{\mathbb{H}} = (w_{14}w_{23})^{-2h} ,$$

and putting everything together one can evaluate the derivative in (3.33) to have [47,48]:

$$\bar{g} = 1 - \frac{\sqrt{3}\left(\log(1-\zeta) - (\zeta-1)\,{}_3F_2\left(1,1,\frac{4}{3};\frac{5}{3},2;1-\zeta\right)\right)}{2\pi} .$$

Using now (2.28) we express ζ in terms of the modular parameter $q = e^{2\pi i\tau}$, where $\tau = iL_T/L$. This yields the conductance for short wires ($L \gg L_T$):

$$\bar{g} = \frac{\sqrt{3}}{2}\frac{L}{L_T} ,$$

predicting an irrational value of the conductivity $\sigma = \frac{\sqrt{3}}{2}$. The other limit can be accessed by a modular transform:

$$\zeta = \left(\frac{\theta_2(\tilde{q})}{\theta_3(\tilde{q})}\right)^4 , \quad \tilde{q} = e^{-2\pi L_T/L} ,$$

yielding the exact amplitude of the conductance of long wires ($L_T \gg L$):

$$\bar{g} = \frac{\Gamma\left(-\frac{1}{3}\right)\Gamma\left(-\frac{1}{6}\right)}{\sqrt{3}\pi^{3/2}} \exp\left(-\frac{\pi}{3}\frac{L_T}{L}\right) .$$

Note correctly the presence of the boundary two-leg exponent $h_{1,3} = 1/3$ in $\bar{g} \sim \exp(-\pi h_{1,3} L_T/L)$.

Conductance of a cylinder

We consider now the geometry of a cylinder, where contacts are put on the bottom and top of the cylinder, and ask what is the conductance predicted by CFT in this case. Denote the circumference of the cylinder W and its length L, and note that this geometry is equivalently to an annulus of width L and length W, a remark already exploited to derive Cardy constraints in section 1.2.3. The disorder averaged two terminal SQH conductance in this geometry will be given by the number of percolation hulls connecting the two boundaries of the annulus.

Consider percolation on an annulus and give a weight β_{12} to loops touching both boundaries while all other loops, contractible or not, are weighted one. Call the ensemble of such loop configurations $\mathcal{L}$ and for a given configuration the number of loops touching both boundaries N_{12}. This coincides with the number of contractible spanning clusters (called N_c in [47]), which does not include spanning clusters N_w wrapping around the cycle of the annulus. Then defining the partition function

$$Z = \sum_{\mathcal{L}} \beta_{12}^{N_{12}} , \tag{3.34}$$

the conductance will be

$$\bar{g} = 2\langle N_{12}\rangle = 2 \lim_{\beta_{12}\to 1} \frac{\partial}{\partial \beta_{12}} Z\,.$$

We will present the computation of Z, using the results of [70] about boundary loop models discussed partly in section 1.2.5. In [70] the authors conjectured the partition function for a loop model on an annulus in which loops are weighted differently depending on homotopy and which boundary they touch.

Parametrize the weight of loops β_{12} in terms of r_{12} by (we use $p = 2, r_1 = r_2 = 1$ in formula (1.62))

$$\beta_{12} = \frac{4}{3}\cos^2\left(\frac{\pi}{6} r_{12}\right)\,,$$

and recall the definition of the modular parameter

$$q := \exp\left(2i\pi\tau\right)\,; \quad \hat{q} := \sqrt{q}\,; \quad \tau := i\frac{W}{L}\,.$$

The partition function (3.34) is[11]:

$$Z = \frac{1}{P(\hat{q})} \sum_{n\in\mathbb{Z}} \hat{q}^{h_{r_{12}-2n,r_{12}}} + \dots$$

where $P(\hat{q})$ is the generating function of integer partitions and $h_{r,s}$ is the Kac table for percolation ($p = 2$ in (1.43)). The dots contain the contribution of sectors with $2j$ non contractible lines through the annulus, and clearly do not depend on β_{12}. Then we get

$$\begin{aligned}
\bar{g} &= 2\frac{1}{P(\hat{q})} \sum_{n\in\mathbb{Z}} \left(-\tfrac{3\sqrt{3}}{\pi}\right) \lim_{r_{12}\to 1} \frac{\partial}{\partial r_{12}} \hat{q}^{h_{r_{12}-2n,r_{12}}} \\
&= -\frac{\sqrt{3}}{2\pi}\frac{1}{P(\hat{q})} \sum_{n\in\mathbb{Z}} (1-6n)\hat{q}^{\frac{1}{2}n(3n-1)} \log(\hat{q}) \\
&= -\frac{\sqrt{3}}{2\pi} \log(\hat{q}) \left(1 - 4\hat{q} + 4\hat{q}^2 + 4\hat{q}^4 + \dots\right) \\
&= -\frac{\sqrt{3}}{2} i\tau\theta_4(\tau)^2\,,
\end{aligned}$$

where

$$\theta_4(\tau) := \sum_{n\in\mathbb{Z}} (-1)^n q^{n^2/2}\,,$$

or in terms of $\eta(\tau) = q^{1/24}\prod_{n=1}^{\infty}(1-q^n)$,

$$\bar{g} = -\frac{\sqrt{3}}{2} i\tau \frac{\eta(\tau/2)^4}{\eta(\tau)^2}\,.$$

[11] Here we used Z formula (6) of [70]. Note that here we did not use formula (67) of [70], which gives the partition function for the Potts model in which also wrapping clusters are weighted β_{12}, and which could be used to compute $\langle N_c + N_w\rangle$.

In the limit $q \to 0$ corresponding to $W/L \to \infty$, we have

$$\bar{g}\,(W/L \to \infty) \sim \frac{\sqrt{3}}{2}\frac{W}{L}\,,$$

correctly coinciding with the expression for a very wide strip. For the opposite limit $\tilde{q} := \exp(-2i\pi/\tau) \to 0$, corresponding to $W/L \to 0$, we use the properties of the conductance under modular inversion $\tau \to -1/\tau$:

$$\begin{aligned}\bar{g} &= \frac{\sqrt{3}}{2}\theta_2(-1/\tau)^2 = 2\sqrt{3}\frac{\eta(-2/\tau)^4}{\eta(-1/\tau)^2} \\ &= 2\sqrt{3}\tilde{q}^{1/4}(1 + 2\tilde{q} + \tilde{q}^2 + 2\tilde{q}^3 + \dots)\,,\end{aligned}$$

where $\theta_2(\tau) := \sum_{n\in\mathbb{Z}} q^{(n+1/2)^2/2}$. So we have

$$\bar{g}\,(W/L \to 0) \sim 2\sqrt{3}\exp\left(-\frac{\pi}{2}\frac{L}{W}\right)\,.$$

Note that correctly in this limit $\bar{g} \sim \text{const}\cdot\exp(-2\pi x_1 L/W)$, where $x_1 = 1/4$ is the bulk 1-hull exponent, the leading contribution.

The formula derived above is not entirely a new result. Cardy derived the generating function of probabilities that there are N_c percolation spanning clusters in the annular geometry in [49]. However in that work the author does not give a closed formula for the mean number of spanning clusters. We have verified that the formula given above coincides with the results given by Cardy from a series expansion up to very high order.

Chapter 4

Boundary criticality at quantum Hall transitions

In this chapter we present the main results of the thesis, building on the several concepts discussed in the previous chapters. In section 4.1 we discuss edge states in network models. We focus on the spin quantum Hall case, for which we describe the edge states in the various formulations of the models for the transition, both from a microscopic and from a field theory point of view. In section 4.2 we present the technical details of the computation of exact critical exponents of the boundary conformal field theories describing higher plateaus transitions in the spin quantum Hall effect. The results obtained allow to predict the scaling of the mean conductance in the network model, and are verified against extensive numerical simulations. This chapter contains original research material published by the author in [27, 28].

4.1 Edge states in network models

4.1.1 Chalker-Coddington model with extra edge channels

The motivation for introducing the Chalker-Coddington (CC) model in section 3.1.2 was the semiclassical picture of electrons moving on isopotential contours of the disordered potential to which the two-dimensional electron gas is subjected. At the boundary the presence of a confining potential allows for propagation of chiral edge states. The original formulation of the CC model [55] however does only account for the possibility of a single pair of counter propagating edge states at the boundary, see figure 3.9. It is the purpose of this section to introduce a new extended network model with extra channels at the boundary modeling higher filling fractions in the quantum Hall sample. Similar ideas were already discussed in [14, 131, 154], and the relevance of perfect conducting channels has been already appreciated in the wire (quasi 1D) limit, as reviewed in [78]. Higher fillings ν require the introduction of ν chiral counter-propagating channels at the boundaries of the network. More generally chiral edge states appear at the interface between two quantum Hall states distinguished by different values of the bulk conduc-

tance, see figure 4.1, the usual case considered so far corresponding to terminate the sample to vacuum (having $\sigma = 0$). This property is the bulk-boundary correspondence of topological insulators, see for example [108] for a review of these general ideas.

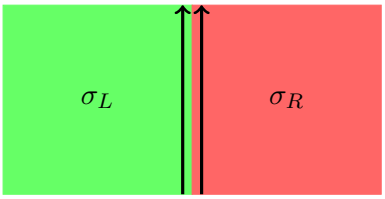

Figure 4.1: σ_R and σ_L are Hall conductances characterizing the two samples put to contact. The number of edge states is given by $|\sigma_R - \sigma_L|$ and their chirality by the sign of $\sigma_R - \sigma_L$.

If we imagine our sample in a topologically non-trivial background, there are four possible networks to be studied, where extra links can be directed up or down at each edge, see figure 4.2. The bulk of width $2L$ contains alternating up- and down-going columns of links. In addition, m (n) extra columns with the *same* chirality are added at the left (right) edge. We label the four possible variants by $(\mathcal{L} = \pm m, \mathcal{R} = \pm n)$; positive labels $(\mathcal{L}, \mathcal{R})$ mean the same direction of the edge links and the closest bulk link. The physics of the $m \to m + 1$ plateau transition[1] can be investigated with the choice $\mathcal{L} = \mathcal{R} = m > 0$, and is the most physically motivated case. Note that $\mathcal{L} = \mathcal{R} = m < 0$ corresponds simply to invert the direction of the magnetic field.

The *boundary* nodes where the fluxes on the extra edge links scatter, are described by matrices of the form of the bulk nodes (3.3), but with new independent transmission amplitudes, t_L and t_R, one for each edge of the system. Note that now in the Feynman expansions of Green functions (3.9) paths at the edge nodes can either turn (left or right, depending on which incoming edge they are visiting) or go straight, and eventually can cross. Transport properties will be drastically affected by the presence of extra channels. Consider for definiteness the strip geometry with open links at the top and bottom of the strip. We imagine a two-probe measurement, where the source of current is put at the bottom of the strip and the drain at the top. The transmission matrix t we have to use in Landauer formula (3.8) can be defined from the scattering matrix of the whole network, relating open incoming to open outgoing links at the two extremities:

$$S_{\text{net}} = \begin{pmatrix} r' & t \\ t' & r \end{pmatrix} .$$

t (t') relates incoming links at the bottom (top) to outgoing at the top (bottom) and r, r' are reflection matrices. We see that if we consider a network with $\mathcal{L} \neq \mathcal{R}$, t and t' are different rectangular matrices, so the bottom-to-top and top-to-bottom conductance, defined respectively as

$$g_{b,t} := \operatorname{Tr} tt^\dagger , \quad g_{t,b} := \operatorname{Tr} t't'^\dagger ,$$

[1] We note that incorporating extra channels in the CC model neglects electron interactions which could be relevant at the edge in experimental realizations of the QH effect, as discussed in [27].

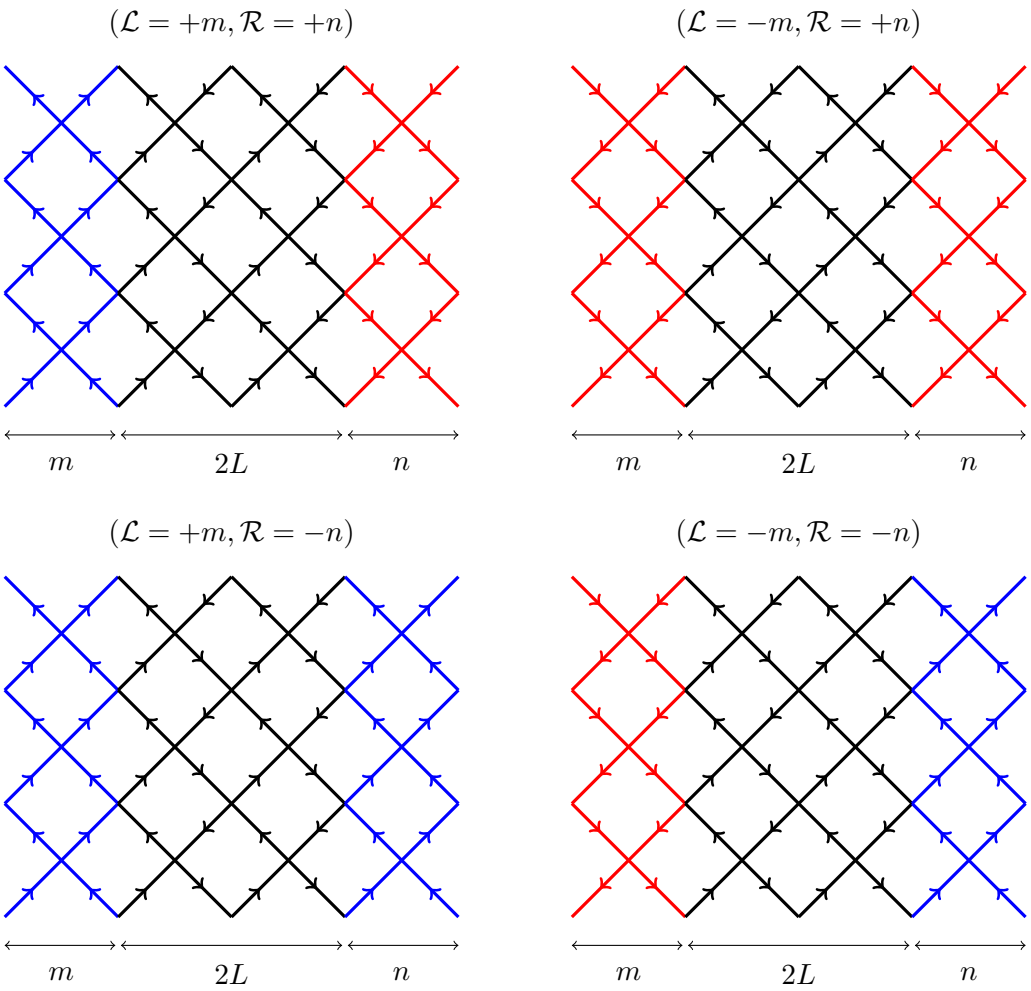

Figure 4.2: The four possible networks with extra chiral edge channels.

are different. Denoted the length and width (without counting extra edges) of the strip $2L_T$ and $2L$ respectively, we expect that in the limit of very long wires, the conductance tends to a non-zero asymptotic value:

$$g_{b,t} \simeq \max(0, \mathcal{L} - \mathcal{R}) + A \exp\left(-\frac{1}{\lambda}\frac{L_T}{L}\right) .$$

Our primary interest is to characterize the decay length λ at criticality using conformal field theory. For this purpose, we will not deal with the CC model with extra edges, since as discussed in the section 3.1.5, no analytical solution of the CC model has been found so far. Instead we will focus our attention on the SQH network, introduced in section 3.2.2, defined by replacing U(1) phases on each link of the CC model with SU(2) ones, relating up and down fluxes.

Before proceeding to the study of the SQH case, we note that more generally one could investigate any network model [135] with extra chiral edge channels. This is an interesting perspective from transport properties, but we remark that this procedure has an interpretation in terms of plateaus transitions like in the IQHE, only in some cases. Apart from the CC model and the network model for the SQHE, another interesting case is the one describing the thermal quantum Hall effect [56], which shows a phenomenology similar to the IQHE and belongs to class D in the symmetry classification discussed in section 3.1.6. Extra edges have already been considered in [131, 154] for a network model describing the quantum spin Hall effect (not to be confused with the SQHE, despite the unfortunate choice of names in the literature) belonging to class AII. In that case, time reversal symmetry requires two counter-propagating channels on each link of the network, and the possible boundary phenomena are reduced to having an even or odd number of channels in the strip, consistent with the $\mathbb{Z}_2$ quantization of the spin conductance in the quantum spin Hall effect [123].

4.1.2 Edge states in loop models and spin chains

Geometrical models for the SQH network model with extra edge channels

We have seen in section 3.2.2 that disorder averaged Feynman paths contributing to the computation of a single Green function or the conductance in the SQH network are of a simple form: they are percolation hulls. In the presence of extra edges, the supersymmetric formulation of observables in the network is straightforwardly generalized. Integration over Haar measure of random SU(2) phases on each link will again project onto a three dimensional space, but this time the interaction at the new boundary vertices is modified and immediately interpreted geometrically: lines can either go through or cross. The resulting geometrical model is no more percolation, but it can nonetheless be formulated as a loop model. The vertices are depicted in figure 4.3, and the corresponding transfer matrices acting on neighboring sites $i, i+1$, at the different types of vertices $s = A, B, L, R$ are:

$$T_{A,i} = (1 - t_A^2)I + t_A^2 E_i, \qquad A \leftrightarrow B, \tag{4.1}$$

$$T_{L,i} = (1 - t_L^2)I + t_L^2 P_{i,i+1}, \qquad L \leftrightarrow R\,. \tag{4.2}$$

E_i is the Temperley-Lieb generator, introduced for the Potts model in section 1.1.1, and $P_{i,i+1}$ is the permutation operator of neighboring strands $i, i+1$. Expanding all the vertices into pieces of oriented loops we end up with a sum over configurations like the one illustrated in figure 4.4. As in the case of no extra edges, the loop orientation is a property of the underlying lattice, not of the loop itself, and in particular no sum over orientations is implied. The weight of loops is $\beta = 1$.

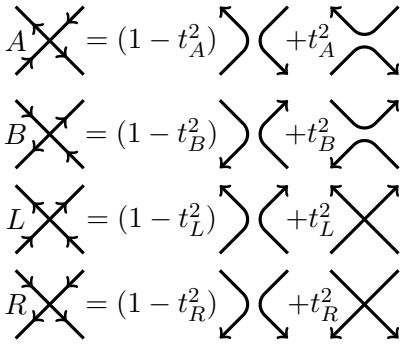

Figure 4.3: Vertices of the model resulting after disorder average in the SQH network with extra edge channels. t_s, $s = A, B, L, R$, refers to the type of vertex.

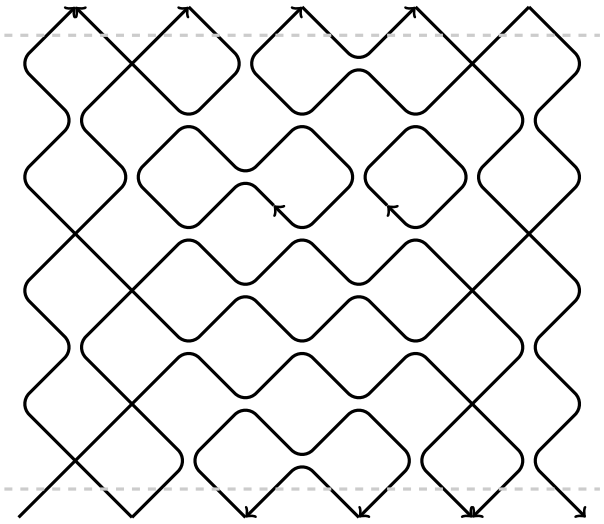

Figure 4.4: A configuration of the loop model in the case $\mathcal{L} = \mathcal{R} = 2$, $2L = 6$. Each loop carries a weight of 1.

The couplings $t_s^2, 1 - t_s^2$ are all positive and have an interpretation as Boltzmann weights of the statistical mechanics model of loops. The critical point is reached by tuning bulk couplings $t_A = t_B$, and in the anisotropic limit, all $t_s \ll 1$, the transfer matrix is approximated by $\exp\big(-t_A t_B H\big)$. The four possible Hamiltonians corresponding to

different choices of $(\mathcal{L},\mathcal{R})$ are

$$\begin{aligned}(m;n):H=&\ H_{\mathcal{L}>0}+H_{\text{bulk}}+H_{\mathcal{R}>0}\\(m;-n):H=&\ H_{\mathcal{L}>0}+H_{\text{bulk}}+H_{\mathcal{R}<0}\\(-m;n):H=&\ H_{\mathcal{L}<0}+H_{\text{bulk}}+H_{\mathcal{R}>0}\\(-m;-n):H=&\ H_{\mathcal{L}<0}+H_{\text{bulk}}+H_{\mathcal{R}<0}\,.\end{aligned}$$

where the bulk critical Hamiltonian is that of percolation

$$H_{\text{bulk}}\ =\ -\sum_{i=m}^{2L+m-2}E_i\ ,$$

while the boundary Hamiltonians are as follows:

$$\begin{aligned}H_{\mathcal{L}>0}\ =&-u\sum_{i=0}^{m-1}P_{i,i+1} &\qquad H_{\mathcal{R}>0}\ =&\ -v\sum_{i=2L+m-1}^{2L+m+n-2}P_{i,i+1}\\H_{\mathcal{L}<0}\ =&-u\sum_{i=0}^{m-2}P_{i,i+1}-t'E_{m-1} &&\qquad (4.3)\\H_{\mathcal{R}<0}\ =&-t''E_{2L+m-1}-v\sum_{i=2L+m}^{2L+m+n-2}P_{i,i+1}\ . &&\qquad (4.4)\end{aligned}$$

The couplings t',t'' are not taken to be equal to 1 despite they correspond to vertices of type A,B since we would like to consider them as boundary couplings, and $u=(t_L/t_A)^2$, $v=(t_R/t_A)^2$ are arbitrary *positive* numbers.

Spin chain formulation

Using the supersymmetric transfer matrix method to deal with disorder average, we found that the Fock space of bosons and fermions are projected onto the fundamental V (dual-fundamental $V^\star$) 3-dimensional irreducible representations of $\mathfrak{sl}(2|1)$ on up links (resp. down links) [101]. In this formulation the node transfer matrices $T_{s,i}$ (4.1)-(4.2), act in the tensor products $V_i\otimes V_{i+1}^\star$ in the bulk and $V_i\otimes V_{i+1}$ or $V_i^\star\otimes V_{i+1}^\star$ in the extra edge regions. Thus, we have four types of supersymmetric spin chains

$$\begin{aligned}(m;n):&\quad V^{\otimes m}\otimes(V\otimes V^\star)^{\otimes L}\otimes\ (V^\star)^{\otimes n}, &(4.5)\\(m;-n):&\quad V^{\otimes m}\otimes(V\otimes V^\star)^{\otimes L}\otimes\ V^{\otimes n}, &(4.6)\\(-m;n):&\quad (V^\star)^{\otimes m}\otimes(V\otimes V^\star)^{\otimes L}\otimes(V^\star)^{\otimes n}, &(4.7)\\(-m;-n):&\quad (V^\star)^{\otimes m}\otimes(V\otimes V^\star)^{\otimes L}\otimes\ V^{\otimes n}. &(4.8)\end{aligned}$$

All tensor products between neighboring sites of these chains decompose into the direct sum of two $\mathfrak{sl}(2|1)$ representations [99]. We note that, while in the bulk these spin chains

are antiferromagnetic since $V \otimes V^\star$ contains the singlet representation, in the boundary, they have a ferromagnetic nature[2].

For understanding the loop model associated to the SQH network with extra channels, it is useful and interesting from a statistical mechanics point of view, to consider a more general problem, where the fugacity of loops is an arbitrary number β. As for the case with no extra edges (the Potts model), when $\beta = M$ integer we can represent the model using $\mathfrak{gl}(N+M|N)$ spin chains. In the case we are after, the space of states will have the form of (4.5)-(4.8), where V and $V^\star$ correspond to the fundamental and dual fundamental representations of $\mathfrak{gl}(N+M|N)$.

4.1.3 Conformal boundary conditions in sigma models

According to the discussion of sections 3.1.4 and 3.2.2, the field theory description of the IQH and SQH transitions is given by a non-linear sigma model with topological θ-term, eq. (3.20). The target space in the IQH case is non-compact and is $\mathrm{U}(1,1|2)/\mathrm{U}(1|1) \times \mathrm{U}(1|1)$, while for the SQH case, it is compact and is the complex projective superspace $\mathbb{CP}^{1|1}$. On a closed worldsheet, we have already stressed that the θ-term is a topological invariant, and the physics depends on $\theta \pmod{2\pi}$. Identifying θ with σ_{xy}, this implies that all plateau transitions have identical universal properties, and one has to face the problem that the integral part of σ_{xy} cannot be predicted.

The solution to this issue is obtained by considering a system with boundaries, as first noticed in [198]. Strictly speaking, in a finite system with boundaries, there are no well defined topologically distinct sectors. One does not expect the behavior of the RG for the bulk properties to change—the standard analysis should still apply provided the equivalent of the instantons (configurations such that the 'topological term' $\mathcal{Q}$ approaches a constant in the core, far from the boundary) are well localized within the system. But boundary properties are expected to now depend on the exact value of θ; in particular, θ can now be expected to affect perturbation theory. It is the purpose of this section to explain the role of the exact value of θ using intuitions from the lattice discretizations discussed above in the case of the SQH network. We expect that the qualitative considerations apply also to the sigma model for the IQH transition.

Mapping on sigma models: the role of boundaries

We now map the spin chains with extra edge states at the boundaries to sigma models using the spin coherent state quantization and the semiclassical approximation described in section 1.1.4. The role of edge states in this mapping has been discussed in [150, 165]. Consider for definiteness the case of the O(3) sigma model. Denote by $\Omega(i)$ the elementary Berry phase for a spin at site i (recall that the Berry phase is the area enclosed by the loop the sigma model field $n_i(t)$ traces on the surface of the target space, the

[2]Ferromagnetic spin chains describing edge states in the IQHE were considered in [103].

sphere). The total phase for the usual antiferromagnetic chain of spin s would read

$$S_{\text{top}} = s\sum_{i=1}^{2L}(-1)^i\Omega(i) \approx \frac{s}{2}\int_0^{2L}\frac{\partial\Omega}{\partial x}\mathrm{d}x = \frac{s}{2}\left[\Omega(2L) - \Omega(0) + 4\pi Q\right] , \tag{4.9}$$

where Q is an integer measuring the number of times the spin configuration $n(x,t)$ covers the surface of the sphere. For a closed chain $\Omega(2L) = \Omega(0)$, while for an open chain the terms $\Omega(2L), \Omega(0)$ correspond to the Berry phase of edge states at the boundaries. Recall also the identification $\theta = \pi$ for $s = 1/2$.

Let us now suppose we have for instance the first chain of eq. (4.5). Since on the boundary we have representations of the same kind, the Berry phase on that side comes unstaggered, so we have (from now on we set the "spin" $s = 1/2$, which is the right value for our spin chain [170]):

$$S_{\text{top}} = -\frac{m}{2}\Omega(0) + \frac{n}{2}\Omega(2L) + \frac{1}{2}\sum_{i=1}^{2L}(-1)^i\Omega(i) \approx \frac{n+1/2}{2}\Omega(2L) - \frac{m+1/2}{2}\Omega(0) + \pi Q\,.$$

This result suggests that the value of θ is replaced in the presence of extra edge states in the spin chains by two new couplings no more periodic in 2π, $\Theta_1 = \frac{\theta}{\pi} + 2m$ for the left boundary and $\Theta_2 = \frac{\theta}{\pi} + 2n$ for the right boundary. Meanwhile, say for the chain of eq. (4.6) we have

$$S_{\text{top}} = -\frac{m}{2}\Omega(0) - \frac{n}{2}\Omega(2L) + \frac{1}{2}\sum_{i=1}^{2L}(-1)^i\Omega(i) \approx \frac{-n+1/2}{2}\Omega(2L) - \frac{m+1/2}{2}\Omega(0) + \pi Q\,.$$

In this case instead the identification is $\Theta_1 = \frac{\theta}{\pi} + 2m$ for the left boundary and $\Theta_2 = \frac{\theta}{\pi} - 2n$ for the right boundary. From this heuristic argument we have that the spin chains with extra edge states will map to a sigma model where, thanks to the presence of boundaries, the bulk periodic coupling θ gets replaced by two real valued couplings:

$$\begin{aligned} \Theta_1 &= \frac{\theta}{\pi} + 2\mathcal{L}\,, \quad \text{left boundary} \\ \Theta_2 &= \frac{\theta}{\pi} + 2\mathcal{R}\,, \quad \text{right boundary}\,. \end{aligned} \tag{4.10}$$

The precise meaning of this statement will be discussed below. Note that in this kind of argument, the exact nature of the couplings on the boundary is irrelevant. Note also that it does not make a difference whether the spins on the boundary are actually projected onto the fully symmetric representation or not.

We now set $\theta = \pi$ and $\mathcal{L} = \mathcal{R} = p \neq 0$. This choice is equivalent to the same model with $\theta = \pi + 2\pi p$ and $\mathcal{L} = \mathcal{R} = 0$, so that shifting θ by multiples of 2π leads to the apparition of extra edge states. Further, we see that considering a system with boundaries reconciles the possibility of describing the integral part of the Hall conductance $\sigma_H^E = \mathcal{L} = \mathcal{R}$, corresponding to the number of extra channels in the network model.

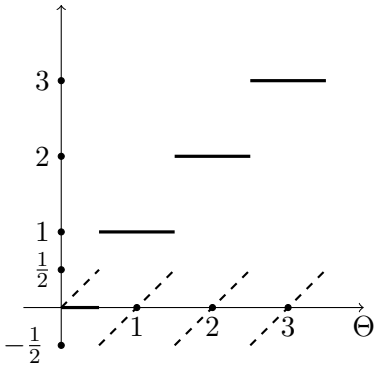

Figure 4.5: The edge (σ_H^E, thick line) and the bulk (σ_H^B, dashed line) parts of the Hall conductance.

$\sigma_H^B = \theta/2\pi$ can then be thought of as a "bulk" property, varying between $(-1/2, 1/2]$, see figure 4.5. In the microscopic model σ_H^B is controlled by staggering the bulk coupling. We refer also to [164] for similar considerations.

The phenomenology described so far is well known in the language of QED (see [58]), to which the $\mathbb{CP}^{M-1}$ model is equivalent at large M, with M flavors and a weak gauge coupling $e^2 \approx \frac{1}{M}$. The $F_{\mu\nu}^2$ term in the action is generated by expanding around the saddle point at large M, see [3] for a review of this mapping.

The topological term is equivalent to a background electrostatic field F in the one-dimensional universe, with $F = \frac{e\theta}{2\pi}$. If this field is too large, it is energetically favorable to produce quark-antiquark pairs. For one such pair the difference in energy per unit length between the state with and without the pair is

$$\Delta E = \tfrac{1}{2}\left[(F-e)^2 - F^2\right] .$$

While it is not energetically favorable for the vacuum to produce a pair if $F \leq \frac{1}{2}e$, it becomes so if $F > \frac{1}{2}e$. Pairs will in fact be produced until F is brought down to a value $F_{\text{screened}} \leq \frac{1}{2}e$. So if $\pi < \theta < 3\pi$, one pair is produced, and more generally if $(2n-1)\pi < \theta < (2n+1)\pi$, n pairs are produced. This is in fact for F positive. If F is negative, that is if $\theta < 0$, things are quite similar, only one produces this time antiquark-quark pairs.

The picture is thus in agreement with the previous findings in the case where there are extra representations V^p on the left and $(V^*)^p$ on the right ($\mathcal{L} = \mathcal{R} = p$), or $(V^*)^p$ on the left and V^p on the right ($\mathcal{L} = \mathcal{R} = -p$), with $\Theta = \frac{\theta}{\pi} + 2\mathcal{R} = 1 + 2\mathcal{R}$. This is once we have identified the chain with no extra representations as corresponding to $\theta = \pi$ ($s = 1/2$). We remark however that nucleation of quark-antiquark pairs in $\mathbb{CP}^{M-1}$ models at large M corresponds to a first order phase transition [1], while in our case it is of second order.

Restricting now to the case $\mathcal{L} = \mathcal{R}$, we observe from eq. (4.9) that another way to have the same physics would be, instead of taking a spin chain with $s = 1/2$ in the bulk and adding edge states by hand, to take directly a chain with spin $s = 1/2 + \mathcal{L} = (1 + 2\mathcal{L})/2$.

In other words, with a spin s (s half an odd integer) chain in the bulk, we expect physics of edge states with $\mathcal{L} = s - 1/2$, which corresponds in turn to a spin on the boundary with value $s' = (s - 1/2)/2$. This is a bulk-boundary correspondence.

In the usual case of the $\mathbb{CP}^1$ model—that is, the O(3) model and the Heisenberg XXX spin chain—all this discussion is somewhat irrelevant. Although edge states still present interesting features, we anticipate that adding extra spins (maybe in a higher dimensional representation) on the boundary does not give rise to new exponents, and the spectrum will in the end coincide with that of the XXX chain with an odd or an even number of sites. This is consistent with the fact that the $SU(2)_1$ WZW model has only two symmetric conformal boundary conditions [9]. In the case of $\mathbb{CP}^{N+M-1|N}$ sigma models however, an infinity of conformal boundary conditions of the corresponding irrational (non-unitary) logarithmic CFT is available, leading to a much richer behavior.

Symmetric conformal boundary conditions in $\mathbb{CP}^{N+M-1|N}$ models

Consider the action of the $\mathbb{CP}^{N+M-1|N}$ sigma model with θ-term, eq. (1.34), on a world-sheet with boundary, say the upper half plane. Imposing vanishing of the action under arbitrary variations of the fields $Z_\alpha, Z_\alpha^\dagger$ (such that $(\delta Z_\alpha^\dagger)Z_\alpha + Z_\alpha^\dagger(\delta Z_\alpha) = 0$), one obtains that the boundary conditions induced by the topological term are

$$(\partial_y + ia_y)Z_\alpha = \frac{\theta}{\pi} g_\sigma^2 (\partial_x + ia_x)Z_\alpha \ ,$$
$$(\partial_y - ia_y)Z_\alpha^\dagger = -\frac{\theta}{\pi} g_\sigma^2 (\partial_x - ia_x)Z_\alpha^\dagger \, ,$$

for $z = \bar{z} < 0$ and a similar condition along the right half $z = \bar{z} > 0$ of the boundary. While in the weak coupling limit the value of θ is irrelevant (and we recover purely Neumann boundary conditions), in general, θ appears explicitly.

Note that the identification of θ and g_σ^2 with the Hall (σ_{xy}) and longitudinal (σ_{xx}) conductance as in (3.21), gives:

$$\gamma = \frac{\theta}{\pi} g_\sigma^2 = \frac{\sigma_{xy}}{\sigma_{xx}} \, .$$

This ratio defines the Hall angle θ_H by $\gamma = \tan(\theta_H)$, which was introduced in [198] (see also the recent discussion in [23]) in the study of the classical limit of the quantum Hall effect. The classical limit can be defined from a network model where we neglect quantum interference. The problem then is that of a directed random walk, leading to diffusive behavior (in high magnetic field) in the continuum limit. At the boundaries (reflecting walls) vanishing of normal current, gives the equation for the probability density $(\partial_y - \gamma \partial_x)\rho = 0$, resembling the boundary conditions for the sigma model field Z_a. In the classical network model γ is given by the ratio of probabilities that the random walker turns left or right at nodes, and the Hall angle is related to the direction at which the random walker moves away from the boundary.

The mapping of spin chains with extra edge states to sigma models seen in the previous section, suggests that the following more general boundary conditions exist for

the sigma model:

$$\begin{aligned}(\partial_y + ia_y)Z_\alpha &= \Theta_1 g_\sigma^2(\partial_x + ia_x)Z_\alpha \ , \\ (\partial_y - ia_y)Z_\alpha^\dagger &= -\Theta_1 g_\sigma^2(\partial_x - ia_x)Z_\alpha^\dagger \, ,\end{aligned} \tag{4.11}$$

for $z = \bar{z} < 0$ and a similar condition with Θ_1 replaced by Θ_2, along the right half $z = \bar{z} > 0$ of the boundary. The parameters Θ_1 and Θ_2 were defined in eq. (4.10).

For $0 < M \leq 2$, we expect that these boundary conditions are conformally invariant at the fixed point theory. In other words, we expect that, in the conformally invariant fixed points of superprojective sigma models $\mathbb{CP}^{N+M-1|N}$ at $\theta = \pi$, there is a discrete family of conformal boundary conditions labeled by the integer $\mathcal{R}, \mathcal{L} \in \mathbb{Z}$.

These boundary conditions were derived in [38] for the case $M = 0$. The strategy used there to solve the model is to start with the so-called minisuperspace (or semi-classical) approximation [95,181] consisting in neglecting the fluctuations around the longitudinal coordinate of the worldsheet, leaving with the study of a one-dimensional sigma model, which is considerably simpler. This approach is valid as g_σ tends to zero (infinite radius), and the result in this limit can be continued to finite values of the couplings, thanks to the existence of a line of fixed points when $M = 0$, see eq. (1.35). However the value $g_\sigma^2 = 1$ which is the one of relevance for us could not be studied with the techniques of [38]. In the case of generic M we are after, we cannot use the minisuperspace technique, and we have to solve the model at finite coupling. The solution of the problem will be presented in section 4.2.2 and is based on the lattice discretizations. We now discuss some interesting considerations done in [38] about the geometrical character of boundary conditions (4.11), which apply also in the general case. A precise derivation of these results would lead us too far from the goal of computing the critical exponents, and we limit ourselves to state the main points.

To discuss the geometrical nature of the boundary conditions we have first to outline some facts about complex projective superspaces. A standard reference for the differential geometry concepts treated (in the bosonic case) is [148]. $\mathbb{CP}^{N+M-1|N}$ is a Kähler manifold of complex dimension $2N + M - 1$ (and superdimension $M - 1$). Choosing the homogeneous coordinates w_i ($i = 1, \ldots, N + M - 1$ bosonic, $i = N + M, \ldots, 2N$ fermionic, $w_{\bar{\imath}} \equiv \bar{w}_i$), its metric

$$\mathrm{d}s^2 = g_{i,\bar{\jmath}}(\mathrm{d}w^{\bar{\jmath}}\mathrm{d}w^i + (-1)^{|i||j|}\mathrm{d}w^i\mathrm{d}w^{\bar{\jmath}}) = 2g_{i,\bar{\jmath}}\mathrm{d}w^{\bar{\jmath}}\mathrm{d}w^i \, ,$$

is given by the $\mathrm{U}(N + M|N)$-invariant Fubini-Study metric:

$$g_{i,\bar{\jmath}} = g(\partial_i, \partial_{\bar{\jmath}}) = \frac{(1 + w^\dagger \cdot w)\delta_{ij} - (-1)^{|j|}w_{\bar{\imath}}w_j}{(1 + w^\dagger \cdot w)^2} \, ,$$

where $w^\dagger \cdot w = w_{\bar{\imath}}w_i$ is the scalar product on $\mathbb{CP}^{N+M-1|N}$. The metric determines the Kähler 2-form ω (which is closed, $\mathrm{d}\omega = 0$) in the following way:

$$\omega = -ig_{i,\bar{\jmath}}\mathrm{d}w^{\bar{\jmath}} \wedge \mathrm{d}w^i \, . \tag{4.12}$$

We consider the second integral cohomology group $H^2(\mathbb{CP}^{N+M-1|N};\mathbb{Z})$, given by the 2-forms which are closed but not exact (recall, exact means $\alpha = \mathrm{d}\beta$). As for its bosonic cousin, $H^2(\mathbb{CP}^{N+M-1|N};\mathbb{Z}) = \mathbb{Z}$, and a generator of it is given by $\omega/(2\pi)$, which satisfies:

$$\int_{\mathbb{CP}^1} \frac{\omega}{2\pi} = 1\,.$$

Indeed if ω were exact, then by Stokes' theorem integration on $\mathbb{CP}^1$ would give zero[3]. We denote by L a complex line bundle over the projective superspace. Recall that a complex line bundle is a fiber bundle with one dimensional fiber $\mathbb{C}$, which in our case can be thought of as the tangent bundle of a sphere. A general result is that isomorphism classes of complex line bundles L_l are in correspondence with elements of $H^2(\mathbb{CP}^{N+M-1|N};\mathbb{Z})$, so they are labeled by $l \in \mathbb{Z}$. For example the trivial line bundle is $L_0 = \mathbb{CP}^{N+M-1|N} \times \mathbb{C}$. When the bundle is not trivial, it cannot be written globally as a product, and the number $l \in \mathbb{Z}$ tells us how the local pieces are twisted when glued together.

We now come back to the sigma model. Considering a local patch where $Z_1 \neq 0$, the coordinates w_i introduced above are related to the Z_α's as follows:

$$Z_1 = Z_1^\dagger = \frac{1}{\sqrt{1 + w^\dagger \cdot w}}\,, \quad w^i = Z_1 Z_{i+1}\,, \quad w^{\bar\imath} = Z_1^\dagger Z_{i+1}^\dagger\,.$$

In these coordinates the action takes the form [38]:

$$S \;=\; \frac{1}{2g_\sigma^2}\int d^2z\, g_{i\bar\jmath}\partial_\mu w^{\bar\jmath}\partial_\mu w^i + \frac{i\theta}{2\pi}\int \omega\,, \tag{4.13}$$

where g is the Fubini-Study metric defined above and the Kähler form ω (4.12) can be written as:

$$\omega = d^2z\,\epsilon^{\mu\nu} i g_{i\bar\jmath}\partial_\nu w^{\bar\jmath}\partial_\mu w^i\,.$$

We now look for boundary conditions which arise from adding to the action (4.13) boundary terms of the form

$$S_b \;=\; \int_{-\infty}^{0} dx\, \left(A_i^L(w,\bar w)\partial_x w^i + A_{\bar\imath}^L(w,\bar w)\partial_x w^{\bar\imath}\right) + \int_0^\infty dx\, (\,L \;\leftrightarrow\; R\,)\,.$$

Here we imagine the boundary being the real axis, and $A^{L(R)} = A_i^{L(R)}dw^i + A_{\bar\imath}^{L(R)}dw^{\bar\imath}$ are one-forms which are at least locally defined on $\mathbb{CP}^{N+M-1|N}$. We now demand invariance of these boundary conditions under global action of $\mathrm{U}(N+M|N)$. The important point is

[3] ω plays the role of a magnetic field B (which is a two-form). Using language of three-dimensional electrodynamics, the fact that B is not exact means that there are no globally defined vector potentials A, such that $\vec B = \nabla \times \vec A$. Indeed if that was the case, using Gauss theorem we will encounter the contradiction:

$$0 \neq \int_{\partial U} \vec B \cdot \mathrm{d}^2\vec n = \int_U \mathrm{d}^3x \nabla\cdot(\nabla\times\vec A) = 0\,,$$

where U is a three dimensional manifold having ∂U as boundary.

that on any irreducible complex symmetric superspace, there is only one invariant closed 2-form, the Kähler form ω. Then denoted $\Omega^{L(R)}$ the curvature two-forms associated to the connection $A^{L(R)}$, invariance of the boundary conditions with respect to the global symmetry requires that [38]

$$\Omega^L \;=\; i\mathcal{L}\omega\,, \quad \Omega^R \;=\; i\mathcal{R}\omega\,,$$

where ω is the Kähler form (4.12). If we now derive the boundary conditions associated to the invariance of the sigma model under arbitrary variations, we would find exactly the twisted Neumann boundary conditions (4.11), see [38] for details. However, in the above discussion $\mathcal{L}, \mathcal{R}$ are arbitrary real numbers. This is indeed the case of the classical theory, but in the quantum theory they assume integer values.

The quantization of $\mathcal{L}, \mathcal{R}$ is analogue to the quantization of magnetic charge in the problem of the Dirac monopole on the sphere (reviewed in [148]), which corresponds to the target space when $N = 0, M = 2$ (for this reason, $\mathcal{L}, \mathcal{R}$ were referred to as monopole numbers in [38]). This can be understood from the minisuperspace limit, where we neglect the σ dependence of $w^i(\sigma, \tau)$, for the theory defined on the strip $[0, \pi] \times \mathbb{R}$. The θ-term is zero, and integrating over σ, we are left with the following one-dimensional sigma model

$$S \;=\; \int_{-\infty}^{\infty} d\tau \left(\frac{\pi}{2g_\sigma^2} g_{i\bar{\jmath}} \dot{w}^{\bar{\jmath}} \dot{w}^i + A_i \dot{w}^i + A_{\bar{\imath}} \dot{w}^{\bar{\imath}} \right) ,$$

where

$$A = A^R - A^L\,.$$

This theory is interpreted as the path integral of a quantum mechanical problem of a particle living on $\mathbb{CP}^{N+M-1|N}$ in the presence of a gauge potential A, and the problem is thus that of a magnetic monopole at the center of the complex projective superspace. Wavefunctions (functions on the superspace) have to be reinterpreted as sections of Hermitian complex line bundles L_l, since as the gauge potential, cannot be defined globally. The usual case of wavefunctions as function from the position space to $\mathbb{C}$, is recovered in the case of trivial bundle L_0, when the connection A is flat (zero curvature). Different local expressions of wavefunctions are related by transition functions which are uniquely defined only if[4]:

$$\Omega = il\omega\,, \quad l \in \mathbb{Z}\,,$$

[4]We recall the reasoning behind the quantization condition in the case of the sphere $S^2 = \mathbb{CP}^1$ [148]. With (θ, ϕ) coordinates on S^2, we consider the two local expressions of the gauge potential

$$A_N = ig(1 - \cos(\theta))\mathrm{d}\phi\,, \quad A_S = -ig(1 + \cos(\theta))\mathrm{d}\phi\,,$$

defined (such that the associated magnetic field $\Omega_{N,S} = \mathrm{d}A_{N,S}$ has no singularities) respectively on the southern $U_S = \{(\theta, \phi) | \frac{\pi}{2} - \epsilon \leq \theta \leq \pi\}$ and northern $U_N = \{(\theta, \phi) | 0 \leq \theta \leq \frac{\pi}{2} + \epsilon\}$ hemispheres. $A_{N,S}$ are related on $U_N \cap U_S$ by the gauge transformation

$$A_N = A_S + 2ig\mathrm{d}\phi\,,$$

which in vector notation is $\vec{A}_N = \vec{A}_S + \vec{\nabla}(2ig\phi)$. We denote ψ_N and ψ_S the wavefunctions (local expressions of global sections) defined on U_N and U_S. These are related by the phase

$$\psi_S = e^{-i2g\phi}\psi_N\,.$$

where Ω is the curvature of the connection $A = A^L - A^R$, and ω is the Kähler form. l represents the cohomology class of the base space $\mathbb{CP}^{N+M-1|N}$ of the bundle. The above quantization condition means that $l = \mathcal{L} - \mathcal{R} \in \mathbb{Z}$ and taking $A^L = 0$ ($A^R = 0$) gives $\mathcal{L} \in \mathbb{Z}$ ($\mathcal{R} \in \mathbb{Z}$). Further details and connections with representation theory (decomposition of the space of sections of bundles on $\mathbb{CP}^{N|N}$ onto representations of $\mathfrak{gl}(N|N)$) can be found in [38].

In summary, we have seen that the number of edge states $\mathcal{L}, \mathcal{R}$ appearing in the twisted Neumann boundary conditions (4.11) label complex line bundles on $\mathbb{CP}^{N+M-1|N}$.

The case $\mathbb{CP}^{0|1}$

To make things more concrete, we investigate now the simplest case of $\mathbb{CP}^{0|1}$ ($N = 1, M = 0$), which is equivalent to symplectic fermions. In this case the θ-term vanishes and the bulk action is

$$S = \frac{1}{2g_\sigma^2} \int d^2z \partial_\mu \xi \partial_\mu \xi^\dagger \,.$$

The boundary conditions are then of the form

$$\begin{aligned} \partial_y \xi &= \Theta \; g_\sigma^2 \; \partial_x \xi \\ \partial_y \xi^\dagger &= -\Theta \; g_\sigma^2 \; \partial_x \xi^\dagger \,, \end{aligned}$$

and can be represented in terms of a gluing automorphism

$$\begin{pmatrix} \partial\xi \\ \partial\xi^\dagger \end{pmatrix} = \Omega \begin{pmatrix} \bar\partial\xi \\ \bar\partial\xi^\dagger \end{pmatrix}$$

where

$$\Omega = \frac{1 + W(\Theta)}{1 - W(\Theta)}, \quad W(\Theta) = i g_\sigma^2 \begin{pmatrix} \Theta & 0 \\ 0 & -\Theta \end{pmatrix} .$$

If we now have two different values of Θ on the left and right boundaries in the upper half plane, going around the insertion of the boundary condition changing operator at the origin in the complex plane gives rise to a monodromy of $\left(\partial\xi, \partial\xi^\dagger\right)^T$ expressed by

$$\Omega_{12} = \Omega_1 \Omega_2^{-1} = \frac{\kappa + W(\Theta_1 - \Theta_2)}{\kappa - W(\Theta_1 - \Theta_2)} \,,$$

where we have set $\kappa = 1 + g_\sigma^4 \Theta_1 \Theta_2$. Of course, Ω_{12} is of the form

$$\Omega_{12} = \begin{pmatrix} e^{2i\pi\lambda} & 0 \\ 0 & e^{-2i\pi\lambda} \end{pmatrix} ,$$

If we set $\theta = \pi/2$ and go around the equator from $\phi = 0$ to $\phi = 2\pi$, demanding that the wavefunctions are single valued implies $2g \in \mathbb{Z}$, which is the quantization condition we were looking for. Lastly we note that the monopole strength g is $l/2$ by computing the flux:

$$2\pi i l = \int_{S^2} \Omega = \int_{U_N} \mathrm{d}A_N + \int_{U_S} \mathrm{d}A_S = \int_{S^1} (A_N - A_S) = 2ig \int_0^{2\pi} \mathrm{d}\phi = 4\pi i g \,.$$

with the twist parameter λ given by $2\cos 2\pi\lambda = \mathrm{Tr}\ \Omega_{12}$:

$$\cos 2\pi\lambda = \frac{(1+g_\sigma^4\Theta_1\Theta_2)^2 - (\Theta_1-\Theta_2)^2 g_\sigma^4}{(1+g_\sigma^4\Theta_1\Theta_2)^2 + (\Theta_1-\Theta_2)^2 g_\sigma^4}\,.$$

The twist parameter vanishes when $\mathcal{L} = \mathcal{R}$, which corresponds to identical boundary conditions for symplectic fermions, and similarly it vanishes when $g_\sigma^2 = 0$. A similar discussion of twisted boundary conditions in symplectic fermions can be found in [61].

In general, the ground state of the theory (which has central charge $c = -2$) in the twisted sector scales with the conformal weight [126]

$$h_\lambda^{\mathrm{gr}} = \frac{1}{2}\lambda(\lambda-1)\,.$$

We remark that λ has in general irrational values, leading to irrational conformal dimensions. The full operator content in this sector is encoded in the $\mathrm{U}(1)\times\mathrm{Vir}$ character [126]

$$\begin{aligned} d_{\mu,\lambda} &= \mathrm{tr}\left(e^{2i\mu J_0} q^{L_0-c/24}\right) = \\ &= e^{-2i\pi\mu\lambda} q^{(1-6\lambda(1-\lambda))/12} \prod_{n=1}^{\infty} \left(1+e^{2i\pi\mu} q^{n+\lambda-1}\right)\left(1+e^{-2i\pi\mu} q^{n-\lambda}\right) \end{aligned}$$

or

$$d_{\mu,\lambda} = \eta^{-1} e^{-2i\pi\mu\lambda} \sum_{m\in Z} e^{2i\pi\mu m} q^{\frac{1}{2}(m+\lambda-\frac{1}{2})^2}\,,$$

where q denotes the modular parameter and η is the Dedekind eta function.

The problem is thus fully solved in this case. We now move to address the general case, where the solution will be obtained using lattice regularizations in terms of spin chains and loop models discussed above.

4.2 Exact exponents for the spin quantum Hall transition in the presence of extra edge channels

In this section we solve the loop model with intersecting loops at the boundaries, and apply the results to higher plateaus SQH transitions.

4.2.1 Algebraic remarks

We first discuss some algebraic properties of the lattice models defined in section 4.1.2. The general problem we would like to address is solving the loop model with loop fugacities β, and the associated $\mathfrak{gl}(N+M|N)$ spin chains.

We start by giving the explicit action of the operators E_i and $P_{i,i+1}$ on the super spin chains (the action of E_i in terms of oscillators was already given in section 1.1.2). Let e_j, with $j = 1,\dots,2N+M$, be a basis of V, and e^j, with $j = 1,\dots,2N+M$, be

the corresponding dual basis of $V^\star$, and let $|j|$ denote the grade of e_j. Then the graded permutation $P_{i,i+1}$ acts on two copies of the same representation by interchanging them with a minus sign if both the elements are odd:

$$P_{i,i+1}\, e_{j_0} \otimes \cdots \otimes e^{j_{m+2L+n-1}} = (-)^{|j_i||j_{i+1}|} e_{j_0} \otimes \cdots \otimes e_{j_{i+1}} \otimes e_{j_i} \otimes \cdots \otimes e^{j_{m+2L+n-1}} .$$

The Temperley-Lieb operator E_i projects onto the singlet in the decomposition of $V \otimes V^\star$ (and $V^\star \otimes V$):

$$E_i\, e_{j_0} \otimes \cdots \otimes e^{j_{m+2L+n-1}} = (-)^{|j_i||j_{i+1}|} \delta_i^{i+1} \sum_{k=1}^{N+M} e_{j_0} \otimes \cdots \otimes e^{j_{i-1}} \otimes \\ \otimes e_k \otimes e^k \otimes e_{j_{i+2}} \otimes \cdots \otimes e^{j_{m+2L+n-1}} .$$

Adding the P generators to the Temperley-Lieb (TL) generators E as needed to define the transfer matrices (4.1)-(4.2), completes the TL relations by additional ones, which define a certain subalgebra of the Brauer algebra.

The full Brauer algebra on $2L$ sites $\mathcal{B}_{2L}(\beta)$ is generated by the permutation operators $P_i (:= P_{i,i+1})$, with $i = 0, \ldots, 2L-2$, and the TL generators E_i, with $i = 0, \ldots, 2L-2$, and is specified by the parameter β. Analogously to the TL algebra, words in $\mathcal{B}_{2L}(\beta)$ can be represented graphically using diagrams composed by rows of dots connected in pairs. The generators I (identity), E_i (TL operator) and P_i (permutation operator) are shown in figure 4.6 in this graphical representation. The product of two words is given by stacking diagrams, and we replace every loop formed by the (complex) weight β. In representation theory, the Brauer algebra plays for the orthogonal group the same role that the symmetric group does for the general linear group in Schur-Weyl duality [30].

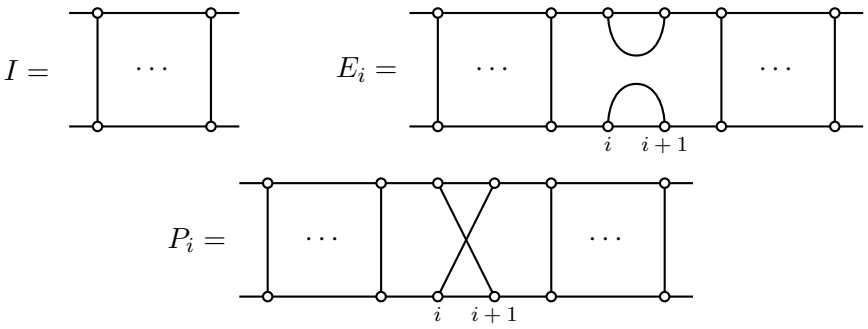

Figure 4.6: Identity, the Temperley-Lieb generator E_i and the permutation operator P_i, in the diagrammatic representation.

In the case we wish to study, the full Brauer algebra $\mathcal{B}_{2L}(\beta)$ is not needed, since we restrict to having permutations on boundary sites only (the Temperley-Lieb generators still act in the bulk). The corresponding subalgebra will be denoted $\mathcal{A}_{2L,\mathcal{L},\mathcal{R}}(\beta)$, and its

generators satisfy the relations

$$P_i^2 = 1, \quad E_i^2 = \beta E_i, \quad E_i P_i = P_i E_i = E_i, \tag{4.14}$$
$$P_i P_{i\pm1} P_i = P_{i\pm1} P_i P_{i\pm1}, \quad E_i E_{i\pm1} E_i = E_i,$$
$$E_i P_{i\pm1} E_i = E_i, \tag{4.15}$$
$$P_i P_j = P_j P_i, \quad E_i E_j = E_j E_i, \quad E_i P_j = P_j E_i\,, \tag{4.16}$$

which can be easily verified by expressing the generators as diagrams.

As already observed, the spin chains (4.5)-(4.8) are representations of the algebra $\mathcal{A}_{2L,\mathcal{L},\mathcal{R}}(\beta)$, with loop fugacity $\beta = \mathrm{Str}_V 1 = M$. A subtle point however is the following. This representation is not faithful: in addition to (4.14)–(4.16), the generators acting on the spin chain satisfy additional relations. These additional relations define a quotient of $\mathcal{A}_{2L,\mathcal{L},\mathcal{R}}(M)$, which we now discuss.

First we note that the algebra $\mathcal{A}_{2L,\mathcal{L},\mathcal{R}}(M)$ as defined by (4.14)–(4.16) is infinite dimensional. We can understand why by considering the simple system with $L = \mathcal{L} = \mathcal{R} = 1$. If we call $W = E_1 P_2 P_0 E_1$, then the word W^p (see figure 4.7) cannot be reduced using the defining relations, and increasing the power p, the dimension of the algebra becomes arbitrarily large.

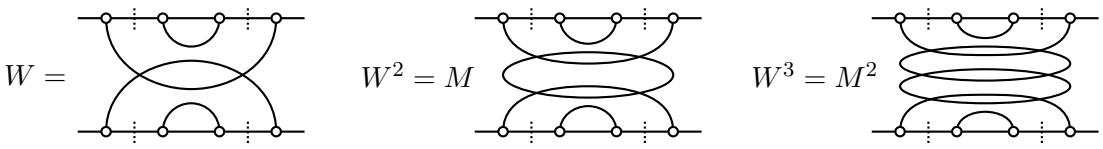

Figure 4.7: The diagrams corresponding to the words $W = E_1 P_2 P_0 E_1$, W^2 and W^3 in $\mathcal{A}_{2L,\mathcal{L},\mathcal{R}}(M)$ with $L = \mathcal{L} = \mathcal{R} = 1$. Here and in the following dotted lines separate bulk and boundary sites.

The additional relation in the spin chain is $P_0 E_1 P_0 P_2 E_1 = P_2 E_1 P_0 P_2 E_1$. Indeed if we compute the action of $E_1 P_0 P_2 E_1$ on the spin chain, we have:

$$E_1 P_0 P_2 E_1\, e_{j_0} \otimes e_{j_1} \otimes e^{j_2} \otimes e^{j_3} = (-)^{|j_1|} \delta_{j_1}^{j_2} \delta_{j_0}^{j_3} \sum_{k,r=1}^{M+N} (-)^{|k|(|j_0|+|j_3|)} \cdot e_k \otimes e_r \otimes e^r \otimes e^k\,,$$

which is invariant under the action of $P_0 P_2$. Note that the additional relations just introduced correctly reduce those words that made the algebra infinite dimensional. We denote the quotient of $\mathcal{A}_{2L,\mathcal{L},\mathcal{R}}(\beta)$ by the additional relations present in the spin chain representation by $\mathcal{Q}_{2L,\mathcal{L},\mathcal{R}}(\beta)$. A complete description of the quotient is possible, but we refer the interested reader to [28] for that. To make things concrete, it is useful to represent diagrammatically the relations. Then the quotient tells us that when intertwined top arcs intersect bottom arcs, their relative intertwining does not matter, and could be disentangled, see for example the reduction of the diagram of figure 4.8. The link states

obtained by cutting in two halves the full diagrams, are rather natural in the quotient: we identify two link states if they have the same connectivities, see the example of figure 4.9

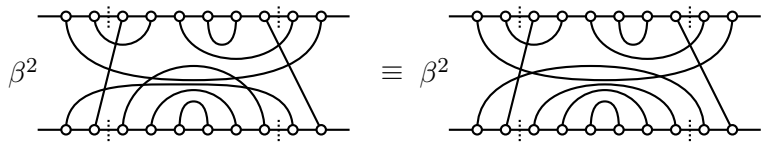

Figure 4.8: The two identified words in the quotient $\mathcal{Q}_{2L,\mathcal{L},\mathcal{R}}(\beta)$ corresponding to figure 4.4.

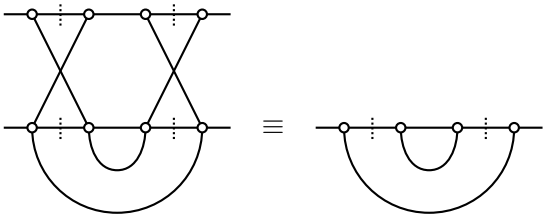

Figure 4.9: Two identified link states in $\mathcal{Q}_{2L,\mathcal{L},\mathcal{R}}(\beta)$.

Another issue is that we have argued in [28] that the representation of the quotient itself on $\mathfrak{gl}(N+M|N)$ spin chains is not faithful for the $\mathfrak{gl}(1|1)$ case (we will comment more on this point at the end of section 4.2.2).

The geometrical model we have to study for understanding the SQH transition is that based on the quotient $\mathcal{Q}_{2L,\mathcal{L},\mathcal{R}}(\beta)$. Note that, except when $\beta = M$ is an integer, we do not know of any spin chain representation of the corresponding algebras, be they $\mathcal{A}, \mathcal{Q}$ or Brauer. This situation has to be contrasted with the ordinary Temperley-Lieb algebra, where the XXZ spin chain provides such a representation for all values of the loop fugacity, as discussed in section 1.1.1. Clearly the presence of loop crossings—even if only between boundary lines—makes the problem considerably more involved. These crossings also make impossible a Coulomb gas approach to the underlying conformal field theory (for essentially the same technical reasons).

We remark that the bulk part of the Hamiltonian of the edge states problem, does not follow from the usual Yang-Baxter construction for alternating fundamental and dual representations of $\mathfrak{gl}(M+N|N)$ [77]. However, being that of the Potts model, the bulk Hamiltonian is exactly solvable, since it belongs to the Temperley-Lieb algebra, and the realization of this algebra in the $\mathrm{U}_q(\mathfrak{sl}(2))$-invariant XXZ spin chain leads to Bethe ansatz equations. We do not know what the situation for our model with boundary interactions might be.

We now launch into the technical problem of determining the critical exponents of the geometrical model. In particular, we focus now on the case $\mathcal{L} = m, \mathcal{R} = n$, for which

the Hamiltonian results:

$$H = -u \sum_{i=0}^{m-1} P_{i,i+1} - \sum_{i=m}^{2L+m-2} E_i - v \sum_{i=2L+n-1}^{2L+n+m-2} P_{i,i+1} \,.$$

This corresponds in spin chain formulation to equation (4.5), which we recall:

$$V^{\otimes m} \otimes (V \otimes V^\star)^{\otimes L} \otimes (V^\star)^{\otimes n} \,.$$

The results for the other values of $\mathcal{L}, \mathcal{R}$ will be derived from this case thanks to symmetries of the exponents.

4.2.2 Solution of the general loop model

One boundary case

We will start by investigating the one boundary problem. Setting $n = 0$, the Hamiltonian we want to study is

$$H = -u \sum_{i=0}^{m-1} P_i - \sum_{i=m}^{2L+m-2} E_i \,. \tag{4.17}$$

Sectors of this Hamiltonian will be indexed now not only by the number of through lines (or "strings"), but also by the action of the symmetric group $\mathfrak{S}_{m+1}$ on the $m+1$ boundary strings which can be permuted, according to its irreducible representations (Specht modules). Then the Hamiltonian (4.17) can be put in a block form, each block indexed by the number of strings and a Young diagram referring to a Specht module. Accordingly the Hilbert space will be decomposed in terms of these subspaces. Numerical diagonalization[5] shows that the lowest eigenvalue of the Hamiltonian always lies in the trivial (fully symmetric) representation of the symmetric group, where permutations act as the identity in the Specht module. So for the purpose of computing the leading critical exponents we can restrict to this sector.

Apart from exact diagonalization of the Hamiltonian, we can have insights on the spectrum using the following argument. We recall first that the one boundary TL algebra (1BTL) [118, 141] is defined by adding to TL a blob operator b acting on the leftmost strand, which we will label m for making easier the connection with our model. By definition, b is idempotent and satisfies the relation (see section 1.2.5)

$$E_m b E_m = \beta_1 E_m \,, \tag{4.18}$$

whose geometrical interpretation is that marked loops get a weight β_1. For the particular case $m = 1$ the lattice algebra underlying our problem is isomorphic to the 1BTL algebra with a given value of β_1. The isomorphism is given by $P_0 = 2b - 1$ (using $b^2 = b$ we get

[5] Numerical diagonalizations are performed using the Arnoldi algorithm, allowing to efficiently determine the lowest part of the spectrum. We use the libraries ARPACK++ [97].

$(P_0)^2 = 1$ as required). So the boundary interaction is proportional to b indeed. The corresponding weight of boundary loops follows from

$$E_1 \frac{1+P_0}{2} E_1 = \frac{1+\beta}{2} E_1 \,,$$

where we have used (4.15). This shows that we are dealing with $\beta_1 = \frac{1+\beta}{2}$.

For higher values $m > 1$ there is no such mapping to the one-boundary loop model. However we now argue that we can replace the boundary interaction in eq. (4.17) with the sum over all possible permutations of the boundary strands without affecting the universal part of the spectrum we are looking at. Intuitively this says that if we act a sufficiently large number of times with $\sum_{i=1}^{m} P_i$, all the permutations are generated and the interaction can be replaced by $\sum_{\sigma \in \mathfrak{S}_{m+1}} \sigma$. Concretely the following modified Hamiltonian

$$\widetilde{H} = -u \frac{1}{(m+1)!} \sum_{\sigma \in \mathfrak{S}_{m+1}} \sigma - \sum_{i=m}^{2L+m-2} E_i \,,$$

is naively expected to have the same critical exponents of the original Hamiltonian (4.17) in the continuum limit[6]. We support this universality hypothesis with strong numerical evidence in table 4.1. Fitting of numerical data is done using formula (1.59), adding a term of order $1/L^2$.

β	j	h	$\tilde{h}$	$h^{2,0}(j)$
0	0	-0.07606 ± 0.00010	-0.07615 ± 0.00015	-0.076068
0	1	0.1099 ± 0.0004	0.1090 ± 0.0006	0.111099
0	2	1.339 ± 0.010	1.321 ± 0.006	1.298266
1	0	0	0	0
1	1	0.33478 ± 0.00009	0.33478 ± 0.00009	1/3
1	2	2.099 ± 0.016	2.099 ± 0.016	2
$\sqrt{2}$	0	0.01374 ± 0.00016	0.01302 ± 0.00021	0.014542
$\sqrt{2}$	1	0.4384 ± 0.0011	0.4432 ± 0.0007	0.438772
$\sqrt{2}$	2	2.4256 ± 0.0013	2.4410 ± 0.0009	2.363001

Table 4.1: Comparison of critical exponents h of the model described by the original Hamiltonian H, and $\tilde{h}$ of the one described by $\tilde{H}$, listed for different values of β and j, the number of bulk through lines, in a system with $m = 2, n = 0$. The values are obtained by fitting eigenvalues for bulk sizes $2L = 12 \to 20$, and although these numbers should be equal when $L \to \infty$, already with these relatively small sizes we find good agreement between the values of the exponents in the model and the exact value predicted in the continuum limit $h^{2,0}(j)$, given in the last column.

[6]We remark that for having this universal behavior, it is crucial that the signs in front of the permutation generators are all negative. In this case, adding to the Hamiltonian (4.17) other terms of the symmetric group than the generators, is a redundant perturbation (see the discussion in [28] for more on this point).

Working with $\widetilde{H}$ rather than H has the advantage that it realizes a representation of 1BTL. First we recognize that $b_{t_1} := \frac{1}{(m+1)!}\sum_{\sigma\in\mathfrak{S}_{m+1}}\sigma$ is idempotent, being the Young symmetrizer associated to the standard Young tableau[7] $t_1 = \boxed{0}\boxed{\cdots}\boxed{m}$. Further b_{t_1} satisfies:

$$E_m b_{t_1} E_m = \beta_1 E_m b_{\hat{t}_1}\,, \tag{4.19}$$

where $\hat{t}_1 = \boxed{0}\boxed{\cdots}\boxed{m-1}$ and

$$\beta_1 = \frac{m+\beta}{m+1}\,. \tag{4.20}$$

To prove formula (4.19) we can use the following simple identity

$$b_{t_1} = \frac{1}{m+1} b_{\hat{t}_1}(1 + (0,m) + (1,m) + \cdots + (m-1,m))\,,$$

(i,j) denoting the transposition of i and j, and the relations of the algebra. Relation (4.18) now follows with our value of β_1 (4.20) if we replace E_i by $\widetilde{E}_i = E_i b_{\hat{t}_1}$, an operation which does not affect relations of the algebra $\mathcal{A}_{2L,\mathcal{L},\mathcal{R}}$. We depict this finding in figure 4.10.

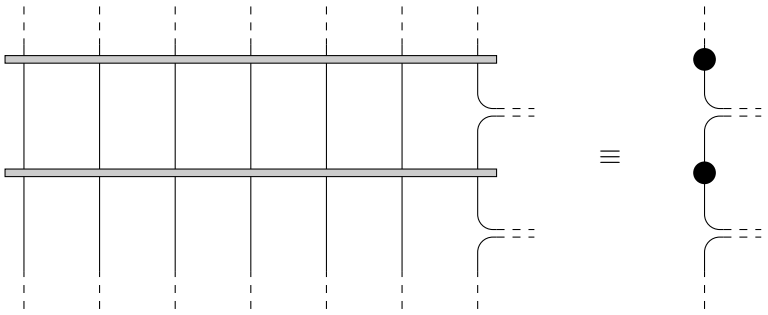

Figure 4.10: Symmetrization (here represented by horizontal gray bars) over the $m+1$ leftmost strands can be interpreted as blobbing the first bulk strand.

Then, the critical exponents of (4.17) are expected to be described by those of a one boundary loop model with fugacity of loops touching the left boundary given by (4.20). The exponents follow then from eq. (1.65):

$$h^{m,0}(j) = h_{r_1(m),r_1(m)+2j}\,,$$

where $r_1(m)$ is given explicitly by

$$r_1(m) = \frac{1+p}{\pi}\arctan\left(\frac{(1+m)\sin\left(\frac{\pi}{p+1}\right)}{m-(m-1)\cos\left(\frac{\pi}{p+1}\right)}\right)\,.$$

[7] In what follows we will adopt the convention of labeling the boxes of a Young diagram of size $m+1$ with the elements of the set $\{0,\ldots,m\}$ when related to the left boundary action of the permutation group

We have checked these results with extensive numerical diagonalizations of the Hamiltonian, see table 4.1. In particular we have verified that the exponents do *not* depend on the coupling u as long as we take it positive, as expected for the 1BTL models, see section 1.2.5. This property should be interpreted in terms of boundary renormalization group flow. The situation is akin to that of the Ising model with a boundary field, where the fixed boundary condition is a stable fixed point, and the free boundary condition an unstable one [6]. At a given non-zero value of the boundary field, there is a crossover, and the system flows to the stable fixed point for a sufficiently large system. In our case, the boundary perturbation to the Lagrangian is $u\phi_{r_1(m),r_1(m)}$, and it drives the system from the $m = 0$ to the $m > 0$ boundary condition. Since the dimension of the field $\phi_{r_1(m),r_1(m)}$ is $h_{r_1(m),r_1(m)}$, by dimensional arguments the relevant length scale in this boundary flow is given by $L^{1-h_{r_1(m),r_1(m)}}$. We have explicitly checked that curves describing the critical exponents as a function of u, collapse after appropriate rescaling in the $\mathfrak{gl}(1|1)$ case, where we can access large sizes of the system thanks to the free fermion realization [28], see figure 4.11.

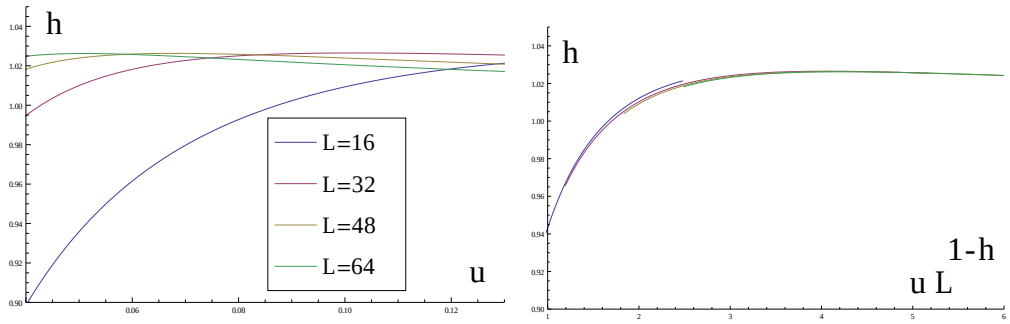

(a) (b)

Figure 4.11: h vs u in the $\mathfrak{gl}(1|1)$ chain for different sizes of the bulk length (here in different colors) and $m = 1, n = 0$. In figure (a) the variable u is not rescaled (the plot shows only very small values of u). In figure (b) we rescale u as $u' = L^{1-h_{r_1(1),r_1(1)}}u$, and we observe a perfect collapse of all curves.

We note also that when $\beta = 1$ (whence $\beta_1 = r_1(m) = 1$ for all m), the case of interest for the applications to the SQH transitions, the exponents are trivial, equal to those of the free boundary case[8]. For general m and u positive when $\beta = 1$ we have found the following relation $\lambda^0_m = -u + \lambda^0_{m-1}$, λ^0_m being the lowest eigenvalues of the Hamiltonian with m boundary lines in a given sector, which implies the same scaling in $1/L$ of the two eigenvalues.

[8] If we think of the case $m = 1$, one intuitive argument supporting this triviality goes as follows. Every time a loop crosses the boundary line, we can think of this configuration as a loop with weight 1 and a straight line times the coupling $-u$:

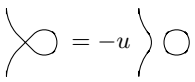

and u can be set to $u = 1$ thanks to universality.

Finally we have numerical evidence that the universality class of H and $\widetilde{H}$ is more general, and that, in particular, the following Hamiltonian also has the same continuum limit:

$$\widetilde{\widetilde{H}} = b_{\hat{t}_1} H b_{\hat{t}_1} \,,$$

corresponding to the case where the m strands on the boundary are fully symmetrized[9]. From an algebraic point of view this version of the model is equivalent to replacing the m copies of the fundamental representation of the superalgebra in the spin chain formulation with a higher-dimensional one.

Two boundary case

We now move to the two boundary problem, which is obviously much richer. In this case we again index sectors by the number k of paired bulk plus boundary through lines (or strings). We will see below that, defined $\mathfrak{m} = \min(m, n)$, the two cases $k > \mathfrak{m}$ and $k \leq \mathfrak{m}$ will have different behaviors. Calling $\ell = |m - n|$, we will refer to the lowest exponent in a sector k as the $(2k + \ell)$-leg exponent, $h^{m,n}(k)$.

We recall that the two boundary problem which we would like to address is described by

$$H = -u \sum_{i=0}^{m-1} P_i - \sum_{i=m}^{2L+m-2} E_i - v \sum_{i=2L+m-1}^{2L+m+n-2} P_i \,. \tag{4.21}$$

By naive analogy with the solution of the one boundary case, we expect the following Hamiltonian to be in the same universality class as our starting problem (4.21):

$$\begin{aligned} \tilde{H} &= -u \, \frac{1}{(m+1)!} \sum_{\sigma \in \mathfrak{S}^{\text{left}}} \sigma - \sum_{i=m}^{2L+m-2} E_i - v \, \frac{1}{(n+1)!} \sum_{\sigma \in \mathfrak{S}^{\text{right}}} \sigma \\ &= -u \, b_{t_1} - \sum_{i=m}^{2L+m-2} E_i - v \, b_{t_2} \end{aligned} \tag{4.22}$$

where we have introduced the symmetric group of the $m + 1$ leftmost and the $n + 1$ rightmost strands:

$$\mathfrak{S}^{\text{left}} = \mathfrak{S}_{\{0,\ldots,m\}} \,, \quad \mathfrak{S}^{\text{right}} = \mathfrak{S}_{\{2L+m-1,\ldots,2L+m+n-1\}} \,,$$

as well as the standard Young tableaux

$$t_1 = \boxed{0}\boxed{\cdots}\boxed{m}, \quad t_2 = \boxed{2L+m-1}\boxed{\cdots}\boxed{2L+m+n-1}.$$

As before b_t stands for the Young symmetrizer related to the tableau t. We have checked numerically the hypothesis that adding these additional permutations to our former Hamiltonian H is a redundant perturbation also in this two boundary case. See table 4.2 for a sample of evidence in the case $m = n = 2$. As in the one boundary case, we

β	k	h	$\tilde{h}$	$h_{2,2}(k)$
0	0	-0.0026 ± 0.0010	-0.0041 ± 0.0013	0
0	1	-0.0026 ± 0.0010	-0.0041 ± 0.0013	0
0	2	0.0504 ± 0.0015	0.0479 ± 0.0021	0.054734
0	3	0.247 ± 0.003	0.238 ± 0.005	0.257230
0	4	1.670 ± 0.007	1.601 ± 0.006	1.631564
1	0	0	0	0
1	1	0.0152 ± 0.0002	0.0147 ± 0.0004	0.015906
1	2	0.0700 ± 0.0012	0.0678 ± 0.0018	0.073136
1	3	0.3346 ± 0.0003	0.3346 ± 0.0003	1/3
1	4	2.118 ± 0.008	2.118 ± 0.008	2

Table 4.2: Comparison of critical exponents h of the model described by the original Hamiltonian H, and $\tilde{h}$ of the one described by the modified one $\tilde{H}$, in a system with $m = 2, n = 2$, listed for different values of β, and k, the number of bulk plus boundary strings. The values are obtained by fitting eigenvalues for bulk sizes $2L = 8 \to 16$, and although these numbers should be equal when $L \to \infty$, already with these relatively small sizes we have good agreement between these two values and with the exact value predicted, given in the last column.

claim that the results are unchanged as long as u and v are taken positive, as we have verified numerically.

The advantage of studying $\widetilde{H}$ is that it can be related to the two boundary analogue of the blob algebra, the two boundary TL algebra, defined in section 1.2.5. In the language of the two boundary loop model (2BLM), loops marked on the left boundary have weight (4.20) and those marked on the right boundary

$$\beta_2 = \frac{n+\beta}{n+1}\,. \tag{4.23}$$

All that remains to be done is to compute β_{12}, the value of loops marked by both blob operators, as expressed in the following algebraic relation (we can consider for simplicity the situation with $L = 1$):

$$E_m b_1 b_2 E_m = \beta_{12} E_m\,,$$

where b_1 and b_2 act respectively on the first and second strand labeled m and $m+1$. Loops marked by both blob operators can appear only if there are no strings in the 2BLM. In our model (4.22), as long as $k \leq \mathfrak{m}$ we can interpret strings as being inserted at the boundary, and we expect that any of the sectors $k \leq \mathfrak{m}$ map to a different quotient of 2BLM with a value of β_{12} depending on k, which we note β_{12}^k. Defining

$$\tilde{E}_m = E_m b_{\hat{t}_1} b_{\hat{t}_2}\,,$$

[9]Note that this is not equivalent to projecting to the sector where the symmetric group acts trivially on strings, since on the thick boundary we may have arcs too.

we would like that the following equation holds for a certain value of β_{12}^k:

$$\tilde{E}_m b_{t_1} b_{t_2} \tilde{E}_m = \beta_{12}^k \tilde{E}_m \,,$$

for $k \leq \mathfrak{m}$.

To make things concrete we discuss in detail the case $m = n = 2$, $L = 1$. First it is convenient to express b_{t_1} and b_{t_2} using the following identities:

$$\begin{aligned} b_{t_1} &= \frac{1}{3} b_{\hat{t}_1} (1 + (0,2) + (1,2)) = \frac{1}{3} b_{\hat{t}_1} (1 + P_1(1 + P_0)) \\ b_{t_2} &= \frac{1}{3} (1 + (3,4) + (3,5)) b_{\hat{t}_2} = \frac{1}{3} (1 + (1 + P_4)P_3) b_{\hat{t}_2} \,. \end{aligned}$$

Then, using the commutation relations of the algebra, we have:

$$\begin{aligned} \tilde{E}_2 b_{t_1} b_{t_2} \tilde{E}_2 &= \frac{1}{9} E_2 b_{\hat{t}_1} (1 + P_1(1 + P_0))(1 + (1 + P_4)P_3) b_{\hat{t}_2} E_2 = \\ &= \frac{1}{9} \left((\beta + 4) \tilde{E}_2 + 4 b_{\hat{t}_1} b_{\hat{t}_2} E_2 P_1 P_3 E_2 b_{\hat{t}_1} b_{\hat{t}_2} \right) \,. \end{aligned} \tag{4.24}$$

The first piece of equation (4.24) is already in the desired form, while the second piece is not proportional to $\tilde{E}_2$. As anticipated, we can only achieve this by fixing a sector k, and computing the action of the operator $W := b_{\hat{t}_1} b_{\hat{t}_2} E_2 P_1 P_3 E_2 b_{\hat{t}_1} b_{\hat{t}_2}$ on the states belonging to the sector. The graphical representation of W and $\tilde{E}_2$ is depicted in figure 4.12.

Figure 4.12: The words W and $\tilde{E}_2$ in the diagram representation. As before, the gray bars indicate symmetrization over the lines and W is obtained using the quotient algebra $\mathcal{Q}_{2L,\mathcal{L},\mathcal{R}}(\beta)$ discussed above.

Let us first consider the case $k = 2$, when no contractions of boundary lines is allowed. It is clear from figure 4.12 that W acts as zero on every state in this sector, since it diminishes the number of strings from 4 to 2. So, we have found that every state of the sector $k = 2$ is in the kernel of the operator

$$R := \left(\tilde{E}_2 b_{t_1} b_{t_2} - \beta_{12}^k \right) \tilde{E}_2 \,,$$

with

$$\beta_{12}^2 = \frac{\beta + 4}{9} \,.$$

We now move to $k = 1$. In this sector we have 18 states. They are drawn in figure 4.13, where we have grouped those related by the action of $b_{\hat{t}_1} b_{\hat{t}_2} = (1 + P_0 + P_1 + P_0 P_1)/4$.

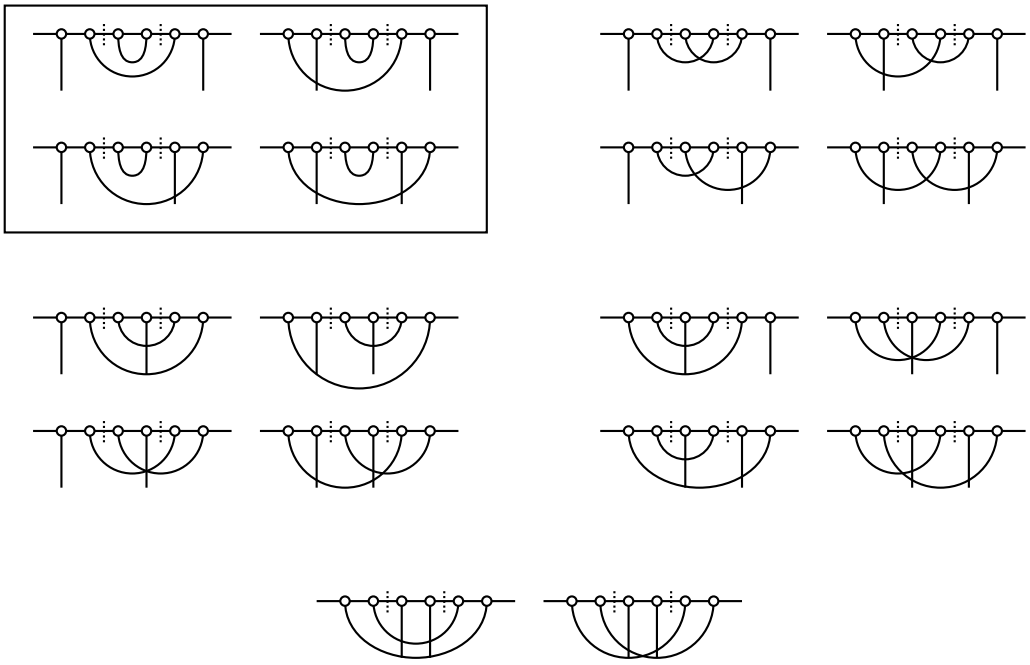

Figure 4.13: The 18 reduced states of the sector $k = 1$, for a system with $m = n = 2, L = 1$. Those related by the action of $b_{\hat{t}_1} b_{\hat{t}_2}$ are grouped together.

Acting with $\tilde{E}_2$ on an arbitrary state will always produce the sum of the four states contained in the box in figure 4.13 times a constant which can eventually be zero, as when E_2 acts on two strings. The role of $\tilde{E}_2$ is indeed to project onto the state in which the boundary strands are fully symmetrized and the bulk ones are contracted. This remark is of crucial importance since it tells us that the action of R is zero on every state, with the same value of β_{12}^k then characterizing this sector. We can evaluate R on a reference state, say the one on the top left in figure 4.13 to obtain the value of β_{12}^k. R on this state is zero if:

$$\beta_{12}^1 = \frac{2\beta + 6}{9} .$$

The last case we have to consider is $k = 0$, when no strings are left. In this sector we have 6 states depicted in figure 4.14, where again we have grouped those connected by the action of $b_{\hat{t}_1} b_{\hat{t}_2}$. As in the previous case, we realize that $\tilde{E}_2$ acting on every such states produces the sum of the two states contained in the box in figure 4.14 times a constant. Then, evaluating R on a given state gives

$$\beta_{12}^0 = \frac{\beta + 2}{3} .$$

The general case can be worked out similarly. The values of β_{12}^k in the general case

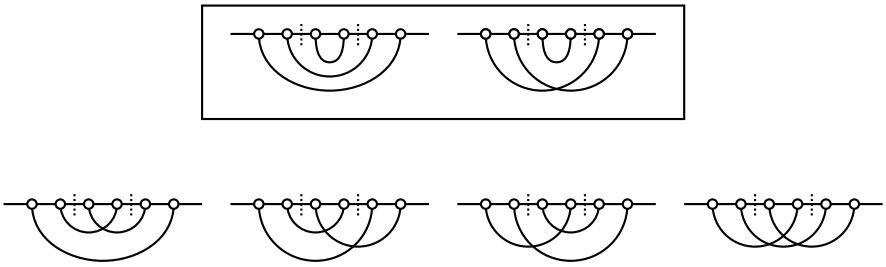

Figure 4.14: The 6 reduced states of the sector $k = 0$, for a system with $m = n = 2, L = 1$. States on top and on bottom grouped together are related by the action of $b_{\hat{t}_1} b_{\hat{t}_2}$.

m, n are found to be [28]:

$$\beta_{12}^k = \begin{cases} \dfrac{(n-k+1)(m+\beta+k)}{(m+1)(n+1)} & \text{if } m \geq n, \\ \dfrac{(m-k+1)(n+\beta+k)}{(m+1)(n+1)} & \text{if } m < n. \end{cases} \tag{4.25}$$

Note that β_{12}^k is symmetric in exchanging m, n, as it should in our problem. The computation of the weights β_{12}^k in the model described by $\tilde{H}$, equation (4.22), concludes the analysis of the sectors $k \leq \mathfrak{m}$.

When $k > \mathfrak{m}$, strings cannot be thought as being a boundary property as before, and the model maps to the 2BLM in the sector with $(k - \mathfrak{m})$ strings without any further issue.

The $(2k + \ell)$-leg exponents $h^{m,n}(k)$ in the model (4.22) are finally listed in table 4.3 where we have used the parametrization of $\beta_1, \beta_2, \beta_{12}^k$ in terms of r_1, r_2, r_{12}^k introduced in (1.62), which we recall:

$$\beta_1 = \frac{\sin\left((r_1+1)\frac{\pi}{p+1}\right)}{\sin\left(r_1\frac{\pi}{p+1}\right)}, \qquad \beta_2 = \frac{\sin\left((r_2+1)\frac{\pi}{p+1}\right)}{\sin\left(r_2\frac{\pi}{p+1}\right)}$$

$$\beta_{12} = \frac{\sin\left((r_1+r_2+1-r_{12})\frac{\pi}{2(p+1)}\right)\sin\left((r_1+r_2+1+r_{12})\frac{\pi}{2(p+1)}\right)}{\sin\left(r_1\frac{\pi}{p+1}\right)\sin\left(r_2\frac{\pi}{p+1}\right)}.$$

Recall also that β_1 and β_2 are simple functions of β and of respectively m and n, equations (4.20) and (4.23), and that $\mathfrak{m}$ is the minimum between m and n.

When the number of legs is between ℓ and $m+n$, the exponents $h_{r_{12}^k, r_{12}^k}$ are computed from our expression of β_{12}^k, equation (4.25). When we have instead $m + n + 2j$ legs, with $j > 0$, we are in the sector j of a 2BLM which is completely described by the two parameters β_1 and β_2, equations (4.20) and (4.23), and the exponents then follow from fusion of the boundary conformal weights of the one-boundary case, the leading exponents in a sector being $h_{r_1+r_2-1, r_1+r_2-1+2j}$.

k	$\#(\text{legs}) = \ell + 2k$	$h^{m,n}(k)$
0	ℓ	$h_{r_{12}^0, r_{12}^0}$
1	$\ell + 2$	$h_{r_{12}^1, r_{12}^1}$
$\vdots$	$\vdots$	$\vdots$
$\mathfrak{m}$	$m + n$	$h_{r_{12}^{\mathfrak{m}}, r_{12}^{\mathfrak{m}}}$
$\mathfrak{m} + 1$	$m + n + 2$	$h_{r_1+r_2-1, r_1+r_2-1+2}$
$\vdots$	$\vdots$	$\vdots$
$\mathfrak{m} + j$	$m + n + 2j$	$h_{r_1+r_2-1, r_1+r_2-1+2j}$
$\vdots$	$\vdots$	$\vdots$

Table 4.3: Critical exponents for the two-boundary problem.

Invoking the usual universality hypothesis—namely that the critical behavior is unchanged upon adding permutations other than the generators to the Hamiltonian H—the above expressions completely determine the critical exponents in our original model (4.21).

Lastly, we have verified that as in the one-boundary case, the version of the model with higher spins on the boundary, $\tilde{\tilde{H}} = b_{\hat{t}_1} b_{\hat{t}_2} H b_{\hat{t}_1} b_{\hat{t}_2}$, is in the same universality class as well.

Symmetries and other cases

We now discuss the other cases with negative values of $\mathcal{L}$ and/or $\mathcal{R}$. Note first that the exponents $h^{\mathcal{L},\mathcal{R}}(k)$ are symmetric in $\mathcal{L}$ and $\mathcal{R}$ by obvious invariance of the spectrum under left-right reflection. Further exponent relations follow from symmetries of the critical spin chains (4.5)–(4.8) (or equivalently of the corresponding graphical formulations). Recall that in each case $V \otimes V^\star$ (and $V^\star \otimes V$) interacts through E_i, and $V \otimes V$ (and $V^\star \otimes V^\star$) through P_i, and the couplings u, v can be set to one thanks to the universality. The same applies to the couplings t', t'' of the boundary Hamiltonians (4.3)-(4.4). Then the top-bottom reflection switching V and $V^\star$ induces a mapping between the chains (sometimes with different lengths of the bulk region): $(\mathcal{L}, \mathcal{R}) \leftrightarrow (-\mathcal{L} - 1, -\mathcal{R} - 1)$, see top of figure 4.15. This implies:

$$h^{\mathcal{L},\mathcal{R}}(k) = h^{-\mathcal{L}-1,-\mathcal{R}-1}(k). \tag{4.26}$$

In particular, this relates pairwise exponents for the chains (4.5), (4.8), as well as for (4.6), (4.7): $h^{-m,-n}(k) = h^{m-1,n-1}(k)$, $h^{-m,n}(k) = h^{m-1,-n-1}(k)$. When the total number of legs in the model (4.8) is smaller than $m + n$, then

$$h^{-m,-n}(k) = h_{r_{12}^k(m-1,n-1), r_{12}^k(m-1,n-1)}\,, \quad \#(\text{legs}) < m + n\,,$$

while when the number of legs equals $m+n+2j$ with $j \geq 0$, the corresponding exponent is:

$$h^{-m,-n}(k) = h_{r_1(m-1)+r_2(n-1)-1, r_1(m-1)+r_2(n-1)-1+2(j+1)}\,, \quad \#(\text{legs}) = m+n+2j\,, j \geq 0\,,$$

since in this case we must write the total number of legs as $(m-1)+(n-1)+2j+2$.

Finally, for the chain (4.7), considering the rightmost site on the left boundary as part of the bulk, and noting that we have identical chiralities at the two boundaries (so that $\ell = m+n$, boundary lines cannot be contracted), the only exponents are the following $(m+n+2j)$-leg exponents:

$$h^{-m,n}(k) = h_{r_1(m-1)+r_2(n)-1,r_1(m-1)+r_2(n)-1+2j+1}\,, \quad j=0,1,\dots$$

Note the presence of $2j+1$, see bottom of figure 4.15. Results for (4.6) easily follow from (4.26): the $(m+n+2j)$-leg exponents are

$$h^{m,-n}(k) = h_{r_1(m)+r_2(n-1)-1,r_1(m)+r_2(n-1)-1+2j+1}\,, \quad j=0,1,\dots$$

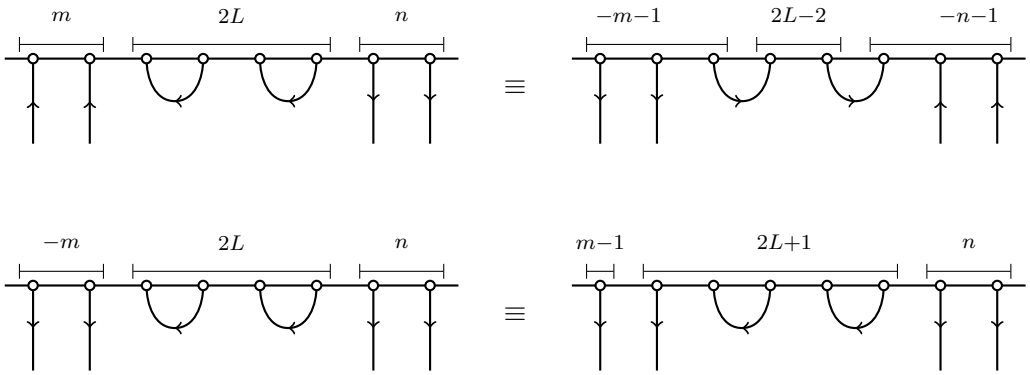

Figure 4.15: Symmetries of the configurations relating different values of $\mathcal{L},\mathcal{R}$. The relation on the top leads to $h^{-m,-n}(k) = h^{m-1,n-1}(k)$, that on the bottom to $h^{-m,n}(k) = h^{m-1,n}(k)$. Note that the number of bulk strands changes in the mapping.

Final remarks

So far we have been able to solve the problem of computing the leading exponents in each sector with fixed number of through lines. This will be enough for the applications to the SQHE we will discuss in section 4.2.3, but clearly the understanding of the (logarithmic) conformal field theories describing the loop models or spin chains with extra edge states require more work.

One first incomplete aspect of our study is that we have not determined all the geometrical exponents: there are definitely plenty of subleading eigenvalues in a given sector. The mapping to a 2BLM involves a quotient version of the latter, and we do not find all the subleading eigenvalues predicted for the 2BLM, see eq. (1.63)–(1.64). In general we do not have full control of which subleading eigenvalues appear. However we expect that the value of possible eigenvalues should be of the form given by the 2BLM conformal weights with some possible omissions and blobbed/unblobbed sectors

mixing, as we have indeed observed in the systems studied numerically. Clearly a deeper algebraic understanding of the problem is needed here to characterize the full spectrum.

The other incomplete aspect is that we lack a clear understanding of the degeneracies. One way to understand these (for the super spin chains) is to think of the generating function of eigenvalues, which could in principle be computed as the modified partition function of a loop model where non-contractible loops are weighted differently [170], using the result of eq. (1.61). In algebraic terms, this generating function would be written as a sum over irreducible representations of the algebra to which the Hamiltonian belongs. The multiplicities of summands would then be the dimensions of irreducibles of the commutant algebra in the Hilbert space at hand; the problem is that very little is known in general about this commutant.

Let us finally recall that the $\mathfrak{gl}(1|1)$ super spin chain—alias symplectic fermions; see appendix of [28]—seems to be the only case where the spin chain representation is not faithful. In particular this manifests itself in the fact that for $m = n$, the spectrum in this chain is equal to that obtained for free ($m = n = 0$) boundary conditions, when the Hamiltonian belongs to the Temperley-Lieb algebra and the critical exponents are those of the conformal field theory of symplectic fermions. Instead, in the case $m = n \neq 0$, the $\mathfrak{gl}(N|N)$ spin chain when $N > 1$ possesses an infinity of new exponents which are not contained in symplectic fermion theory. Note that these exponents in general are *not rational*—a rather unusual feature in conformal field theory.

4.2.3 Applications to the spin quantum Hall effect

We will now describe quantitatively how the presence of extra edge channels modifies the boundary critical behavior of the SQH network model.

We first set the fugacity of loops to one ($p = 2$) in the formulas of table 4.3. In this case the result simplifies, and is reproduced in table 4.4. There $h_{r,s} = \big[(3r-2s)^2-1\big]/24$, $\mathfrak{m} = \min(m, n)$ and the parameter r_k is given in terms of m, n and k for $m \geq n$ (if $m < n$ exchange m and n) by

$$r_k = \frac{6}{\pi} \arccos\left(\frac{\sqrt{3}}{2}\sqrt{\frac{(m+1+k)(n+1-k)}{(m+1)(n+1)}}\right).$$

Note that for number of legs greater than $n + m$, they no more depend on m, n and coincide with those of percolation, a phenomenon already observed in the one boundary case above. However when the number of legs is between ℓ and $n+m$, they are far from trivial and irrational.

Similarly, the exponents for the other values of $\mathcal{L}, \mathcal{R}$ are simplified. When the total number of legs in the model ($\mathcal{L} = -m, \mathcal{R} = -n$) equals $m + n + 2j$ with $j \geqslant 0$, the corresponding exponent is $h_{1,3+2j} = (j+1)(2j+1)/3$, and the $(m+n+2j)$-leg exponents are $h_{1,2+2j} = j(2j + 1)/3$ in both models ($\mathcal{L} = -m, \mathcal{R} = n$), ($\mathcal{L} = m, \mathcal{R} = -n$).

Now we recall from section 3.2.3 that the disorder averaged Green function for a point at the boundary is related to the probability that the point belongs to a loop of given length. This observable is governed by the operator creating two lines in the loop

k	#(legs) $= \ell + 2k$	$h^{m,n}(k)$
0	ℓ	$h_{r_0,r_0} = 0$
1	$\ell + 2$	h_{r_1,r_1}
$\vdots$	$\vdots$	$\vdots$
$\mathfrak{m}$	$n + m$	$h_{r_\mathfrak{m},r_\mathfrak{m}}$
$\mathfrak{m} + 1$	$n + m + 2$	$h_{1,3} = 1/3$
$\vdots$	$\vdots$	$\vdots$
$\mathfrak{m} + j$	$n + m + 2j$	$h_{1,1+2j} = j(2j-1)/3$
$\vdots$	$\vdots$	$\vdots$

Table 4.4: The watermelon exponents for fugacity of loops equal to one, of interest for the SQHE. k is the number of paired through lines on top of ℓ unpaired ones and $\mathfrak{m} = \min(m, n)$.

model with extra edge channels, which now has scaling dimension $h^{\mathcal{L},\mathcal{R}}(1)$. From this consideration we see that the boundary local density of states (3.31) becomes:

$$\overline{\rho^{\mathcal{L},\mathcal{R}}(e,\epsilon)} \sim |\epsilon|^{h^{\mathcal{L},\mathcal{R}}(1)/d_f} = |\epsilon|^{\frac{4}{7}h^{\mathcal{L},\mathcal{R}}(1)} .$$

The critical exponent of the local density of states at the boundary gets smaller with increasing the number of edge channels, see figure 4.16.

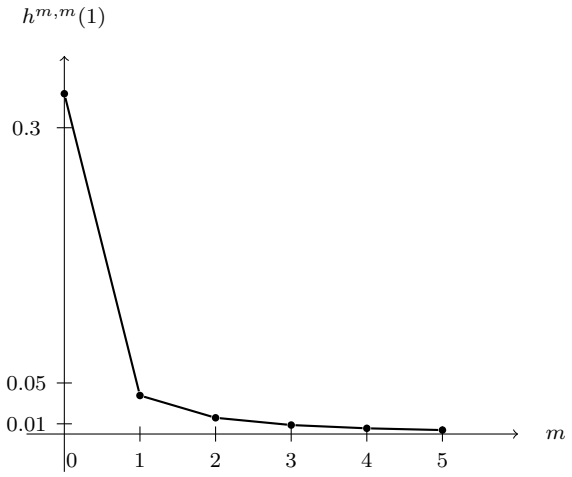

Figure 4.16: The behavior of $h^{\mathcal{L},\mathcal{R}}(1)$ when $\mathcal{L} = \mathcal{R} = m$ as a function of m. We see that the value for the case $m = 0$, $h^{0,0}(1) = 1/3$, gets smaller very rapidly by increasing the number of edge channels. Lines are guides for the eyes.

Scaling of conductance

We now move on to see how the extra edges affect transport properties by considering the conductance in the strip geometry, generalizing the discussion for $\mathcal{L} = \mathcal{R} = 0$ presented in section 3.2.3.

We have discussed in section 4.1.1 general transport properties of the networks with extra edge channels. Here we consider the mean conductance $\bar{g}^{\mathcal{L},\mathcal{R}}$ with the source at the bottom and the drain at the top of the strip. In the mapping to the geometrical model, the conductance is given by the average number of through lines going from the source to the drain of the current, times 2 for the spin. The minimal number of available through lines is $k_{\min}^{\mathcal{L},\mathcal{R}} = \max(0, \mathcal{L} - \mathcal{R})$, as already pointed out in section 4.1.1, whence

$$\bar{g}^{\mathcal{L},\mathcal{R}} = 2k_{\min}^{\mathcal{L},\mathcal{R}} + 2\sum_{k=1}^{\infty} kP(k, L_T/L, L_T/\xi), \tag{4.27}$$

where $P(k, L_T/L, L_T/\xi)$ is the probability (symmetric in $\mathcal{L}$ and $\mathcal{R}$) that exactly $2k$ "paired" through lines run through the system of size $2L_T$ by $2L + m + n$, and ξ is the bulk correlation length. At the transition, $\xi = \infty$. We refer to figure 4.17 for an illustration.

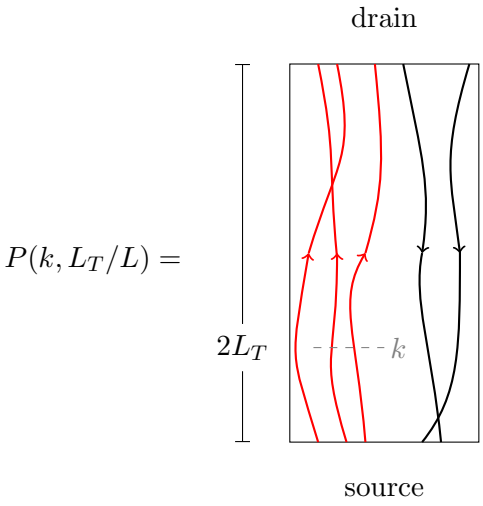

Figure 4.17: The probability that there are $2k$ paired through lines in the rectangle, contributing to the mean conductance. Source is on the bottom and the drain is on the top of the rectangle.

Using the transfer matrix T of the loop model we rewrite the mean conductance as

$$\bar{g} = \langle D|T^{L_T}|S\rangle\,, \tag{4.28}$$

where $|S\rangle$ and $\langle D|$ are two boundary states for the semirectangular geometries describing the source and the drain. We do not know exactly how to write these states in terms of links states (even for the case $\mathcal{L} = \mathcal{R} = 0$, as was pointed out in [46]). What we

know is that they are symmetric under any permutation of the incoming channels from the Landauer formula (3.8), so that only the block of the transfer matrix respecting this symmetry will couple to them. Further, we know that the boundary states will be symmetric under left-right reflection only if $\mathcal{L} = \mathcal{R}$. This observation is lifted in the continuum limit by saying that only even descendants of whatever primary field present in the BCFT will couple to the boundary state when $\mathcal{L} = \mathcal{R}$ [10].

Although we do not control these boundary states, we expect from conformal invariance that for large L_T/L, $P(k, L_T/L, 0) \sim e^{-\pi h^{\mathcal{L},\mathcal{R}}(k) L_T/L}$. The exponents $h^{\mathcal{L},\mathcal{R}}(k)$ are exactly the conformal dimensions we have computed above. For $L_T/L \gg 1$ the sum in Eq. (4.27) for $\bar{g}$ is dominated by $k = 1$:

$$\bar{g}^{\mathcal{L},\mathcal{R}} \sim 2k_{\min}^{\mathcal{L},\mathcal{R}} + C_1 e^{-\pi h^{\mathcal{L},\mathcal{R}}(1) \frac{L_T}{L}} . \tag{4.29}$$

We predict that the decay length of the conductance in the strip geometry is governed by the exponents $h^{\mathcal{L},\mathcal{R}}(1)$, whose numerical value can be read from table 4.4.

Numerical checks

In [27] we have presented extensive numerical computations of the conductance of critical SQH networks with extra channels in the strip geometry. The conductance is computed for a given realization of disorder from the Landauer formula, eq. (3.8), and the top-to-bottom transmission matrix t of the network using the transfer matrix method [135].

We compare the numerical value of the exponent governing the decay of the conductance obtained by fitting eq. (4.29) with the analytical prediction. The results are presented in table 4.5 for several values of $\mathcal{L}, \mathcal{R}$. The ratio of L_T/L in the system simulated is typically $[2, 40]$, and the number of disorder realizations over which we average is of the order of 10^5, 10^6. The numerical results are always very close to the analytical predictions, which we stress once again are irrational small number in most of the cases. Further, the numerical simulations confirm also that the results are independent on the choice of boundary couplings $t_{L,R}$ (of the boundary scattering matrices) and agree with the symmetry relation (4.26).

More remarks and details of the numerical simulations can be found in [27]. In particular [27] contains also results for $\gamma^{\mathcal{L},\mathcal{R}}$, the subleading corrections to $\bar{g}^{\mathcal{L},\mathcal{R}}$:

$$\bar{g}^{\mathcal{L},\mathcal{R}} \sim 2k_{\min}^{\mathcal{L},\mathcal{R}} + C_1 e^{-\pi h^{\mathcal{L},\mathcal{R}}(1) \frac{L_T}{L}} + C_2 e^{-\pi \gamma^{\mathcal{L},\mathcal{R}} \frac{L_T}{L}} .$$

The value of $\gamma^{\mathcal{L},\mathcal{R}}$ is not completely under control from the theoretical point of view. Conformal invariance implies that the exponential corrections to the conductance are given by conformal dimensions in the theory, see (4.28). $\gamma^{\mathcal{L},\mathcal{R}}$ is then the minimum among $h^{\mathcal{L},\mathcal{R}}(2)$ and dimensions of certain primary and descendant fields in the sector $k = 1$. Unfortunately, the analysis of section 4.2.2 is not sufficient to identify all the fields contributing to $\bar{g}^{\mathcal{L},\mathcal{R}}$ in the general case.

[10] Odd descendants are odd under left-right symmetry, think as performing the transformation $z \to -z$, under which the field with dimension h transforms with $(-)^h$.

$\mathcal{L}, \mathcal{R}$	numerics	analytical
	$h^{\mathcal{L},\mathcal{R}}(1)$	$h^{\mathcal{L},\mathcal{R}}(1)$
$0, 0$	0.3333(12)	$1/3$
$0, 1$	0.3330(7)	$1/3$
$0, 10$	0.3325(24)	$1/3$
$1, 1$	0.03775(25)	0.037720
$2, 2$	0.01600(2)	0.015906
$1, 2$	0.0520(25)	0.052083
$2, 4$	0.02954(7)	0.029589
$-2, -2$	0.0377(4)	0.037720
$-3, -2$	0.0522(2)	0.052083
$-1, 0$	0.999(9)	1
$-2, 0$	0.999(3)	1
$-2, 1$	0.998(3)	1

Table 4.5: The numerical values of the exponent governing the decay of the mean conductance (column "numerics") and the analytical prediction (column "analytical").

Conclusion and outlook

In this thesis we have discussed several aspects of lattice models and conformal field theories, together with their applications to the study of quantum Hall transitions.

The major achievement presented is the quantitative understanding of how critical behavior at higher spin quantum Hall plateau transitions is modified. Higher plateaus are distinguished by the presence of edge states at the boundary of the sample, and in a first place, we have discussed how to extend network models for Anderson transitions to include extra channels at the boundaries. Then, we have focused on the case of the spin quantum Hall effect. The network model for this transition enjoys a very special status among other models. We gave a detailed review of how in the bulk or in the presence of reflecting boundaries, the model can be mapped to the problem of classical percolation on a square lattice, allowing the exact determination of critical properties. Then we generalized this mapping to the case of networks with extra edges, leading to the study of a new loop model with crossings at the boundaries. For fugacity of loops M, this model discretizes $\mathbb{CP}^{N+M-1|N}$ super sigma models, where the edge states in the lattice formulation label in field theory language symmetric conformal boundary conditions for the fields. The computation of the critical exponents of these theories is quite intricate and required a lengthy discussion of lattice algebras and relations with boundary loop models. The outcome of this technical analysis is the exact expression of critical exponents, which turn out to be irrational in the general case, a rather unusual feature in conformal field theory (CFT). These irrational exponents govern the boundary critical behavior at higher spin quantum Hall plateau transitions, and in particular, they give the decay length of the mean spin conductance in the strip geometry. Our analytical predictions are corroborated by extensive numerical simulations of the network models.

The study of the conductance of network models in the rectangular geometry motivated also another result obtained in this thesis, the extension of the notion of CFT boundary states, commonly used to describe cylindrical geometries, to the rectangular ones. These objects are the continuum limit of incoming and outgoing states for lattice models defined on a strip, and have potentially several other applications, for example to quenches in 1D gapless quantum systems. Despite they appear as natural as cylinder boundary states from a statistical mechanics perspective, rectangular boundary states have been discussed very little in the literature and offers interesting technical challenges. We have developed a general theory allowing to describe rectangular geometries with different boundary conditions in an arbitrary CFT. In the general case these boundary

states have a rather complicated expression, depending on the operators implementing the conformal mapping from the upper half plane to the rectangle, and on the fusion of boundary condition changing operators. However for the case of free theories they take simple coherent states forms. Further, we have applied these results to loop models, giving a geometrical interpretation of rectangular amplitudes. An interesting outcome of the analysis is the derivation of formulas for probabilities of self-avoiding walks, which contain the indecomposability parameters of logarithmic CFTs.

The work presented in this thesis leaves a variety of interesting directions for future research. In general the geometrical language of edge states we have uncovered should have a broader range of applicability to other models describing topological properties of matter. We now list some concrete proposals of further developments, some of which are under investigation.

- Geometrical models derived from network models pertaining to any symmetry class can be formulated, and truncations amenable to exact solutions in any of such cases can be studied, generalizing the recent work done in [111] for the Chalker-Coddington model.

  There are plenty of questions that arise once the geometrical models have been set up, and in particular it is interesting to see if in some case the approximations provided by the truncations become exact. These ideas are the basis of work in progress with E. Vernier, H. Saleur and J. Jacobsen.

- The study of edge states developed in this thesis for the spin quantum Hall network paves the way for investigating more generally boundary critical behaviors at other Anderson transitions. The drastic influence of extra edge channels we have pointed out, is of immediate relevance for the integer quantum Hall transition and the thermal quantum Hall transition in class D. Some numerical studies discussing extra channels in network models have also already appeared in the literature [14, 131, 154]. However a general picture is definitely lacking. It could be also interesting to quantitatively investigate the role of edge states in the truncated geometrical models.

- Quantum transport properties of disordered wires (quasi 1D geometry) in a given symmetry class are related to diffusion in a corresponding Riemannian symmetric superspace [144, 201, 202]. We think that crucial topological considerations of the problem, related to transport at higher plateaus in quantum Hall-like systems, are missing in the literature, and an interesting direction could be to discuss those in a quantitative way.

  Indeed, we have discussed in this thesis how the symmetric conformal boundary conditions in the $\mathbb{CP}^{N+M-1|N}$ models are related in the minisuperspace (quasi 1D) limit to the monopole problem. Concretely, one could generalize the results of [144, 201, 202] to the case of open boundaries corresponding to the presence of extra edge channels in the lattice models. This would need to study Hamiltonians of the monopole problem on Riemannian symmetric superspaces, where the possibility of

having extra edge channels should emerge as twisting of the associated complex line bundles.

We remark that for having quantitative results in the wire limit an alternative route to the 1D sigma model is available, and is known as the DMPK equation, see the discussion and references in [78]. Without entering any detail here, we point out that exact results for the conductance of wires with extra edge channels (also called perfectly conducting channels) have been obtained, as reviewed in [78]. However, rederiving these results, together with the topological interpretation sketched above, would be a very interesting exercise both from a physical and a mathematical perspective.

- One of the motivations for discussing rectangular amplitudes was the exact computation of conductance at high spin quantum Hall plateaus in the strip geometry. In this thesis we did not carry out fully this program. Indeed this would require extending our results for boundary states to the case of blobbed loop models, since for computing the mean number of lines crossing the rectangle, we need to weight differently loops touching different boundaries. Unfortunately, difficulties in understanding the fusion rules of boundary fields in blobbed loop models, require more work to complete this project.

- As a last outlook, we point out the need to improve our understanding of logarithmic conformal field theories. Although in this thesis we did not deal explicitly with formal aspects of these theories, it is clear that a better understanding of those is vital for studying disordered critical points. By now, there are several examples of understood boundary logarithmic CFTs (for example see [88, 172]), and recent research is focusing more on the case of bulk logarithmic CFTs. As interesting perspectives in this direction, we mention the lattice approach [92–94], and the bulk-boundary correspondence of [89, 174] built on a formal algebraic framework.

Bibliography

[1] I. Affleck, *The quantum hall effects, σ-models at $\theta = \pi$ and quantum spin chains*, Nuclear Physics B **257** (1985), no. 0, 397 –406.

[2] ———, *Universal term in the free energy at a critical point and the conformal anomaly*, Phys. Rev. Lett. **56** (1986), 746–748.

[3] ———, *Field theory methods and quantum critical phenomena*, Fields, strings and critical phenomena: Les houches summer school, session xlix, 1988, pp. 563–640.

[4] ———, *Exact results on the dimerisation transition in $SU(n)$ antiferromagnetic chains*, Journal of Physics: Condensed Matter **2** (1990), no. 2, 405–415.

[5] ———, *Quantum Impurity Problems in Condensed Matter Physics*, Exact Methods in Low-Dimensional Statistical Physics and Quantum Computing: Lecture Notes of the Les Houches Summer School: Volume 89, July 2008, 2010.

[6] I. Affleck and A. W. W. Ludwig, *Universal non integer ground-state degeneracy in critical quantum systems*, Phys. Rev. Lett. **67** (1991), no. 2, 161–164.

[7] ———, *The Fermi edge singularity and boundary condition changing operators*, Journal of Physics A: Mathematical and General **27** (1994), no. 16, 5375.

[8] F. C. Alcaraz, M. N. Barber, M. T. Batchelor, R. J. Baxter, and G. R. W. Quispel, *Surface exponents of the quantum XXZ, Ashkin-Teller and Potts models*, Journal of Physics A: Mathematical and General **20** (1987), no. 18, 6397.

[9] A. Alekseev and V. Schomerus, *D-branes in the WZW model*, Phys. Rev. D **60** (1999), no. 6, 061901.

[10] A. Altland and B. Simons, *Condensed Matter Field Theory*, Cambridge University Press, 2006.

[11] A. Altland and M. R. Zirnbauer, *Nonstandard symmetry classes in mesoscopic normal-superconducting hybrid structures*, Phys. Rev. B **55** (1997), 1142–1161.

[12] G. E. Andrews, R. J. Baxter, and P. J. Forrester, *Eight-vertex SOS model and generalized Rogers-Ramanujan-type identities*, Journal of Statistical Physics **35** (1984), 193–266. 10.1007/BF01014383.

[13] E. Ardonne and G. Sierra, *Chiral correlators of the Ising conformal field theory*, Journal of Physics A: Mathematical and Theoretical **43** (2010), no. 50, 505402.

[14] C. Barnes, B. L. Johnson, and G. Kirczenow, *Quantum railroads: Introducing directionality to Anderson localization*, Phys. Rev. Lett. **70** (1993), 1159–1162.

[15] M. Bauer and D. Bernard, *Conformal Transformations and the SLE Partition Function Martingale*, Annales Henri Poincare **5** (2004), 289–326. 10.1007/s00023-004-0170-z.

[16] ———, *2D growth processes: SLE and Loewner chains*, Physics Reports **432** (2006), no. 34, 115 –221.

[17] R. J. Baxter, *Exactly Solved Models in Statistical Mechanics*, Dover Books on Physics Series, Dover Publications, 2008.

[18] E. J. Beamond, J. Cardy, and J. T. Chalker, *Quantum and classical localization, the spin quantum Hall effect, and generalizations*, Phys. Rev. B **65** (2002), 214301.

[19] A. A. Belavin, A. M. Polyakov, and A. B. Zamolodchikov, *Infinite conformal symmetry in two-dimensional quantum field theory*, Nuclear Physics B **241** (1984), no. 2, 333 –380.

[20] D. Bernard and A. LeClair, *A classification of 2D random Dirac fermions*, Journal of Physics A: Mathematical and General **35** (2002), no. 11, 2555.

[21] B. A. Bernevig, T. L. Hughes, and S.-C. Zhang, *Quantum Spin Hall Effect and Topological Phase Transition in HgTe Quantum Wells*, Science **314** (2006), no. 5806, 1757–1761.

[22] M Bershadsky, *PSL$(n|n)$ sigma model as a conformal field theory*, Nucl. Phys. B **559** (1999), no. 1-2, 205–234.

[23] E. Bettelheim, I. A. Gruzberg, and A. W. W. Ludwig, *Quantum Hall transitions: an exact theory based on conformal restriction*, ArXiv e-prints (2012), available at 1202.4573.

[24] H. W. J. Blöte, J. Cardy, and M. P. Nightingale, *Conformal invariance, the central charge, and universal finite-size amplitudes at criticality*, Phys. Rev. Lett. **56** (1986), 742–745.

[25] R. Blumenhagen and E. Plauschinn, *Introduction to Conformal Field Theory: With Applications to String Theory*, Lecture Notes in Physics, Springer, 2009.

[26] R. Bondesan, J. Dubail, J. L. Jacobsen, and H. Saleur, *Conformal boundary state for the rectangular geometry*, Nuclear Physics B **862** (2012), no. 2, 553 –575.

[27] R. Bondesan, I. A. Gruzberg, J. L. Jacobsen, H. Obuse, and H. Saleur, *Exact Exponents for the Spin Quantum Hall Transition in the Presence of Multiple Edge Channels*, Phys. Rev. Lett. **108** (2012), 126801.

[28] R. Bondesan, J. L. Jacobsen, and H. Saleur, *Edge states and conformal boundary conditions in super spin chains and super sigma models*, Nuclear Physics B **849** (2011), no. 2, 461 –502.

[29] Roberto Bondesan, Jesper L. Jacobsen, and Hubert Saleur, *Rectangular amplitudes, conformal blocks, and applications to loop models*, Nuclear Physics B **867** (2013), no. 3, 913 –949.

[30] R. Brauer, *On Algebras Which are Connected with the Semisimple Continuous Groups*, Ann. Math. **38** (1937), no. 4, pp. 857–872.

[31] S. B. Bravyi and A. Y. Kitaev, *Quantum codes on a lattice with boundary*, eprint arXiv:quant-ph (1998), available at arXiv:quant-ph/9811052.

[32] J. Budczies and M. R. Zirnbauer, *Howe Duality for an Induced Model of Lattice U(N) Yang-Mills Theory*, ArXiv Mathematical Physics e-prints (2003), available at arXiv:math-ph/0305058.

[33] M. Büttiker, *Absence of backscattering in the quantum Hall effect in multiprobe conductors*, Phys. Rev. B **38** (1988), 9375–9389.

[34] P. Calabrese and J. Cardy, *Quantum quenches in extended systems*, Journal of Statistical Mechanics: Theory and Experiment **2007** (2007), no. 06, P06008.

[35] C. G. Callan, C. Lovelace, C. R. Nappi, and S. A. Yost, *Adding holes and crosscaps to the superstring*, Nuclear Physics B **293** (1987), no. 0, 83 –113.

[36] C. Candu, T. Creutzig, V. Mitev, and V. Schomerus, *Cohomological Reduction of Sigma Models*, J. High Energy Phys. **2010** (2010), 1–39.

[37] C. Candu, J. L. Jacobsen, N. Read, and H. Saleur, *Universality classes of polymer melts and conformal sigma models*, J. Phys. A: Math. Gen. **43** (2010), 142001.

[38] C. Candu, V. Mitev, T. Quella, H. Saleur, and V. Schomerus, *The sigma model on complex projective superspaces*, J. High Energy Phys. **2010** (2010), no. 2, 59.

[39] C. Candu and H. Saleur, *A lattice approach to the conformal supercoset sigma model. Part I: Algebraic structures in the spin chain. The Brauer algebra*, Nuclear Physics B **808** (2009), no. 3, 441 –486.

[40] S. Caracciolo, J. L. Jacobsen, H. Saleur, A. D. Sokal, and A. Sportiello, *Fermionic Field Theory for Trees and Forests*, Phys. Rev. Lett. **93** (2004), 080601.

[41] J. Cardy, *Conformal invariance and surface critical behavior*, Nuclear Physics B **240** (1984), no. 4, 514 –532.

[42] ———, *Conformal invariance and universality in finite-size scaling*, Journal of Physics A: Mathematical and General **17** (1984), no. 7, L385.

[43] ———, *Operator content of two-dimensional conformally invariant theories*, Nuclear Physics B **270** (1986), no. 0, 186 –204.

[44] ———, *Boundary conditions, fusion rules and the Verlinde formula*, Nuclear Physics B **324** (1989), no. 3, 581 –596.

[45] ———, *Critical percolation in finite geometries*, Journal of Physics A: Mathematical and General **25** (1992), no. 4, L201.

[46] ———, *The number of incipient spanning clusters in two-dimensional percolation*, Journal of Physics A: Mathematical and General **31** (1998), no. 5, L105.

[47] ———, *Linking Numbers for Self-Avoiding Loops and Percolation: Application to the Spin Quantum Hall Transition*, Phys. Rev. Lett. **84** (2000), 3507–3510.

[48] ———, *Conformal Invariance and Percolation* (2001), available at arXiv:math-ph/0103018.

[49] ———, *Crossing formulae for critical percolation in an annulus*, Journal of Physics A: Mathematical and General **35** (2002), no. 41, L565.

[50] ———, *Network Models in Class C on Arbitrary Graphs*, Communications in Mathematical Physics **258** (2005), 87–102. 10.1007/s00220-005-1304-y.

[51] ———, *The $O(n)$ Model on the Annulus*, Journal of Statistical Physics **125** (2006), 1–21. 10.1007/s10955-006-9186-8.

[52] ———, *Conformal Field Theory and Statistical Mechanics*, Exact Methods in Low-Dimensional Statistical Physics and Quantum Computing: Lecture Notes of the Les Houches Summer School: Volume 89, July 2008, 2010.

[53] J. Cardy and D. Lewellen, *Bulk and boundary operators in conformal field theory*, Physics Letters B **259** (1991), no. 3, 274 –278.

[54] J. Cardy and I. Peschel, *Finite-size dependence of the free energy in two-dimensional critical systems*, Nuclear Physics B **300** (1988), 377 –392.

[55] J. T. Chalker and P. D. Coddington, *Percolation, quantum tunnelling and the integer Hall effect*, Journal of Physics C: Solid State Physics **21** (1988), no. 14, 2665.

[56] J. T. Chalker, N. Read, V. Kagalovsky, B. Horovitz, Y. Avishai, and A. W. W. Ludwig, *Thermal metal in network models of a disordered two-dimensional superconductor*, Phys. Rev. B **65** (2001), 012506.

[57] S.-J. Cheng and W. Wang, *Dualities and Representations of Lie Superalgebras*, American Mathematical Society, 2013.

[58] S. Coleman, *More about the massive Schwinger model*, Ann. Phys. (New York) **101** (1976), no. 1, 239 –267.

[59] T. Creutzig, *Geometry of branes on supergroups*, Nucl. Phys. B **812** (2009), no. 3, 301–321.

[60] T. Creutzig, T. Quella, and V. Schomerus, *Branes in the $GL(1|1)$ WZNW model*, Nuclear Physics B **792** (2008), no. 3, 257 –283.

[61] T. Creutzig and P. B. Rønne, *The $GL(1|1)$-symplectic fermion correspondence*, Nuclear Physics B **815** (2009), no. 12, 95 –124.

[62] A. D'Adda, M. Lüscher, and P. Di Vecchia, *A $1/n$ expandable series of non-linear σ models with instantons*, Nuclear Physics B **146** (1978), no. 1, 63 –76.

[63] S. Das Sarma and A. Pinczuk, *Perspectives in Quantum Hall Effects: Novel Quantum Liquids in Low-Dimensional Semiconductor Structures*, John Wiley & Sons, 2008.

[64] P. G. de Gennes, *Scaling Concepts in Polymer Physics*, G - Reference, Information and Interdisciplinary Subjects Series, Cornell University Press, 1979.

[65] P. di Francesco, H. Saleur, and J. B. Zuber, *Relations between the Coulomb gas picture and conformal invariance of two-dimensional critical models*, Journal of Statistical Physics **49** (1987), 57–79. 10.1007/BF01009954.

[66] N. Diamantis and P. Kleban, *New percolation crossing formulas and second-order modular forms*, ArXiv e-prints (2009), available at http://arxiv.org/abs/0905.1727.

[67] A. Doikou and P. P. Martin, *Hecke algebraic approach to the reflection equation for spin chains*, Journal of Physics A: Mathematical and General **36** (2003), no. 9, 2203.

[68] V. S. Dotsenko and V. A. Fateev, *Four-point correlation functions and the operator algebra in 2D conformal invariant theories with central charge $C \leq 1$*, Nuclear Physics B **251** (1985), 691 –734.

[69] J. Dubail, *Conditions aux bords dans des theories conformes non unitaires*, PhD Thesis, 2010 (French).

[70] J. Dubail, J. L. Jacobsen, and H. Saleur, *Conformal two-boundary loop model on the annulus*, Nuclear Physics B **813** (2009), no. 3, 430 –459.

[71] ———, *Conformal field theory at central charge $c = 0$: A measure of the indecomposability (b) parameters*, Nuclear Physics B **834** (2010), no. 3, 399 –422.

[72] J. Dubail and J.-M. Stéphan, *Universal behavior of a bipartite fidelity at quantum criticality*, Journal of Statistical Mechanics: Theory and Experiment **2011** (2011), no. 03, L03002.

[73] B. Duplantier and F. David, *Exact partition functions and correlation functions of multiple Hamiltonian walks on the Manhattan lattice*, Journal of Statistical Physics **51** (1988), 327–434. 10.1007/BF01028464.

[74] F. J. Dyson, *The Threefold Way. Algebraic Structure of Symmetry Groups and Ensembles in Quantum Mechanics*, Journal of Mathematical Physics **3** (1962), no. 6, 1199–1215.

[75] K. Efetov, *Supersymmetry in Disorder and Chaos*, Cambridge University Press, 1999.

[76] I. Ellwood, B. Feng, Y.-H. He, and N. Moeller, *The identity string field and the tachyon vacuum*, Journal of High Energy Physics **2001** (2001), no. 07, 016.

[77] F. H. L. Essler, H. Frahm, and H. Saleur, *Continuum limit of the integrable superspin chain*, Nuclear Physics B **712** (2005), no. 3, 513 –572.

[78] F. Evers and A. D. Mirlin, *Anderson transitions*, Rev. Mod. Phys. **80** (2008), 1355–1417.

[79] A. Feiguin, S. Trebst, A. W. W. Ludwig, M. Troyer, A. Kitaev, Z. Wang, and M. H. Freedman, *Interacting Anyons in Topological Quantum Liquids: The Golden Chain*, Phys. Rev. Lett. **98** (2007), 160409.

[80] G. Felder, J. Fröhlich, J. Fuchs, and C. Schweigert, *Conformal Boundary Conditions and Three-Dimensional Topological Field Theory*, Phys. Rev. Lett. **84** (2000), 1659–1662.

[81] P. Fendley and N. Read, *Exact S -matrices for supersymmetric sigma models and the Potts model*, Journal of Physics A: Mathematical and General **35** (2002), no. 50, 10675.

[82] C. M. Fortuin and P. W. Kasteleyn, *On the random-cluster model*, Physica **57** (1972), no. 4, 536–564.

[83] E. Fradkin, *Field Theories of Condensed Matter Systems*, Advanced Books Classics Series, Perseus Books, 1998.

[84] P. Di Francesco, P. Mathieu, and D. Sénéchal, *Conformal Field Theory*, Graduate Texts in Contemporary Physics, Springer, 1997.

[85] D. Friedan, Z. Qiu, and S. Shenker, *Conformal Invariance, Unitarity, and Critical Exponents in Two Dimensions*, Phys. Rev. Lett. **52** (1984), 1575–1578.

[86] M. R. Gaberdiel, *D-branes from conformal field theory*, Fortschritte der Physik **50** (2002), 783–801.

[87] ———, *An Algebraic approach to logarithmic conformal field theory*, Int.J.Mod.Phys. **A18** (2003), 4593–4638.

[88] M. R. Gaberdiel and I. Runkel, *The logarithmic triplet theory with boundary*, Journal of Physics A: Mathematical and General **39** (2006), no. 47, 14745.

[89] ———, *From boundary to bulk in logarithmic CFT*, Journal of Physics A: Mathematical and Theoretical **41** (2008), no. 7, 075402.

[90] R. Gade, *Anderson localization for sublattice models*, Nuclear Physics B **398** (1993), no. 3, 499 –515.

[91] R. Gade and F. Wegner, *The $n = 0$ replica limit of $U(n)$ and $U(n)/SO(n)$ models*, Nuclear Physics B **360** (1991), no. 23, 213 –218.

[92] A. M. Gainutdinov, N. Read, and H. Saleur, *Bimodule structure in the periodic $gl(1|1)$ spin chain*, ArXiv e-prints (2011), available at 1112.3407.

[93] ———, *Continuum limit and symmetries of the periodic $gl(1|1)$ spin chain*, ArXiv e-prints (2011), available at 1112.3403.

[94] ———, *Associative algebraic approach to logarithmic CFT in the bulk: the continuum limit of the $gl(1|1)$ periodic spin chain, Howe duality and the interchiral algebra*, ArXiv e-prints (2012), available at 1207.6334.

[95] D. Gepner and E. Witten, *String theory on group manifolds*, Nuclear Physics B **278** (1986), no. 3, 493 –549.

[96] S. M. Girvin, *The Quantum Hall Effect: Novel Excitations and Broken Symmetries*, Topological Aspects of Low Dimensional Systems, 1999, pp. 53.

[97] F. Gomes and Danny C. Sorensen, *ARPACK++: An object-oriented version of ARPACK eigenvalue package*, 2000.

[98] G. Götz, T. Quella, and V. Schomerus, *Tensor products of $psl(2|2)$ representations*, ArXiv High Energy Physics - Theory e-prints (2005), available at arXiv:hep-th/0506072.

[99] ———, *Representation theory of $sl(2|1)$*, Journal of Algebra **312** (2007), no. 2, 829–848.

[100] ———, *The WZNW model on $PSU(1,1|2)$*, Journal of High Energy Physics **2007** (2007), no. 03, 003.

[101] I. A. Gruzberg, A. W. W. Ludwig, and N. Read, *Exact Exponents for the Spin Quantum Hall Transition*, Phys. Rev. Lett. **82** (1999), 4524–4527.

[102] I. A. Gruzberg, N. Read, and A. W. W. Ludwig, *Network models for quantum Hall transitions: the supersymmetry approach*, 2009.

[103] I. A. Gruzberg, N. Read, and S. Sachdev, *Scaling and crossover functions for the conductance in the directed network model of edge states*, Phys. Rev. B **55** (1997), 10593–10601.

[104] V. Gurarie, *Logarithmic operators in conformal field theory*, Nuclear Physics B **410** (1993), no. 3, 535 –549.

[105] V. Gurarie and A. W. W. Ludwig, *Conformal Field Theory at central charge c=0 and Two-Dimensional Critical Systems with Quenched Disorder*, ArXiv High Energy Physics - Theory e-prints (2004), available at arXiv:hep-th/0409105.

[106] F. D. M. Haldane, *Nonlinear Field Theory of Large-Spin Heisenberg Antiferromagnets: Semiclassically Quantized Solitons of the One-Dimensional Easy-Axis Néel State*, Phys. Rev. Lett. **50** (1983), 1153–1156.

[107] B. I. Halperin, *Quantized Hall conductance, current-carrying edge states, and the existence of extended states in a two-dimensional disordered potential*, Phys. Rev. B **25** (1982), 2185–2190.

[108] M. Z. Hasan and C. L. Kane, *Colloquium: Topological insulators*, Rev. Mod. Phys. **82** (2010), 3045–3067.

[109] P. Heinzner, A. Huckleberry, and M. R. Zirnbauer, *Symmetry Classes of Disordered Fermions*, Communications in Mathematical Physics **257** (2005), 725–771.

[110] R. Howe, *Remarks on classical invariant theory*, Trans. Amer. Math. Soc. **313** (1989), 539–570.

[111] Y. Ikhlef, P. Fendley, and J. Cardy, *Integrable modification of the critical Chalker-Coddington network model*, Phys. Rev. B **84** (2011), 144201.

[112] Y. Ikhlef, J. L. Jacobsen, and H. Saleur, *A Temperley-Lieb quantum chain with two- and three-site interactions*, Journal of Physics A: Mathematical and Theoretical **42** (2009), no. 29, 292002.

[113] Y. Imamura, H. Isono, and Y. Matsuo, *Boundary States in the Open String Channel and CFT near a Corner*, Progress of Theoretical Physics **115** (2006), no. 5, 979–1002.

[114] ———, *Boundary State of Superstring in Open String Channel*, Progress of Theoretical Physics **119** (2008), no. 4, 643–662.

[115] N. Ishibashi, *The Boundary and Crosscap States in Conformal Field Theories*, Mod.Phys.Lett. **A4** (1989), 251.

[116] E. V. Ivashkevich, *Correlation functions of dense polymers and $c = -2$ conformal field theory*, Journal of Physics A: Mathematical and General **32** (1999), no. 9, 1691.

[117] J. L. Jacobsen, *Conformal Field Theory Applied to Loop Models*, Polygons, polyominoes and polycubes, 2009, pp. 347–424.

[118] J. L. Jacobsen and H. Saleur, *Conformal boundary loop models*, Nuclear Physics B **788** (2008), no. 3, 137 –166.

[119] J. K. Jain, *Composite Fermions*, Cambridge University Press, 2007.

[120] M. Janssen, M. Metzler, and M. R. Zirnbauer, *Point-Contact Conductances at the Quantum Hall Transition*, Phys. Rev. B **59** (1999), 15836.

[121] V. G. Kac, *Vertex Algebras for Beginners*, University Lecture Series, American Mathematical Society, 1998.

[122] V. Kagalovsky, B. Horovitz, Y. Avishai, and J. T. Chalker, *Quantum Hall Plateau Transitions in Disordered Superconductors*, Phys. Rev. Lett. **82** (1999), 3516–3519.

[123] C. L. Kane and E. J. Mele, *Quantum Spin Hall Effect in Graphene*, Phys. Rev. Lett. **95** (2005), 226801.

[124] C. Kassel, *Quantum Groups*, Graduate Texts in Mathematics, Springer-Verlag, 1995.

[125] L. H. Kauffman and S. Lins, *Temperley-Lieb Recoupling Theory and Invariants of 3-Manifolds*, Annals of Mathematics Studies, Princeton University Press, 1994.

[126] H. Kausch, *Curiosities at $c = -2$* (1995), 26.

[127] ———, *Symplectic fermions*, Nucl. Phys. B **583** (2000), no. 3, 513–541.

[128] A. Kitaev, *Periodic table for topological insulators and superconductors*, American institute of physics conference series, 2009, pp. 22–30.

[129] P. Kleban and I. Vassileva, *Free energy of rectangular domains at criticality*, Journal of Physics A: Mathematical and General **24** (1991), no. 14, 3407.

[130] P. Kleban and D. Zagier, *Crossing Probabilities and Modular Forms*, Journal of Statistical Physics **113** (2003), 431–454.

[131] K. Kobayashi, K. Hirose, H. Obuse, T. Ohtsuki, and K. Slevin, *Transport properties in network models with perfectly conducting channels*, Journal of Physics: Conference Series **150** (2009), no. 2, 022041.

[132] J. Kondev and J. B. Marston, *Supersymmetry and localization in the quantum Hall effect*, Nuclear Physics B **497** (1997), no. 3, 639 –657.

[133] M. König, S. Wiedmann, C. Brüne, A. Roth, H. Buhmann, L. W. Molenkamp, X.-L. Qi, and S.-C. Zhang, *Quantum Spin Hall Insulator State in HgTe Quantum Wells*, Science **318** (2007), no. 5851, 766–770.

[134] W. M. Koo and H. Saleur, *Representations of the Virasoro algebra from lattice models*, Nuclear Physics B **426** (1994), no. 3, 459 –504.

[135] B. Kramer, T. Ohtsuki, and S. Kettemann, *Random network models and quantum phase transitions in two dimensions*, Physics Reports **417** (2005), no. 56, 211 –342.

[136] A. LeClair and D. Bernard, *Holographic classification of Topological Insulators and its 8-fold periodicity*, ArXiv e-prints (2012), available at 1205.3810.

[137] A. Leclair, M. E. Peskin, and C. R. Preitschopf, *String field theory on the conformal plane (I).: Kinematical Principles*, Nuclear Physics B **317** (1989), no. 2, 411 –463.

[138] D. C. Lewellen, *Sewing constraints for conformal field theories on surfaces with boundaries*, Nuclear Physics B **372** (1992), no. 3, 654–682.

[139] A. W. W. Ludwig, M. P. A. Fisher, R. Shankar, and G. Grinstein, *Integer quantum Hall transition: An alternative approach and exact results*, Phys. Rev. B **50** (1994), 7526–7552.

[140] J. B. Marston and S.-W. Tsai, *Chalker-Coddington Network Model is Quantum Critical*, Phys. Rev. Lett. **82** (1999), 4906–4909.

[141] P. Martin and H. Saleur, *The blob algebra and the periodic Temperley-Lieb algebra*, Letters in Mathematical Physics **30** (1994), 189–206. 10.1007/BF00805852.

[142] P. P. Martin, *Potts Models and Related Problems in Statistical Mechanics*, Series on Advances in Statistical Mechanics, World Scientific, 1991.

[143] A. D. Mirlin, F. Evers, and A. Mildenberger, *Wavefunction statistics and multifractality at the spin quantum Hall transition*, Journal of Physics A: Mathematical and General **36** (2003), no. 12, 3255.

[144] A. D. Mirlin, A. Müller–Groeling, and M. R. Zirnbauer, *Conductance Fluctuations of Disordered Wires: Fourier Analysis on Supersymmetric Spaces*, Annals of Physics **236** (1994), no. 2, 325 –373.

[145] V. Mitev, T. Quella, and V. Schomerus, *Principal chiral model on superspheres*, J. High Energy Phys. **2008** (2008), no. 11, 086.

[146] G. Moore and N. Seiberg, *Lectures on RCFT*, Physics, geometry, and topology, 1990, pp. 263 –361.

[147] G. Mussardo, *Statistical Field Theory: An Introduction to Exactly Solved Models in Statistical Physics*, Oxford Graduate Texts, Oxford University Press, 2009.

[148] M. Nakahara, *Geometry, Topology, and Physics*, Graduate Student Series in Physics, Institute of Physics Publishing, 2003.

[149] C. Nayak, S. H. Simon, A. Stern, M. Freedman, and S. Das Sarma, *Non-Abelian anyons and topological quantum computation*, Rev. Mod. Phys. **80** (2008), 1083–1159.

[150] T.-K. Ng, *Edge states in antiferromagnetic quantum spin chains*, Phys. Rev. B **50** (1994), no. 1, 555–558.

[151] A. Nichols, V. Rittenberg, and J. de Gier, *One-boundary Temperley-Lieb algebras in the XXZ and loop models*, Journal of Statistical Mechanics: Theory and Experiment **2005** (2005), no. 03, P03003.

[152] B. Nienhuis, *Exact Critical Point and Critical Exponents of* O(n) *Models in Two Dimensions*, Phys. Rev. Lett. **49** (1982), 1062–1065.

[153] ———, *Coulomb gas formulation of two-dimensional phase transitions*, Phase transitions and critical phenomena, 1987, pp. 1–54.

[154] H. Obuse, A. Furusaki, S. Ryu, and C. Mudry, *Boundary criticality at the Anderson transition between a metal and a quantum spin Hall insulator in two dimensions*, Phys. Rev. B **78** (2008), 115301.

[155] H. Obuse, I. A. Gruzberg, and F. Evers, *Finite Size Effects and Irrelevant Corrections to Scaling near the Integer Quantum Hall Transition*, ArXiv e-prints (2012), available at 1205.2763.

[156] G. Parisi and N. Sourlas, *Self avoiding walk and supersymmetry*, Journal de Physique Lettres **41** (1980), no. 17, 403–405.

[157] V. Pasquier and H. Saleur, *Common structures between finite systems and conformal field theories through quantum groups*, Nuclear Physics B **330** (1990), no. 23, 523 –556.

[158] P. A. Pearce, J. Rasmussen, and J.-B. Zuber, *Logarithmic minimal models*, Journal of Statistical Mechanics: Theory and Experiment **2006** (2006), no. 11, P11017.

[159] A. M. Perelomov, *Coherent states for arbitrary Lie group*, Communications in Mathematical Physics **26** (1972), no. 3, 222–236.

[160] V. B. Petkova and J.-B. Zuber, *Conformal boundary conditions and what they teach us*, Non-perturbative qft methods and their applications, 2001, pp. 1–35.

[161] A. M. Polyakov, *Supermagnets and Sigma Models*, Quarks, hadrons, and strong interactions, 2006, pp. 409–428.

[162] R.E. Prange and S.M. Girvin, *The Quantum Hall effect*, Springer-Verlag, 1987.

[163] A. M. M. Pruisken, *On localization in the theory of the quantized hall effect: A two-dimensional realization of the θ-vacuum*, Nuclear Physics B **235** (1984), no. 2, 277 –298.

[164] ———, *Super universality of the quantum Hall effect and the "large N picture" of the ϑ angle*, Int. J. Theor. Phys. **48** (2009), 1736–1765.

[165] S. Qin, T.-K. Ng, and Z.-B. Su, *Edge states in open antiferromagnetic Heisenberg chains*, Phys. Rev. B **52** (1995), no. 17, 12844–12848.

[166] T. Quella, V. Schomerus, and T. Creutzig, *Boundary spectra in superspace σ-models*, J. High Energy Phys. **2008** (2008), no. 10, 024–024.

[167] L. Rastelli and B. Zwiebach, *Tachyon potentials, star products and universality*, Journal of High Energy Physics **2001** (2001), no. 09, 038.

[168] N. Read, 1987.

[169] N. Read and S. Sachdev, *Some features of the phase diagram of the square lattice $SU(N)$ antiferromagnet*, Nuclear Physics B **316** (1989), no. 3, 609 –640.

[170] N. Read and H. Saleur, *Exact spectra of conformal supersymmetric nonlinear sigma models in two dimensions*, Nuclear Physics B **613** (2001), no. 3, 409–444, available at 0106124.

[171] ———, *Associative-algebraic approach to logarithmic conformal field theories*, Nuclear Physics B **777** (2007), no. 3, 316–351.

[172] ———, *Enlarged symmetry algebras of spin chains, loop models, and S-matrices*, Nuclear Physics B **777** (2007), no. 3, 263–315.

[173] I. Runkel, *Boundary structure constants for the A-series Virasoro minimal models*, Nuclear Physics B **549** (1999), no. 3, 563–578.

[174] I. Runkel, M. R. Gaberdiel, and S. Wood, *Logarithmic bulk and boundary conformal field theory and the full centre construction*, Conformal field theories and tensor categories, 2011.

[175] B.E. Sagan, *The Symmetric Group: Representations, Combinatorial Algorithms, and Symmetric Functions*, Graduate Texts in Mathematics, Springer, 2001.

[176] H. Saleur, *Super spin chains and super sigma models: a short introduction*, Exact Methods in Low-Dimensional Statistical Physics and Quantum Computing: Lecture Notes of the Les Houches Summer School: Volume 89, July 2008, 2010.

[177] H. Saleur and M. Bauer, *On some relations between local height probabilities and conformal invariance*, Nuclear Physics B **320** (1989), no. 3, 591 –624.

[178] H. Saleur and B. Duplantier, *Exact Determination of the Percolation Hull Exponent in Two Dimensions*, Phys. Rev. Lett. **58** (1987), 2325–2328.

[179] A. P. Schnyder, S. Ryu, A. Furusaki, and A. W. W. Ludwig, *Classification of Topological Insulators and Superconductors*, American institute of physics conference series, 2009, pp. 10–21.

[180] V. Schomerus, *Lectures on branes in curved backgrounds*, Classical and Quantum Gravity **19** (2002), no. 22, 5781.

[181] V. Schomerus and H. Saleur, *The GL(1|1) WZW-model: From supergeometry to logarithmic CFT*, Nuclear Physics B **734** (2006), no. 3, 221 –245.

[182] A. Sen, *Open string field theory in a non-trivial background field: (I). Gauge invariant action*, Nuclear Physics B **334** (1990), no. 2, 350 –394.

[183] T. Senthil, J. B. Marston, and Matthew P. A. Fisher, *Spin quantum Hall effect in unconventional superconductors*, Phys. Rev. B **60** (1999), 4245–4254.

[184] R. Shankar and N. Read, *The $\theta = \pi$ nonlinear sigma model is massless*, Nuclear Physics B **336** (1990), no. 3, 457 –474.

[185] A. D. Sokal, *The multivariate Tutte polynomial (alias Potts model) for graphs and matroids* (2005), 54 pp., available at 0503607.

[186] A. R. Subramaniam, I. A. Gruzberg, and A. W. W. Ludwig, *Boundary criticality and multifractality at the two-dimensional spin quantum hall transition*, Phys. Rev. B **78** (2008), 245105.

[187] H. N. V. Temperley and E. H. Lieb, *Relations between the 'Percolation' and 'Colouring' Problem and other Graph-Theoretical Problems Associated with Regular Planar Lattices: Some Exact Results for the 'Percolation' Problem*, Proceedings of the Royal Society of London. Series A, Mathematical and Physical Sciences **322** (1971), no. 1549, pp. 251–280.

[188] D. J. Thouless, M. Kohmoto, M. P. Nightingale, and M. den Nijs, *Quantized Hall Conductance in a Two-Dimensional Periodic Potential*, Phys. Rev. Lett. **49** (1982), 405–408.

[189] S. A. Trugman, *Localization, percolation, and the quantum Hall effect*, Phys. Rev. B **27** (1983), 7539–7546.

[190] R. Vasseur, A. Gainutdinov, J. L. Jacobsen, and H. Saleur, *Puzzle of Bulk Conformal Field Theories at Central Charge $c = 0$*, Phys. Rev. Lett. **108** (2012), 161602.

[191] R. Vasseur, J. L. Jacobsen, and H. Saleur, *Indecomposability parameters in chiral logarithmic conformal field theory*, Nuclear Physics B **851** (2011), no. 2, 314 –345.

[192] G. Volovik, *On edge states in superconductors with time inversion symmetry breaking*, JETP Letters **66** (1997), 522–527. 10.1134/1.567563.

[193] K. von Klitzing, *The quantized Hall effect*, Rev. Mod. Phys. **58** (1986), 519–531.

[194] F. Wegner, *The mobility edge problem: Continuous symmetry and a conjecture*, Zeitschrift für Physik B Condensed Matter **35** (1979), 207–210. 10.1007/BF01319839.

[195] ———, *Four-loop-order β-function of nonlinear σ-models in symmetric spaces*, Nucl. Phys. B **316** (1989), no. 3, 663 –678.

[196] H. A. Weidenmüller, *Single electron in a random potential and a strong magnetic field*, Nuclear Physics B **290** (1987), no. 0, 87 –110.

[197] E. Witten, *Perturbative Gauge Theory as a String Theory in Twistor Space*, Commun. Math. Phys. **252** (2004), no. 1-3, 189–258.

[198] S. Xiong, N. Read, and A. D. Stone, *Mesoscopic conductance and its fluctuations at a nonzero Hall angle*, Phys. Rev. B **56** (1997), 3982–4012.

[199] Z. Yin, *Conformal Invariance on Orbifolds and Excitations of Singularity*, Modern Physics Letters A **24** (2009), 2089–2097.

[200] C. M. Yung and M. T. Batchelor, *Integrable vertex and loop models on the square lattice with open boundaries via reflection matrices*, Nuclear Physics B **435** (1995), no. 3, 430 –462.

[201] M. R. Zirnbauer, *Fourier analysis on a hyperbolic supermanifold with constant curvature*, Communications in Mathematical Physics **141** (1991), 503–522. 10.1007/BF02102812.

[202] ———, *Super fourier analysis and localization in disordered wires*, Phys. Rev. Lett. **69** (1992), 1584–1587.

[203] ———, *Towards a theory of the integer quantum Hall transition: From the nonlinear sigma model to superspin chains*, Annalen der Physik **506** (1994), no. 7-8, 513–577.

[204] ———, *Riemannian symmetric superspaces and their origin in random-matrix theory*, Journal of Mathematical Physics **37** (1996), no. 10, 4986–5018.

[205] ———, *Supersymmetry for systems with unitary disorder: circular ensembles*, Journal of Physics A: Mathematical and General **29** (1996), no. 22, 7113.

[206] ———, *Toward a theory of the integer quantum Hall transition: Continuum limit of the Chalker–Coddington model*, Journal of Mathematical Physics **38** (1997), no. 4, 2007–2036.

[207] ———, *Conformal field theory of the integer quantum Hall plateau transition*, ArXiv High Energy Physics - Theory e-prints (1999), available at arXiv:hep-th/9905054.

[208] ———, *Symmetry classes in random matrix theory*, Encylopedia of Mathematical Physics, 2005.

[209] ———, *Symmetry Classes*, Oxford Handbook of Random Matrix Theory, 2011.